Université de Liège
Faculté des Sciences Appliquées

Steel and composite building frames:

sway response under conventional loading and development of membrane effects in beams further to an exceptional action

Thèse présentée par

Jean-François Demonceau

en vue de l'obtention du grade scientifique de
Docteur en Sciences de l'Ingénieur

Année académique 2007 – 2008

Université de Liège
Faculté des Sciences Appliquées

Steel and composite building frames:

sway response under conventional loading and development of membrane effects in beams further to an exceptional action

Thèse présentée par

Jean-François Demonceau

en vue de l'obtention du grade scientifique de
Docteur en Sciences de l'Ingénieur

Année académique 2007 – 2008

Members of the Jury

Prof. **André PLUMIER** (President of the Jury)
University of Liège, Department Argenco
Chemin des Chevreuils, 1 B52
4000 Liège – Belgium

Prof. **Jean-Pierre JASPART** (Promoter of the thesis)
University of Liège, Department Argenco
Chemin des Chevreuils, 1 B52
4000 Liège – Belgium

Prof. **René MAQUOI**
University of Liège, Department Argenco
Chemin des Chevreuils, 1 B52
4000 Liège – Belgium

Prof. **Philippe BOUILLARD**
University of Bruxelles
Campus du Solbosch
CP 194/02, Avenue F.D. Roosvelt, 50
1050 Bruxelles – Belgium

Dr. **Louis-Guy CAJOT**
ArcelorMittal Belval et Differdange S.A.
Rue de Luxembourg, 66
4009 Esch-Sur-Alzette - Grand Duchy of Luxembourg

Prof. **Luis SIMOES DA SILVA**
University of Coimbra, Departemento de Engenharia Civil
Rua Luis Reis Santos
Polo II da Universida. Pinhal de Marrocos
3030-688 Coimbra – Portugal

Prof. **BASSAM IZZUDINE**
Imperial College London; Department of Civil and Environmental Engineering
Skempton Building
Imperial College London
London SW7 2AZ – United Kingdom

Table of contents

Acknowledgements

The present thesis is the result of six years of research at Liège University and is the fruit of kind collaborations. Within the present acknowledgement, I would like to express my gratitude to different persons who significantly contributed to the achievement of the present work.

I would like to thank first Prof. Jean-Pierre Jaspart, the promoter of the thesis, for his support and his advices. During this six year period, he created the best conditions to make possible the achievement of this work, offering me the possibility to participate actively to European projects and actions.

My gratitude goes also to Prof. Maquoi for his encouragements and all the interesting discussions we had, in particular on the rules of Eurocode 4.

Then, my acknowledgments go to the technical staff of the Argenco laboratory and in particular, to Carl Vroomen and Etienne Rondia who contributed actively to the success of the experimental tests I had the opportunity to realise within the present work.

I would like also to thank my "office" colleague, Dr. Lam Ly with whom I have the chance to collaborate since my arrival at University, for his help and for all the interesting discussions we had.

Now, I will switch to French to thank my friends and my family. Je tiens à remercier mes amis et ma famille et en particulier, mes parents, pour toutes les marques de soutien qu'ils ont manifesté.

Je terminerai en remerciant mon épouse, Valérie, pour son soutien permanent et ma petite Nora qui, dès ses premiers jours, a dû supporter les absences répétées de son papa.

Notations

Latin letters:

A : total area of a cross section

A_{IPE200} : cross section area of an IPE200 profile

A_s : steel rebars area of a concrete or composite slab

$A_{s,2}$: total area of the transverse slab rebars behind the column in the vicinity of an external composite joint

$ASMM$: amplified sway moment method

A_w : area of the web of a double T cross section

b : width of the flanges of a double T cross section

b_c : width of a column profile flange

b_{eff} : effective width of a composite slab

$b_{eff,conn}$: effective width of the concrete/composite slab contributing to the composite joint resistance subjected to sagging moments

DL : dead loads

E : Young elastic modulus

E_a : Young elastic modulus for the steel material

E_c *or* E_{cm} : secant Young modulus for the concrete

$\varepsilon_{u,average}$: average ultimate strain of a material

f_{ck} : characteristic resistance stress for the concrete

$f_{ck,actual}$: actual resistance stress for the concrete obtained through cylinder tests

$f_{ck,column}$: characteristic resistance stress for the concrete of a composite column

$f_{ck,slab}$: characteristic resistance stress for the concrete of a composite or reinforced concrete slab

FE : Finite Elements

FEM : Finite Element Method

F_i : load in row i within a connection

F_{Rd} : resistance of the indirectly affected part subjected to horizontal loads

$F_{Rd,i}$: design resistance load of the component i

f_{sk} : characteristic resistance stress for steel rebars

f_u : ultimate stress of a material

$f_{u,average}$: average value of a ultimate stress

$f_{u,flange}$: ultimate stress of the flanges of a double T cross section

$f_{u,long.}$: longitudinal ultimate stress of a plate (according to the rolling process)

$f_{u,trans.}$: transversal ultimate stress of a plate (according to the rolling process)

$f_{u,web}$: ultimate stress of the web of a double T cross section

f_y : yielding stress of a material

$f_{y,average}$: average value of a yielding stress

$f_{y,flange}$: yielding stress of the flanges of a double T cross section

f_{yk} : characteristic yielding stress of a material

$f_{y,long.}$: longitudinal yielding stress of a plate (according to the rolling process)

$f_{y,overstrength}$: yielding stress affected by an overstrength coefficient

$f_{y,trans.}$: transversal yielding stress of a plate (according to the rolling process)

$f_{y,web}$: yielding stress of the web of a double T cross section

h : height of a storey, of a column or of an element cross section

h_c : height of a column profile cross section

$h_{concrete}$: total height of a concrete slab

$H_{Ed,i}$: design value of the horizontal reaction at the bottom of storey i

h_i : height of storey i or position of row according to the beam reference point within a connection

h_{struc} : total height of a structure

I *or* I_b : moment of inertia of a beam according to the major axis

I_{IPE200} : moment of inertia of an IPE200 profile according to the major axis

K : lateral restraint coming from the indirectly affected part of a structure losing a column

k_{csc} : stiffness of the component "concrete slab in compression"

k_i : stiffness of the component i

L : span or length of a beam

LL : live loads

m : number of columns in a row

M : bending moment

M_e : elastic resistance to bending moments of a joint

M_{Ed} : design applied moment on an element or a joint

MMR : modified Merchant-Rankine

$M_{N,Rd}$: design resistance to bending moments of a cross section associated to N_{Ed}

$M_{pl,Rd}$: design plastic resistance to bending moments of a structural element

MR : Merchant-Rankine

M_{Rd} : design resistance to bending moments of a joint

M_{Rd1} : resistance to bending moments of the plastic hinges 1 and 4 in the simplified substructure modelling associated to the axial resistance N_{Rd1}

M_{Rd2} : resistance to bending moments of the plastic hinges 2 and 3 in the simplified substructure modelling associated to the axial resistance N_{Rd2}

M_u : ultimate resistance to bending moments of a joint

n : total number of storeys in a structure or of rows within a connection

N : axial load

N_b : number of bolt rows within a connection

N_{Ed} : design normal applied load

N_{lo} : axial load in a loss column

$N_{pl,Rd}$: plastic resistance to normal forces of a cross section

N_{Rd1} : resistance to normal forces of the plastic hinges 1 and 4 in the simplified substructure modelling associated to the resistance in bending M_{Rd1}

N_{Rd2} : resistance to normal forces of the plastic hinges 2 and 3 in the simplified substructure modelling associated to the resistance in bending M_{Rd2}

N_{up} : axial load in the column just above a loss column

p : uniformly distributed load applied to the simplified substructure

Q : concentrated load to be support by the simplified substructure

$S_{j,ini}$: initial stiffness of a joint

$S_{j,post\text{-}limit}$: post-limit stiffness of a joint

SLS : serviceability limit states

t_f : thickness of a profile flange

ULS : ultimate limit states

V_1 and V_2 : shear loads at the extremities of the left and right beams connected at the top of the loss column

V_{cr} : critical vertical load of a structure associated to a global sway mode of instability

V_{Ed} : total vertical load applied to a structure

$V_{Ed,i}$: design vertical load on the structure at the bottom of storey i

V_{Rd} : design resistance to shear forces of a joint

z : height of the concrete/composite slab contributing to the composite joint resistance subjected to sagging moments

Greek letters:

α_h : reduction factor for height h applicable to columns

α_m : reduction factor for the number of columns in a row

β : transformation parameter for the column web panel in shear in a joint

χ : reduction factor used in the Ayrton-Perry formulation

χ_{beam} : reduction factor associated to a beam plastic mechanism in the developed new method

$\chi_{combined}$: reduction factor associated to a combined plastic mechanism in the developed new method

χ_{panel} : reduction factor associated to a panel plastic mechanism in the developed new method

Δ : horizontal displacement at the top of a structure

Δ_a : vertical displacement of the top of the loss column

$\delta_{H,Ed,i}$: horizontal displacement at the top of storey i, relative to the bottom of storey i, when the frame is loaded with horizontal loads which are applied at each floor level

δ_K : elongation of the horizontal spring simulating the lateral restraint coming from the indirectly affected part in the simplified substructure

δ_{N1} : elongation of the plastic hinges 1 and 4 in the simplified substructure

δ_{N2} : elongation of the plastic hinges 2 and 3 in the simplified substructure

ε_{cu} : ultimate deformation which can be reached in the concrete in compression

ϕ : rotation of a joint

Φ_0 : basic value for global initial sway imperfection

Φ_{ini} : global initial sway imperfection

ϕ_u : rotation associated to the ultimate bending moment M_u of a joint

γ : rotation associated to a column web panel in shear

γ_c : safety coefficient associated to the concrete material

γ_s : safety coefficient associated to the steel rebar material

φ : rotation associated to a connection within a joint

$\overline{\lambda}$: non dimensional relative slenderness

$\overline{\lambda}_0$: length of the plateau in a χ - $\overline{\lambda}$ graph

$\overline{\lambda}_{beam}$: non dimensional relative slenderness associated to a beam plastic mechanism in the developed new method

$\overline{\lambda}_{combined}$: non dimensional relative slenderness associated to a combined plastic mechanism in the developed new method

$\overline{\lambda}_{panel}$: non dimensional relative slenderness associated to a panel plastic mechanism in the developed new method

λ_{cr} : critical load factor ($= V_{cr}/V_{Ed}$)

$\lambda_{cr,cracked}$: critical load factor of a composite structure with the concrete assumed to be cracked in the hogging moment zone

$\lambda_{cr,uncracked}$: critical load factor of a composite structure with the concrete assumed to be uncracked

λ_{Ed} : design load factor associated to the applied load

λ_{p} : load factor associated to the collapse mode obtained through a first order rigid-plastic analysis

$\lambda_{p,beam}$: plastic load factor associated to the development of a beam plastic mechanism

$\lambda_{p,combined}$: plastic load factor associated to the development of a combined plastic mechanism

$\lambda_{p,panel}$: plastic load factor associated to the development of a panel plastic mechanism

λ_{u} : load factor associated to the collapse mode obtained through a fully non-linear analysis

$\lambda_{u,beam}$: ultimate load factor obtained through the developed new method and associated to the beam plastic load factor

$\lambda_{u,combined}$: ultimate load factor obtained through the developed new method and associated to the combined plastic load factor

$\lambda_{u,panel}$: ultimate load factor obtained through the developed new method and associated to the panel plastic load factor

μ : parameter influencing the shape of the curve obtained through the Ayrton-Perry formulation

μ_{beam} : value of μ associated to a beam plastic mechanism in the developed new method

$\mu_{combined}$: value of μ associated to a combined plastic mechanism in the developed new method

μ_{panel} : value of μ associated to a panel plastic mechanism in the developed new method

θ : rotation of the plastic hinges at the simplified substructure extremities

σ : axial stress

τ : shear stress

Ψ : parameter influencing the shape of the non-linear part of a moment-rotation curve of a joint

Ψ_{braced} : lateral flexibility of the structure with the bracing system

$\Psi_{unbraced}$: lateral flexibility of the structure without the bracing system

Summary

The present thesis is dedicated to the study of the behaviour of steel and composite steel-concrete building frames with a particular attention paid to the beam-to-column joint behaviour. Two main topics are investigated herein:

- the behaviour of sway building frames subjected to "conventional" loadings and;
- the development of the membrane forces in structural beams further to the loss of a column.

Regarding the first topic, the main objective is to propose a simplified analytical method to predict the ultimate load factor of composite sway building frames, a case not yet covered by the actual codes and standards.

To achieve this goal, the behaviour of composite joints subjected to bending moments is first studied through experimental and analytical investigations; indeed, the joints are key elements influencing the response of sway frames. Through these investigations, a new collapse mode is identified for single-sided composite joints subjected to hogging moments and an analytical method is proposed and validated to introduce this new collapse mode in the joint design. In addition, an analytical method is also proposed and validated to predict the response of composite joints subjected to sagging moment, a situation which can occur in composite sway frames subjected to horizontal loads but not yet covered by the actual codes.

Afterwards, the numerical tool used to predict the response of composite sway frames is validated through a benchmark study and through comparisons with experimental test results coming from two tests performed in European laboratories. With the so-validated software, the behaviour of actual sway building frames (i.e. frames extracted from existing buildings) is investigated, highlighting their particularities.

The applicability to composite sway frames of two simplified analytical method initially developed for steel sway frames (an elastic one called the "amplified sway moment method" and a plastic one called the "Merchant-Rankine approach") is then studied. From these investigations, it is demonstrated that the elastic method can be applied with good confidence to composite sway frames while the plastic one illustrates the same problems of accuracy already observed in previous studies on steel sway frames; in particular, the plastic method may prove to be very unsafe if the collapse mode associated to the ultimate limit state is a panel plastic mechanism.

Finally, according to these results, a simplified analytical method is developed for the prediction of the ultimate load factor of steel and composite sway frames. The proposed method is founded on the Ayrton-Perry formulation and is validated through comparison to results obtained with full non-linear numerical analyses performed on more than 300 steel and composite frames. The so-validated method is easy to apply and permits to predict with a very good accuracy the ultimate load factor of a sway frame and the collapse mode appearing at the ultimate limit state.

Founded on the knowledge gained from the previous topic on the structural behaviour of steel and composite structures, the behaviour of such structures subjected to an exceptional event is investigated within the second topic. The main objective is to propose a simplified analytical procedure to predict the development of the membrane forces within a structure further to the loss of a column and their effects on the structural response.

In a first step, a general procedure allowing the prediction of the response of a structure further to the loss of a column is first defined, with a particular attention paid to the influence of the development of the catenary action on this response.

Then, an experimental test performed at Liège University and simulating the loss of a column in a composite frame is described. The objective of this test is to observe the development of the catenary action within the tested structure and its effect on the joint behaviour. The described test constitutes a European first in this domain.

Also, as for the previous topic, the behaviour of joints is investigated in details. Here, the particularity is the fact that the joints are subjected to combined bending moments and axial loads when the membrane effects developed in the structure. In a previous PhD thesis presented at Liège University, an analytical procedure founded on the component method was developed to predict the response of steel joints subjected to such loading. Within the present thesis, this method is extended to composite joints and validated through comparisons to experimental tests.

Afterwards, the numerical tool used for the numerical investigations is validated through a benchmark study and through comparisons with the results of the experimental test performed at Liège University. In particular, the difficulty of simulating the actual behaviour of beam-to-column joints subjected to combined bending moments and axial loads is illustrated.

With the so-validated software, a simplified substructure modelling, on which the developed analytical method is founded, is then validated. In addition, parametric

numerical studies are performed on the substructure modelling in order to identify the parameters to be considered within the developed method.

Finally, the developed simplified analytical method is described and validated through comparisons between the experimental results and the analytical prediction. With this "easy-to-apply" method, a very good accuracy is achieved; in particular, it is possible to predict the requested deformation capacity in the structural elements where plastic hinges are developed and the membrane forces which have to be supported by the structure.

Résumé

La présente thèse est dédiée à l'étude du comportement des portiques de bâtiments en acier et mixte acier-béton avec une attention particulière portée sur le comportement des assemblages poutre-colonne. Deux sujets principaux sont abordés :

- l'étude du comportement des portiques à nœuds transversalement déplaçables soumis à un chargement "classique" et ;
- l'étude du développement des efforts membranaires dans les poutres d'un portique suite à la perte d'une colonne.

Concernant le premier sujet, l'objectif principal est de proposer une méthode analytique simplifiée permettant de prédire le multiplicateur de charge ultime de portiques mixtes à nœuds transversalement déplaçables, cas non encore couvert par les codes actuels.

Pour atteindre cet objectif, le comportement des assemblages mixtes soumis à des moments de flexion est étudié dans un premier temps aux travers d'études expérimentales et analytiques, les assemblages étant des éléments clés dans l'étude du comportement des portiques à nœuds transversalement déplaçables. Via ces études, un nouveau mode de ruine est mis en évidence pour les assemblages mixtes externes et une méthode analytique est proposée et validée pour la prise en compte de ce nouveau mode de ruine dans le dimensionnement de ces assemblages. De plus, une méthode analytique est également proposée et validée pour prédire la réponse des assemblages mixtes soumis à moment positif, situation pouvant apparaître dans les portiques mixtes à nœuds transversalement déplaçables soumis à un chargement horizontal mais non encore couverte par les codes actuels.

Ensuite, l'outil numérique utilisé pour prédire la réponse des portiques est validé par une étude comparative réalisée avec différents logiciels et par une comparaison à des résultats expérimentaux provenant de deux essais réalisés dans des laboratoires Européens. Avec cet outil ainsi validé, le comportement de portiques mixtes réels (c'est-à-dire extraits de bâtiments existants) est étudié en mettant en évidence leurs particularités.

L'applicabilité à des structures mixtes de deux méthodes simplifiées initialement développées pour des portiques en acier à nœuds transversalement déplaçables (une élastique intitulée "amplified sway moment method" et une plastique intitulée "approche de Merchant-Rankine") est alors étudiée. Suite à cette étude, il est démontré que la méthode élastique peut être assurément appliquée aux portiques mixtes tandis que la méthode plastique démontre les mêmes problèmes de précision que ceux déjà observés dans des études précédentes réalisées sur des portiques en acier ; en particulier, la méthode

peut se révéler être très insécuritaire si le mécanisme de ruine associé à l'état limite ultime est un mécanisme plastique de panneau.

Finalement, suite à cette dernière observation, une méthode analytique simplifiée est développée pour la prédiction du multiplicateur de charge ultime de portiques mixtes et en acier à nœuds transversalement déplaçables. La méthode proposée est fondée sur la formulation d'Ayrton-Perry et est validée par des comparaisons à des résultats obtenus via des analyses non-linéaires réalisées sur plus de 300 portiques en acier et mixtes. La méthode ainsi validée est facile à utiliser et permet d'obtenir le multiplicateur de ruine d'un portique avec une très bonne précision ainsi que le mode de ruine apparaissant à l'état limite ultime.

Suite à l'expérience acquise sur le comportement des structures en acier et mixtes soumises à un chargement « classique », le comportement de celles-ci soumises à une action exceptionnelle a alors été étudié. L'objectif principal est la proposition d'une méthode analytique simplifiée permettant de prédire le développement des forces membranaires dans une structure suite à la perte d'une colonne et leurs effets sur la réponse structurale.

Dans un premier temps, une procédure générale permettant de prédire la réponse d'une structure lors de la perte d'une colonne est définie, mettant en évidence l'influence du développement des efforts membranaire sur cette réponse.

Un essai expérimental réalisé à l'Université de Liège et simulant la perte d'une colonne dans un portique mixte est ensuite présenté. L'objectif de cet essai est d'observer le développement des efforts membranaires dans la structure testée et leurs effets sur le comportement des assemblages. L'essai présenté constitue une première Européenne dans ce domaine.

Comme pour le sujet précédent, le comportement des assemblages est aussi étudié en détail. Ici, la particularité est le fait que les assemblages sont soumis à la fois à des moments de flexion et à des efforts axiaux lorsque les effets membranaires se développent dans la structure. Dans une thèse de doctorat précédente présentée à l'Université de Liège, une procédure analytique fondée sur la méthode des composantes a été développée pour prédire la réponse d'assemblages en acier soumis à un tel chargement. Dans la présente thèse, cette méthode est étendue au cas des assemblages mixtes et validées via des comparaisons à des résultats expérimentaux.

Ensuite, l'outil numérique utilisé est validé par une étude comparative réalisée avec différents logiciels et par des comparaisons aux résultats de l'essai réalisé à l'Université de Liège. En particulier, la difficulté de simuler le comportement réel d'assemblages soumis à une action combinée d'efforts de flexion et d'efforts axiaux est illustrée.

Avec le logiciel ainsi validé, un modèle simplifié de sous-structure permettant de développer la méthode analytique simplifiée est défini et validé via des études numériques. De plus, des études paramétriques sont réalisées sur ce modèle afin d'identifier les paramètres à prendre en compte dans la méthode développée.

Finalement, la méthode simplifiée développée est décrite et validée via des comparaisons entre les résultats expérimentaux et les prédictions analytiques. Avec cette méthode facile à utiliser, une très bonne précision est obtenue ; en particulier, il est possible de prédire la demande en terme de capacité de déformation au niveau des éléments structuraux où se forment des rotules plastiques et de déterminer les efforts membranaires devant être supportés par la structure.

I. General introduction

I.1. Generalities

Since long time, the behaviour of steel and steel-concrete composite building frames has been the topic of a lot of researches worldwide; the results of these researches had significant impacts in the understanding of their behaviour, in the development of design procedures for such frames and, also, in the development of the associated codes and standards.

In particular, in the last decade, the M&S department of Liège University (department which is now integrated in a bigger department called Argenco) had the opportunity to participate to European projects dedicated to the behaviour of steel-concrete composite sway building frames and to the behaviour of steel and composite buildings (or of their structural elements) subjected to exceptional actions; these projects are summarised here below:

- An ECSC (European Coal and Steel Community) project titled "Applicability of composite structures to sway frames" (contract N° 7210-PR-250 – acronym: Sway frame) *[1]*: the objective of this project was to provide background information on the behaviour of composite framework structures under monotonous and cyclic loads. Particular attention was paid to the sway behaviour and to the beam-to-column joint behaviour. In particular, limitations or particular provisions for such structures for both the serviceability and ultimate limit state were provided.
- An ECOLEADER project titled "3-D full scale seismic testing of a steel-concrete composite building at ELSA" (EUR 21299 EN) *[2]*: this project was dedicated to the performance of an experimental test to investigate the behaviour of a high ductile steel-concrete composite frame structure characterized by partially encased columns and dissipative partial strength joints, where both the column web panel, not surrounded by concrete, and the beam-to-column connection share the energy dissipation demands. The performed test allows promoting the development of design rules currently not covered by Eurocode 8.
- An RFCS (Research Fund for Coal and Steel) project titled "Prefabricated composite beam-to-concrete filled tube or partially reinforced-concrete-encased column connections for severe seismic and fire loadings" (Project N° RFS-PR-02002 – acronym: Precious) *[3]*: this research programme intended to develop fundamental data, design procedures and promotion of two types of ductile and fire-resistant composite beam-to-column joints with: partially reinforced-concrete-encased column with I-section and concrete filled tubular column with circular hollow steel section.

- An RFCS project titled "Robust structures by joint ductility" (Project N° RFS-CR-04046 – acronym: Robustness) *[4]*: robustness ensures structural safety by preventing the collapse of the total structure when only one part of the structure is damaged or destroyed. By intelligent design the possibility of force redistribution is given after extensive plastification of joints and single structural elements. Thus the structure keeps its strength even under exceptional loading and under large deformations. Profiting from the inherent ductile behaviour of steel, this project analysed the requirements for robustness and developed new ductile joint solutions to allow for this force redistribution. Criteria for robust structures, especially concerning steel and composite joints were elaborated and illustrated by drawings in a handbook for an easy understanding and realisation by the constructor.

The present thesis reflects activities which were initiated in 2001. Part of the developments presented herein is directly linked to the activities of the department within these European projects. In particular, two investigated topics are addressed:

- the behaviour of steel-concrete composite building frames subjected to significant second-order effects when subjected to "conventional" loading and;
- the development of membrane effects in structural steel or composite beams further to an exceptional event.

For each topic, the performed investigations include experimental, numerical and analytical aspects. The plan of the thesis is detailed in the following paragraph.

I.2. General plan of the thesis

The present thesis is divided in six main parts (divided in paragraphs, themselves divided in sections). The first one is the present one and contains the general introduction of the thesis.

The second one is dedicated to the study of the behaviour of steel-concrete composite sway frames subjected to "conventional" loading. The main objective of this study is to propose simplified analytical methods to predict the response of these frames. Within the study, a particular attention is paid to the behaviour of the beam-to-column composite joints as the latter are key elements influencing significantly the global sway frame behaviour. Also, the behaviour of actual composite building frames, i.e. frames extracted from "real" buildings, is numerically and analytically investigated. At the end, an analytical method, founded on the Ayrton-Perry formulation and applicable to steel and composite sway frames, is developed and validated to predict the ultimate load factor of

these frames with a very good accuracy and to predict the collapse mode occurring at the ultimate limit state.

Founded on the knowledge gained from the previous part on the structural behaviour of steel and composite structures subjected to significant second order effects, the third part is devoted to the study of such structures subjected to an exceptional event: loss of a column further to an impact. In particular, the development of the membrane effects in steel or composite structural beams associated to the column loss is investigated. The performed developments (including experimental, numerical and analytical approaches) are part of a general concept which is first described. Then, an experimental test simulating the loss of a column in a composite building performed at Liège University is presented; the performed test constitutes a European first. The behaviour of joints subjected to combined bending moments and axial loads (associated to the membrane forces) is also investigated in details through experimental and analytical studies; in particular, an analytical method to predict the response of composite joints subjected to such loadings is proposed and validated. Finally, a simplified analytical method to predict the development of the membrane forces in a steel or composite frame and their influence on the frame response is developed and validated.

The fourth part presents the general conclusions of the thesis and perspectives. To ensure a fluidity of the lecture of the previous parts, the personal contributions to the presented developments are not highlighted within the text; however, a paragraph dedicated to these personal contributions is included in the fourth part.

Finally, the fifth and the sixth parts are devoted to the references and appendixes respectively. In the appendixes, some additional information concerning the performed experimental tests or the performed computations are given.

II. Sway response of composite building frames subjected to "conventional" loading

II.1. Introduction

II.1.1. Context

Most steel-concrete composite structures are laterally restrained by efficient bracing systems, such as concrete cores. This practice does not favour the use of composite structures. Indeed, once concrete construction companies are involved into major parts of a building, the reason for using composite structures for subsequent parts is often questionable.

As an alternative, moment resisting frames, without bracing systems, offer a flexible solution to the user of the buildings, especially for the internal arrangements and the exploitation of the buildings. When sufficient stiffness and strength with regard to lateral forces are achieved, such frames offer a structural solution, which can resist lateral loads. In seismic regions, properly designed moment resisting frames are the best choice regarding the available ductility and the capacity to dissipate energy. This is stated in Eurocode 8 *[5]* devoted to earthquake engineering in which high values of the behaviour factor are recommended.

Obviously, the construction of tall buildings and large industrial halls without wind bracing systems is susceptible to make global instability a relevant failure mode; this is not yet well covered by Eurocode 4 *[6]* and other references (*[7]*, *[8]* and *[9]*) which mainly deals with composite construction under static loading. Indeed, as far as the European codes are concerned, Eurocode 4 contains design procedures for non-sway composite buildings and gives design rules for composite slabs, beams, columns and joints; composite sway frames are allowed in Eurocode 4 but no information on how to design them are given.

That is the reason why two European research projects on composite sway frames, in which Liège University was involved, have been conducted recently:

- the first one involving seven institutions and titled "Applicability of composite structures to sway frames" (Contract N° 7210-PR-250) *[1]* was funded by the European Coal and Steel Community (ECSC) for three years (from July 2000 to June 2003);
- the second one was an Ecoleader project (from July 2000 to June 2003) titled "3-D full scale seismic testing of a steel-concrete composite building at ELSA" involving six institutions *[2]*.

The objective of these projects was to provide background information on the behaviour of such frames under static and seismic loads and to provide simplified design rules as a result of experimental, numerical and analytical investigations (see *§ I.1*).

Concerning the experimental investigations, two main experimental tests were planned within these projects:

- a 3-D composite building under dynamic loading tested in Ispra (Italy), called the "Ispra" structure;
- a 2-D composite frame under static loading tested in Bochum (Germany), called the "Bochum" structure.

Beside these tests, cyclic and static tests on isolated joints were also performed in different European laboratories (involving the Argenco Laboratory of liege University) so as to get the actual behaviour of the constitutive structural joints of these two structures; indeed, the behavioural responses of the joints are known to significantly influence the global behaviour of structures.

Concerning the analytical and numerical investigations performed at Liège University, they were divided in three parts:

- validation and development of an analytical procedure to predict the response of composite joints subjected to hogging and sagging bending moments
- numerical analyses of existing structures further to the validation of the numerical tools used for the numerical investigations;
- development of design guidance with proposals of simple analytical methods to design composite sway structures.

Part of the investigations presented within *Part II* reflects the investigations carried out at Liège University as partner of the above-mentioned European projects. The objectives of the performed work and the research steps followed within the present study are briefly described in the following paragraph.

II.1.2. Objectives and research steps

Composite sway structures are prone to global instability phenomena and to second-order effects; the latter have to be predicted carefully because they may govern the design. These second-order effects are amplified by an additional source of deformability with regards to steel sway structures: the concrete cracking. Indeed, this effect, which is specific to concrete and composite constructions, tends to increase the lateral deflection of the frame, amplifies consequently the second-order effects and reduces the ultimate resistance

of the frames. In other words, for a same number of hinges formed at a given load level in a steel frame and in a composite frame, larger sway displacements are reported in the composite one.

The objective of the present part of the thesis is to investigate the effects of these phenomena on the behaviour of composite sway frames, to highlight the particularities of their behaviour and to propose simplified analytical procedures for the design of such frames; these objectives will be achieved by means of numerical and analytical studies on 2-D plane frames extracted from realistic or actual buildings. The research steps are the following:

- *§ II.2* first gives a general overview of the available knowledge on sway composite structures and the design methods for sway structural systems. So, details about the sway effects in steel building frames and the design methods available in Eurocode 3 for steel sway frames are first given; then, the few information concerning the design of composite sway frames are introduced.
- As previously mentioned, the behavioural response of the joints is known to significantly influence the global behaviour of sway structures. Accordingly, *§ II.3* presents the experimental and analytical investigations devoted to the study of the behaviour of composite joints. In particular, the tests performed at the Argenco Laboratory of Liège University on a single-sided composite joint *[10]* are first described, highlighting a particular failure mode which occurred during the experimental test and which had not yet been detected previously. Then, an analytical formula covering this particular phenomenon and based on a theoretical model is presented; it is validated through comparisons with experimental results. Finally, as no method is proposed in the codes to predict the behaviour of composite joints under sagging bending moments, an analytical procedure to predict the response of composite joints under such loadings is proposed and validated through comparison to experimental test results; indeed, the prediction of the joint response under such loading is needed as this type of loading can occurred in sway composite frames at the joint level.
- Then, in *§ II.4*, the finite element software used for the prediction of the composite sway frame responses has been validated through a benchmark study and through comparison with experimental test results performed in two European laboratories.
- *§ II.5* summarises numerical and analytical investigations performed with the so-validated tool on frames extracted from actual buildings and presented in a Master Thesis submitted at Liège University *[11]*. The main conclusions are also reminded, putting into sight the particular behaviour of composite sway frames.

- Afterwards, according to the results obtained through the investigations presented in the previous paragraph, a new design method for the design of steel and composite sway building frames is proposed and validated through parametrical studies presented in *§ II.6*. The developed method is founded on the Ayrton-Perry formulation which is the method recommended in the Eurocodes to deal with the instability phenomena and permits to compute the ultimate load factor of a sway frame and the associated collapse mode.
- Conclusions are finally drawn in *§ II.7* to conclude the second part of the thesis.

The followed strategy is illustrated in *Figure II.1*.

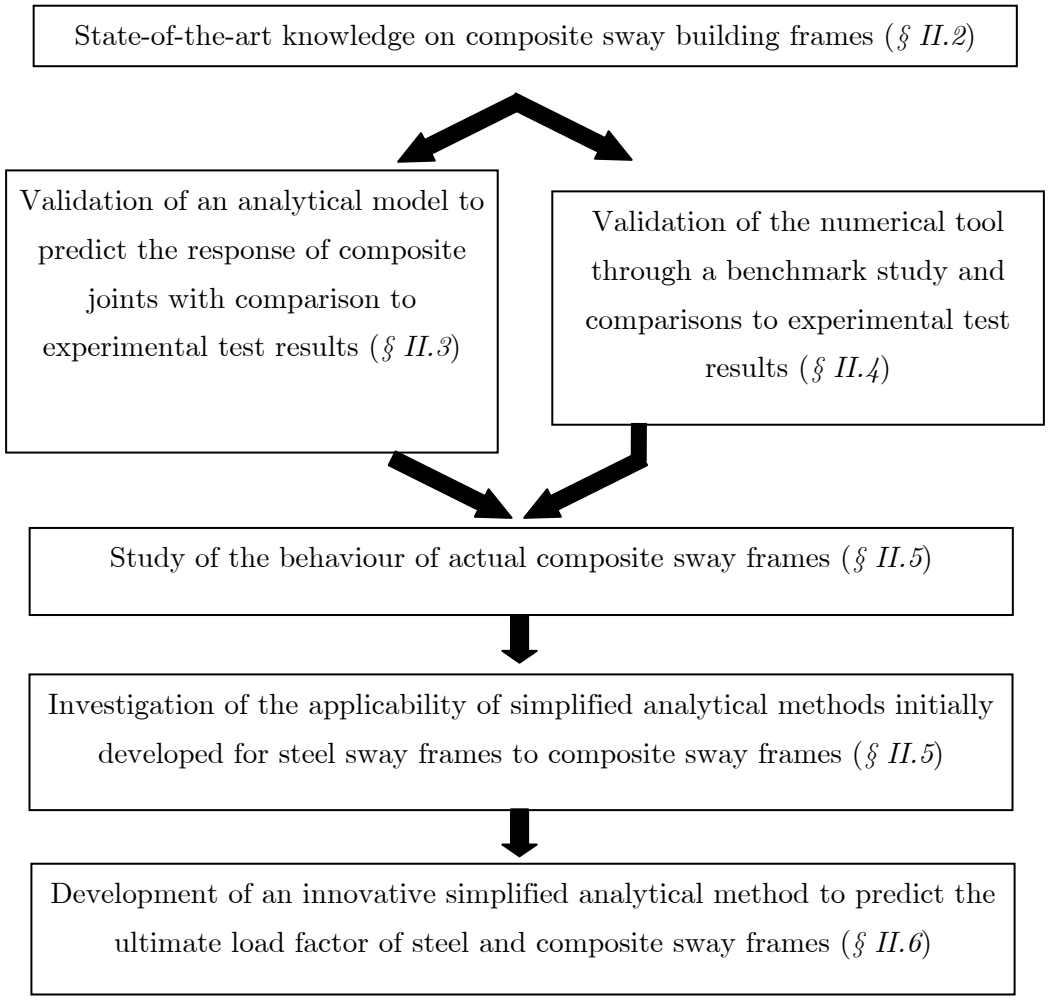

Figure II.1. Strategy followed within Part II

II.2. State-of-the-art knowledge on composite sway building frames

II.2.1. Introduction

As said in *§ II.1.1*, Eurocode 4 *[6]* limits its scope to "non-sway" composite buildings under static loading, giving rules to analyse and to check elements like composite slabs, beams, columns and joints. No rules are given for the analysis and the verification of "sway" composite building frames; Eurocode 4 only recommends using "appropriate" design rules for such frames.

The present paragraph introduces the different concepts available in the actual codes, which will be the starting points for the developments presented in this thesis:

- *§ II.2.2* first introduces concepts, important definitions and design methods proposed in Eurocode 3 *[12]* for the analysis and the check of steel sway building frames;
- then, *§ II.2.3* presents few information available on the behaviour of composite sway building frames mentioning recent researches.

II.2.2. Sway effects in steel building frames

II.2.2.1. Introduction

Sway frames are characterised by significant lateral displacements. The latter can generate a global instability phenomenon under the gravity loads, as a result of second-order effects called "*P-Δ* effects" which can significantly influence the behaviour of the frame. Furthermore, under increasing single-sided loading, the appearance of plastic hinges in the frame decreases progressively its lateral stiffness; this has a detrimental influence on the maximum vertical loads leading to a global frame instability.

Eurocode 3 *[12]* dedicated to steel buildings, is the only structural code providing indications on how to deal with the instability and, in particular, with the global frame analysis methods. Global frame analysis aims at determining the distribution of the internal forces and of the corresponding deformations in a structure subjected to a specified loading. It requires the adoption of adequate models which incorporate assumptions on the behaviour of the structure and in particular of its constitutive members and joints. And, these assumptions may be different if the structural building is "sway" or "non-sway".

In this section, the procedure proposed in Eurocode 3 for the analysis and the verification of a steel sway frame is described; the applicability of the latter to sway composite frames is investigated latter on in *§ II.5.* this section is organised as follows:

- First, a general description of the criteria for the classification of member cross sections and frames is given in *§ II.2.2.2* and *§ II.2.2.3* respectively.
- The possible global frame analyses are then briefly described in *§ II.2.2.4* together with the different criteria which govern their choice; the different verifications to perform according to the selected analysis method are also presented.
- Finally, simplified analytical methods developed for steel sway frames are introduced in *§ II.2.2.5*; these methods allow the designer to proceed to a rather simple structural design (not requiring a high capacity software to take account of the sway effects and the non-linearities).

Remark: these paragraphs are largely inspired by the following lecture notes prepared within a European project in which Liège University has been deeply involved: "Structural Steelwork Eurocodes – Development of a Trans-national Approach (SSEDTA)" (*[13]* & *[14]*).

II.2.2.2. Member cross section classification

Member sections, be they rolled or welded, may be considered as an assembly of individual plate elements, some of which are internal (e.g. the webs of open beams or the flanges of boxes) and others are outstand (e.g. the flanges of open sections and the legs of angles). As the plate elements in structural sections are relatively thin compared with their width, when loaded in compression (as a result of axial loads applied to the whole section and/or from bending) they may buckle locally. The disposition of any plate element within the cross section to buckle may limit the axial load carrying capacity, or the bending resistance of the section, by preventing the attainment of yield. Avoidance of premature failure arising from the effects of local buckling may be achieved by limiting the width-to-thickness ratio for individual elements within the cross section. This is the basis of the section classification approach.

Eurocode 3 *[12]* (and also Eurocode 4 *[6]*) defines four classes of cross section. The class into which a particular cross section falls depends upon the slenderness of each element (defined by a width-to-thickness ratio) and the compressive stress distribution i.e. uniform or linear. The classes are defined in terms of performance requirements for resistance of bending moments and for the rotational capacity (*Figure II.2*):

- **Class 1** cross sections are those which can form a plastic hinge with the required rotational capacity for plastic analysis.
- **Class 2** cross sections are those which, although able to develop a plastic moment (M_{pl}), have limited rotational capacity and are therefore unsuitable for structures designed by plastic analysis.
- **Class 3** cross sections are those in which the calculated stress in the extreme compression fibre can reach yield but local buckling prevents the development of the plastic moment.
- **Class 4** cross sections are those in which local buckling limits the moment resistance (or compression resistance for axially loaded members); the elastic moment (M_{el}) cannot develop in such sections. Explicit allowance for the effects of local buckling is necessary.

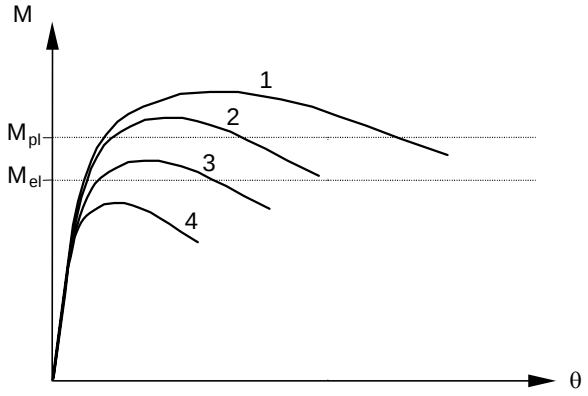

Figure II.2. Shape of the moment-rotation curves according to the class of the section

So, the choice between an elastic and a plastic analysis will be mainly govern by the class of the cross sections of the structural members (see *§ II.2.2.4*).

II.2.2.3. Frame classification

A. Braced and unbraced

At a preliminary design stage, a decision usually has to be made as to whether the structure is to have a braced or unbraced classification. This determines how the vertical and horizontal load effects (including those due to frame imperfections) are to be considered in the analysis.

When bracing is provided it is normally used to prevent, or at least to restrict, sway in multi-storey frames. Common bracing systems are trusses or shear walls (*Figure II.3*).

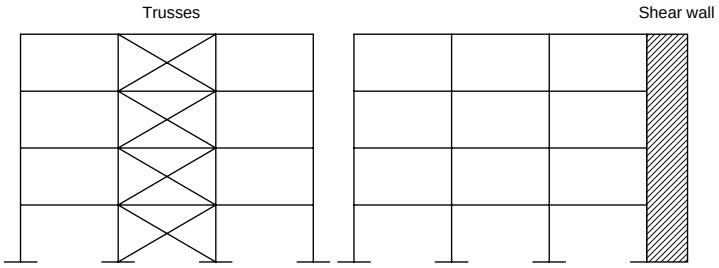

Figure II.3. Common bracing systems

For a frame to be classified as a braced frame, it must possess a bracing system which is adequately stiff. Indeed, the existence of a bracing system in a structure does not guarantee that the frame structure is to be classified as braced. Only when the bracing system reduces the horizontal displacements by at least 80 % can the frame be classified as braced:

- if no bracing system is provided, the frame is unbraced;
- if a bracing system is provided, the frame is braced when $\Psi_{braced} \leq 0{,}2\ \Psi_{unbraced}$ where Ψ_{braced} is the lateral flexibility of the structure with the bracing system and $\Psi_{unbraced}$ is the lateral flexibility of the structure without the bracing system.

When it is justified to classify the frame as braced, it is possible to analyse the frame and the bracing system separately as follows:

- The frame without the bracing system can be treated as fully supported laterally and as having to resist the action of the vertical loads only.
- The bracing system resists all the horizontal loads applied to the frames it braces, any vertical loads applied to the bracing system and the effects of the initial sway imperfections from the frames it braces and from the bracing system itself.

For frames without a bracing system and also for frames with a bracing system but which is not sufficiently stiff to allow classification of the frame as braced, a single structural system, consisting of the frame and of the bracing when present, shall be analysed for both the vertical and horizontal loads acting together as well as for the effects of imperfections.

B. Sway and non-sway

Second-order effects

Prior to the definition of the sway – non-sway classification, it is important to define the underlying concept of "second-order effects".

The second-order theory consists in expressing the equilibrium between the internal and external forces of the structure in the deformed shape; in opposite, a first-order theory expresses the equilibrium in the undeformed shape. As an example, *Figure II.4* shows that an additional lever arm for the vertical loads appears with account for the deformation of the structure; so, additional bending moments develop in the structure (called "second-order bending moments").

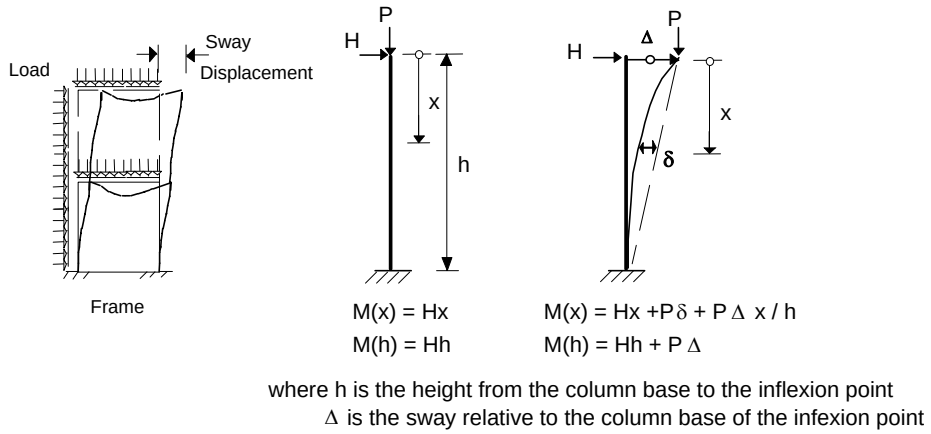

Figure II.4. First-order and second-order moments in a beam-column

These global second-order moments are commonly referred to as the *P-Δ* effects. In addition a local second-order moment, commonly referred to as the *P-δ* effects, arises in the axially loaded member due to the deflections (δ) relative to the chord line connecting the member ends (*Figure II.4*). These second-order effects are initiated by the global frame imperfections and the local member imperfections which are present in all structures (*Figure II.5*).

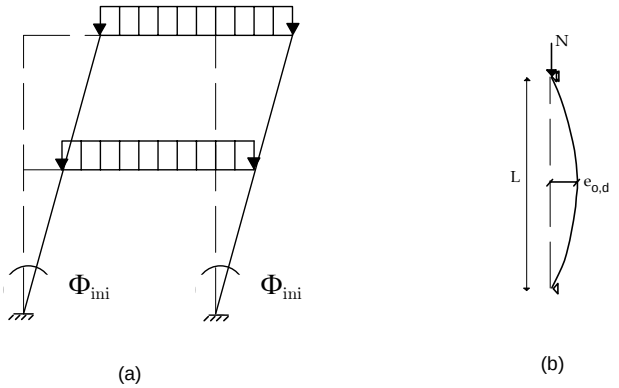

Figure II.5. Global frame initial imperfection (a) and local member initial imperfections (b)

Sway – non-sway classification

The term non-sway frame is applicable when the frame response to in-plane horizontal forces is sufficiently stiff for it to be acceptable to neglect any additional forces or moments arising from horizontal displacements of its nodes. The global second-order

effects (i.e. the *P-Δ* sway effects) may be neglected for a non-sway frame. When the global second-order effects are not negligible, the frame is said to be a sway frame.

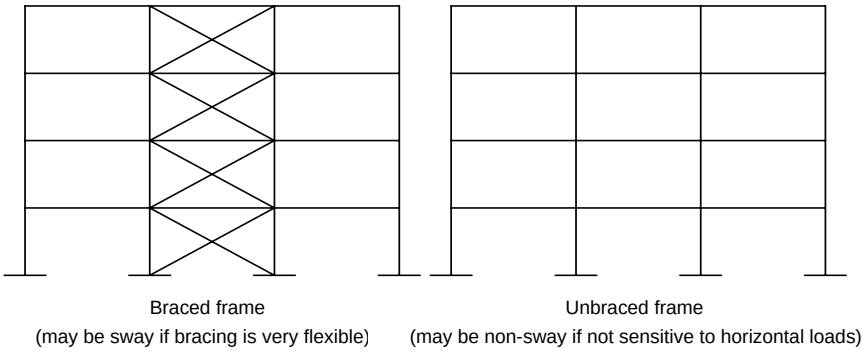

Figure II.6. Braced and unbraced frame

Normally a frame with bracing is likely to be classified as non-sway, while an unbraced frame is likely to be classified as sway. However, it is important to note that it is theoretically possible for an unbraced frame to be classified as non-sway (this is often the case of one storey portal frame buildings) while a frame with bracing may be classified as sway (possible for multi-storey buildings) (*Figure II.6*).

When a frame is classified as non-sway, a first-order analysis may always be used; when a frame is classified as sway, a second-order analysis shall be used.

The classification of a frame structure as sway or non-sway is based on the value of the ratio of the design value of the total vertical load V_{Ed} applied to the structure to its elastic critical value V_{cr} producing sway instability (failure in the sway mode). Obviously, the closer that the applied load is to the critical load, the greater is the risk of instability and the greater are the global second-order effects on the structure (the *P-Δ* effects). According to Eurocode 3 *[12]*, the classification rules are as follows:

- For elastic analysis:
  - o if $\frac{V_{Ed}}{V_{cr}} \leq 0.1$ (2.1), the structure is classified as non-sway;
  - o if $\frac{V_{Ed}}{V_{cr}} > 0.1$ (2.2), the structure is classified as sway.
- For plastic analysis:
  - o if $\frac{V_{Ed}}{V_{cr}} \leq 0.067$ (2.3), the structure is classified as non-sway;
  - o if $\frac{V_{Ed}}{V_{cr}} > 0.067$ (2.4), the structure is classified as sway.

These rules can also be expressed in the following way:

- For elastic analysis:

- o if $\lambda_{cr} = \frac{V_{cr}}{V_{Ed}} \geq 10$ (2.5), the structure is classified as non-sway;
- o if $\lambda_{cr} = \frac{V_{cr}}{V_{Ed}} < 10$ (2.6), the structure is classified as sway.

- For plastic analysis:
  - o if $\lambda_{cr} = \frac{V_{cr}}{V_{Ed}} \geq 15$ (2.7), the structure is classified as non-sway;
  - o if $\lambda_{cr} = \frac{V_{cr}}{V_{Ed}} < 15$ (2.8), the structure is classified as sway.

The more restrictive limit for plastic analyses is justified in Eurocode 3 *[12]* by the fact that, when the material non linearities are included in the analysis, the global second-order effects are more important.

C. Summary

The different possibilities of frame classification can be summarized by *Table II.1* where all the possible combinations between braced/unbraced and sway/non-sway are presented. The choice between a first-order and a second-order theory for the global structural analysis will mainly be governed by the frame classification (see *§ II.2.2.4*).

Table II.1. Possibilities of frame classification

	Braced	**Unbraced**
Non-sway	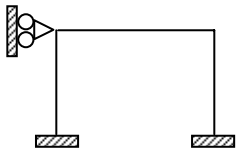	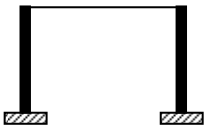
Sway	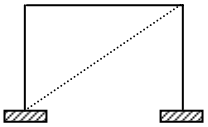	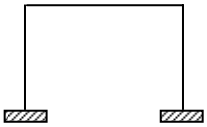

II.2.2.4. Types of structural analyses and associated verifications

A. Introduction

The previous sections have introduced the different classifications for the member cross sections and the frames; these classifications will mainly influence the selection of the global structural analysis to perform on the frame.

On one hand, the class of the member cross section influences the choice between a plastic or an elastic analysis: plastic analyses can only be applied to structures which present

member cross sections of class 1 where plastic hinges take place; if it is not the case, only the realization of an elastic analysis is authorized.

On the other hand, the classification of the frame will influence the choice between a first-order and a second-order theory. The different possibilities are presented in *Table II.2*.

Table II.2. Influence of the frame classification on the choice between a first or second-order theory

	Braced	**Unbraced**
Non-sway	First-order theory or Second-order theory	First-order theory or Second-order theory
Sway	Second-order theory	Second-order theory

One aspect which has also to be considered in this choice is that the design checks to be carried out after the analysis depend on the sophistication of the analysis "tool" (see *Figure II.7*): the number of design checks decreases with the increase of the analysis sophistication (from first-order elastic analysis to "full" non-linear analysis).

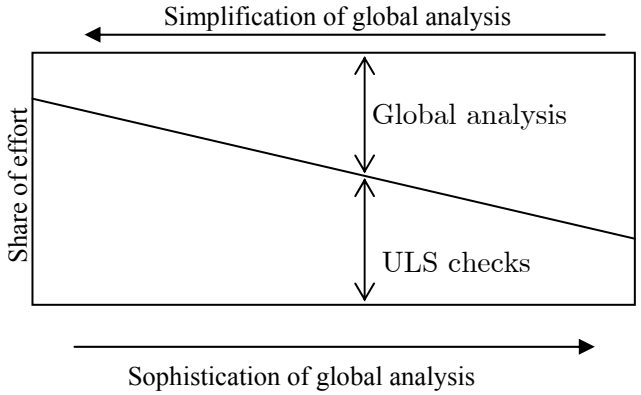

Figure II.7. Balance between global analysis and ultimate limit states (ULS) checks

The present section presents the different type of structural analyses which can be applied to frames. For each type, the different ultimate limit states (ULS) checks to perform are described. The serviceability limit states (SLS) have also to be verified; the different limitations recommended in Eurocode 3 *[12]* (and in Eurocode 4 *[6]*) are presented in *Table II.3* where L is the length of a beam, h_{struc} the total height of the structure and h the height of a storey. A last section compares the results obtained through the different analyses described in this paragraph through a qualitative illustration in *Figure II.8*.

Table II.3. Deflection limitations recommended in Eurocode 3 and 4

Verification	Limitation
Beam deflection	$L/300$
Top sway displacement	$h_{struc}/500$
Sway displacement for each storey	$h/300$

Remark: for all the presented analyses, the out-of-plane stabilities have to be checked. This point will not be reminded in the following paragraphs.

B. First-order elastic analysis

Linear elastic analysis implies an indefinite linear response of sections and joints. This analysis is applicable to non-sway buildings. It can be used for sway frames under certain conditions and provided that appropriate corrections are made to allow for the second-order effects when necessary (see *§ II.2.2.5*); this is the only restriction to this type of analysis. The main advantage of such analysis is that the superposition principle is applicable.

When elastic analysis is used, it would seem appropriate to consider the attainment of the yield stress in the extreme fibres of the most loaded section as the design condition for a member; however, in usual cases, it is generally accepted that an elastic analysis can be safely used to determine the load corresponding to when the first plastic event occurs (if the class of the member cross section where the plastic event occurs permits it). However, this assumes that the structure (in case of sway frames) and its members remain stable. So, it is important to check the stability of the structure and its members to be sure that an instability phenomenon does not decrease the design resistance value.

C. Critical elastic analysis

This analysis is based on the same assumption as the previous one (sections and joints indefinitely linear elastic) and is achieved so as to derive the elastic critical load V_{cr} (or the elastic critical load factor λ_{cr}) that corresponds to the first mode of global instability. According to Eurocode 3 *[12]*, this value is used through the evaluation of the V_{Ed}/V_{cr} (or $\lambda_{Ed}/\lambda_{cr}$) ratio – V_{Ed} being the design vertical applied load – to determine whether a frame is laterally rigid or, in contrast, prone to sway (see *§ II.2.2.3.B*).

D. Second-order elastic analysis

In this type of analysis, the indefinitely linear-elastic response of sections and joints is still applied. The distribution of the double-sided forces is now computed on the basis of a

second-order theory (i.e. equilibrium equations express in the deformed structure). This type of analysis is applicable to all structures.

As for the first-order elastic analysis, the failure is assumed to be reached when the extreme fibres of the most loaded section yields or when the first plastic hinge takes place in the structure (if the member cross section class permits it). The resistance of the sections and of the joints has to be checked. As the *P-Δ* effects (*§ II.2.2.3.B*) are considered in a second-order analysis, it is not needed to check the global stability of the structure. If the *P-δ* (*§ II.2.2.3.B*) effects are also included in the analysis, neither have the local stability to be checked; if it is not the case, it has to be verified but by computing the buckling length with the assumption of a non-sway structure, as the sway effects are included in the analysis.

E. First-order rigid-plastic analysis

In such analysis, the elastic deformations are ignored. This type of analysis is especially appropriate for non-sway frames while its use for sway frames is limited to specific cases; the latter is only applicable to structures which fulfil some conditions given in Eurocode 3 *[12]* (steel properties, cross section class,...). This calculation results in the first-order rigid-plastic load factor λ_p; the latter is often called the first-order "limit" load factor. It can be obtained easily by hand-calculation, or by using appropriate software. The first-order rigid-plastic load factor is required, for instance, to apply the simplified design method known as the "Merchant-Rankine approach" (see *§ II.2.2.5.D*).

Adequate design requires that the value of the load multiplier λ_p be at least unity. As the first-order plastic method does not make allowance for any buckling phenomena as well at a local as at a global level, these checks shall be carried out with due allowance being made for the presence of plastic hinges.

F. Second-order rigid-plastic analysis

This analysis may be used in all cases for which a plastic analysis is allowed. This analysis differs from the previous one by the fact that equilibrium equations are now expressed with reference to the deformed frame configuration.

A second-order rigid-plastic analysis gives an indication on how second-order effects develop once the first-order rigid-plastic mechanism is formed and how much they affect the post-limit resistance. Because second-order effects are without significant influence on the plastic beam mechanisms, the second-order rigid-plastic response curve will not diverge notably from the one obtained from a first-order rigid-plastic analysis. In contrast,

for panel and combined beam-panel plastic mechanisms, the larger the sway displacement, the more the second-order rigid-plastic load factor is reduced when gravity loads increase.

Concerning the stability of the studied structure and its constitutive elements, the remarks introduced for the first-order rigid-plastic analysis (in the previous paragraph) are also valid for the second-order rigid-plastic analysis except that it is not needed here to check the global stability of the structure as the P-Δ effects are involved in the analysis.

G. Non-linear analysis

A non-linear analysis is applicable to all cases. In this type of analysis, all the geometrical and material non-linearities are considered: realistic material stress-strain curves, semi-rigid response of the joints and second-order effects induced by frame and element geometrical imperfections. The initial deformation of the buildings is introduced in the analysis. Such an analysis enables an accurate estimation of the actual ultimate load factor λ_u. The stability of the structure and the constitutive elements does not need to be checked, as P-Δ and P–δ effects are involved in the non-linear analysis.

H. Overview of the considered frame analyses

In *Figure II.8*, the results of the different analyses described in this paragraph are qualitatively illustrated. This figure shows how the sway displacement Δ influences the value of the load factor λ got from the several types of analysis.

The line "OA" corresponds to a purely elastic first-order analysis. The result of the elastic critical analysis is given by the horizontal line "ML", the ordinate of which corresponds to the elastic critical load factor λ_{cr}. Curve "OJL" corresponds to the second-order elastic analysis; this curve approaches asymptotically the horizontal line "ML" corresponding to the elastic critical analysis result. The first-order rigid-plastic analysis is represented by the curve "OBC"; when the first-order rigid-plastic load factor λ_p is reached (in "B"), the failure develops under constant load ("BC" line). The behaviour got from the second-order rigid-plastic analysis is represented by the "OBD" curve: when the rigid-plastic load factor λ_p is reached (in "B"), its value decreases with an increasing transverse displacement ("BD" curve). The "OFG" curve results from a non-linear analysis; it is likely to reflect the "actual" frame behaviour. The ultimate load factor λ_u corresponds to the peak ordinate of the load-displacement curve (in "F"). If, at λ_u, the failure of the structure is due to the formation of a full plastic mechanism, the "actual" behavioural curve "OFG" obtained through the non-linear analysis and the line "OBD" relative to the second-order rigid-plastic analysis join at point "F", in this particular case, point "F" should correspond to point "K" in *Figure II.8*. If a global frame instability occurs before the development of a plastic mechanism, the "actual" curve remains below the second-order

rigid-plastic one "OBD" and point "F" differs from point "K". This situation is the one illustrated in *Figure II.8*.

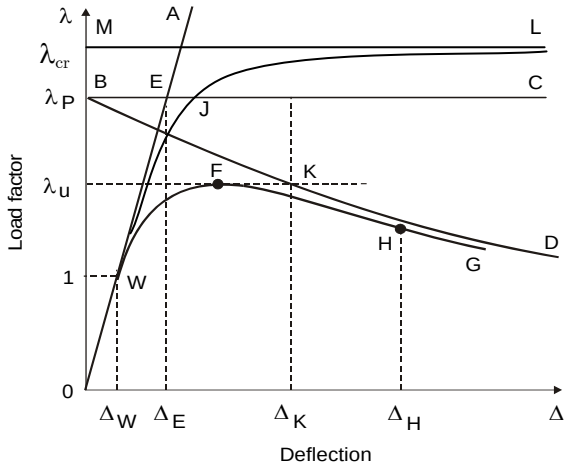

Figure II.8. Graphical representation of the results obtained through the different frame analyses

II.2.2.5. Simplified analytical methods for steel sway frames

A. Introduction

Several simplified analytical methods for frame analysis and design exist and some of them are proposed in Eurocode 3 *[12]*. These methods allow the designer to proceed to structure design without high capacity software which could take account of the sway effects and the non-linearities. Some of them are briefly described in this paragraph.

These methods assume that the materials and the joints have linear or rigid-plastic behaviours and are based on physical and empirical approaches of the problem; the proportion between the two types of approaches depends of the chosen method.

They permit to derive a design load resistance which allows verifying the ULS; nevertheless, the SLS should also be verified for the studied structure. This point will not be recalled in the following paragraphs.

B. Amplified sway moment method

This simplified analytical method is proposed in Eurocode 3 *[12]*. In this method, first-order linear elastic analyses are first carried out; then, the resulting internal forces are amplified by a "sway factor" so as to ascertain for second-order sway effects. Finally, the design load resistance of the frame is derived by computing the load at which a first plastic hinge develops in the frame (→ the elastic load factor λ_e is derived).

The steps to be crossed when applying this elastic design procedure are as follows:

- A first-order elastic analysis is performed on the frame fitted with horizontal supports at the floor levels (*Figure II.9.A*); it results in a distribution of bending moments in the frame and reactions at the horizontal supports.
- Then, a second first-order elastic analysis is conducted on the initial frame subjected to the sole horizontal reactions obtained in the first step (*Figure II.9.B*); the resulting bending moments are the so-called "sway moments".

Approximate values of the "actual" second-order moments result from the summing up of the moments obtained respectively in the two frame analyses, after having amplified the sole sway moments by means of the sway factor:

$$\frac{1}{1 - \frac{V_{Ed}}{V_{cr}}} \tag{2.9}$$

where V_{Ed} is the design vertical applied load and V_{cr} is the lowest elastic critical load associated to a global sway instability.

The maximum elastic resistance of the frame is reached as soon as a first plastic hinge forms in the frame.

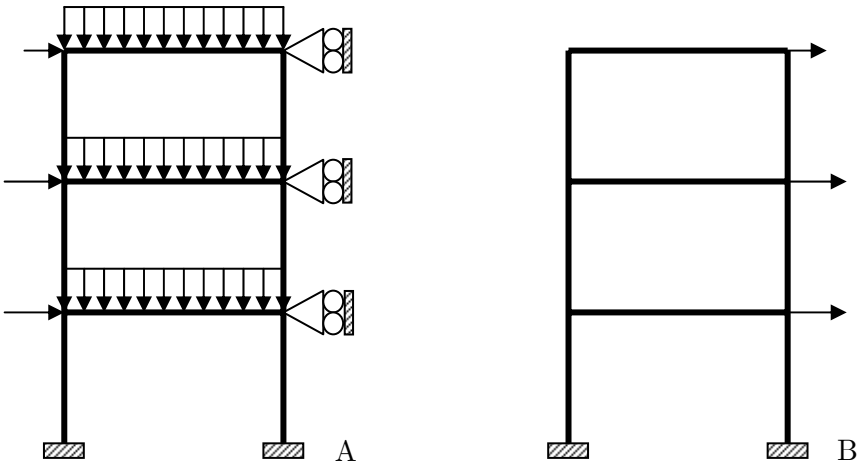

Figure II.9. Static schemes used for the amplified sway moment method

Above design procedure is rather simple, as it only requires first-order elastic analyses. Also the principle of superposition remains applicable, what is especially useful when having to combine several individual loading cases. According to Eurocode 3 *[12]*, the amplified sway moment method is restricted to structures characterized by V_{Ed}/V_{cr} ranging from 0.1 to 0.3.

The global stability check is involved in the method. For the in-plane local buckling check of the members, the buckling length for the non-sway mode is used in conjunction with the amplified moments and forces. Out-of-plane stability has also to be checked.

C. Sway-mode buckling length method

The Sway-mode buckling length method is another indirect method to allow for second-order sway effects when using a first-order elastic analysis and is close to the previous method. It may be adopted for structures for which the sway sensitivity is unknown.

The internal forces (moments, shear and axial forces) are computed on the basis of a first-order analysis. The sway moments in beams and joints are then amplified by a nominal factor of 1,2 and afterwards added to the remainder of the moments (those not due to sway).

The so-obtained amplified forces are used for the design checks of joints and member cross sections and member in-plane and out-of-plane stability. The global stability check is included in the method; when checking in-plane local buckling of the members, the sway mode buckling length must be used for member design, which is a main difference according to the amplified sway moment method. Out-of-plane stability must also be checked. This method often gives too safe results, which explains the fact that this method is rarely used.

D. Merchant-Rankine approach

The origin of this method is described in *[15]*. The Merchant-Rankine method is a second-order elasto-plastic approach, which was developed for bare steel frames; it allows to assess the ultimate load factor through a formula that takes account of interactions between plasticity *(λ_p)* and instability (λ_{cr}) in a simplified and empirical way. A direct comparison with the ultimate load factor λ_u got through a non-linear analysis may be achieved. The Merchant-Rankine basic formula ("MR") writes:

$$\frac{1}{\lambda_u} = \frac{1}{\lambda_{cr}} + \frac{1}{\lambda_p} \tag{2.10}$$

or:

$$\lambda_u = \frac{\lambda_p}{1 + (\lambda_p / \lambda_{cr})} \not> \lambda_p \tag{2.11}$$

Should the frame be very stiff against sway displacements, then λ_{cr} is much larger than λ_p with the result of a low λ_p/λ_{cr} ratio: a minor influence of the geometrical second-order effects is expectable and the ultimate load is therefore close to the first-order rigid-plastic load. In contrast, a flexible sway frame is characterised by a large value of the λ_p/λ_{cr} ratio. It shall collapse according to a nearly elastic buckling mode at a loading magnitude, which approaches the elastic bifurcation load.

Strain hardening tends to raise plastic hinge moment resistances above the values calculated from the yield strength. Therefore most practical frames with only a few storeys

in height attain a failure load at least equal to the theoretical rigid-plastic resistance. When the ratio λ_{cr}/λ_p is commonly greater than 10, the effects of material strain hardening more than compensate those of changes in geometry. Sometimes, additional stiffness due to cladding is sufficient to compensate such changes. To allow, in a general treatment for the minimum beneficial effects to be expected from both strain hardening and cladding, Wood suggested a slightly modified Merchant-Rankine formula ("MMR"):

$$\lambda_u = \frac{\lambda_p}{0.9 + (\lambda_p / \lambda_{cr})} \not> \lambda_p \tag{2.12}$$

in the range $\lambda_{cr}/\lambda_p \geq 4$. He recommended not to use it in practice when $\lambda_{cr}/\lambda_p < 4$ but to carry a non-linear analysis in this range.

When $\lambda_p/\lambda_{cr} \leq 0.1$, λ_u is limited to λ_p, what means that the frame can be designed according to the simple first-order rigid-plastic theory. A clear and direct relationship may be established between this criterion and the one, which enables, according to Eurocode 3 *[12]*, to classify steel frames as sway ($V_{Ed}/V_{cr} > 0{,}1$) or non-sway ($V_{Ed}/V_{cr} \leq 0{,}1$).

The use of *Formula (2.12)* is commonly restricted to frames in buildings, in which:

1. the frame is braced perpendicular to its own plane;
2. the average bay width in the plane of the frame is not less than the greatest storey height;
3. the frame does not exceed 10 storeys in height;
4. the sway at each storey, due to non-factored wind loading, does not exceed 1/300 of the storey height;
5. $\lambda_{cr}/\lambda_p \geq 4$.

From complementary studies carried out at Liège University *[15]*, the "MMR" approach is seen to exhibit a different degree of accuracy according to the type of first-order rigid-plastic failure mode which characterises the frame under consideration:

- safe for beam plastic mechanisms;
- adequate for combined plastic mechanisms;
- unsafe for panel plastic mechanisms.

As a result, the application of the "MMR" approach to structures exhibiting a first-order panel plastic mechanism should therefore be prohibited.

Also, in *[15]*, the scope of the "MMR" formula is extended to structures with semi-rigid and/or partial-strength joints.

The global stability check is involved in the "MR" and "MMR" methods but the local stability of the members must be checked.

E. Simplified second-order plastic analysis

As an alternative to a second-order elastic-plastic analysis, Eurocode *[12]* allows the use of rigid-plastic first-order analysis for particular types of sway frames. As for the indirect methods with first-order elastic analysis, the second-order sway effects are accounted for indirectly by multiplying moments (and associated forces) by a similar magnification factor. However in this case, all of the internal moments (and associated forces) are magnified (and not just those due to sway alone as it is done in the elastic analysis case). The limitation imposed on its use excludes the use of slender members for which member imperfections would have to be accounted for. The magnification factor is the same as for the first-order elastic analysis (*Formula (2.9)*).

In a diploma work *[16]*, it was demonstrated that this method is equivalent to the Merchant-Rankine approach if this method is used so as to predict the ultimate load factor λ_u; so, this method will not be presented with more details.

F. Wind moment method

The wind moment method is a British one (mainly used in North America and UK) which is fully empirical. It is closer to a pre-design method than an analytical one. It permits the pre-design of sway structures with semi-rigid joints.

The distinguishing factors of this method, that set it apart from other methods, are the assumptions that are used during the design stage *[17]*:

- under gravity loads, the connections are assumed to act as pins (*Figure II.10.a*);
- under wind loads the connections are assumed to behave as rigid joints, with points of contraflexure occurring at mid-height of the columns and at mid-span of the beams (*Figure II.10.b*).

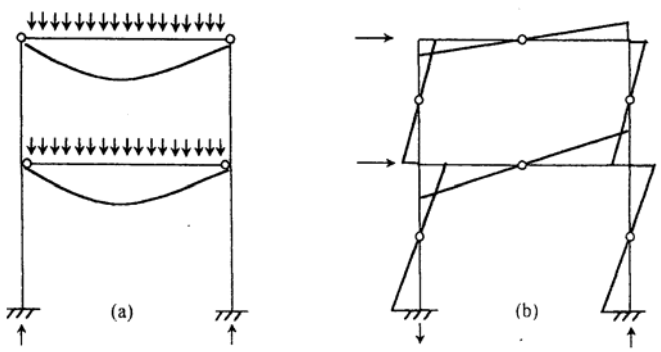

Figure II.10. Double-sided moments and forces according to the wind-moment method [17]

The first step in the design sequence is to design the beams under gravity loads. Then, the frame is analysed under horizontal wind loads, with the assumption that the beam-to-column connections behave in a rigid manner. The so-obtained internal forces and moments are combined using the principle of superposition. The design for ULS is finally completed by amending the initial section sizes and connection details, to withstand the combined effects.

P-Δ effects are accounted for by designing the columns using effective lengths that are greater than the true column lengths. The sway displacements are computed assuming the beam-to-column joints are rigid; a sway factor is used to account for their true behaviour.

The advantage of this method is its simplicity, as the frame is rendered statically determinate. Nevertheless, the horizontal beams tend to be overdesigned (as the joints at their extremities are assumed to be hinges) when vertical columns tend to be underdesigned (as the bending moments coming from the beams are neglected). The joints are also underdesigned as hogging moments coming from the vertical loads are neglected.

II.2.2.6. Conclusions

In *§ II.2.2*, the different steps to be crossed for the selection of a global structural analysis according to Eurocode 3 and the structural analyses available for the determination of the internal forces of a frame have been described in details; the different verifications to perform which are associated to the chosen analysis have also been detailed. In addition, simplified analytical methods available for steel sway frames have been introduced in *§ II.2.2.5*.

Some of the global structural analyses presented in this section will be applied to sway steel and composite frames through the investigations presented in *§ II.5* and *§ II.6*. The applicability of some simplified analytical methods developed for steel sway frames to composite ones will also be investigated in *§ II.5*.

II.2.3. Sway effects in composite building frames

As already mentioned, few information is available concerning this type of structures. Eurocode 4 *[6]* permits the erection of sway composite frames (i.e. frames with a elastic critical load factor smaller than 10 (rule (3) of *§ 5.2.1* of Eurocode 4 *[6]*)) but "*second-order effects may be included indirectly by using a first-order analysis with appropriate amplification*" (rule (2) of § 5.2.2 of Eurocode 4); however, no information is given on how to amplify the obtained results through the first-order analysis.

First investigations in this field have been carried out in the last years. As already mentioned, two European projects on this topic were initiated in 2000 (see *§ II.1.1*). Also,

the applicability of the wind-moment method (see *§ II.2.2.5.F*) to unbraced composite frames was first examined in a PhD thesis (*[17]* and *[18]*) submitted by J.S. Hensman at Nottingham University.

In the latter, it was demonstrated that the remarks concerning the application of this method to steel sway frames presented in *§ II.2.2.5.F* are still valid for composite ones. However, this method is closer to a pre-design method than to an analytical one and it is difficult to use it so as to predict a failure load factor.

II.2.4. Conclusions

Until now, the knowledge about the behaviour of sway composite frames is weak; few investigations in this field have been performed.

In this chapter, different concepts available in Eurocode 3 for the analysis of steel sway frames have been introduced, focusing on the member cross section and frame classification (and its influence on the choice of the structural analysis), the possible structural analyses and the available simplified analytical methods for the design of steel sway frames.

The applicability of these concepts to composite sway building frames will be investigated later on in *§ II.5* but, before that, the behaviour of the composite joints subjected to bending moments is investigated in the next paragraph (see strategy defined in *Figure II.1*).

II.3. Behaviour of beam-to-column composite joints subjected to bending moments

II.3.1. Introduction

As already mentioned, the beam-to-column joint behaviour is a key parameter regarding the response of sway frames; accordingly, a particular attention is paid to this topic within the thesis.

Looking the moment-rotation curve of joints, different properties can be identified (see *Figure II.11*):

- the initial stiffness $S_{j,ini}$;
- the post-limit stiffness $S_{j,post\text{-}limit}$;
- the resistance design moment M_{Rd};

- the ultimate moment M_u;
- the shear design resistance V_{Rd};
- the rotation ϕ_u associated to M_u.

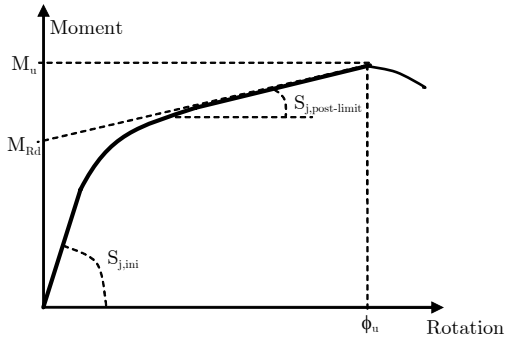

Figure II.11. M-ϕ behaviour curve of a joint

These properties can be determined through three main approaches: experimental, numerical and analytical. Within the thesis, experimental and analytical studies are conducted on composite joints; the present paragraph is organised as follows:

- First, experimental tests performed on composite joints in isolation within the previously mentioned European projects (see *§ I.1*) are detailed in *§ II.3.2*. In particular, the experimental tests performed at Liège University on single-sided composite joints are presented.
- Then, the validity of the analytical method proposed in the Eurocodes for the joint design is investigated in *§ II.3.3* through comparisons with the experimental results. In particular, a new formula is developed to take into account of a new collapse mode identified through the experimental tests performed at Liège University. Also, in sway frames, sagging moments can occur at the joint level; however, no analytical procedure to predict the response of composite joints under such loading is proposed in the codes. So, a design method is proposed and validated in order to analytically predict the composite joint response under sagging bending moment.
- Finally, conclusions are drawn for this paragraph in *§ II.3.4*.

II.3.2. Available experimental data for composite beam-to-column joints

II.3.2.1. Introduction

In the present section, the experimental tests performed on composite joints in isolation within three European projects in which Liège University was involved are presented. In

particular, the main properties requested later on for the validation of the analytical methods such as the geometrical dimensions or the material mechanical properties are detailed.

II.3.2.2. "Sway frames" project

A. Description of the tested joint configuration

As said in *§ II.1.1*, cyclic and static tests on isolated joints were performed in different European laboratories so as to get the actual behaviour of the constitutive joints of the two structures tested within the European project "Applicability of composite structures to sway frames": the "Ispra" and the "Bochum" structures.

As part of this project, Liège University performed four tests on isolated single-sided joints belonging to these two structures *[10]*:

- TEST 1 - static test on the single-sided composite joint configuration at the first storey of the "Ispra" structure (hogging moment);
- TEST 2 - cyclic test on the single-sided composite joint configuration at the first storey of the "Ispra" structure;
- TEST 3 - static test on the single-sided steel joint configuration at the first storey of the "Bochum" structure (hogging moment);
- TEST 4 - static test on the single-sided steel joint configuration at the top of the "Bochum" structure (hogging moment).

As the scope of this part is to investigate the behaviour of sway composite frames under static loading, the investigations presented herein only focus on TEST 1, i.e. on the static test on the single-sided composite joint.

In the "Ispra" structure (*[1]* and *[2]*), semi-rigid and partial-strength composite joints with sufficient rotational capacity (minimum 0,035 rad) have been selected so as to enable the development of plastic hinges and the dissipation of energy in the joints under seismic loading. To achieve this goal, as many ductile components as possible are activated in the joint at plastic failure (i.e. web panel in shear, reinforcement in tension and end-plate in bending). *Figure II.12* presents the so-obtained configuration of the single-sided composite joint tested at Liège University (TEST 1). The beam is an IPE300 one, and the column a HEB260 one (partially encased). The slab is 150 mm thick and the hollow rib is an EGB 210 one from BROLLO (Italy), with ribs perpendicular to the beam axis. The composite slab is connected to the upper beam flange by means of shear studs. The layout of the rebars in the slab is given in *Figure II.13*. The mesh is made of rebars with a diameter of

6 mm and a spacing of 150 mm. The column is surrounded by two 12 mm rebars. Additional transversal rebars of 12 mm of diameter are placed close to the column. More details about these specimens are given in *[10]*.

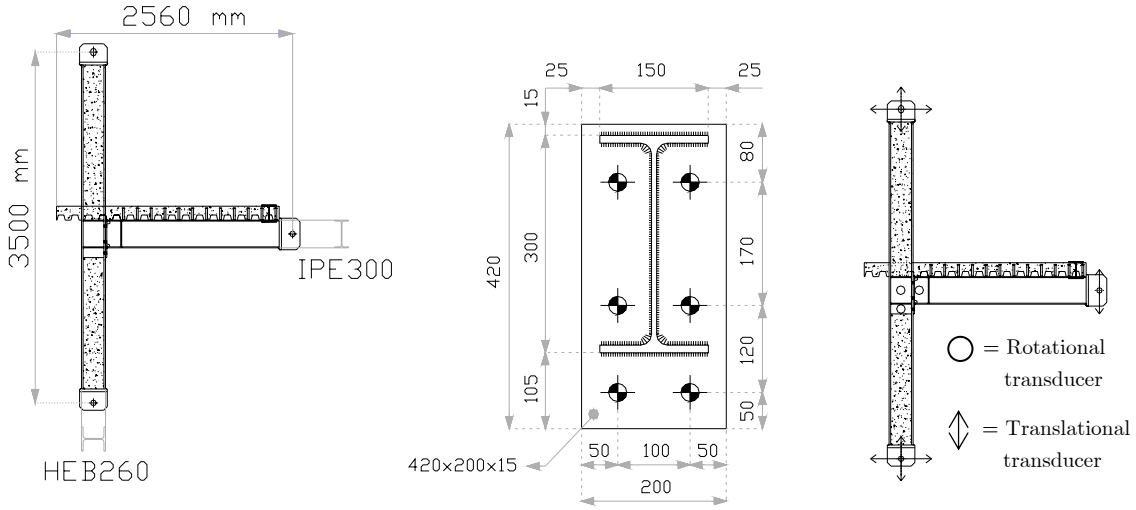

Figure II.12. Properties (in mm) and instrumentation of the single-sided composite joint specimen

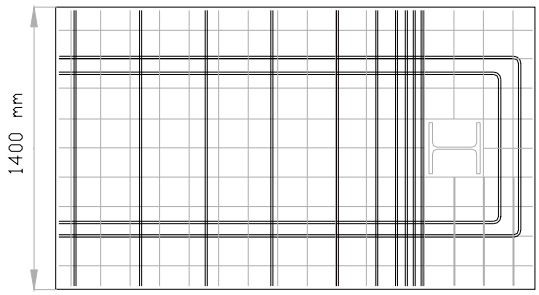

Figure II.13. Distribution of the rebars in the slab

S235 steel grades were ordered for the beams, the columns and the beam end-plates; rebars are made of S500C steel. C25/30 concrete is used for the slabs and the composite columns. The bolts are M24 10.9 ones; they are preloaded at 75% with an additional rotation of 60°.

Remark: All the steel elements used to test the Ispra structure and the corresponding isolated joints in Liège come from the same producer and from the same production so as to reach a full adequacy between the experimental results.

B. Experimental results

Compression tests on concrete cubes have been performed on the same day as the experimentation on the joint specimens. Coupons have also been extracted from the different steel elements. All the so-measured mechanical properties for steel and concrete are reported in *Appendix VI.1.1.*

Two independent measurement systems have been used to derive the moment-rotation curve of the joints: rotational and translational transducers, as shown in *Figure II.12* (respectively circles and arrows). The way on how moment-rotation curves are obtained in both cases is explained in *Appendix VI.2*. The objective of this rather complex instrumentation is to draw two independently measured joint moment-rotation curves, to compare them and, in the case of good agreement, to ensure the accuracy of the reported experimental results.

Figure II.14 presents the *M-ϕ* behavioural curves obtained for joint "TEST 1" by means of the translational and rotational transducers measurements. In agreement with the Eurocodes, the moment is evaluated at the connection level. Main joint properties are listed in *Table II.4*; the initial stiffness is estimated at the "unloading-reloading" part of the graph (see *Figure II.14*). During the test, first cracks in the concrete slab appeared i) transversally, close to connection and ii) longitudinally, just behind the column, as shown in *Figure II.14*. The transversal cracks result from the tension forces in the longitudinal rebars while the longitudinal ones are due to shear forces. Then, at a higher loading step, new cracks developed until a shear failure occurred behind the column (hatched part in *Figure II.14*) for a bending moment of 201,6 kNm and a rotation of 31 mrad (less than the requested one, i.e. 35 mrad). In addition to these cracks, significant yielding developed in the steel joint components: column web panel in shear and end-plate in bending first, beam flange in compression and beam web in tension later on. Photographs of this test are given in *Figure II.15*; others are available in *[10]*. The test was stopped with the appearance of a crack in the beam web in the vicinity of the connection as shown in *Figure II.15*.

The shear failure of the concrete slab behind the column was not expected and had therefore not been considered in the design phase; the same collapse mode was observed during TEST 2 performed on the same joint configuration but under cyclic loading. This aspect will be further investigated in *§ II.3.3.2.*

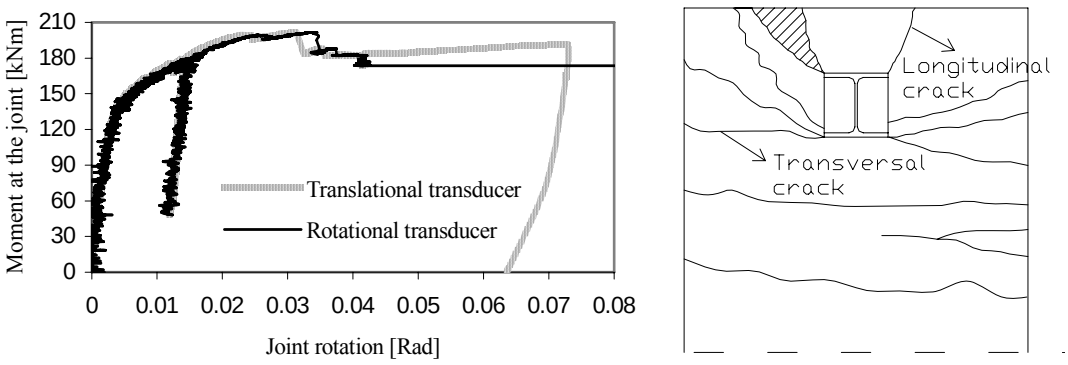

Figure II.14. Moment-rotation curves for the tested single-sided composite joint with the distribution of the cracks at the end of the test

Figure II.15. Photos of the joint at the end of the test

Table II.4. Main mechanical properties of the "TEST 1" joint

	Test results
$S_{j,ini}$ [kNm/rad]	± 65000
M_u [kNm]	201,58
ϕ_u [rad]	0,031

II.3.2.3. "Robustness" project

A. Description of the tested joint configuration

The joint experimental tests presented herein are part of the European project titled "Robust structures by joint ductility" (see *§ I.1*) involving five partners (including Liège University). Within the present paragraph, only the joint tests performed at Stuttgart University are considered *[19]*.

The performed tests can be subdivided into two main series: one series on composite double-sided joints and a second series on pure steel double-sided joints; all the joints were symmetrically loaded during the tests. Only the first series will be considered. These tests have been performed so as to derive the behaviour of composite joints under bending moment and normal force combined actions. In order to achieve this goal, five experimental tests have been conducted on the same joint configuration:

- Three tests under hogging moments:
    - one test with the joint first loaded under hogging bending moments until reaching the ultimate resistance in bending and secondly, after having slightly reduced the applied bending moment, loaded under tension loads until the collapse of the joint (TEST 1) and;

- two tests with the joint, first, loaded under hogging bending moments with the loading stopped just before reaching the ultimate resistance to bending and, secondly, loaded under tension loads until the collapse of the joint (TEST 2 & TEST 3).

- Two tests under sagging moments:

  - one test with the joint first loaded under sagging bending moments until reaching the ultimate resistance in bending and secondly, after having slightly reduced the applied bending moment, loaded under tension loads until the collapse of the joint (TEST 4) and;

  - one test with the joint, first, loaded under sagging bending moments with the loading stopped just before reaching the ultimate resistance to bending and, secondly, loaded under tension loads until the collapse of the joint (TEST 5).

This paragraph will only focus on TEST 1 and TEST 4 as the ultimate resistances to bending moments were reached only with these tests; the other tests will be presented and analysed later on in *§ III.5.2* investigating the behaviour of composite joints subjected to combined bending moments and axial loads.

The dimensions as well as the used profiles for the joint configuration are given in *Figure II.16*. The tested joint configuration was designed so as to exhibit a ductile behaviour at collapse and with account of the *M-N* combined loading *[20]*.

The materials were ordered as follows: S355 steel for the profiles and the end-plates, ductile S450C steel for the rebars and C25/30 for the concrete. As for the "sway frames" project, all the profiles used for the different tests came from the same production so as to be able to make comparisons between the obtained results. The actual properties of the materials are given in *Appendix VI.1.2*.

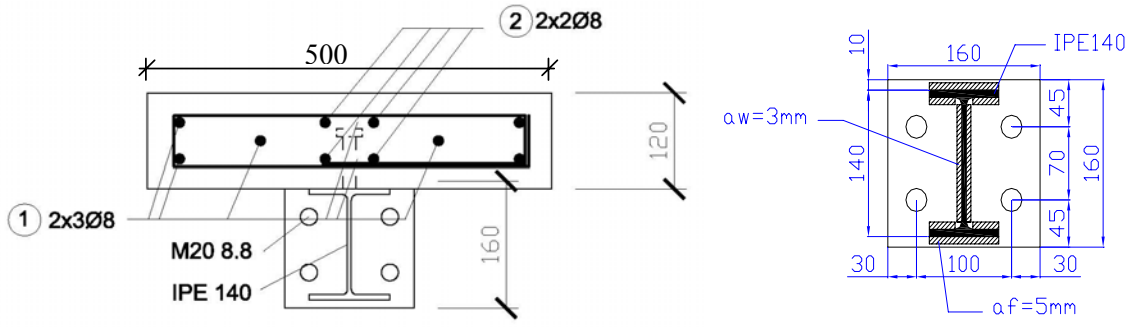

Figure II.16. Tested double-sided composite joint configuration

The arrangement of the transducers at the composite joints was chosen in order to characterise the response of the joint components which contribute to the rotation capacity of the joint and to derive the moment-rotation curves of the tested joints.

B. Experimental results – TEST 1 (hogging moment)

By increasing the bending moment, the cracks in the concrete slab developed at the column section. Close to the ultimate moment M_u, the slab at the column section was cracked over the total height. During the test, plasticity developed in some steel components: the column flange in bending first, followed by the column web and the beam flange in compression and the end-plate in bending. The collapse mode of the joint under bending moment was associated to the buckling of the beam flange in compression. Some photographs of the joint when the ultimate bending resistance is reached are given in *Figure II.17*; the moment-rotation curve of the joint is given in *Figure II.18*. The main mechanical properties of the joint are listed in *Table II.5*. More details about the test are given in *[19]*.

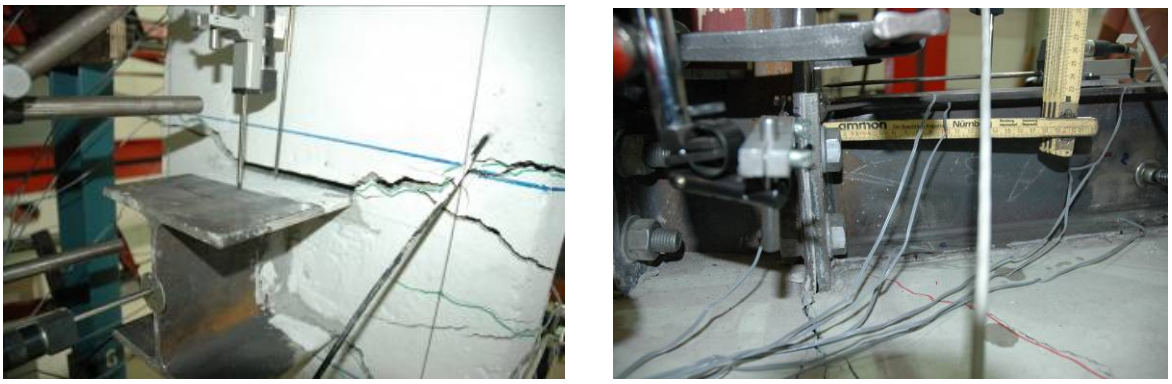

Figure II.17. Photos of the joint at the end of TEST 1 [19]

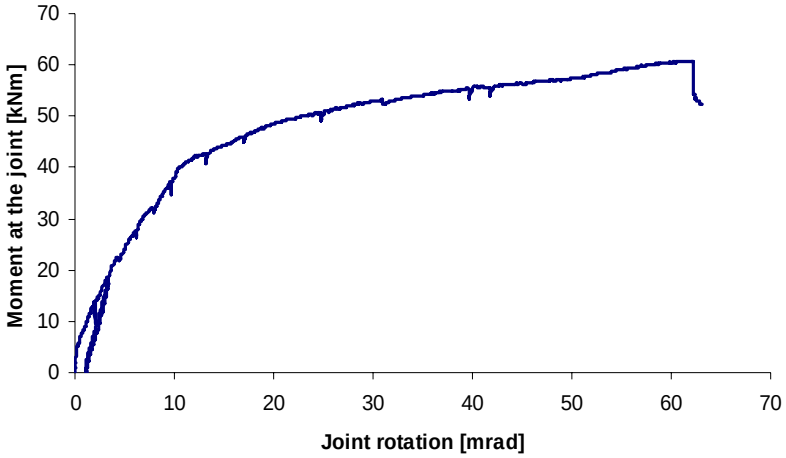

Figure II.18. Moment-rotation curve of the joint obtained through TEST 1 [19]

Table II.5. Main mechanical properties of the "TEST 1" joint

	Test results
$S_{j,ini}$ [kNm/rad]	± 9530
M_u [kNm]	60,6
ϕ_u [rad]	0,062

C. Experimental results – TEST 4 (sagging moment)

For the test under sagging moment, the crushing of concrete slab in compression against the column was observed at the end of the test. As for TEST 1, plasticity also developed in some steel components: the column flange and the end-plate in bending and the column web in tension. The collapse mode associated to the ultimate bending resistance was associated to the concrete crushing with the yielding of the column flange in bending. Some photographs of the joint when the ultimate resistance is reached are given in *Figure II.19*; the moment-rotation curve of the joint is given in *Figure II.20*. The main mechanical properties of the joint are listed in *Table II.6*. More details about this test can be found in *[19]*.

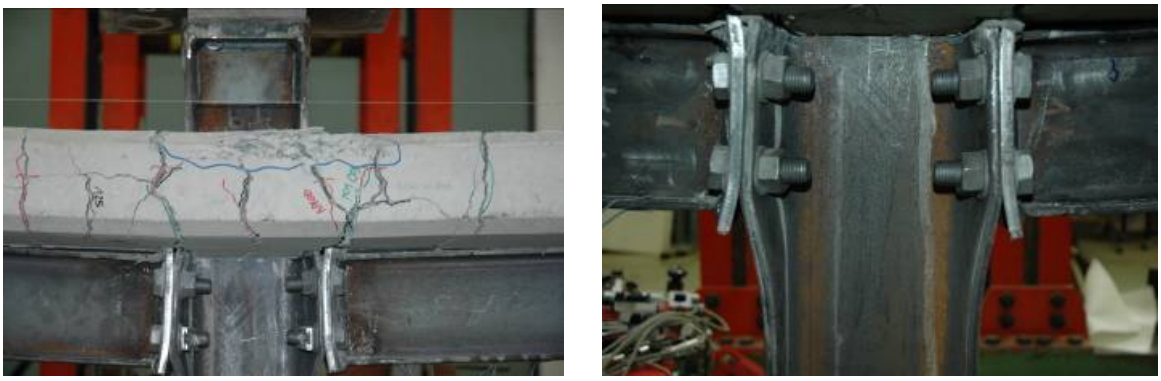

Figure II.19. Photos of the joint at the end of TEST 4 [19]

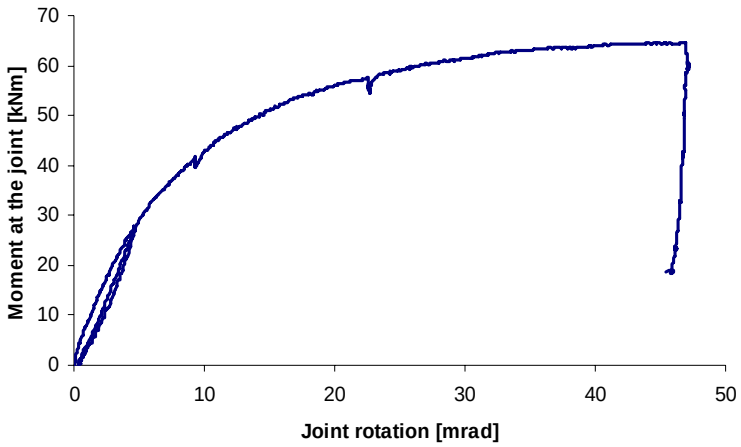

Figure II.20. Moment-rotation curve of the joint obtained through TEST 4 [19]

Table II.6. Main mechanical properties of the "TEST 4" joint

	Test results
$S_{j,ini}$ [kNm/rad]	$\pm$ 6400
M_u [kNm]	64,5
ϕ_u [rad]	0,047

II.3.2.4. "Precious" project

A. Description of the tested joint configuration

The present paragraph described experimental tests which have been performed within the European project "Precious"; the latter is briefly described in *§ I.1.* Within this project, four joint configurations were tested:

- beam-to-column composite joints with partially encased composite columns and steel sheeting composite slabs;
- beam-to-column composite joints with partially encased composite columns and prefabricated concrete slabs;
- beam-to-column composite joints with concrete filled tubular columns and steel sheeting composite slabs;
- beam-to-column composite joints with concrete filled tubular columns and prefabricated concrete slabs.

Only the two first configurations are investigated within the thesis; indeed, the behaviour of structures composed of composite tubular columns is not considered herein.

The double-sided and single-sided joint configurations were tested under monotonic and cyclic loadings at room and elevated temperatures. Within the thesis, only the joint tests conducted at room temperature under monotonic loading are considered. Also, as the test results for the double-sided joint configurations are not yet available, only the behaviour of the single-sided composite joints will be investigated in the present section.

These joints have been tested at Trento University, as part of the above-mentioned project. In total, three tests have been realised:

- TEST 1 – one monotonic test under hogging moment with a steel sheeting composite slab (configuration A in *Figure II.21*);
- TEST 2 – one monotonic test under sagging moment with a steel sheeting composite slab (configuration A in *Figure II.21*);

- TEST 3 – one monotonic test under sagging moment with a prefabricated concrete slab (configuration B in *Figure II.21*).

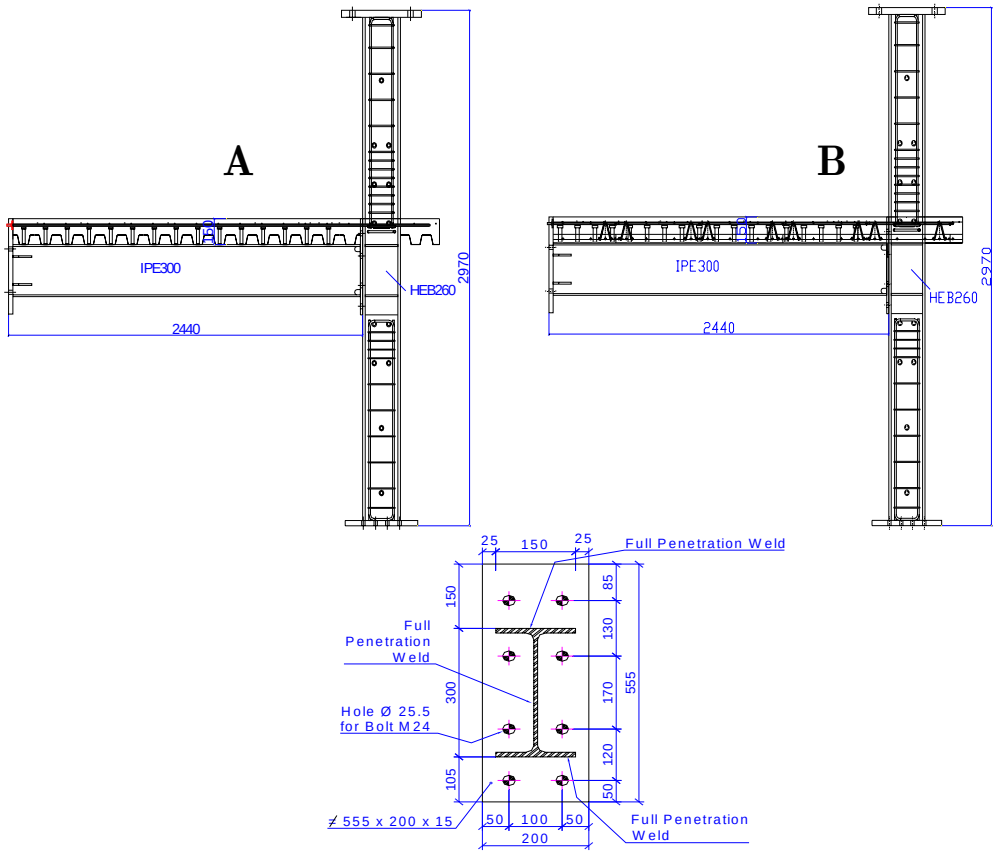

Figure II.21. Precious project - tested joint configurations at Trento University [21]

The beams are made of IPE300 profiles with the upper flange connected to the composite or concrete slab (full connection); the columns are partially encased HEB260 profiles. The materials were ordered as follows: S355 steel for the profiles and the end-plates, ductile S450C steel for the rebars and C25/30 for the concrete. The bolts are M24 10.9 ones. As for the other projects, all the profiles used for the different tests came from the same production so as to be able to make comparisons between the obtained results. The actual properties of the materials are given in *Appendix VI.1.3*. More details are available in *[21]*.

B. Experimental results – TEST 1 (hogging moment)

The moment-rotation curve for TEST 1 is given in *Figure II.22*. During the test, the development of cracks was observed in the concrete slab in the vicinity of the column; in particular, cracks with an inclination of 45° were observed behind the column (see *Figure II.23*) which is a clear indication of the "strut-and-tie" behaviour described later on in *§ II.3.3.3.A*. In parallel, yielding developed in some steel components (mainly column web in shear and beam flange in compression) with non-negligible deformations of the latter (see *Figure II.24*). In *Figure II.22*, a loss of resistance is observed for a rotation of more or less

50 mrad in the moment-rotation curve; the latter is associated to the concrete slab crushing in the vicinity of the column induced by the development of the "strut-and-tie" behaviour.

The main properties of the tested joint are summarised in *Table II.7*.

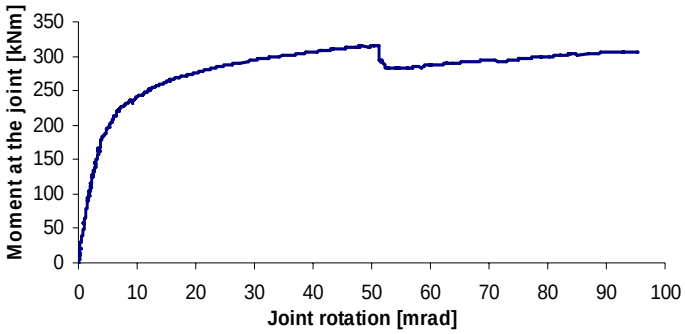

Figure II.22. Moment-rotation curve of the joint obtained through TEST 1

Left side Right side

Figure II.23. Test 1 – Development of cracks in the composite slabs (at the end of the test)

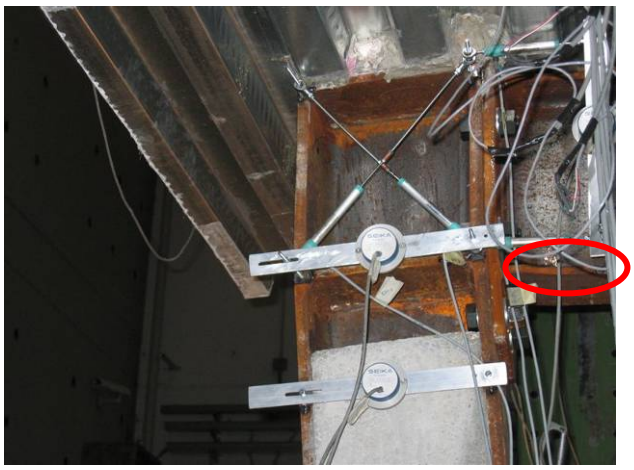

Figure II.24. Test 1 – Deformation of the steel components at the end of the test

Table II.7. Main mechanical properties of the "TEST 1" joint

	Test results
$S_{j,ini}$ [kNm/rad]	$\pm$ 57450
M_u [kNm]	316
ϕ_u [rad]	0,051

Remark: the bending moment which are reported here for the experimental results are not the same than the ones presented in *[21]*. Indeed, a different assumption concerning the lever arm to be used for the computation of the bending moment than the one presented in *Appendix VI.6* have been used for the moments reported in *[21]*. Indeed, in *[21]*, the lever arm is taken as equal to the distance between the load application point and the middle of the column web while in *Appendix VI.6*, the lever arm is equal to the distance between the load application point and the middle of the column flange on the connection side. So, the moments reported in *[21]* have been modified so as to respect the assumption presented in *Appendix VI.6* and to be coherent within the thesis. This remark is also valid for the results reported in the next section.

C. Experimental results – TEST 2 & 3 (sagging moment)

The moment-rotation curves obtained through TEST 2 & 3 are given in *Figure II.25*. In the latter, it can be observed that the curves are similar until a joint rotation of more or less 29 mrad. At this rotation, a loss of resistance appeared for TEST 2 joint while the latter was not observed for TEST 3 joint. This loss of resistance is linked to the crushing of the concrete against the column flange which is more accentuated for TEST 2 than for TEST 3, as shown in *Figure II.26*. This can be justified by the different slab configurations which are used within the two tests. Indeed, the TEST 2 slab is a composite one with a steel sheeting which means that only the concrete above the steel sheeting ribs contributes to the resistance, i.e. 95 mm, while the TEST 3 slab is a prefabricated one which means that the full height of the concrete can contribute to the joint resistance, i.e. 150 mm.

During these tests, the yielding of steel components was also observed, in particular the column web panel in shear and the end-plate in bending, as illustrated in *Figure II.27*.

The main properties of the tested joints are summarised in *Table II.8*.

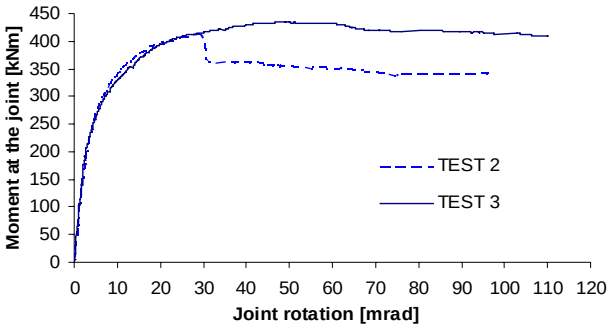

Figure II.25. Moment-rotation curves of the joint obtained through TEST 2 & 3

TEST 2 TEST 3

Figure II.26. Crushing of the concrete in front of the column at the end of TEST 2 & 3

TEST 2 TEST 3

Figure II.27. Yielding of steel components at the end of TEST 2 & 3

Table II.8. Main mechanical properties of the "TEST 2" and "TEST 3" joints

	Test 2 results	**Test 3 results**
$S_{j,ini}$ [kNm/rad]	$\pm$ 64900	$\pm$ 64900
M_u [kNm]	411	435
ϕ_u [rad]	0,029	0,110

II.3.3. Analytical prediction of the composite beam-to-column joint response

II.3.3.1. Introduction

In the previous section, the behaviour of joints has been determined through the experimental approach. However, the only practical option for the designer is the analytical one. Within the present section, the accuracy of an analytical method proposed in the Eurocodes (*[6]*, *[12]* and *[22]*) called "the component method" is investigated through comparisons of the analytical predictions obtained with this method to the experimental results presented in the previous section.

In *§ II.3.3.2*, the component method is first briefly described. Then, *§ II.3.3.3* presents the studies performed to investigate the accuracy of the presented method to predict the behaviour of composite beam-to-column joints under hogging bending moments while *§ II.3.3.4* investigates the accuracy of this method to predict the behaviour of these joints under sagging bending moments. In particular, new methods are developed in order to improve the component method and to complete it with a new component allowing computing composite joints under sagging bending moments.

II.3.3.2. Brief description of the component method

A. General principles

Nowadays, the component method is a widely recognised procedure for the evaluation of the design properties of structural joints. As previously mentioned, this method is the one recommended in the Eurocodes and applies to any type of steel or composite joints, whatever the geometrical configuration, the type of loading (axial force and/or bending moment, ...) and the type of member sections. This method considers any joint as a set of individual basic components. For the particular joint shown in *Figure II.28* (composite joint configuration with a flush end-plate connection subjected to hogging bending moments), the relevant components are given in *Table II.9*.

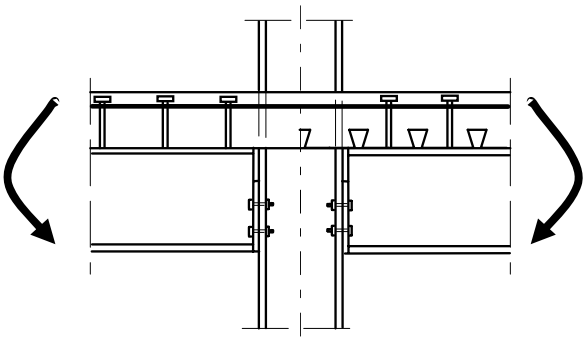

Figure II.28. Composite joint with a flush end-plate connection subjected to hogging moments

Table II.9. Components to be considered for a flush end-plate connection subjected to hogging moments

Zones	**Components**
Compression zone	column web in compression
	beam flange and web in compression
Tension zone	column web in tension
	column flange in bending
	bolts in tension
	end-plate in bending
	beam web in tension
	slab rebars in tension
Shear zone	column web panel in shear

Each of these basic components possesses its own strength and stiffness either in tension or in compression or in shear (spring model – see *Figure II.29*). The column web is subject to coincident compression, tension and shear. This coexistence of several components within the same joint element can obviously lead to stress interactions that are likely to decrease the resistance of the individual basic components; the latter is taken into account within the method.

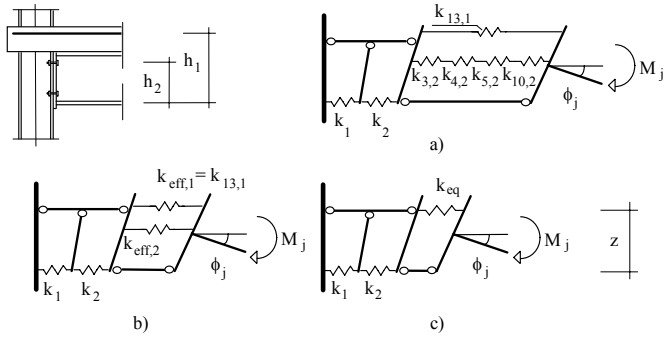

Figure II.29. Example of a spring model for a composite flush end-plate connection [23]

The application of the component method requires the following steps:

- identification of the active components in the joint being considered;
- evaluation of the stiffness and/or resistance characteristics for each individual basic component (specific characteristics - initial stiffness, design resistance, ... - or the whole deformability curve);

- assembly of all the constituent components and evaluation of the stiffness and/or resistance characteristics of the whole joint (specific characteristics - initial stiffness, design resistance, ... - or the whole deformability curve).

The assembly procedure consists in deriving the mechanical properties of the whole joint from those of all the individual constituent components. This requires a preliminary distribution of the forces acting on the joint into internal forces acting on the components in a way that satisfies equilibrium. In Eurocode 3 and 4 (*[12]* and *[6]*), the analytical assembly procedures are described for the evaluation of the initial stiffness $S_{j,ini}$ and the design moment resistance M_{Rd} of steel and composite joints.

Table II.10. Components covered by Eurocode 3 and Eurocode 4

N°	**Components**
1	Column web panel in shear
2	Column web in compression
3	Beam flange and web in compression
4	Column flange in bending
5	Column web in tension
6	End-plate in bending
7	Beam web in tension
8	Flange cleat in bending
9	Bolts in tension
10	Bolts in shear
11	Bolts in bearing (on beam flange, column flange, end-plate or cleat)
12	Plate in tension or compression
13	Reinforcement in tension
14	Contact plate in compression

The application of the component method requires a sufficient knowledge of the behaviour of the basic components. Those covered by Eurocode 3 for steel joints are listed in *Table II.10* (components 1 to 12); those covered by Eurocode 4 for composite joints are the same than for steel joints with two additional components *[23]* also presented in *Table II.10* (components 13 and 14). The combination of these components allows to cover a wide range of joint configurations.

B. Joint classification

The joints can be classified according to three different criteria: their stiffness, their resistance and their ductility. The classification of the joint depends of the stiffness and resistance properties of the closest beam cross section (I_b and $M_{pl,Rd}$ respectively).

The classification criterion according to the stiffness properties for sway frames is the following (E = young modulus of the beam material and L = span of the beam):

- if $S_{j,ini} > 25\dfrac{EI_b}{L}$, the joint is classified as rigid → there is no relative rotations between the connected members;
- if $S_{j,ini} < 0.5\dfrac{EI_b}{L}$, the joint is classified as nominally pinned → a free rotation is assumed at the joint level;
- in all the other cases, the joint is classified as semi-rigid.

The classification criterion according to the resistance properties is the following:

- if $M_{Rd} \geq M_{pl,Rd}$, i.e. the joint resistance is higher than the beam one, the joint is classified as full strength;
- if $M_{Rd} < 0.25M_{pl,Rd}$, it is assumed that the joint transmits no moments and the latter is classified as nominally pinned;
- in all the other cases, the joint is classified as partial strength.

The classification according to the ductility of the joint is associated to the rotation capacity of the joint which depends of its collapse mode. If the collapse mode is associated to the yielding of component 1, 4, 6, 8 or 13 (see *Table II.10*), the joint can be classified as ductile; if it is not the case, it is assumed that the joint is not a ductile one. Also, when plastic hinges form at the joint level in a structure, the realisation of a plastic analysis is only possible if the joints are ductile ones.

C. Joint modelling and idealisation

For the joint modelling, Eurocode 3 *[12]* and Eurocode 4 *[6]* propose a simple solution resulting from the "concentration" of the joint behaviour in a rotational spring placed at the intersection between the beam and column axes. This solution for the joint modelling is used in the different numerical investigations performed in the following sections.

Depending on the software available for frame analysis, either the full non-linear shape of the joint characteristics or multi-linear simplifications can be assigned to the rotational

springs (*Figure II.30*). Further simplifications may also result from the nature of the method used for global analysis:

- if an elastic analysis is performed (see *§ II.2.2.4.B*, *§ II.2.2.4.C* and *§ II.2.2.4.D*), only the joint stiffness is important as the structural members and joints are assumed to be indefinitely elastic;

- if a rigid-plastic analysis is performed (see *§ II.2.2.4.E* and *§ II.2.2.4.F*), only the joint resistance to bending moments is important as the joints are assumed to be rigid until their yielding;

- if a full non-linear analysis is performed (see *§ II.2.2.4.G*), both the stiffness and the resistance properties are important and must be involved in the analysis.

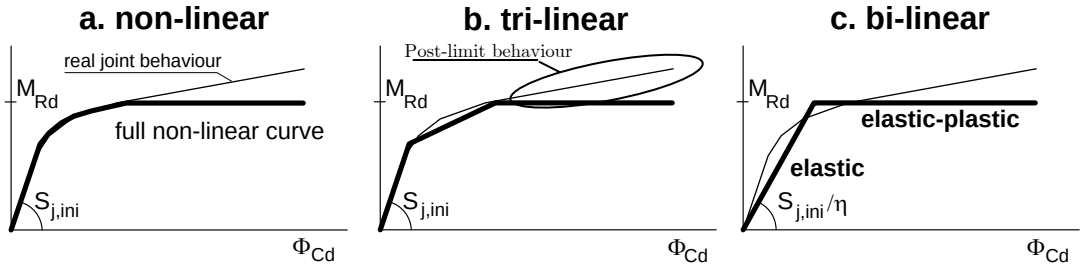

Figure II.30. Possibilities for curve idealisation to simulate the behaviour of a joint

The simplest approximation is to represent the joint characteristic by a bi-linear curve (*Figure II.30.c*). The joint stiffness is constant for all values of bending moment smaller than the design moment resistance. An appropriate stiffness can be calculated by dividing the initial stiffness $S_{j,ini}$ by a modification factor, denoted η. This depends on the type of steelwork connection and on the joint configuration. For example, η is equal to 2,0 for a beam-to-column joint with a flush end-plate and 1,5 for a joint with a contact plate. For an indefinitely elastic analysis, the following assumptions are proposed in Eurocode 3 and 4:

- if $M_{Ed} \leq \frac{2}{3} M_{Rd}$, the joint stiffness is assumed to be equal to $S_{j,ini}$;

- otherwise, the joint stiffness is assumed to be equal to $S_{j,ini}/\eta$.

In the following sections comparing the analytical predictions to the experimental results, the full non-linear curve idealisation (*Figure II.30.a*) will be used: the curve is first linear until the elastic resistance to bending moments M_e (= 2/3 M_{Rd}) and then non-linear until the resistance bending moment M_{Rd}. The formula to be used for the non-linear part of the curve is the following *[23]*:

$$S_j = \frac{S_{j,ini}}{\left(\frac{1,5.M_{j,Ed}}{M_{Rd}}\right)^{\psi}} \tag{2.13}$$

where S_j and $M_{j,Ed}$ are parameters defined in *Figure II.31* and Ψ is a parameter which depends of the configuration of the joint (for instance, for joints with bolted end-plates, Ψ = 2,7).

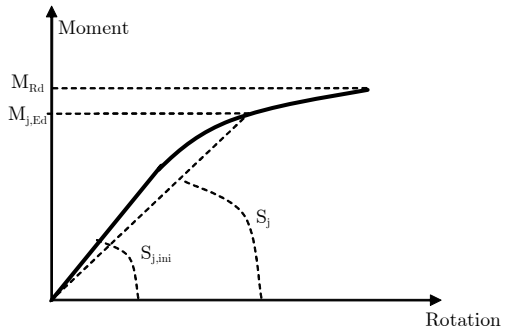

Figure II.31. Definition of the parameters of Formula (2.13)

II.3.3.3. Composite joints subjected to hogging moments

A. Introduction

In *§ II.3.2*, three tests on composite joints subjected to hogging bending moments have been presented. The validity of the component method recommended in the Eurocodes is investigated in this section through comparisons between the moment-rotation curves analytically predicted and the ones experimentally determined.

For the analytical predictions, the material properties which are used are the actual ones (presented in *Appendix VI.1* – no safety coefficients). Part of the component characterisation has been realised with two software:

- CoP *[24]*, dedicated to the computation of steel joints (under bending moments and axial loads) and developed by Liège and Aachen Universities;
- a homemade software based on an Excel sheet presented in *[11]* and dedicated to the computation of composite joints with bolted end-plates.

As mentioned in the previous section, the component method proposed in the Eurocodes only permits to compute the design bending resistance M_{Rd} and the initial stiffness $S_{j,ini}$. In order to be able to compare the moment-rotation curve until the ultimate moment M_u, it is also needed to compute the post-limit stiffness $S_{j,post\text{-}limit}$, the ultimate bending resistance M_u and the rotation ϕ_u (see *Figure II.11*); the latter has been computed according the

method proposed in the PhD thesis of Jean-Pierre Jaspart *[25]* which is in full agreement with the component method.

B. First comparison – TEST 1 of the "sway frames" project

The first comparison deals with the joint configuration tested in the "sway frame" project and presented in *§ II.3.2.2*. The comparison of the moment-rotation curves is given in *Figure II.32*. The component method prediction has been obtained applying the rules as actually recommended in Eurocode 3 and Eurocode 4 (*[6]*, *[12]* and *[22]*).

The failure mode associated to the analytically predicted resistant and ultimate bending moments involves two components: "rebars in tension" and "end-plate in bending". From *Figure II.32*, it can be observed that the initial and the strain hardening stiffnesses are well estimated while the resistant and ultimate bending moments and the ultimate rotation are overestimated with the analytical approach. To explain this difference, reference is made to *§ II.3.2.2* where experimental observations have been reported. As already stated, first cracks developed in the concrete slab, transversally in the vicinity of the connection and longitudinally just behind the column (see *Figure II.14*). The transverse cracks are due to the tension forces acting in the longitudinal rebars (each side of the column); this failure mode is covered by Eurocode 4 ("slab rebars in tension" component – see *Table II.10*). But nothing is said in the normative documents as far as longitudinal shear cracks are concerned. Actually, Eurocode 4 *[6]* only prescribes a minimum section area for the transversal rebars to be placed behind the column (see *Formula (2.18)* here below) so as to avoid the crushing of the concrete slab against the column when the joint is subjected to hogging moments.

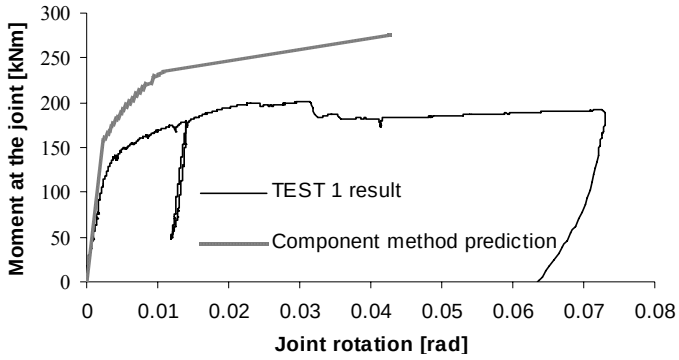

Figure II.32. Comparison between the component method prediction and the experimental test result

In reality, as soon as the longitudinal cracks in shear develop, the concrete no more contributes to the slab resistance. So the transversal rebars are alone to resist the forces acting along these cracks. These forces can be divided in two parts (*Figure II.33*):

- tension forces resulting from the "strut-and-tie" behaviour (phenomenon which is described in details in *[26]* and *[27]*);

- shear forces induced by the longitudinal rebars in tension.

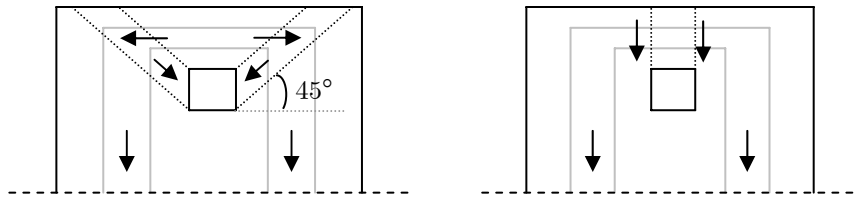

Figure II.33. Forces acting along the shear cracks in the slab

Obviously, an interaction between the tension and the shear forces has to be considered. So, the resistance criteria, which may be roughly estimated by means of the Von Mises criterion, can be expressed as follows:

$$\sqrt{(\sigma^2 + 3\,\tau^2)} \leq f_{sk} \tag{2.14}$$

where σ are the tension stresses induced by the "strut-and-tie" behaviour, τ, the shear stresses induced by the shear forces and f_{sk}, the yield strength of the rebars.

In the present case, the truss rods are assumed to be inclined by 45° (see *Figure II.33*), which is close to the reality (observation coming from tests – see *[26]*, *[27]* and *[28]*) ; the tension and shear stresses are then equal ($\sigma = \tau$) and *Formula (2.14)* becomes:

$$\sigma \leq f_{sk} / 2 \tag{2.15}$$

According to *Formula (2.15)*, half of the resistance is allocated to tension and half to shear. To take this into account, a modification of the procedure to predict the resistance of the rebars is suggested here below for single-sided joint configurations.

In Eurocode 4 (and in *[23]*), the resistance of the component "slab rebars in tension" is defined as:

$$F_{Rd,13} = \frac{A_s\, f_{sk}}{\gamma_s} \tag{2.16}$$

where A_s is the total area of the longitudinal slab rebars in tension with a diameter higher than 6 mm and γ_s, the safety coefficient to be applied to the rebar material (equal to 1,15 according to Eurocode 4). As previously mentioned, this formula only considers the resistance of the longitudinal rebars.

The formula which is suggested, to include the shear-tension interaction, is the following:

$$F_{Rd,13} = \min\left[\frac{A_s\, f_{sk}}{\gamma_s}; \frac{2\,A_{s,2}\,(f_{sk}/2)}{\gamma_s}\right] \tag{2.17}$$

where $A_{s,2}$ is the total area of the transverse slab rebars behind the column. The factor "2" in front of $A_{s,2}$ is justified by the presence of two sections of failure (one at each side of the column – *Figure II.33*).

So, the resistance of the component "rebars in tension" is governed by the weakest of the loaded rebars: the longitudinal or the transversal ones.

Another solution would be to define new requirements for the minimum area of transverse rebars to be placed behind the column so as to avoid the failure of the concrete slab behind the column (by assuming a truss rod inclination of 45°):

$$A_{S,2} \geq A_S \tag{2.18}$$

instead of:

$$A_{S,2} \geq \frac{A_s}{2} \tag{2.19}$$

as actually stated in Eurocode 4 for such joint configurations.

The computed moment-rotation curve obtained through the component method by substituting *Formula (2.17)* to *Formula (2.16)* for the evaluation of the resistance of the "slab rebars in tension" component is given in *Figure II.34*. Key values are reported in *Table II.11*. Two assumptions have been used to perform the computations as far as the area of the rebars is concerned:

- total area of the rebars ($A_{s,tot}$) or;
- area of the rebars with a diameter higher than 6 mm only, as recommended in Eurocode 4 ($A_{s,12\ mm}$).

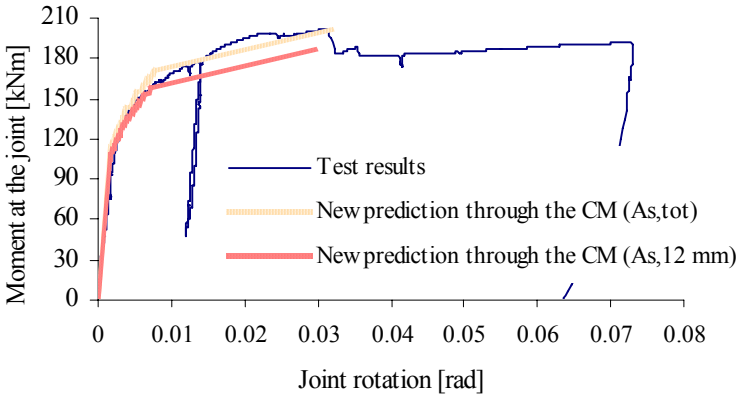

Figure II.34. Comparison between the "new" component method predictions and the experimental test result

Table II.11. Key values obtained experimentally (TEST 1) and analytically through the new prediction approach

	Exp. results	**New formula: $A_{s,tot}$**	**New formula: $A_{s,12\ mm}$**
$S_{j,ini}$ [kNm/rad]	65000	64312	64312
M_u [kNm]	201,58	201,54	186,4
ϕ_u [rad]	0,031	0,032	0,030

Figure II.34 and *Table II.11* show the good agreements between the test results and the component method predictions using the new resistance formula for the "slab rebars in tension" component. Also, it can be observed that the loss of resistance at a rotation of more or less 0,031 rad can be justified by the collapse of the 6 mm rebars; indeed, the experimental curve at this rotation passes from the "$A_{s,tot}$" analytical curve to the "$A_{s,12mm}$" curve. This is confirmed by *Figure II.35* where it can be seen that the 6 mm transversal rebars behind the column are collapse at the end of the test (the concrete slab has been carefully removed to inspect the rebars). It is justified by the low ductility of the 6 mm rebars if compared to the 12 mm ones. It is the reason why Eurocode 4 recommends that the rebars to be considered in the joint calculation are only those with a diameter higher than 6 mm.

Figure II.35. Photo of the rebars behind the column at the end of the test

Remark: In the tests on double-sided composite joint configurations performed by other partners involved in the above-mentioned "Sway frames" project (*[29]* and *[30]*), the appearance of shear cracks in the concrete slab has not been observed. This can be explained by the amount of concrete available behind the column to resist to the shear loads that is higher than in a single-sided joint configuration.

C. Second comparison – TEST 1 of the "Precious" project

The analytical characterisation of the joint has been performed through the component method, as recommended in the Eurocodes (i.e. with *Formula (2.16)* – namely "Old"

method) and with the new proposal presented in the previous section (i.e. with *Formula (2.17)* – namely "New" method). All the rebars are considered in the computation, i.e. rebars with a diameter of 12 mm and 6 mm.

The obtained results with the "old" and the "new" methods are presented in *Table II.12*. The analytically determined collapse mode associated to the resistant and ultimate bending moments is "Beam flange in compression" with the two methods, what is in good agreement with the experimental test observations. Even if the component "Rebars in tension" is not directly involved in the collapse mode, it can be seen that the obtained results with the two methods are significantly different. It can be justified by the fact that the distribution of the internal forces amongst the bolts rows (and, accordingly, the moments) is affected by the maximum load which can be sustained by the rebars.

Table II.12. Computed resistant and ultimate bending moments with the two methods

Methods	**M_{Rd} [kNm]**	**M_u [kNm]**
"Old" method	319,1	391,0
"New" method	272,5	335,8
Difference	*14,6 %*	*14,1 %*

The comparison between the analytical predictions and the experimental results is given in *Figure II.36* and *Table II.13*. From this comparison, it can be observed that the ultimate moment obtained with the "old" method is widely overestimated (difference of -19,1 %) while the one obtained with the "new" method is more accurate (difference of -5,9 %). The experimental curve and the analytical one obtained with the new method are in very good agreement until a joint rotation of more or less 51 mrad. After this, a loss of resistance of the joint is observed for the experimental result which is linked to a concrete crushing (associated to a lack of ductility) in the "strut-and-tie" behaviour (see *§ II.3.2.4.B*); this phenomenon is not yet taken into account in the component method. Additional investigations should be realised in future in order to characterise this phenomenon which can limit the value of the resistant and/or ultimate bending moments and the rotation capacity.

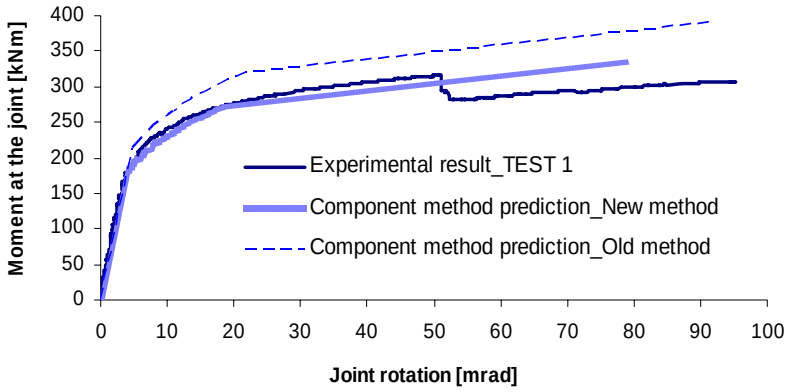

Figure II.36. Comparison between the component method predictions and the experimental test result

Table II.13. Comparison of the ultimate moment between the analytical predictions and the experimental result (TEST 1)

Methods	M_u [kNm]	$M_{u,exp.}$ [kNm]	Difference
"Old" method	391	316	-19,1 %
"New" method	335,8	316	-5,9 %

D. Third comparison – TEST 1 of the "Robustness" project

The comparison between the analytical prediction and the experimental results is presented in *Figure II.37* and in *Table II.14*. The analytically determined collapse mode is "beam flange in compression" (for the resistant and ultimate bending moment) which is in line with what was identified during the experimental test.

From the comparison, it can be observed that the initial stiffness (compared to the unloading-reloading branch) and the resistant bending moment are in good agreement with the experimental test while the ultimate moment and the post-limit stiffness are underestimated; indeed, a difference of 10 % exists between the "experimental" ultimate moment and the "analytical" one.

One phenomenon which could explain these differences is the development of membrane forces in the components "end-plate in bending" and "column flange in bending", phenomenon which is not actually covered by the component method. Indeed, the tested specimen is composed of a thin end-plate (thickness of 8 mm) and a thin column flange (thickness of 9 mm) which deformed significantly at the end of the test; these deformations can then lead to the development of membrane forces within these components (see *Figure II.38*) which can increase the resistance and the stiffness of the latter. The same phenomenon was already identified in the "sway frame" project through

TEST 3 and 4 (see *§ II.3.2.2.A*) performed on steel joints with thin end-plate (*[1]* and *[10]*).

Within the "Robustness" project, tests in isolation on each component of the joints have been performed at Trento University. So, it will be possible to confirm this observation when the results of the experimental tests performed on the components will be available, what is not yet the case at the time of redaction of the thesis.

Remark: a parallelism with the theory proposed in *Part III* for the prediction of the development of the membrane forces in structural beams will be put into sight later on in the perspectives presented in *§ IV.2*.

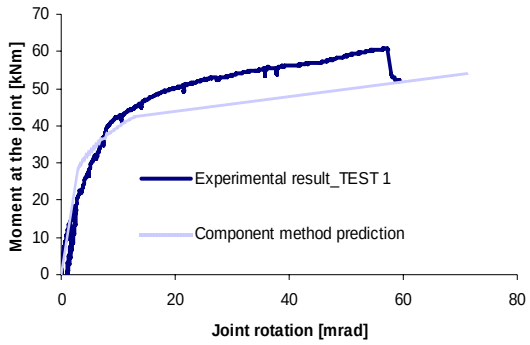

Figure II.37. Comparison between the component method prediction and the experimental test result

Table II.14. Key values obtained experimentally (TEST 1) and analytically

	Exp. results	**Component method results**
$S_{j,ini}$ [kNm/rad]	$\pm$ 9530	9850
M_u [kNm]	60,6	54,07
ϕ_u [rad]	0,062	0,071

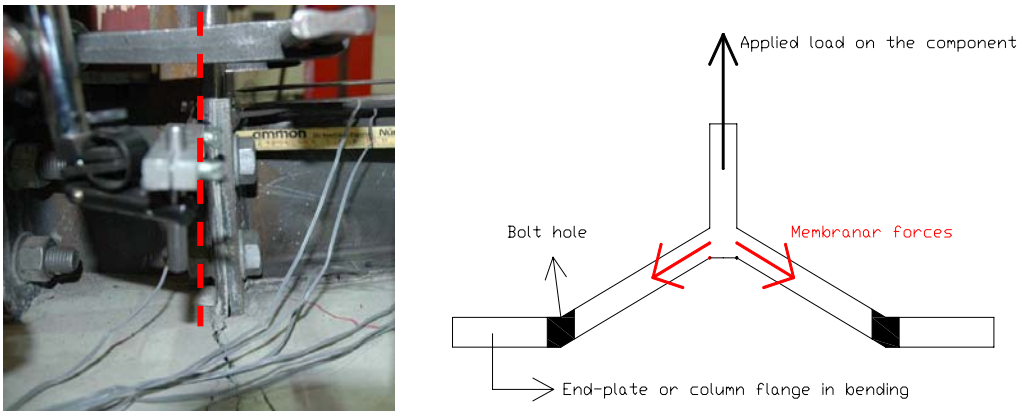

Figure II.38. Deformation of the end-plate and the column flange at the end of the bending test

II.3.3.4. Composite joints subjected to sagging moments

A. Introduction

In *§ II.3.2*, two tests on composite joints subjected to sagging bending moments have been presented. As previously mentioned (*§ II.3.1*), the component method as actually proposed in the Eurocodes is not yet able to predict the behaviour of composite joints subjected to such loading. Indeed, no method is available to characterise one of the activated components: concrete slab in compression.

In recent researches, methods to characterise this component in term of « resistance » are proposed. Their aim is to define a rectangular cross section of concrete participating to the joint resistance.

The procedure which is proposed in this section combined two methods proposed respectively by Fabio Ferrario in *[28]* and by J.Y. Richard Liew in *[31]*. The combination of these two methods permits to reflect in a more appropriate way how the concrete resists to the applied load in the vicinity of the joint. Also, a formula for the characterisation of this component in term of "stiffness" is proposed and validated.

The proposed procedure is described first in *§ II.3.3.4.B*; then, the validity of the latter is investigated through comparisons with experimental tests results in *§ II.3.3.4.C* and *§ II.3.3.4.D*.

As in the previous section, the actual material properties (given in *Appendix VI.1*) without safety factors are used for the analytical predictions. Also, the resistant bending moment M_{Rd} and the initial stiffness $S_{j,ini}$ are computed in full agreement with the component method recommended in Eurocode 4 while the ultimate moment M_u, the post-limit stiffness $S_{j,post\text{-}limit}$ and the rotation capacity ϕ_u are computed according the method proposed in the PhD thesis of Jean-Pierre Jaspart *[25]*.

B. Proposed method for the characterisation of the new component "Concrete slab in compression"

The objective of the proposed method is to define a rectangular cross section of concrete in order to characterise the contribution of the concrete/composite slab to the joint resistance. As previously mentioned, this method is a combination of two methods proposed in the PhD thesis of Fabio Ferrario *[28]* and in an article of J.Y. Richard Liew et al *[31]*.

In the PhD thesis of Fabio Ferrario *[28]*, a formula is proposed to compute the width of the concrete $b_{eff,conn}$ which has to be taken into account for the joint component "concrete slab in compression":

$$b_{eff,conn} = b_c + 0,7h_c \leq b_{eff} \tag{2.20}$$

where b_c is the width of the column profile flange, h_c the height of the column profile cross section and b_{eff}, the effective width of the concrete/composite slab to be considered in the vicinity of the joint; b_c represents the contribution of the concrete directly in contact with the column flange while $0,7.h_c$ the contribution of the developed concrete rods *[28]* in the "strut-and-tie" behaviour (see *Figure II.39*).

In the article of J.Y. Richard Liew et al *[31]*, the width of the concrete is taken as equal to the width of the column flange ($b_{eff,conn} = b_c$) and the development of the concrete rods in compression through the "strut-and-tie" model is neglected.

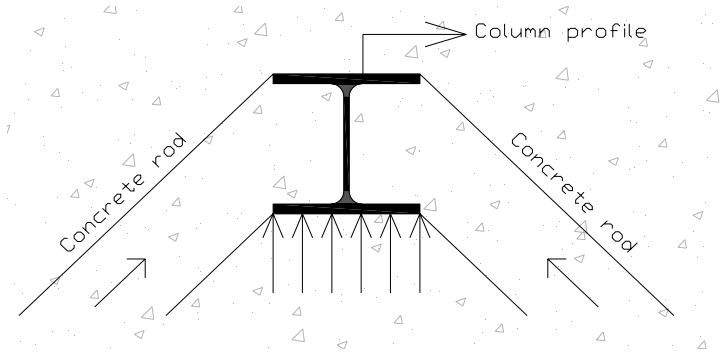

Figure II.39. Plane view of the slab in the vicinity of the joint - development of concrete rods in compression under sagging moment

The definition of the width given in *[28]* (i.e. *Formula (2.20)*) will be used in the developed procedure as this definition reflects in a more appropriate way the mechanism developing in the concrete slab according to the observations reported during the experimental tests presented in *§ II.3.2.*

Another difference between the two methods is linked to the definition of the height of concrete to be considered and, accordingly, to the position of the centre of compression within the joint. In *[28]*, the centre of compression is assumed to be at mid-height of the concrete slab while in *[31]*, the following procedure is given to compute the position of this point:

- the characterisation of the components in tension and eventually in shear is performed according to the rules recommended in the Eurocodes;
- then, the height of the concrete/composite slab contributing to the joint behaviour is computed by expressing the equilibrium of the load developing in the

concrete/composite slab in compression with the components in tension or in shear and assuming a rectangular stress distribution in the concrete (equal to 0,85 f_{ck}/γ_c in a design and to $f_{ck,actual}$ in the following sections). For instance, in the example illustrated in *Figure II.40*, the concrete height to be considered is equal to:

$$z = \frac{F_{Rd,1} + F_{Rd,2} + F_{Rd,3}}{b_{eff,conn}.(0{,}85.f_{ck}/\gamma_c)} \leq h_{concrete} \tag{2.21}$$

where $h_{concrete}$ is the total height of the concrete slab (in case of a composite slab, $h_{concrete}$ is equal to the concrete above the ribs);

- finally, the characterisation of the joint is performed assuming that the centre of compression is situated at the middle of the height of the contributing part of the concrete slab (z).

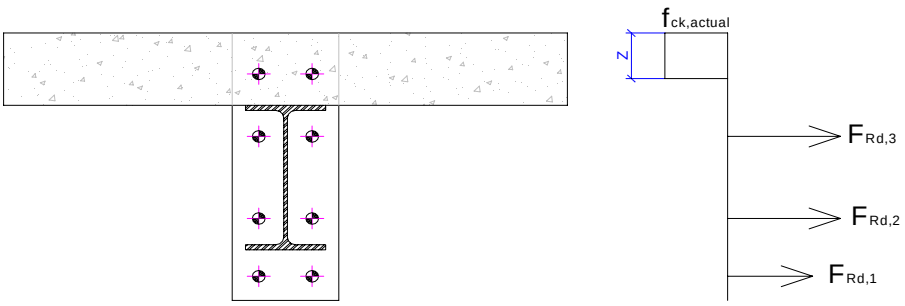

Figure II.40. Height of the concrete to be considered in the characterisation of the new component

It is the latter procedure which is considered in the developed procedure as it reflects in a more appropriate way the actual behaviour of the joint according to the observations made during the experimental tests.

So, the resistance of the component "concrete slab in compression" can be computed through the following formula:

$$F_{Rd,CSC} = b_{eff,conn}.z.(0{,}85.f_{ck}/\gamma_c) \tag{2.22}$$

with $b_{eff,conn}$ and z computed according to *Formula (2.20)* and *Formula (2.21)* respectively.

The two previously mentioned references only deal with the characterisation of the component "concrete slab in compression" in term of resistance but no formulas are proposed to characterise the latter in term of stiffness; however, the latter is requested in order to be able to predict the initial stiffness of the joint (and to derive the moment-rotation curve).

If reference is made to *[32]*, a formula is proposed to predict the stiffness of a concrete block against a rigid plate. In the present case, the steel column encased in the concrete slab can be considered as a rigid plate; so, the formula proposed in *[32]* can be extended to the present situation to compute the stiffness of the component under consideration:

$$k_{csc} = \frac{E_c \cdot \sqrt{b_{eff,conn} \cdot z}}{1{,}275 . E_a} \tag{2.23}$$

where E_C is the secant Young modulus for the concrete, E_a, the elastic Young modulus for the steel and k_{CSC}, the stiffness of the component "concrete slab in compression" to be considered in the component method.

In conclusion, with *Formula (2.22)* and *(2.23)*, it is possible to characterise the "new" component "concrete slab in compression" and so, through the component method, to predict the behaviour of composite joints subjected to sagging moments. The validity of the proposed method is investigated in the two following sections.

C. First comparison – TEST 4 of the "Robustness" project

The comparison between the component method prediction (with the characterisation of the component « concrete slab in compression » according to the proposed method) and the experimental result of TEST 4 realised within the "Robustness" project (see *§ II.3.2.3.C*) is given in *Figure II.41* and *Table II.15*.

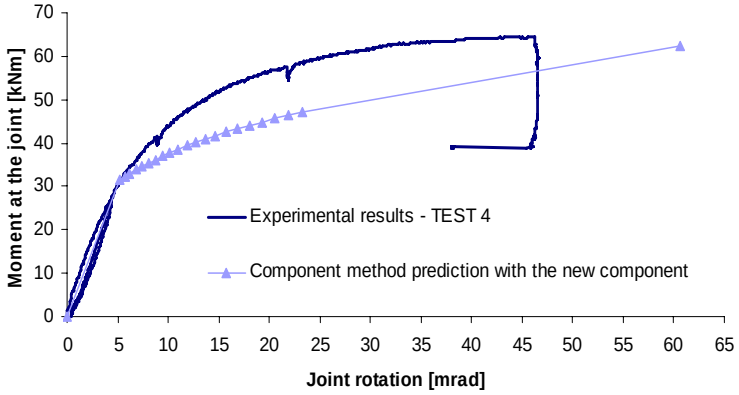

Figure II.41. Comparison between the component method prediction and the experimental test result

Table II.15. Key values obtained experimentally (TEST 4) and analytically through the component method

	Exp. results	**Component method results**
$S_{j,ini}$ [kNm/rad]	± 6400	6061
M_u [kNm]	64,5	62,4
ϕ_u [rad]	0,047	0,062

Through this comparison, it can be observed that a good agreement is obtained between the analytical and the experimental results for $S_{j,ini}$ and the resistance and ultimate bending moments while the post-elastic stiffness is widely under-estimated which is confirmed by the over-estimated value of ϕ_u (see *Table II.15*). The analytically determined collapse mode for the resistant and ultimate bending moments is "column flange in bending" which is in full agreement with the experimental observation (see *§ II.3.2.3.C*). The difference on the value of the ultimate moment is equal to 3 %.

Remark: for the computation of the ultimate moment M_u, the resistance of the concrete which has been used is the actual resistance obtained through cylinder compression test + 8 Mpa as recommended in Eurocode 2 *[33]*. This remark is also valid for the next section

As explained in *§ II.3.3.3.D* comparing the analytical prediction and the experimental result for the same joint configuration subjected to hogging bending moments, the difference observed for the post-elastic stiffness can be explained by the development of membrane forces in the components "column flange in bending", phenomenon which is not actually covered by the component method and the characterisation of this component (see *Figure II.38*). The effects of these membrane forces on the joint response is more important under sagging moment than under hogging moment because, under sagging moment, the component "column flange in bending" is directly involved in the collapse mode which leads to an important deformation of the latter. It will be possible to confirm this observation when the results of the experimental tests performed at Trento University on the joint components will be available. At the time of redaction of the thesis, it is not yet the case.

As mentioned in *§ II.3.3.2.C*, the non-linear part of the analytical behavioural curve of a joint is computed through *Formula (2.13)*. The shape of the latter is influence by the parameter Ψ. The value proposed in *[23]* for a joint with a bolted end-plate is 2,7; if this value is modified in order to take into account the additional stiffness coming from the development of the membrane forces within the component "column flange in bending" (for instance, $\Psi = 1$), a better accuracy between the analytical prediction and the experimental results can be obtained, as illustrated in *Figure II.42*.

Additional researches are requested to study the effects of membrane forces on the behaviour of the components in bending (i.e. column flange and end-plate in bending). This point will be addressed in the perspective presented in *§ IV.2*.

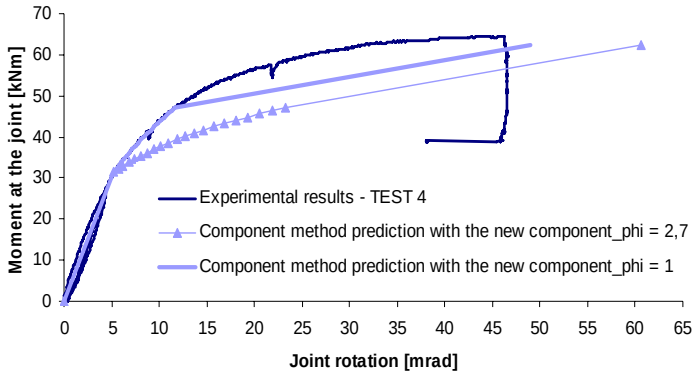

Figure II.42. Comparison between the component method prediction and the experimental test result

D. Second comparison – TEST 2 & 3 of the "Precious" project

Through the analytical computation, the collapse mode associated to the resistant and ultimate bending moments is "Column web panel in shear" which is in line with the observations during the test (see *§ II.3.2.4.C*). In *Figure II.43* comparing the analytical and the experimental curves, it can be observed that there is a good agreement between the TEST 3 experimental result and the analytical prediction. For TEST 2, there is a good agreement until a rotation of 29 mrad; after this joint rotation, a loss of resistance in the joint is observed for TEST 2 as already mentioned and justified in *§ II.3.2.4.C*, what is not reflected in the analytical prediction.

The fact that the analytical model is not yet able to predict the concrete crushing (responsible of the resistance loss) is linked to the fact that, until now, the analytical model does not consider the collapse of the concrete slab associated to a lack of ductility of this component. Future researches should be performed in order to investigate in more details this phenomenon.

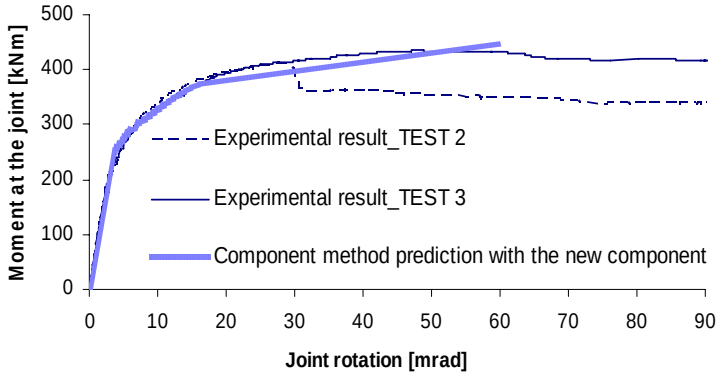

Figure II.43. Comparison between the component method prediction and the experimental test results

Table II.16. Key values obtained experimentally (TEST 2 and 3) and analytically through the component method

	Component method results	**Test 2 results**	**Test 3 results**
$S_{j,ini}$ [kNm/rad]	69860	± 64900	± 64900
M_u [kNm]	448	411	435
ϕ_u [rad]	0,060	0,029	0,110

II.3.4. Conclusions

Within this section, the behaviour of beam-to-column composite joints subjected to bending moments has been investigated through experimental and analytical studies.

Through the experimental approach, a new collapse mode has been identified for the single-sided beam-to-column composite joints subjected to hogging bending moments: the collapse of the transversal rebars behind the column under combined tensile and shear loads. This new failure mode is not actually covered by the component method which is the analytical procedure recommended in Eurocode 4 *[6]* for the joint design. Accordingly, an analytical expression covering this new failure mode has been developed and integrated in the component method. The latter has been validated through comparisons with experimental test results; it has been shown that the new analytical expression allows reaching a very good agreement with the test results.

In composite sway frames, the beam-to-column composite joints can be subjected to sagging bending moments; however, Eurocode 4 *[6]* is not yet able to characterise composite joints subjected to such loading as no method is available to characterise one of the activated components which is "concrete slab in compression". Within this section, a procedure to characterise this component (in term of resistance and stiffness) has been proposed and validated through comparison with experimental results, the analytical predictions obtained with this new method being in good agreement with the experimental results.

From the presented investigations, it can be concluded that accurate analytical tool is available to predict the beam-to-column composite joint behaviour subjected to hogging and sagging bending moments. These analytical tools will be used later on (in *§ II.5* and *§ II.6*) so as to introduce the joint behaviour in the numerical modellings.

II.4. Description and validation of the numerical tool

II.4.1. Introduction

All the performed numerical investigations within the thesis are performed through the homemade finite element software FINELG. In this section, a description of this software (*§ II.4.2*) and of the main assumptions needed to model the investigated composite structures (*§ II.4.3*) is first given. Then, two studies devoted to the validation of the FINELG software for the numerical simulation of the non-linear behaviour of composite structures are presented:

- The first one, in *§ II.4.4*, is a benchmark study performed within the "sway frame" project and coordinated by Liège University. The reference structure is a braced composite building tested in U.K. because both the detailed data and test results are available (*[34]* and *[35]*). Even if the building is braced and therefore does not exhibit sway effects, it has been initially used as a benchmark to demonstrate the ability of different FEM software (and in particular of FINELG) to simulate the behaviour of composite systems.

- The second one, in *§ II.4.5*, is a comparison between the numerical prediction obtained through a "full" non-linear analysis performed with FINELG and the experimental results obtained through a test performed at Bochum University on a composite sway frame.

Finally, a brief conclusion is given in *§ II.4.6*.

II.4.2. Brief description of the homemade FEM software FINELG

The computer program FINELG *[36]* is a homemade finite element program developed at the Liège University (Argenco department) and at Greisch design office (Liège, Belgium) and is especially used for research purposes. It originated in 1974 and is continuously growing up. The software is linked to homemade "satellite" graphical and post-processor software such as DESFIN, FINGL (graphical interactive programs), SELFIN (interactive program allowing the post-treatment of the FINELG output file), …

The software allows solving:

- geometrically and materially nonlinear solid or structural problems under static dead loads;

- linear and nonlinear instability problems, leading to buckling loads and instability modes by an eigenvalue computation;
- dynamic problems, leading to eigenfrequencies and vibration modes with taking account, or not, of the double-sided stresses.

Also, the software FINELG allows performing different types of analyses listed here below:

- First-order elastic analysis;
- Non-linear static analysis;
- Stability analysis;
- Dynamic analysis – eigenfrequencies;
- Dynamic analysis - Seismic spectrum analysis;
- Linear step-by-step dynamic analysis;
- Non linear step-by-step dynamic analysis and;
- Stochastic dynamic analysis

Within the thesis, stability and non-linear static analyses are performed. For the non-linear analyses, a step-by-step computation is used with Newton-Raphsons steps and the arc-length method for the load increment; for the stability analyses, the eigenvalues and the corresponding eigenvectors are computed through the subspace iteration method.

II.4.3. Assumptions relative to the modelling of the composite structures

For all the studied 3-D buildings, a 2-D frame is isolated as allowed in Eurocode 4 *[6]* and a 2-D modelling of these isolated frames is performed; this procedure is based on the assumption that the frames are braced in the out-of-plane direction (what is assumed for the studied frames within the thesis).

The beam and column members are modelled by means of plane beam elements with three nodes (*Figure II.44*). Node 1 and 3 present three degrees of freedom (u, v and θ - see *Figure II.44*); node 2 only presents one degree of freedom (u) which allows to take into account of an eventual relative displacement between the concrete and the steel profile *[37]*. This type of elements does not permit to involve the cross section local buckling phenomenon. As a 2-D numerical analysis is performed, the out-of-plane buckling phenomena as lateral-torsional buckling are not taken into account in the computation.

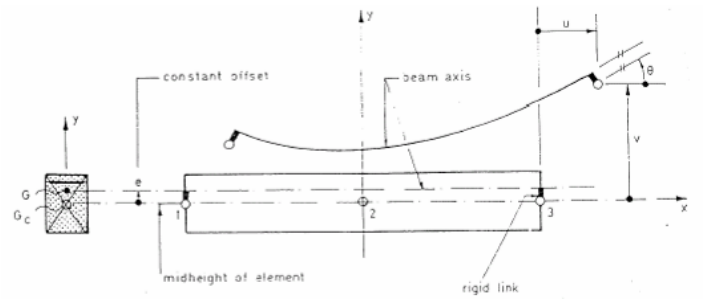

Figure II.44. Plane beam finite element with three nodes

For all the materials, the characteristic values for the resistance are used (security coefficients for the materials equal to 1) as the objective of the study is not to perform a frame design but to investigate the behaviour of composite sway frames.

For the steel elements (steel profiles and steel rebars), a linear law ("Hooke's law") is used for the elastic analyses and a bilinear one for the non-linear analyses (*Figure II.45*). The FINELG software also permits to take into account of the influence of the residual stresses; the latter are not introduced in the computations presented herein as the objective of the presented studies is to investigate the global behaviour of the structure (the residual stresses only influence the local behaviour of the members).

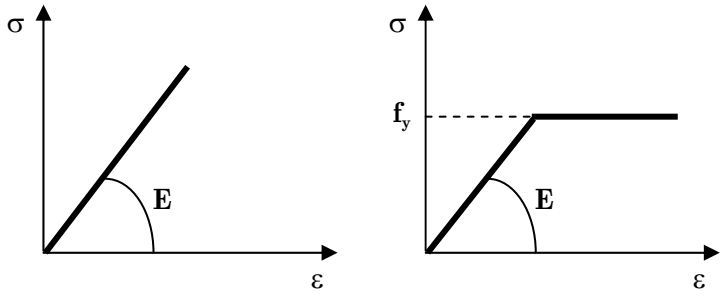

Figure II.45. Linear and bilinear behaviour laws used for the steel materials

For the concrete material, a parabolic law with tension stiffening is introduced in the modelling (*Figure II.46*). Shrinkage and creep phenomena are not introduced in the computation; the long term loading effect is taken into account by multiplying the concrete resistance by a factor equal to 0.85 (α coefficient).

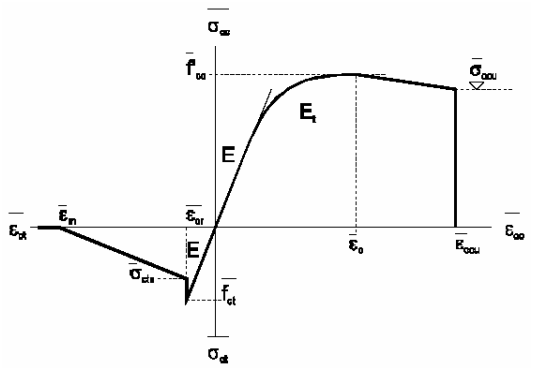

Figure II.46. Parabolic law with tension stiffening used for the concrete materials

The concept of effective width is used for the composite beam modelling (as recommended in Eurocode *4*). The connection between the concrete or composite slabs and the steel profiles is assumed to be complete. All the columns are assumed to be continuous on all the height of the studied frames.

Concerning the semi-rigid and partial-strength joint modelling, the simplified approach as proposed in *[22]* and *[23]* is used, i.e. the deformability of the joints is concentrated at the intersection between the beam and the column axes. Rotational springs with tri-linear behaviour laws (*Figure II.47*) are introduced in the frame modelling to model and to idealize the joint behaviour; with such idealisation, the post-limit behaviour of the joint (including the strain hardening effects, the eventual membrane effects, ...) is neglected (see *Figure II.11*). For the critical elastic analysis performed later on, these tri-linear laws are replaced by linear ones as presented in *Figure II.45* with a stiffness equal to $S_{j,ini}$ (as recommended in the Eurocodes).

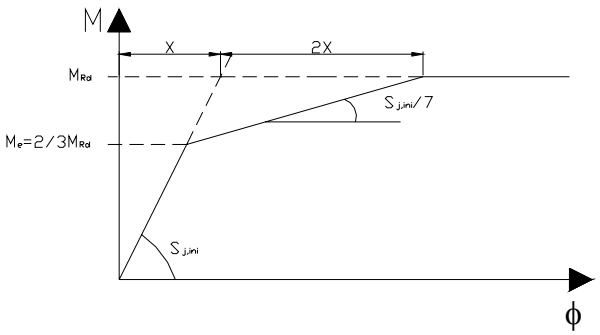

Figure II.47. Trilinear idealisation of the non-linear joint behaviour

As the behaviour of the constitutive joints of the "UK" building and of the "Bochum" frame are available from test results (see *§ II.4.4* and *§ II.4.5* here after), these test results are used to idealize the joints. For the other structures, the properties of the composite joints are computed by means of the component method presented in *§ II.3.3*.

II.4.4. Benchmark study – UK building

II.4.4.1. Introduction

In this paragraph, a benchmark study aimed at validating the use of several finite element software for the numerical simulation of the non-linear behaviour of composite structures is summarized. More details may be found in *[38]*. The Institutions which contributed to the benchmark study were partners involved in the numerical studies of the "sway frames" project presented in *§ I.1*:

- LABEIN (Spain) – ABAQUS 6.2 software;
- RWTH Aachen (Germany) – DYNACS software;

- Pisa University (Italy) – ADINA 7.5 software;
- Liège University (Belgium) – FINELG software.

The reference structure for the benchmark study is a 3-D braced composite building composed of two main frames (*Figure II.48*) tested at BRE (Building Research Establishment) in UK because both the detailed data and test results are available (*[34]* and *[35]*). The test report is well documented (yield strengths, dimensions, type of loading); in particular, the behavioural curves of the structural joints are given. The "203x203 UC 46" bare steel columns support floors consisting in composite slabs; the latter are connected by shear studs to the top flanges of the sole "254x102 UB 25" primary beams. As the main purpose of the frame tests was to investigate semi-rigid joint effects on overall frame behaviour, a finite width of concrete slab (1 m) was used instead of the full floor slab layout; in the latter four 12 mm and four 10 mm high yield bars were used as longitudinal reinforcement. Flush end-plate joint configurations were used for all beam-to-column joints.

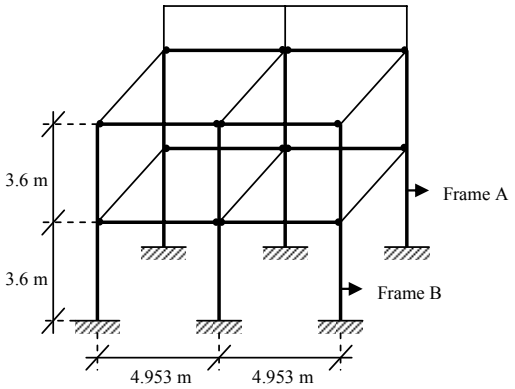

Figure II.48. General layout of the "UK" building tested at BRE laboratory

The structure is composed of two parallel two-storey two-bay main frames (namely "Frame A" and "Frame B" – see *Figure II.48*) connected by secondary beams. In Frame A, all the columns are bent about their major axis, while they are about their minor axis in Frame B. Both frames are subjected to concentrated loads F applied at one third and two thirds of each beam span (*Figure II.49*). These ones are proportionally increased (λ load factor) until failure is reached, except for the lower right beam where these loads are kept constant as equal to "F". For Frame A, the nominal value of F is equal to 37 kN; for Frame B, the latter is equal to 39 kN.

Though the reports *[34]* and *[35]* are well documented, some data are nevertheless missing; therefore reasonable assumptions *[38]* have been agreed on so as to ensure a complete similarity of the data used by the above partners for performing their respective numerical simulations.

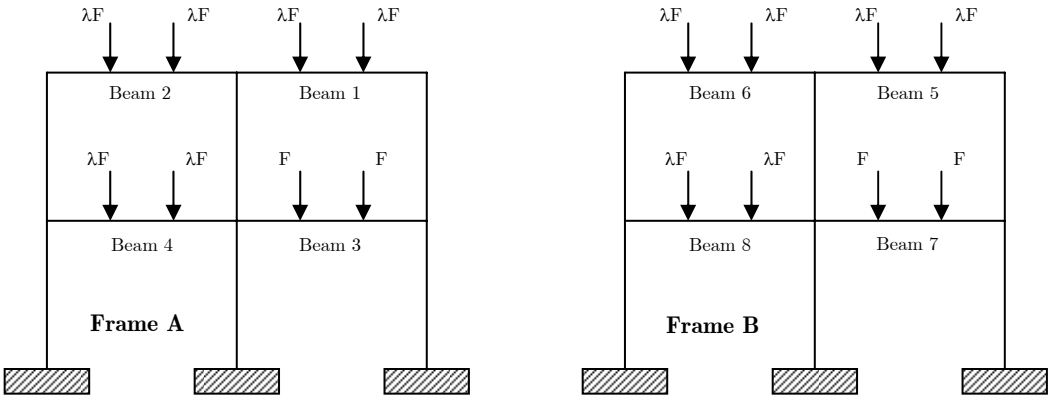

Figure II.49. Static schemes of Frame A and Frame B extracted from the "UK" building

The validation of the different software is subordinated to a successful comparison of the results obtained numerically by the above partners with the ones recorded during the tests.

Remark: For the numerical investigations performed through the FINELG software, the different assumptions presented in *§ II.4.3* have been applied. However, the strain hardening effect is introduced in the definition of the steel behaviour law (which constitutes a deviation with regards to these assumptions) so as to be as close as possible to the actual behaviour of the steel material.

II.4.4.2. Obtained results

In general, the numerical simulations are in a rather good agreement with the test results got at BRE *[35]*. The comparison between FEM simulations and test for the ultimate load factor is presented in *Table II.17* and *Table II.18*.

Table II.17 and *Table II.18* values show that the ultimate load factors are under estimated in all cases (except for Pisa in Frame A). The maximum difference with the test results is obtained by Labein (24,1 %).

The numerical results fit better to the test for Frame B than for Frame A (except for Labein where no difference is observed). The failure of the two frames results from the development of beam plastic mechanisms in all the numerical simulations as in the test but for different beams; indeed, for the numerical simulations, the beam mechanisms develop in beam 4 and beam 5 for Frame A and Frame B respectively when, for the test, they develop in beam 1 and beam 8 (see *Figure II.49* for the position of the beams). The reasons which could explain this difference are developed later on in *§ II.4.4.2.C*.

Table II.17. Ultimate load factor λ_u – Frame A

Partner	Simulations	Test Results	Difference (%)
Labein	4,59	6,05	24,1
Pisa	6,32	6,05	-4,5
Aachen	5,31	6,05	12,2
Liège	5,48	6,05	9,4

Table II.18. Ultimate load factor λ_u – Frame B

Partner	Simulations	Test Results	Difference (%)
Labein	3,97	5,23	24,1
Pisa	5,03	5,23	3,8
Aachen	4,66	5,23	10,9
Liège	5,02	5,23	4,0

A. Displacements in the frames

During the test, the mid-span relative deflections of the beams (relative to the displacement of the extremities) have been measured. These deflections are reported in *[35]* as a function of the total applied load on the beam (sum of the two applied concentrated loads).

Figure VI.5 to *Figure VI.10* in *Appendix VI.3* present comparisons between load – deflection curves numerically derived and experimentally measured for the primary beams of Frame A and Frame B. It may be seen in these figures that, for the two frames, the ultimate loads are under estimated (except for Pisa University – Frame A) as it was already shown in the previous section. The response of the beams is quite similar in the test and in the simulations (except for Labein where the simulations are always below the test curves). In Frame B, at the beginning of the loading, the curves obtained by the simulations are more linear than in the test curves. But at the yielding phase, the simulation curves and the test curves are quite alike. Nevertheless, it can be observed that, at this phase, for Pisa University simulations (see *Appendix VI.3*), the stiffness remains bigger than the other simulations. This can be explained by the type of steel constitutive law chosen for the modelling (without a plateau in the yielding phase) which is different from the other partners.

Again, some differences between the simulations and the test results may be explained by different reasons developed in *§ II.4.4.2.C.*

B. Bending moment diagrams

In *Figure VI.11* of *Appendix VI.3*, the diagrams of bending moments at failure obtained from the test and the simulations are compared.

Again, the numerical simulations predict rather well the actual frame response (except for Labein). The maximum difference between the test results and the numerical results (in percentage) is observed for the "almost non-loaded" beams; it is not surprising as the moments are rather small in these beams.

C. Reasons explaining the result differences

Looking the obtained results, some minor differences have been identified which can be justified through some observations.

For the differences between the simulation results, they can be justified by some small differences in the assumptions adopted by each partner for their modelling *[38]*.

For the differences between the simulations and the test results, a detailed analysis of the test results (*[34]* and *[35]*) allows to identify unclear and doubtful points which can explain some differences with the simulation results:

- The applied loads on Frame A at failure are not the same for all the beams what is in contradiction with the definition of the applied loads in *[34]* which should be proportionally loaded.
- Test results for the joints in Frame A look inconsistent: joints 4 and 8 have the same mechanical properties but joints 1 and 4 don't have at all the same behaviour (*Figure II.50*).

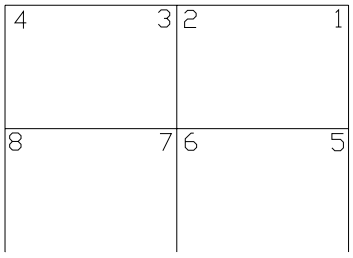

Figure II.50. Position of the joints in Frame A

- In the test, rotations with the joints were calculated by taking the difference between the measured beam end rotations and column rotations for every load increment. The moments at beam end were also evaluated through strain measurements and both have been used to build the joint moment-rotation curves. But, it is well known that it is very difficult to obtain a correct moment-rotation

curve by this technique; so, the experimentally obtained moment-rotation curves used in the numerical simulations may be not so close to the actual ones.

These points can explain the greater difference between the numerical and experimental failure load factor for Frame A and the fact that the failure appears in beam 4 (in the simulations) instead of beam 1 (in the test).

II.4.5. Comparison to experimental test results – Bochum test

II.4.5.1. Introduction

Within the "sway frame" project, a test on a 2-D composite sway frame has been performed at Bochum University *[39]*. The objectives of this test were to identify the particular behaviour of such frames and to validate the numerical tools. To achieve this goal, tests in isolation were also performed on the structural joints in order to obtain their bending moment-rotation curve; the partners involved in these joint tests were:

- Liège University;
- Aachen University and;
- Labein (Spain).

Liège University was deeply involved in the preparation of this test campaign, in particular in the design of the joints *[40]* and in the definition of the loading sequence so as to obtain a failure by global in-plane instability *[41]*.

In *§ II.4.5.2*, a brief description of the tested frame is first given. Then, the main results obtained through the frame test and the isolated joint tests are presented in *§ II.4.5.3*. Finally, the frame test results are compared to the numerical prediction in *§ II.4.5.4* so as to validate the homemade software FINELG for the prediction of the behaviour of composite sway frames.

II.4.5.2. Brief description of the Bochum frame

The Bochum frame (*Figure II.51*) is a two-bay two-storey frame. The total height is 4,99 m and the total width is 9,76 m.

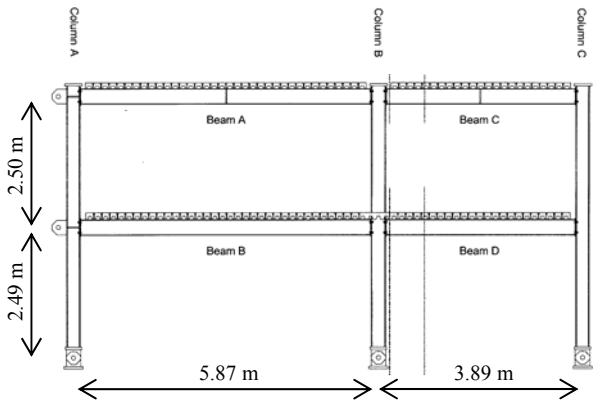

Figure II.51. General layout of the Bochum frame test

Columns A and C are made of HEB260 profiles and column B of a HEB280 one. The IPE300 beams have their upper flange connected to the composite slab by means of shear studs. The composite slab thickness and width are 120 and 1200 mm respectively. The slab reinforcement is constituted of a T6x6x150x150 mesh with four additional rebars with a diameter of 12 mm at the first storey internal composite joint vicinity; the covering of the rebars is equal to 25 mm. The collaborating hollow rib is a EGB210 one from BROLLO (Italy).

All the moment resistant joints are steel ones except the double-sided joint at the first storey which is a composite one (*Figure II.52*); these joints were designed so as to develop ductile modes of collapse with account of over-strength effects *[40]*. The configuration of the steel components of the steel joints is the same. According to Eurocode 3 and 4 (*[12]* and *[6]* respectively), all the joints are classified as semi-rigid and partial-strength ones (see *§ II.3.3.2.B*). The main details of these joints are given in *Figure II.52*.

The steel grades of the different structural elements are the same than the ones presented for the TEST 1 presented in *Appendix VI.1.1* as all the steel elements used for the tests within the "sway frame" project come from the same rolling. For the concrete, tests on cylinder were performed in Bochum the day of the frame test and an average concrete grade (f_{ck}) equal to 44,9 MPa was obtained.

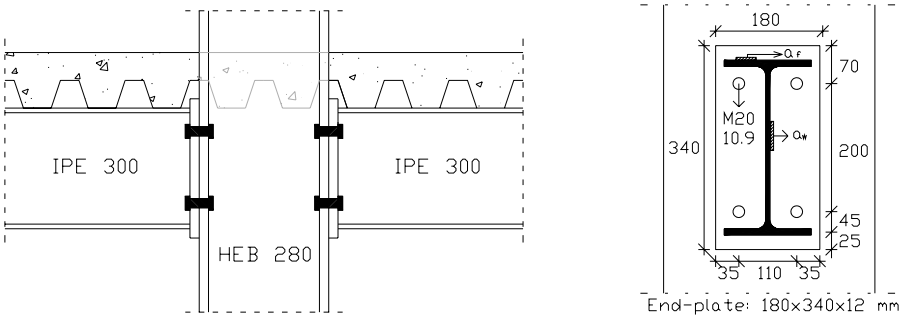

Figure II.52. Double-sided composite joint and joint details of the Bochum frame

In accordance with the experimental facilities at Bochum University, the applied loads on the frame are as follows:

- a vertical load of 400 kN applied at the top of each column; it is supposed to represent the gravity loads transmitted by the upper storeys;
- uniform and concentrated gravity loads as indicated in *Figure II.53*;
- horizontal loads of 50 kN applied at both floor levels.

For testing, the loading sequence was the following: all the gravity loads are first increased up to their nominal values; they are then kept constant while the horizontal loads are progressively magnified by a load factor λ till failure (see *Figure II.53*). More details about this structure are given in *[39]*.

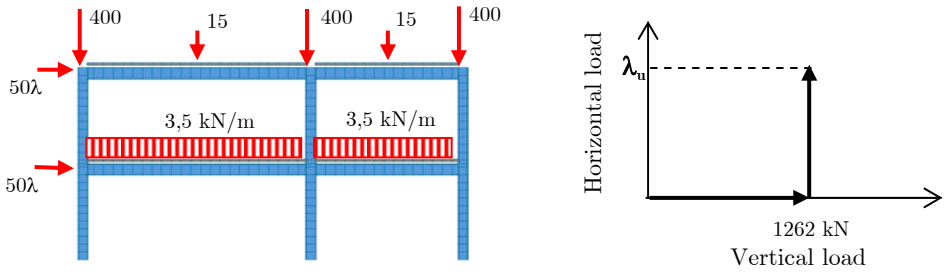

Figure II.53. Loading conditions and loading sequence for the "Bochum" frame [kN]

II.4.5.3. Test results

The test results which are reported here are the results which are needed to perform the numerical investigations and to validate the FEM software. More details concerning these tests are available in *[1]*, *[10]* and *[39]*.

A. Isolated joint test results

As mentioned previously, tests in isolation have been performed at Liège and Aachen Universities and at Labein on the steel and composite joint configurations which are met in the tested frame: the steel joint configurations were tested at Liège University (TEST 3 and 4 mentioned in *§ II.3.2.2*) while the composite double-sided joint configuration was tested at Aachen University and at Labein (double-sided composite joint configuration). Some pictures of the tests performed at Liège University are presented in *Figure II.54*.

TEST 3 configuration

TEST 3 at the end of the test

TEST 4 at the end of the test

Figure II.54. Photos of the tests on the single-sided steel joints performed at Liège University

In order to model the actual behaviour of the joints in the numerical simulation, the actual bending moment-rotation curves of each joint are requested. The latter are reported in *Figure II.55* and *Figure II.56*.

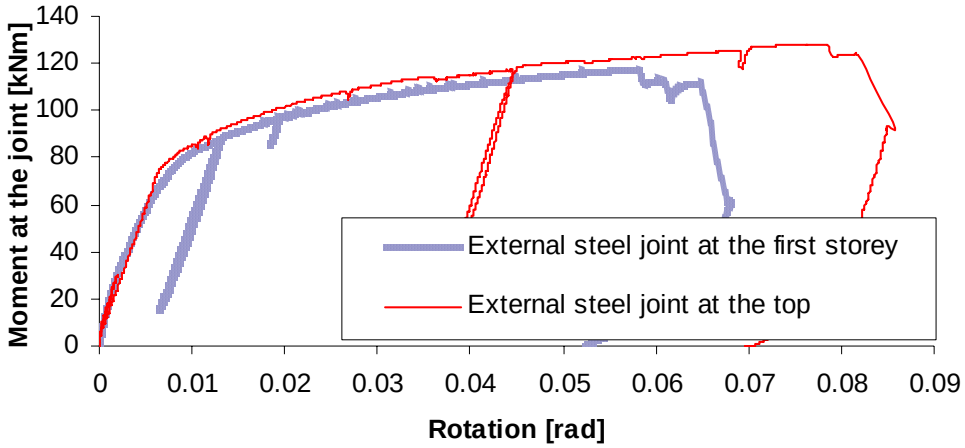

Figure II.55. Bending moment-rotation curves for the single-sided steel joints of the Bochum frame experimentally obtained at Liège University

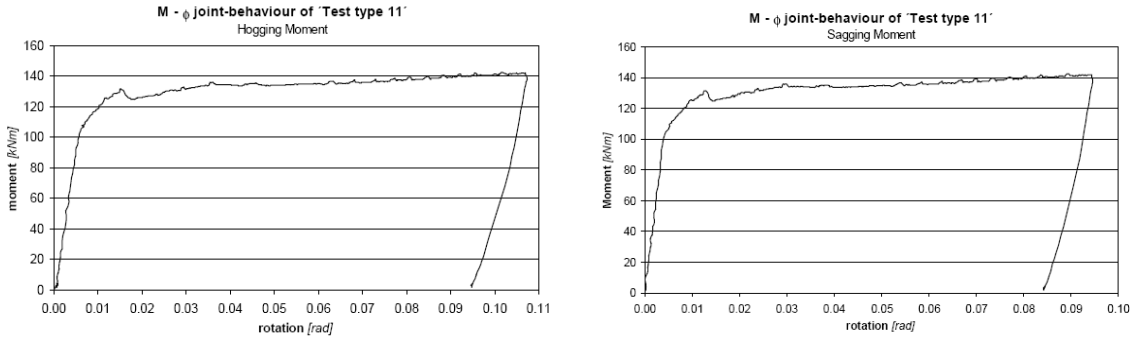

Figure II.56. Bending moment-rotation curves for the double-sided composite joint of the Bochum frame obtained experimentally at Aachen University [1]

Remark: the results of the tests carried out in Labein are not reported herein because the loading sequence followed during the joint test was not in line with the one appearing at the joint level during the frame test.

Within the "Sway frames" project, one joint configuration which is met in the frame has not been tested: the double-sided steel joint at the second storey. This joint has exactly the same configuration than the single-sided steel joint at the same storey but, at the double-sided joint level, the component "web panel in shear" is not activated in the same way. In order to have a prediction of the bending moment-rotation curve for the double-sided joint as accurate as possible, the following procedure has been followed:

- First, the contribution of the web panel in shear to the single-sided joint response has been analytically estimated and its contribution has been removed from the experimental bending moment-rotation curve;
- Then, the contribution of the web panel in shear to the double-sided joint response has been analytically estimated and its contribution has been added to the bending moment-rotation curve defined through the previous step.

Also, for the single-sided steel joints between column A and the beams, horizontal steel plates have been placed at the column web level (see *Figure II.57*) so as to avoid the buckling of the latter at the horizontal load introduction points; however, the steel plates were not present in the specimens tested in isolation at Liège University. Through the same procedure than the one described above, the influence of these plates on the joint response has been first analytically computed and then, taken into account in the bending moment-rotation curves introduced in the numerical simulations.

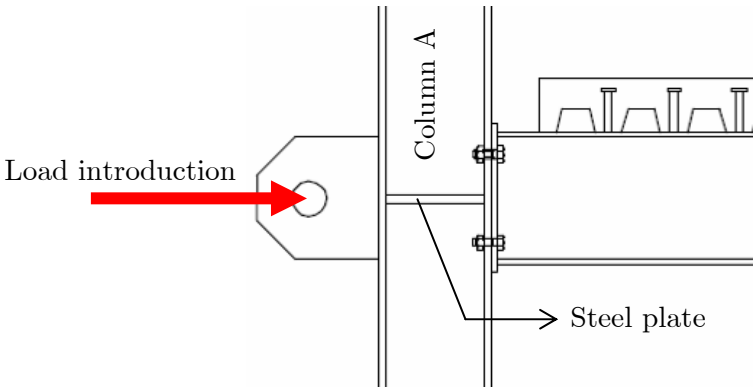

Figure II.57. Steel plate at the single-sided joints between column A and the beams

B. Frame test results

In *Figure II.58*, a scheme of the frame load setup is shown. Pretension loads of 400 kN were applied at the top of the columns; the latter simulates the loads coming from upper storeys. The upper beams were loaded by single loads of 15,7 kN at mid-span while the

lower ones with a uniformly distributed load of 3,5 kN (through sand bags). After the application of these loads, the horizontal actuator applied a displacement "s" until the collapse of the frame. The latter was executed as quasi static with an actuator speed of 2 mm/min (displacement control).

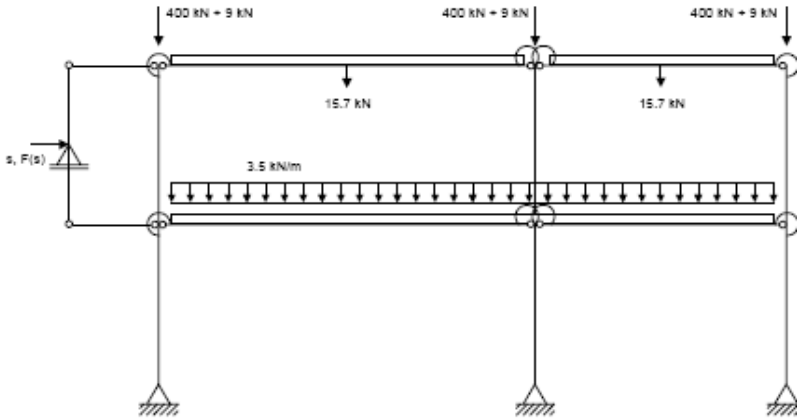

Figure II.58. Loads applied to the tested frame [1]

The failure mode which occurred during the test is a global instability mode as expected. Photos of the frame at the end of the test are given in *Figure II.59*. According the strain gauge measurements (place in the beams and in some joints components), this global instability was accompanied by yielding of some parts of the frame but the yielded zones were not sufficient to form a plastic mechanism. The applied load at the actuator vs. the horizontal displacement "s" at the actuator curve which will be used to validate the numerical tool is reported in *Figure II.60*.

Figure II.59. Deformation of the "Bochum" frame at the end of the test [1]

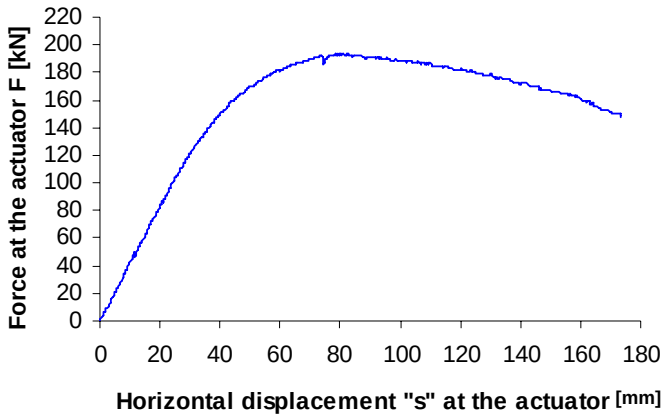

Figure II.60. Bochum test - applied load by the actuator vs. horizontal displacement "s" at the actuator curve [1]

II.4.5.4. Comparison numerical prediction vs. experimental results

As previously mentioned, the "Bochum" frame has been numerically simulated so as to validate the homemade software FINELG. The loading sequence which has been described in the previous section is also the one used for the numerical analysis. The material properties introduced in the modelling are the actual ones given in *Appendix VI.1.1*; the bending moment-rotation curves for the joints have been derived from the test results presented in the previous section and introduced within the modelling through multi-linear laws.

The comparison between the numerical prediction and the experimental result is given in *Figure II.61*. It can be observed that a good agreement is obtained between the two curves; a difference of 4,8 % is obtained for the maximum force *F*. Accordingly, this comparison permits to validate the use of FINELG to predict the response of composite sway frames

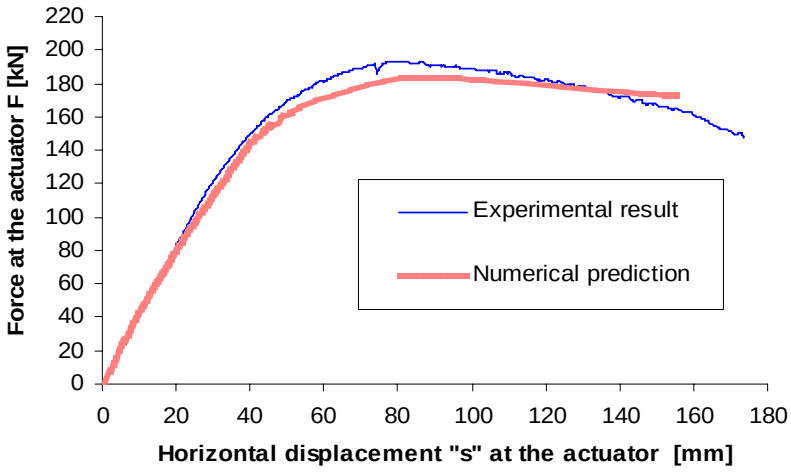

Figure II.61. Bochum test – comparison between the numerical prediction and the experimental result

II.4.6. Conclusions

In this paragraph, studies dedicated to the validation of numerical tools for the prediction of composite sway frame responses have been detailed.

In a first step, the homemade finite element software FINELG and the main modelling assumptions has been presented.

Then, a benchmark study dedicated to the FE simulation of a braced composite building tested at BRE in UK has been described; this benchmark study was coordinated by Liège University *[38]*. Through the latter, it has been demonstrated that the simulations conducted with different software (including FINELG) show a reasonably good agreement with the test results except for ABAQUS used by Labein (Spain).

In a last section, the validity of FINELG to simulate the behaviour of composite sway frames has been verified and confirmed through a comparison with experimental results obtained from a test performed at Bochum University on a composite sway frame which was designed at Liège University in collaboration with Bochum University so as to fail by global in-plane instability.

In conclusion, the studies presented in this paragraph justify its further use when investigating sway composite frames.

II.5. Numerical and analytical investigations of actual composite sway frames

II.5.1. Introduction

The studies presented in this paragraph summarize the investigations presented in *[11]*. The objective of this work was to analyse the behaviour of sway composite frames under static loading through numerical analyses and to investigate the applicability of simplified analytical methods initially developed for steel sway frames (see *§ II.2.2.5*) to composite ones.

Through the previous paragraph, it has been demonstrated that the homemade finite element software FINELG can be used with a good confidence to investigate the behaviour of composite sway structures. Also, the analytical method (i.e. the component method) to predict the bending moment-rotation curve of steel and composite joints which has been extended and validated in *§ II.3* is used to compute the behavioural curves of the joints met in the investigated structures.

Different numerical analyses on actual composite sway buildings submitted to horizontal and vertical static loads with the so-validated FINELG software have been first performed so as to understand their behaviour and to highlight some particularities. The performed numerical investigations respect the assumptions presented in *§ II.4.3*. These investigations are summarised in *§ II.5.2*.

Then, the applicability to composite sway structures of two simplified analytical methods is investigated in *§ II.5.3*: the "Amplified sway moment method" and the "Merchant-Rankine approach", initially developed for steel structures and respectively based on elastic and plastic design philosophies.

As already mentioned, composite sway structures present a particularity according to steel ones: the concrete cracking. This phenomenon leads to an amplification of the lateral deflections and, consequently, to an amplification of the second-order effects, which reduces the ultimate resistance of the frames. In other words, for a same number of hinges formed at a given load level in a steel frame and in a composite frame respectively, larger sway displacements are reported in the composite one.

In *[42]*, it is proposed to take into account of this phenomenon in the simplified design methods through the computation of a cracked critical load factor (i.e. the concrete is assumed to be cracked in the hogging moment zones by assuming that the concrete has no stiffness when loaded in tension) instead of an uncracked one (i.e. the concrete is assumed to be uncracked in the hogging moment zones even if the concrete is loaded in tension in these regions). The simplified analytical methods studied here will be applied with these two values so as to compare the so-predicted results and to know if the observations made in *[42]* can be extended to the structures studied herein.

II.5.2. Numerical investigations of actual composite sway frames

Five actual composite buildings have been studied herein:

- the "Ispra" building;
- the "Bochum" building;
- the "UK" building;
- the "Eisenach" building;
- and the "Luxembourg" building.

The three first ones are full-scale buildings which have been tested in European laboratories, the "Eisenach" building is a factory in Germany and the last one is a bank in

Luxembourg. The difficulty in this task was to collect, for each building, enough data such as those on geometry, material properties and joint details; these ones strongly influence the global structural response. These buildings are described in detailed in *Appendix VI.4.*

The different analyses which have been performed on these structures are the following:

- Critical elastic analyses with, as previously mentioned, two different assumptions with regards to the concrete cracking:
    - in the first case, the concrete is assumed to be uncracked all along the beam and to have the same stiffness in tension than in compression (→ $\lambda_{cr,uncracked}$);
    - in the second case, the concrete is assumed to be cracked when loaded in tension by assuming that the concrete has no stiffness in these zones (→ $\lambda_{cr,cracked}$).
- First-order and second-order plastic analyses (→ λ_p).
- Non-linear analyses (→λ_e when the first plastic hinge is formed and λ_u when the failure of the structure is reached)

As previously mentioned, the assumptions presented in *§ II.4.3* have been respected to model the structures. However, for the Bochum structure modelling, the strain hardening of the steel materials has been taken into account, what is not in line with these assumptions.

The results obtained through these different analyses are summarized for each studied structures in *Table II.19.*

Table II.19. Summary of the obtained results through the numerical investigations

Building	$\lambda_{cr,uncracked}$	$\lambda_{cr,cracked}$	λ_p	**Plastic mechanism associated to λ_p**	λ_e	λ_u	**Failure associated to λ_u**
Ispra	6,49	5,95	1,84	beam	1,61	1,79	global instability
Bochum	9,83	9,42	1,82	panel	1,26	1,41	global instability
Eisenach	4,35	4,27	1,55	beam	1,14	1,14	panel plastic mechanism
UK	9,31	8,77	2,36	combined	1,71	2,01	global instability
Luxembourg	5,15	4,62	1,58	beam	0,99	1,21	panel plastic mechanism

From this table, the following remarks may be drawn:

- All the computed critical load factors are smaller than 10; in other words, the V_{Ed}/V_{cr} $(= \lambda_{Ed}/\lambda_{cr})$ ratios for all the studied structures are higher than 0.1. So, these structures can be classified as sway if reference is made to the Eurocode 4 or the Eurocode 3 criteria (see *§ II.2.3* and *§ II.2.2.3.B* respectively) and that for elastic and plastic analyses.

- When the failure associated to λ_u is a global instability phenomenon, it can be observed that the load factor at which it occurs is significantly smaller than the elastic critical load factor. This demonstrates the great influence of the yielding of the structure on the instability phenomena.

- For the "Eisenach" and the "Luxembourg" buildings, the failure associated to λ_u is a panel plastic mechanism while the one associated to λ_p is a beam one. This can be explained by the fact that panel plastic mechanisms are strongly influenced by the second-order effects while the latter have no significant effects on the beam ones. This phenomenon is illustrated in *Figure II.62* and in *Figure II.63* for the "Eisenach" and "Luxembourg" buildings respectively; indeed, these figures show that the results obtained through the second-order rigid-plastic analyses (determined through an analytical computation) and the non-linear ones (obtained through the software FINELG) are in good agreement (i.e. the failure of the frame obtained through a non-linear analysis is reached when the "non-linear curve" in the load – top displacement graph intersects the "second-order rigid-plastic curve" associated to the panel mechanism). More details about this phenomenon can be found in *[11]*.

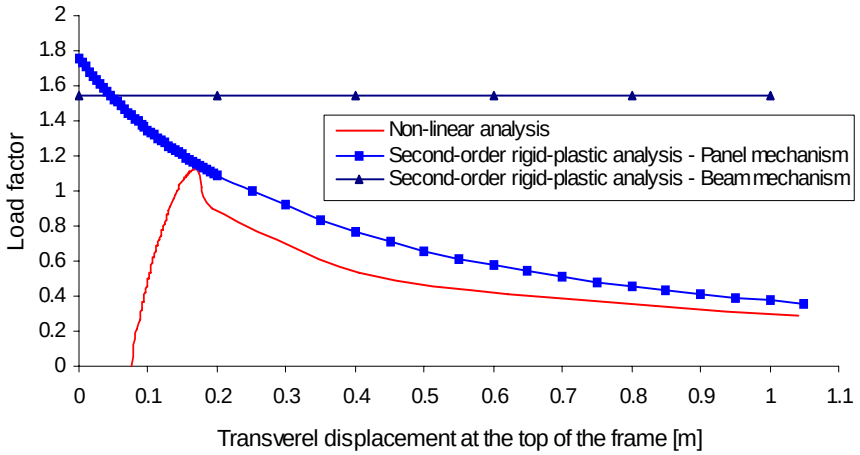

Figure II.62. Second-order effects in the "Eisenach" building

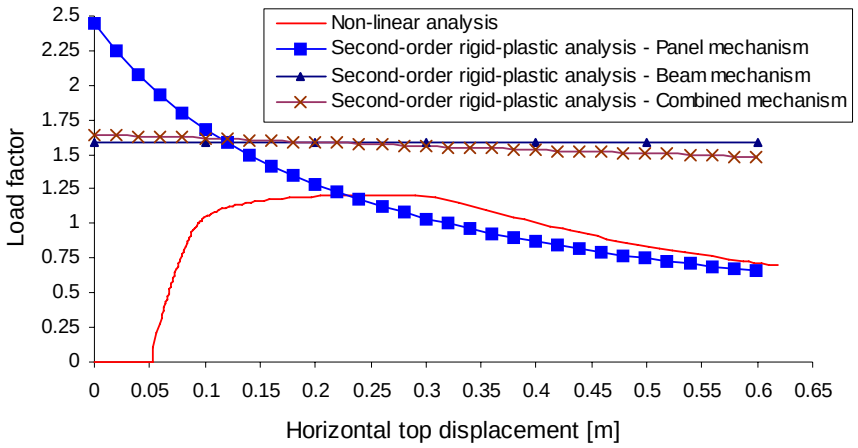

Figure II.63. Second-order effects in the "Luxembourg" building

From the numerical studies performed on the five above-mentioned composite sway buildings (presented in *[11]* and summarised in this paragraph), it has been demonstrated that the general behavioural response of such structures to static vertical and horizontal loads is quite similar to the one exhibited by steel sway frames. Starting from this observation, the applicability to composite sway frames of simplified analytical methods initially dedicated to steel ones is investigated in the next section.

II.5.3. Applicability of simplified analytical methods

II.5.3.1. Introduction

Several simplified analytical methods exist for the study of steel sway frames and some of them are presented in *§ II.2.2.5*. The objective here is to investigate whether and how these design procedures can be generalized to composite sway frames. Two of these methods are focused on in the following sections: the amplified sway moment method (*§ II.2.2.5.B*) and the Merchant-Rankine approach (*§ II.2.2.5.D*).

The applicability of the other simplified analytical methods presented in *§ II.2.2.5* is not investigated herein, what is justified here below:

- The applicability of the wind moment method to composite sway frames (see *§ II.2.3*) has already been investigated in a PhD thesis of Nottingham University *[17]*; in the latter, it was demonstrated that the remarks concerning the application of this method to steel sway frames presented in *§ II.2.2.5.F* are still valid for composite ones. In addition, this method is closer to a pre-design method than to an analytical one and it is then difficult to use it so as to predict a failure load factor. So, this method is no more investigated herein.

- The sway-mode buckling length method (see *§ II.2.2.5.C*) gives too safe results for steel sway frames, which explains the fact that this method is rarely used for such frames. Accordingly, this method is not investigated herein.
- In *[16]*, it was demonstrated that the simplified second-order plastic analysis is equivalent to the Merchant-Rankine approach if this method is used so as to determine the ultimate load factor λ_u.

The predicted values will be compared to the "non-linear" ones obtained through the numerical investigations presented in the previous chapter (considered as "reference" results).

Also, the Merchant-Rankine approach cannot be applied to the "Bochum" structure in a straightforward way, as the latter is based on the concept of "proportional loading"; an alternative method is nevertheless developed and analysed in this section to assess the ultimate load factor of the "Bochum" structure.

II.5.3.2. Amplified sway moment method ("ASMM")

This method is applied to the here-above mentioned frames so as to predict the elastic load factor λ_e at which a first plastic hinge forms. As said previously, the influence of concrete cracking on the results predicted by this method is investigated through the computation of 2 critical load factors: "cracked" and "uncracked" (computed through the software FINELG). The results are presented in *Table II.20*, in *Table II.21* and in *Figure II.64* where the so-predicted values are compared to the ones numerically obtained through the previously mentioned numerical investigations.

Table II.20. Comparison between the non-linear analysis results and the "ASMM" predictions (with $\lambda_{cr,uncracked}$)

Structures	$\lambda_{cr,uncracked}$	$\frac{1}{1-\frac{V_{Ed}}{V_{cr}}}$	λ_e **"ASMM"**	λ_e **Non-linear analysis**	**Difference (in %)**
"Ispra" building	6,49	1,18	1,56	1,61	3,1
"Bochum" building	9,83	1,11	1,21	1,26	4
"Eisenach" building	4,33	1,3	1,18	1,14	-3,4
"UK" building	9,31	1,12	1,63	1,71	4,7
"Luxembourg" building	5,15	1,24	0,96	0,99	3,4

Table II.21. Comparison between the non-linear analysis results and the "ASMM" predictions (with $\lambda_{cr,cracked}$)

Structures	$\lambda_{cr,cracked}$	$\frac{1}{1-\frac{V_{Ed}}{V_{cr}}}$	λ_e **"ASMM"**	λ_e **Non-linear analysis**	**Difference (in %)**
"Ispra" building	5,95	1,20	1,55	1,61	3,7
"Bochum" building	9,42	1,12	1,20	1,26	4,9
"Eisenach" building	4,27	1,31	1,18	1,14	-3,4
"UK" building	8,77	1,13	1,63	1,71	4,7
"Luxembourg" building	4,62	1,28	0,95	0,99	4

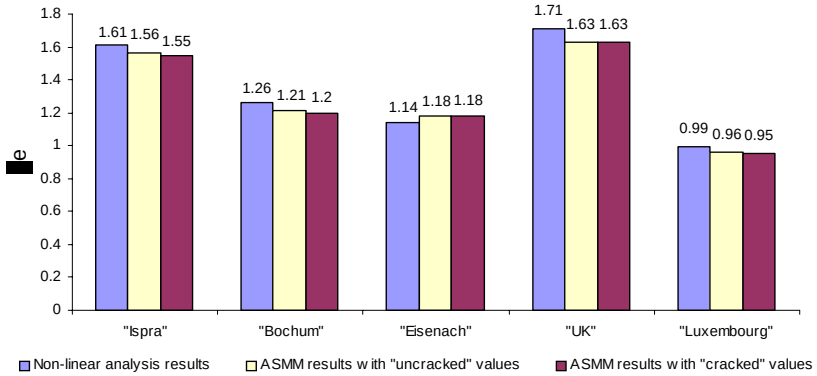

Figure II.64. Comparison between the results numerically obtained and the "ASMM" results

Through these investigations, it is demonstrated that:

- The values predicted by the amplified sway moment method are in very good agreement with the ones numerically obtained; indeed, the maximum difference is equal to 4.9 % for the "Bochum" building.
- All the predicted values are on the safe side with regards to the numerical ones (except for the "Eisenach" building).
- The formation of the first plastic hinge occurs, for all the studied frames, at the same location through the "ASMM" and through the non-linear analysis.
- The assumption concerning the concrete cracking has no significant influence on the values predicted by the "ASMM".

So, accordingly, it can be concluded that the amplified sway moment method can be applied with confidence to sway composite structures with no needs to introduce the concrete cracking in the computation of λ_{cr}.

As previously mentioned, the critical load factor λ_{cr} has been computed through FINELG, which constitutes a precise way to compute this value. If reference is made to Eurocode 4

[6] (which makes reference to Eurocode 3 *[12]*), a simplified method is proposed to compute the critical load factor through the following formula:

$$\lambda_{cr} = \min(\alpha_{cr,i}) \text{ with } \alpha_{cr,i} = \left(\frac{H_{Ed,i}}{V_{Ed,i}}\right).\left(\frac{h_i}{\delta_{H,Ed,i}}\right) \text{ with i = 1 to } n \qquad (2.24)$$

where (see *Figure II.65*) i is the number of the storey under consideration, $H_{Ed,i}$ is the design value of the horizontal reaction to the horizontal loads at the bottom of storey i, $V_{Ed,i}$ is the total design vertical load on the structure at the bottom of storey i, $\delta_{H,Ed,i}$ is the horizontal displacement at the top of storey i, relative to the bottom of storey i, when the frame is loaded with horizontal loads which are applied at each floor level, h_i is the height of storey i and n is the total number of storeys.

If *Formula (2.24)* is used to compute the critical load factor of the investigated building frames and if the latter is used in the "ASMM", the obtained results are still in good agreement with the results obtained through the non-linear analyses performed with FINELG as illustrated in *Figure II.66*.

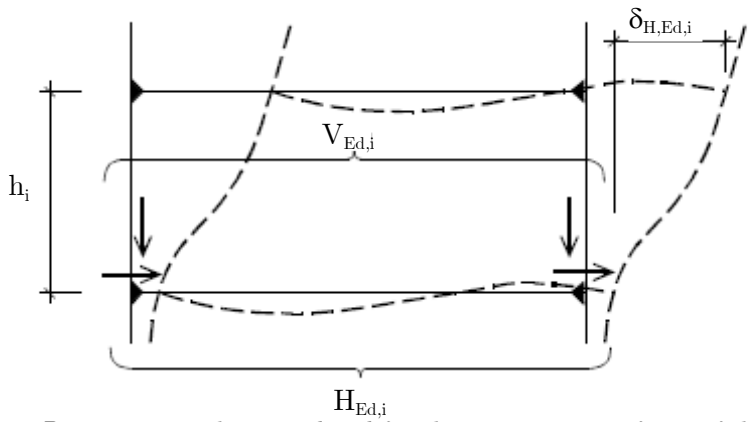

Figure II.65. Parameters to be considered for the computation of $\alpha_{cr,i}$ of the storey i [12]

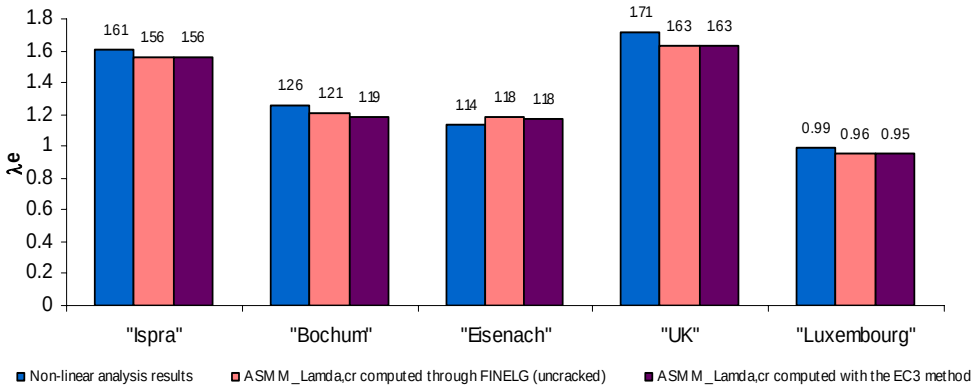

Figure II.66. Comparison between the results numerically obtained and the "ASMM" results with λ_{cr} analytically computed with the Eurocode 4 method

II.5.3.3. Merchant-Rankine approach ("MR")

The Merchant-Rankine approach allows assessing the ultimate load factor through a formula that takes account of interactions between plasticity (λ_p) and instability (λ_{cr}) in a simplified and empirical way (see *Formula (2.10)* in *§ II.2.2.5.D*). Again, this method is applied to the five reference frames.

However, this method cannot be applied to the "Bochum" frame in a straightforward way as it is characterised by a non-proportional loading and this is in opposition with the Merchant-Rankine approach which covers proportional loading. To bypass this problem, an alternative method is developed so as to estimate the ultimate load factor of such frames, with due account of their actual loading path. This method is detailed later on in this section.

As for the amplified sway moment method, the influence of the concrete cracking on the critical load factor when predicting ultimate load factors through the Merchant-Rankine approach is also investigated.

The results obtained for 4 of the 5 frames characterised by a proportional loading are presented and compared in *Table II.22*, in *Table II.23* and in *Figure II.67*.

Table II.22. Comparison between the non-linear analysis results and the "MR" predictions (use of $\lambda_{cr,uncracked}$)

Structures	λ_p	$\lambda_{cr,uncracked}$	λ_u **"MR"**	λ_u **Non-linear analysis**	**Difference (in %)**
"Ispra" building	1,84	6,49	1,43	1,79	20,1
"Eisenach" building	1,545	4,33	1,139	1,138	-0,1
"UK" building	2,36	9,31	1,88	2,01	6,5
"Luxembourg" building	1,58	5,15	1,210	1,209	-0,2

Table II.23. Comparison between the non-linear analysis results and the "MR" predictions (use of $\lambda_{cr,cracked}$)

Structures	λ_p	$\lambda_{cr,cracked}$	λ_u **"MR"**	λ_u **Non-linear analysis**	**Difference (in %)**
"Ispra" building	1,84	5,95	1,41	1,79	21,2
"Eisenach" building	1,545	4,27	1,137	1,138	0,1
"UK" building	2,36	8,77	1,86	2,01	7,5
"Luxembourg" building	1,58	4,62	1,181	1,209	2,3

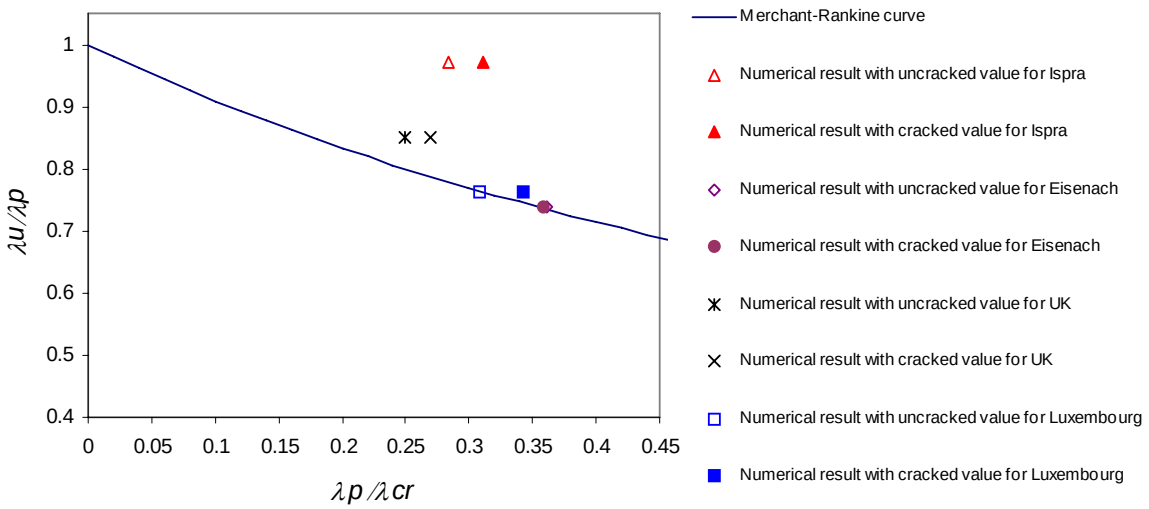

Figure II.67. Comparison between the "MR" curve and the results numerically obtained

First, it can be observed on this figure that all the points does not enter in the field of application of the Merchant-Rankine approach as defined in *§ II.2.2.5.D* ($\lambda_p/\lambda_{cr} \in [0.1;0.25]$); however, the studied frames are not too far from this domain.

A rather good agreement between numerical simulations and the "MR" calculation model seems to be obtained, except for the "Ispra" building. In *Figure II.67*, it can be observed that the use of the $\lambda_{cr,cracked}$ value instead of the $\lambda_{cr,uncracked}$ one permits to pass from the unsafe to the safe side of the graph (the points corresponding to the "Luxembourg" and the "Eisenach" buildings pass from the lower to the upper part of the graph according to the "MR" curve), which confirms the observations presented in *[42]*.

However, the obtained results have to be discussed:

- The somewhat too safe character of the "MR" approach for the "Ispra" building results from the nature of the first-order rigid-plastic mechanism, which corresponds to the plastic failure of a beam; the same phenomenon was also observed for steel structures presenting a beam plastic mechanism through a first-order rigid-plastic analysis (see *§ II.2.2.5.D*). In fact, the formation of plastic beam mechanisms is not affected in a significant way by the second-order effects which can justified the too conservative result obtained through the "MR" approach.
- The good prediction of the ultimate load factor through the "MR" approach for the "UK" building results of the nature of the first-order rigid-plastic mechanism, which is a combined one. Again, the same phenomenon was observed for steel structures presenting such first-order rigid-plastic mechanism.
- It can be observed that the "MR" approach gives very good results for the "Eisenach" and "Luxembourg" buildings although the plastic mechanism

associated to a first-order rigid-plastic analysis is a beam one. This observation seems to be in contradiction with the obtained results for steel structures. In fact, if reference is made to the numerical investigations presented in the previous chapter, it was shown that the failure of these frames through a non-linear analysis is associated to the formation of panel mechanisms influenced by the second-order effects. So, the first-order rigid-plastic load factor associated to a beam plastic mechanism, which is involved in the "MR" approach, does not correspond to the plastic mechanism occurring at failure. It can be then concluded that the good agreement between the "MR" predictions and the non-linear analysis results for these two structures occurs quite by chance; for instance, if the second-order effects had a greater influence on the behaviour of these structures and especially on the formation of the panel plastic mechanism, the "MR" approach could have given unsafe results.

For the non-proportionally loaded "Bochum" structure, an alternative method which enables to estimate the ultimate load factor with account of the loading sequence is proposed. This alternative method consists:

- in deriving a "MMR" interaction curve in a "V – H" diagram (*Figure II.68*), V and H being respectively the total vertical and horizontal applied loads at failure;
- in reporting in this diagram the actual loading path followed during the test (see *Figure II.53* in *§ II.4.5.2*);
- in defining the failure load at the intersection between the "MMR" interaction curve and the one representing the actual loading path.

For the Bochum frame, the modified Merchant-Rankine approach (MMR – see *Formula (2.12)* is used as the strain hardening effect is taken into account in the numerical investigations (see *§ II.5.2*).

This approach is based on the assumption that the ultimate load factor of a structure is independent of the loading history; this is not theoretically exact but it usually appears as acceptable.

In practice, the "MMR" interaction curve is obtained as follows:

- first, the V and H loads in *Figure II.68* are normalised by dividing them by their values V_{serv} and H_{serv} at serviceability limit state, respectively 1262,4 kN and 100 kN (see *§ II.4.5.2*);
- in a second step, different load combinations between V_{serv} and H_{serv} are considered (i.e. 0,5 V_{serv} + H_{serv} or V_{serv} +0,5 H_{serv} or ...);

- for each particular load combination, the corresponding vertical and horizontal service loads are then assumed to be proportionally increased until failure (load factor λ_{prop}); through this assumption, the critical load factor ($\lambda_{prop,cr}$) and the first-order rigid-plastic load factor ($\lambda_{prop,p}$) are computed and an estimation of the ultimate load factor ($\lambda_{prop,u}$) is derived, for each load combination, by means of the "MMR" approach;
- finally, the ultimate load factors are reported in the "$V - H$" diagram so as to obtain the MMR interaction curve.

The "MMR" interaction curve computed for the "Bochum" structure is presented in *Figure II.68* (curve "DIAC"). The points reported on this graph have been computed with $\lambda_{cr,cracked}$ values as it has been demonstrated previously that the use of the latter in the MR approach sometimes permits to pass from the unsafe to the safe side.

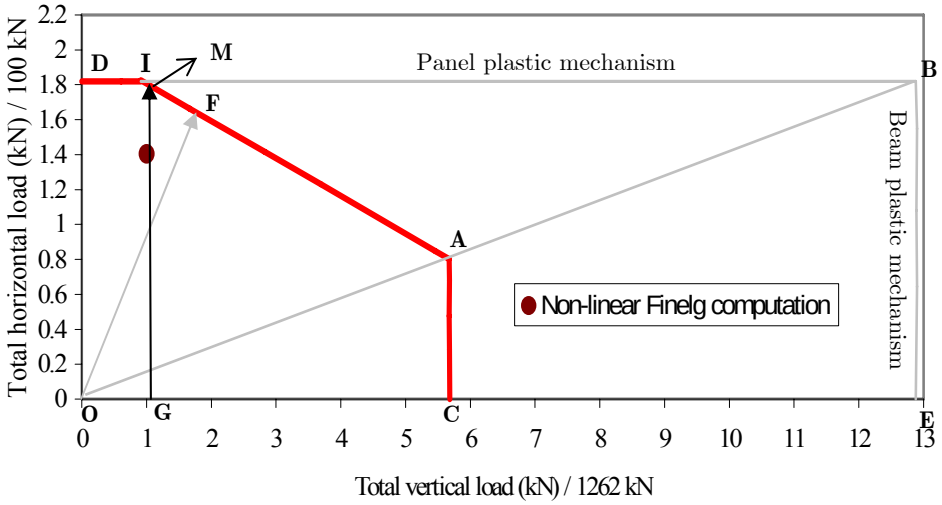

Figure II.68. "MMR" interaction curve

The curve "DBE" corresponds to the first-order rigid-plastic resistance interaction curve; the horizontal line "DB" relates to the development of a first-order panel plastic mechanism ($\lambda_{prop,p}$ only depends on the horizontal loads) and the vertical line "BE" to the development of a beam plastic mechanism in beam A (see *Figure II.51* in *§ II.4.5.2*) ($\lambda_{prop,p}$ only depends on the vertical loads). In *Figure II.68,* the diagram is seen to be separated in two zones by the line "OAB":

- development of a first-order rigid-plastic panel mechanism for load combinations relative to the upper part of the diagram;
- development of a first-order rigid-plastic beam mechanism in beam A for load combinations relative to the lower part of the diagram.

Figure II.68 shows that no combination of V and H leads to the development of a combined plastic mechanism, as far as the "Bochum" structure is concerned.

The shape of the "MMR" interaction curve presented in *Figure II.68* can be explained as follows:

- When no vertical loads are applied to the structure, the ultimate load factor $\lambda_{prop,u}$ corresponds to the development of a panel plastic mechanism (point "D"); no instability phenomena occur as no vertical loads are applied. In this case, $\lambda_{propr,u}$ is equal to 1,82 (H = 182 kN), which is equal to the first-order rigid-plastic load factor λ_p.
- For small vertical loads, a panel plastic mechanism still appears at failure (line "DI"). This indicates that second-order effects are quite negligible in this loading range.
- Beyond point "I", second-order effects can no more be neglected and the "MMR" computed values $\lambda_{prop,u}$ reduce when the importance of the vertical loads in the load combinations increases. At point "I", the ratio $\lambda_{cr,cracked}/\lambda_p$ is equal to 10.
- When no horizontal loads are applied to the structure, the first-order rigid-plastic load factor corresponds to the development of a beam mechanism ($\lambda_{prop,p}$ = 12,88); the "MMR" ultimate load factor $\lambda_{prop,u}$, which is equal to 5,68, takes into account the interaction between the plasticity and the instability phenomena under high vertical loads.
- The value $\lambda_{prop,u}$ is constant and equal to 5,68 when the first-order rigid-plastic mechanism is a beam one (vertical line "CA" of the "MMR" interaction curve) as, in this specific case, λ_p, and therefore the "MMR" load factor, are strictly depending on the vertical loads.

For the "Bochum" structure, if the service loads were proportionally increased (loading path "OF"), an ultimate load factor $\lambda_{prop,u}$ equal to 1,66 would be found by means of the "MMR" approach (V = 2095,6 kN and H = 166 kN). But, as stated in *§ II.4.5.2*, this is not the case and therefore the load factor $\lambda_{prop,u}$ equal to 1,66 can not be compared with the one (λ_u = 1,41) obtained by means of FINELG (*§ II.5.2); *indeed, the latter has not been computed with a proportional loading, but with the actual one.

The actual loading path is represented in *Figure II.68* by the arrow "OGM". At its intersection with the interaction curve, a "MMR" estimated failure load multiplier λ_u equal to 1,8 is derived, which may be now compared to the FINELG numerical result. The difference between the two approaches is equal to 22 % and the analytical predicted value is seen to be quite unconservative. Such a conclusion has already been drawn from

previous studies on steel structures characterised by the development of a first-order rigid-plastic panel mechanism.

Through the investigations performed within the present section, it is finally demonstrated that the conclusions which were drawn for steel sway structures *[15]* are still appropriate for the composite ones:

- safe for beam plastic mechanisms;
- adequate for combined plastic mechanisms;
- unsafe for panel plastic mechanisms.

II.5.3.4. Conclusions

In this chapter, the applicability of the "Amplified sway moment method" and the "Merchant-Rankine approach" (respectively based on elastic and plastic design philosophies) to composite sway structures has been investigated. Also, the influence on the accuracy of these methods of the chosen assumption with regards to the concrete cracking in the computation of the elastic critical load factor has been investigated.

First, for the "amplified sway moment method", it has been demonstrated that:

- The chosen assumption concerning the concrete cracking for the computation of λ_{cr} has no significant influences on the predicted value through this method for the studied cases.
- A good accuracy of this method is obtained when applied to sway composite structures; the maximum difference between the amplified sway moment method results and the numerically obtained results (results obtained through a non-linear analysis) is equal to 4.9 %, which is reasonable.
- The simplified method proposed in Eurocode 3 for the computation of λ_{cr} permits to obtain an accurate prediction of the latter which, consequently, do not significantly affect the accuracy of the amplified sway moment method.

Secondly, the applicability of the Merchant-Rankine approach has been investigated and it has been shown that:

- The conclusions concerning the accuracy of this method which were drawn for steel sway structures *[15]* still appropriate for the composite sway structures:
  - safe for beam plastic mechanisms;
  - adequate for combined plastic mechanisms;
  - unsafe for panel plastic mechanisms.

- The use of the $\lambda_{cr,cracked}$ value instead of the $\lambda_{cr,uncracked}$ one in the Merchant-Rankine approach permits, for some cases, to pass from the unsafe to the safe side for the estimation of the λ_u with respect to the non-linear analysis results; this result is in agreement with the conclusions of a previous work *[42]*.
- The nature of the plastic mechanism considered in the Merchant-Rankine does not always correspond to the one occurring at failure of the frame (computed through a non-linear analysis); this phenomenon is due to the second-order effects which differently influence the yielding of the structure according to the nature of the considered plastic mechanism.

Finally, an alternative method for the estimation of the ultimate load factor of frames subjected to a non-proportional loading, which is the case of the "Bochum" structure investigated herein has been proposed and described in details.

According the lack of accuracy and sometimes the unsafe character of the "Merchant-Rankine approach", a new simplified analytical method able to predict the ultimate load factor of a steel or composite sway frame is developed and validated in the next paragraph.

II.6. Development of a simplified design method for steel and composite sway frames

II.6.1. Introduction

For the Merchant-Rankine approach, it has been shown in the previous paragraph that the plastic mechanism associated to the plastic load factor introduced in the Merchant-Rankine formula does not always correspond to the one occurring at failure of the frame which can lead to an unsafe prediction of the ultimate load factor. This phenomenon is associated to the fact that the different types of plastic mechanisms are not affected the same way by the second-order effects developing in a structure.

The solution proposed here is to develop a procedure based on three formulas, one for each type of plastic mechanisms which could appear in the studied frame (i.e. beam, panel and combined plastic mechanisms):

- Formula1($\lambda_{p,beam}$, λ_{cr}) → $\lambda_{u,beam}$;
- Formula2($\lambda_{p,panel}$, λ_{cr}) → $\lambda_{u,panel}$;
- Formula3($\lambda_{p,combined}$, λ_{cr}) → $\lambda_{u,combined}$.

Through these formulas, three predicted ultimate load factors are computed; the smallest one is then considered as the ultimate load factor of the studied frame: $\lambda_u = \min(\lambda_{u,beam}, \lambda_{u,panel}, \lambda_{u,combined})$.

These new formulas could be developed from the Merchant-Rankine one; in fact, the actual Merchant-Rankine formula could be used as "Formula3" as it was demonstrated herein and in previous studies on steel sway frames *[15]* that this formula gives satisfactory results for frames with a the first-order rigid-plastic mechanism associated to a combined one. Nevertheless, it is chosen to develop these formulas from the Ayrton-Perry formulation (see *Table II.24*), which is already used in the Eurocodes to treat the member instability phenomena (plane buckling, lateral buckling and lateral torsional buckling); this proposal is in agreement with the recommendation of the last draft of Eurocode 3 *[12]* where it is stated that such formulation should be used to verify "*the resistance to lateral and lateral torsional buckling for structural components such as single members (built-up or not, uniform or not, with complex support conditions or not) or plane frames or subframes composed of such members which are subject to compression and/or mono-axial bending in the plane...*" (*§ 6.3.4 (1)* of Eurocode 3 *[12]*). A great advantage is that the Ayrton-Perry formulation implicitly permits to respect the limit conditions which are:

- when λ_{cr} is very high, no instability phenomena will appear and the failure occur through the appearance of a plastic mechanism ($\lambda_u \rightarrow \lambda_p$);
- when λ_p is very high, no yielding appears in the frame and the failure occurs through an instability phenomenon ($\lambda_u \rightarrow \lambda_{cr}$).

Table II.24. From the Ayrton-Perry formulation to the formulas to be included in the new simplified analytical design method

Ayrton-Perry formulation – Eurocode 3 *[12]*	**Formulas included in the new simplified design method for sway frames**
$N_{b,Rd} = \dfrac{\chi \alpha_{ult,op}}{\gamma_{M1}}$	$\lambda_u = \chi \lambda_p$
$\chi = \dfrac{1}{\phi + \sqrt{\phi^2 - \overline{\lambda}_{op}^{\,2}}}$	$\chi = \dfrac{1}{\phi + \sqrt{\phi^2 - \overline{\lambda}_{op}^{\,2}}}$
$\overline{\lambda}_{op} = \sqrt{\dfrac{\alpha_{ult,k}}{\alpha_{cr,op}}}$	$\overline{\lambda}_{op} = \sqrt{\dfrac{\lambda_p}{\lambda_{cr}}}$
$\phi = 0,5\left[1 + \alpha(\overline{\lambda}_{op} - \overline{\lambda}_0) + \overline{\lambda}_{op}^{\,2}\right]$	$\phi = 0,5\left[1 + \mu(\overline{\lambda}_{op} - \overline{\lambda}_0) + \overline{\lambda}_{op}^{\,2}\right]$

Within this formulation, χ is called the reduction factor and $\overline{\lambda}_{op}$ the non-dimensional relative slenderness. The parameter $\overline{\lambda}_0$ represents the length of the plateau in a $\overline{\lambda}_{0p}$ - χ graph when χ equal to 1 (see *Figure II.69*), i.e. the length on which the ultimate resistance is assumed to be equal to the plastic resistance and, accordingly, where the influence of the second-order effects is neglected; as no strain hardening and cladding effects are considered within the thesis, the plateau length will be taken equal to 0 as in the Merchant-Rankine approach.

So, to develop this new method, only the parameter μ has to be determined. The parameter μ is used to implicitly take into account of the second order effects within the developed procedure. In fact this parameter influences the shape of the curve presented in *Figure II.69*; the highest μ is, the smallest the reduction factor χ is and, accordingly, the smallest the predicted λ_u is.

Three values of the parameter μ have to be calibrated, one for each plastic mechanism (i.e. μ_{beam} for the beam plastic mechanism, $\mu_{combined}$ for the combined plastic mechanism and μ_{panel} for the panel plastic mechanism), as each type of plastic mechanisms are influence differently by the second order effects. These values will be calibrated through parametrical studies. At the end of this calibration, it is intended to obtain a higher value of μ for the panel plastic mechanism than the one for the combined plastic mechanism and the latter higher than the one for the beam plastic mechanism ($\rightarrow \mu_{panel} > \mu_{combined} > \mu_{beam}$). Indeed, it has been shown previously that the influence of the second order effects is more important for the panel plastic mechanism than for the combined one and is not significant for the beam plastic mechanism.

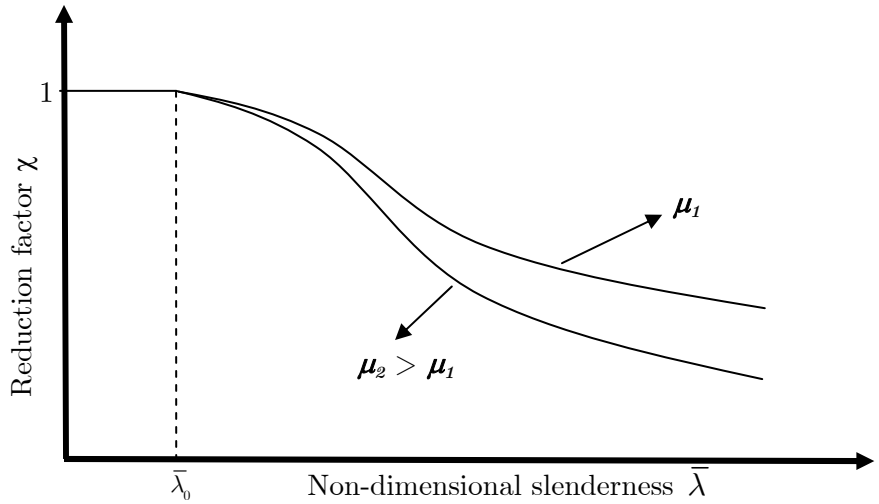

Figure II.69. Example of "Ayrton-Perry" curves

As the same problems of accuracy are met with the Merchant-Rankine approach for steel and composite sway frames, the proposed method will be developed for steel sway frame in

§ II.6.2 and for composite sway frames in *§ II.6.3*. Then, in *§ II.6.4*, the developed method will be applied to the actual composite frames investigated in the previous paragraph. In these sections, the method presented here is called "New method".

II.6.2. Parametrical study on steel sway frames

II.6.2.1. Introduction

The parametric study presented here has been realised in strong collaboration with a Vietnamese student Tuyen Van Nguyen *[43]*. Within the thesis, four types of 2-D "academic" simple frames are investigated (from *Figure II.70* to *Figure II.73*); in total, 181 frames are analysed.

The beams and the columns are steel hot-rolled profiles of class 1 (to be able to develop plastic mechanism) bent around their major axis; the steel material is modelled through a bilinear law. The finite element is the same than the one used for the modelling of the composite structures and is presented in *§ II.4.3* (*Figure II.44*).

The beam-to-column joints are partial-strength and semi-rigid ones with a sufficient ductility to develop plastic hinges (modelled through a bilinear law – see *Figure II.30*) and to allow plastic analyses; they are modelled with rotational springs. The column base joints are assumed to be rigid and fully resistant. The properties of the frames have been defined so as to cover the three types of plastic mechanisms, i.e. beam, combined and panel plastic mechanisms (obtained through first-order rigid-plastic analyses) with each type of structures and to obtain different types of collapse modes (plastic mechanisms or instability) through the full non-linear analyses. The parameters which are modified within these frames are:

- the height of the columns;
- the properties of the joints;
- the beam and column cross sections and;
- the applied loads.

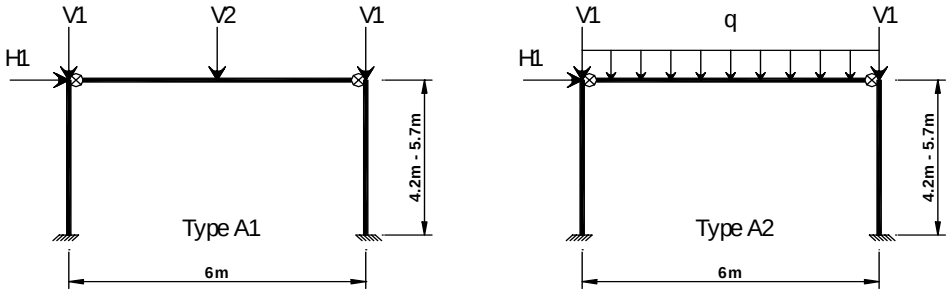

Figure II.70. Structure type A [43]

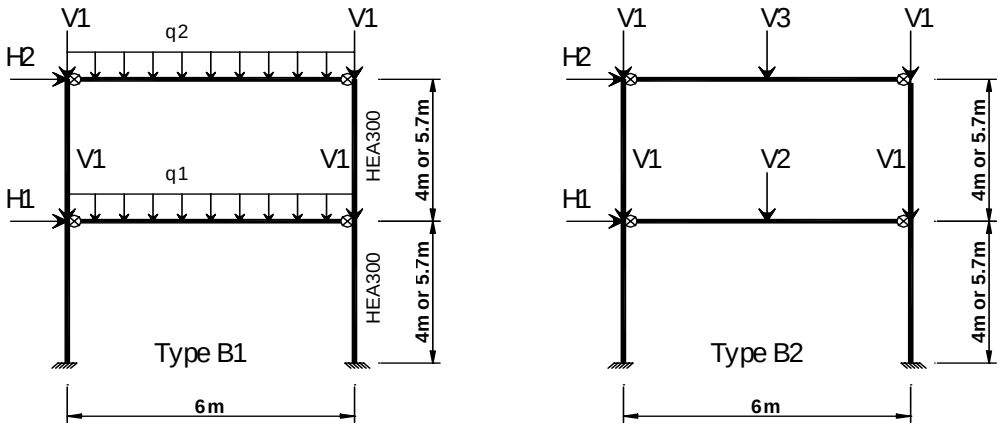

Figure II.71. Structure type B [43]

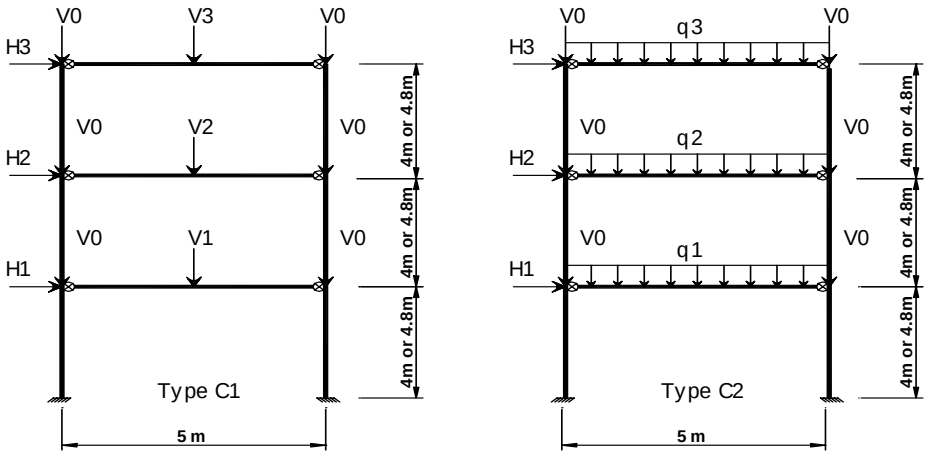

Figure II.72. Structure type C [43]

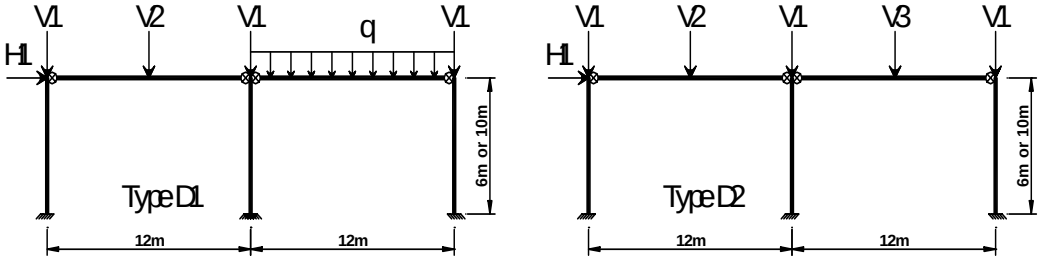

Figure II.73. Structure type D [43]

For all these structures, the serviceability limit states have been checked and the displacements respect the limitations recommended in *Table II.3*.

The types of analyses which have been performed are:

- Critical elastic analyses (λ_{cr});
- First-order rigid-plastic analyses (computation of the three plastic load factors, i.e. $\lambda_{p,beam}$, $\lambda_{p,combined}$ and $\lambda_{p,panel}$);
- Full non-linear analyses (λ_u).

For the computation of λ_{cr} and λ_u, the software FINELG is used. As recommended in Eurocode 3 *[12]*, an initial deformation is introduced in the computation (see *Figure II.5* in *§ II.2.2.3*). A formula is proposed in Eurocode 3 *[12]* so as to estimate a value for the initial out-of-plumb ϕ to impose to the structure:

$$\boldsymbol{\Phi}_{ini} = \alpha_m \, \alpha_h \, \boldsymbol{\Phi}_0 \tag{2.25}$$

where:

- $\boldsymbol{\Phi}_0 = 1/200$ (2.26)
- $\alpha_h = \frac{2}{\sqrt{h_{struc}}}$ but $\frac{2}{3} \leq \alpha_h \leq 1$ (2.27)
- $\alpha_m = \sqrt{0,5.(1+\frac{1}{m})}$ (2.28)

with h_{struc}, the total height of the structure in meters and m, the number of columns in a row including only those columns which carry a vertical load N_{Ed} not less than 50 % of the average value of the loads supported by the columns in the vertical plane considered.

The shape of the initial deformation introduced in the computations is proportional to the first global instability mode obtained through the critical elastic analysis (which is in agreement with the Eurocode recommendations); this permits to introduce at the same time a global initial deformation (to initiate *P-Δ* effects) and local initial deformations for the members (to initiate *P-δ* effects). In practice, the FINELG software produces a first global instability mode with a displacement at the top of the structure equal to the unity; so, to introduce the initial deformation in the computations, this mode is multiplied by $\phi_{ini}.h_{struc}$ where ϕ_{ini} is the initial out-of-plumb computed through *Formula (2.25)*. For the computation of the plastic load factors, a software (based on an Excel sheet and Visual Basic modules) has been developed and validated through comparisons to numerical results. The *M-N* interaction in the columns for the computation of the plastic load factors is taken into account through formulas proposed in the PhD thesis of M. Vilette *[44]* (*Formula (2.29)* and *Formula (2.30)*); the latter permits to analytically predict the *M-N* interaction curve of a double-T cross section with a very good accuracy:

- If $0 \leq \frac{N_{Ed}}{N_{pl,Rd}} \leq \frac{A_w}{A}$,

$$M_{N,Rd} = M_{pl,Rd}.\left[1-\left(\frac{N_{Ed}}{N_{pl,Rd}}\right)^2.\frac{1}{2.\left(\frac{h-t_f}{h-2.t_f}\right).\left(1-\frac{A_w}{A}\right).\frac{A_w}{A}+\left(\frac{A_w}{A}\right)^2}\right] \tag{2.29}$$

- If $\frac{A_w}{A} \leq \frac{N_{Ed}}{N_{pl,Rd}} \leq 1$,

$$M_{N,Rd} = b.t_f.\left(h - t_f\right).f_y - \frac{1}{2}.(N_{Ed} - A_w.f_y).\left[\left(h - 2.t_f\right) + \frac{N_{Ed} - A_w.f_y}{2.b.f_y}\right] \quad (2.30)$$

where N_{Ed} is the normal force applied on the cross section, $N_{pl,Rd}$ is the plastic resistance to normal forces of the cross section, $M_{N,Rd}$ is the resistant moment of the cross section associated to N_{Ed}, $M_{pl,Rd}$ is the plastic resistance to bending moments of the cross section, h is the total height of the profile, t_f is the thickness of the profile flange, A_w is the area of the profile web, A is the total area of the cross section and b is the width of the profile flange.

The main results of the parametrical study are presented in *§ II.6.2.2*; then, conclusions are drawn in *§ II.6.2.3*.

II.6.2.2. Parametrical study results

The behaviour of 181 steel frames is investigated. For each frame, the results obtained with the new method and with the Merchant-Rankine method are compared to the numerical results obtained through the performed non-linear analyses considered as the "reference" ones. In the analytical methods, the values of λ_{cr} which are used are the numerical ones obtained through FINELG. An example of frame investigation is given in *Appendix VI.5*.

The investigated frames were defined so as to cover a wide range of λ_p/λ_{cr} values (from 0,09 to 0,61), λ_p being the minimum value of the three plastic load factors $\lambda_{p,beam}$, $\lambda_{p,combined}$ and $\lambda_{p,panel}$.

The three values of μ, i.e. μ_{beam}, $\mu_{combined}$ and μ_{panel}, have been calibrated so as to minimize the difference between the predicted values of λ_u through the new method and the ones numerically predicted. The three values which have been obtained are the following:

- $\mu_{beam} = 0{,}07$;
- $\mu_{combined} = 0{,}29$ and;
- $\mu_{panel} = 0{,}596$.

The comparison between the predicted values of λ_u obtained through the analytical methods (the new one and the Merchant-Rankine approach) and the numerical simulations is given in *Figure II.74* and *Figure II.75* for all the frames.

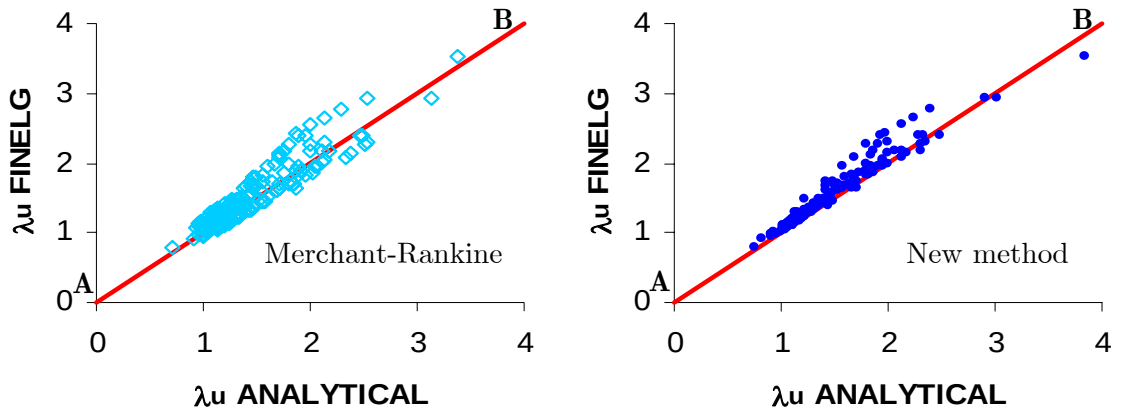

Figure II.74. Comparison between the analytical and the numerical results for the prediction of λ_u (all the investigated steel frames)

In *Figure II.74*, the abscissa represents the values of λ_u analytically predicted while the ordinate, the values of λ_u numerically computed. If the analytical methods were perfectly accurate, all the points of the figures would exactly be on the line "AB", i.e. the analytical prediction would be equal to the numerical computation results; so, the more accurate the analytical method is, the closer to the line "AB" the points are. Also, all the points which are in the upper zone of the graph according to the line "AB" are cases where the analytical method underestimates the ultimate load factors (i.e. "safe side" of the graph) while the points in the lower zone are cases where the analytical method overestimates the ultimate load factors (i.e. "unsafe side" of the graph). From *Figure II.74*, it can be observed that the new method gives more accurate results than the Merchant-Rankine approach; indeed, the points obtained with the new method are closer to the line "AB" than the ones obtained with the Merchant-Rankine approach. Also, more points on the "unsafe side" of the graph are present with the Merchant-Rankine approach than with the new method; indeed, 66 cases (i.e. 36 % of the investigated frames) are unsafe through the Merchant-Rankine approach for only 13 (i.e. 7 % of the investigated frames) cases through the new method.

These observations are confirmed by the graph presented in *Figure II.75*. The latter represents the number of frames which are included in ranges of differences, expressed in %, between the analytical predictions and the numerical results; for instance, it can be seen on this graph that the number of frames for which the difference between the λ_u analytically predicted and the λ_u numerically computed is included in the range [0 % ; 1 %] is equal to 23 with the new method and to 4 with the Merchant-Rankine approach.

From *Figure II.75*, it can be observed that the number of frames for which the differences on the value of λ_u is between 0 % and 10 % is equal to 148 with the new method (i.e. 81,8 % of the frames) and to 57 with the Merchant-Rankine approach (i.e. 31,5 % of the frames) which confirms the better accuracy of the proposed method.

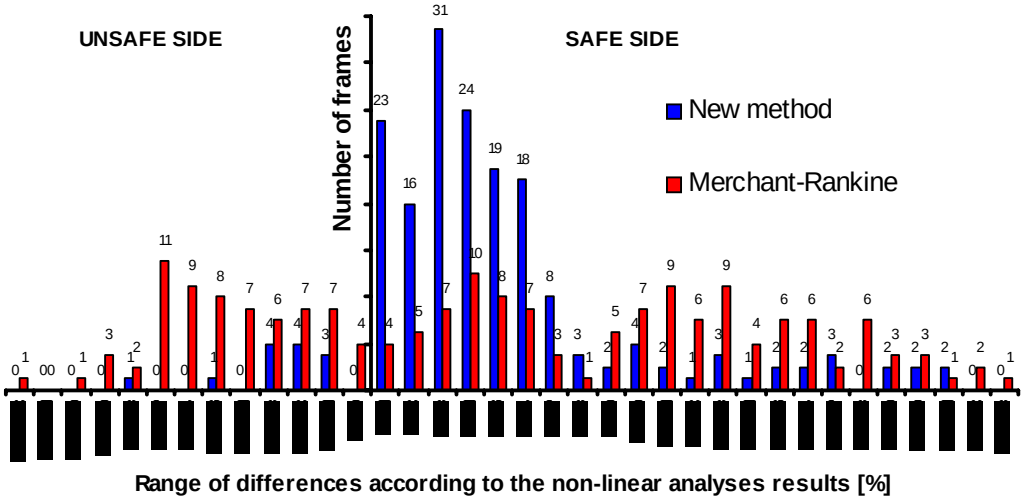

Figure II.75. Evaluation of the accuracy of the analytical methods (all the investigated steel frames)

Also, as mentioned in *§ II.5.3.4*, the collapse mode associated to the ultimate load factor λ_u does not necessary correspond to the one associated to the plastic load factor λ_p (which is the case, for instance, for the detailed example presented *Appendix VI.5*); it reflects the situation of 112 of the investigated frames. It is interesting to underline that, with the new method, the type of plastic mechanism associated to the minimum value of λ_u corresponds to the one appearing through the fully non-linear numerical analysis for 93 % of the investigated frames.

In the presented results, the Merchant-Rankine approach is applied to all the frames with values of the λ_p/λ_{cr} ratio from 0,09 to 0,61; however, as mentioned in *§ II.2.2.5.D*, it is recommended to apply this approach to structures with this ratio between 0,1 and 0,25. If only the frames respecting this condition are considered (which is the case for 133 of the investigated structures), the results presented in *Figure II.76* and in *Figure II.77* are obtained. From the latter, the previous observations are still valid; it can be observed that:

- Only 4 unsafe situations (i.e. 3 % of the considered frames) are obtained with the new method for 45 (i.e. 34 % of the considered frames) with the Merchant-Rankine approach.
- The number of frames for which the differences on the value of λ_u is between 0 % and 10 % is now equal to 123 with the new method (i.e. 92,5 % of the considered frames) and to 47 with the Merchant-Rankine approach (i.e. 35,3 % of the considered frames) what confirms the better accuracy of the proposed method.
- The type of plastic mechanism associated to the minimum value of λ_u obtained with the proposed new method corresponds to the one appearing through the fully non-linear numerical analysis for 93 % of the investigated frames.

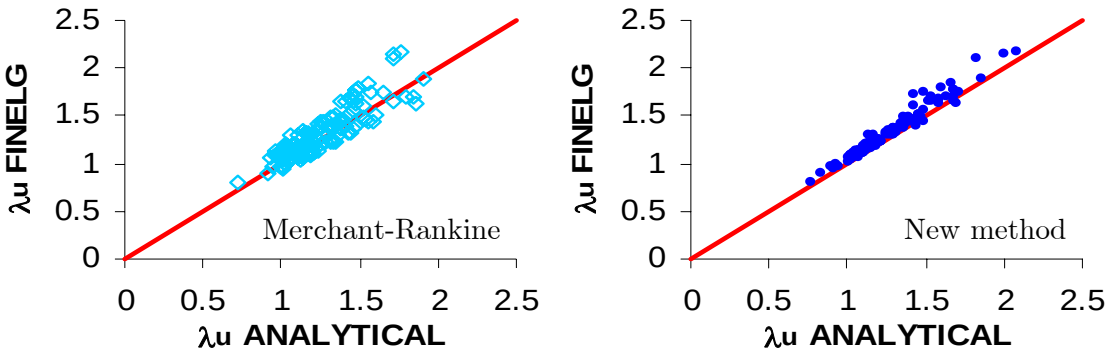

Figure II.76. Comparison between the analytical and the numerical results for the prediction of λ_u ($\lambda_p/\lambda_{cr} \in [0,1 ; 0,25]$)

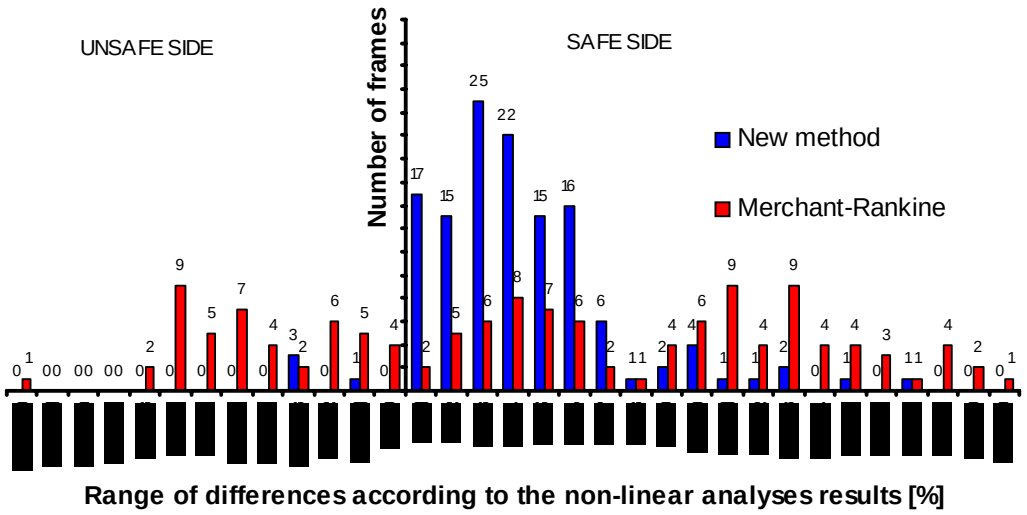

Figure II.77. Evaluation of the accuracy of the analytical methods ($\lambda_p/\lambda_{cr} \in [0,1 ; 0,25]$)

II.6.2.3. Conclusions

The calibration of the parameters μ needed to apply the new method to steel sway frames has been realised through a parametrical study on 181 steel frames. The main results of this parametrical study have been presented within this section.

Through the latter, it has been demonstrated that the new method permits to obtain accurate results (if compare to the results obtained through a fully non-linear numerical analysis) which is not the case through the Merchant-Rankine approach.

Also, it has been shown that the number of unsafe situations is limited if the new method is used while, with the Merchant-Rankine approach, it is not the case (an unsafe result is obtained with the Merchant-Rankine approach for more than one third of the investigated frames).

Finally, the new method is able to predict the collapse mode appearing at the ultimate limit state; indeed, there is a very good agreement between the collapse modes appearing through the non-linear numerical analyses and the ones associated to the minimum values of the ultimate load factor obtained through the new method.

II.6.3. Parametrical study on composite sway frames

II.6.3.1. Introduction

In the previous section, a parametrical study has been performed on steel frames to investigate the validity of the proposed analytical method based on the Ayrton-Perry formulation and to calibrate some coefficients which are requested within the latter. Within the present section, the same procedure is followed for the composite sway frames.

The parametric study presented here has been realised in strong collaboration with a colleague Ly Dong Phuong Lam *[45]*. Within this study, three types of 2-D "academic" simple frames have been investigated (*Figure II.80*); in total, 199 frames have been studied. Different types of structural elements are met within the investigated frames as described here below:

- Two types of composite beam configurations bent around their major axis:
  - upper hot-rolled profile flange fully connected to a concrete slab (*Figure II.78.A*) or;
  - upper hot-rolled profile flange fully connected to a composite slab (*Figure II.78.B*).
- Two types of columns bent around their major axis:
  - steel hot-rolled profile ones (*Figure II.79.A*) or;
  - partially encased composite ones (*Figure II.79.B*).
- The beam-to-column composite joints are rigid or semi-rigid ones and full-strength or partial-strength ones; the column bases are assumed to be rigid and fully resistant. The beam-to-column joints are assumed to have a sufficient ductility to develop plastic hinges and to allow a plastic analysis.

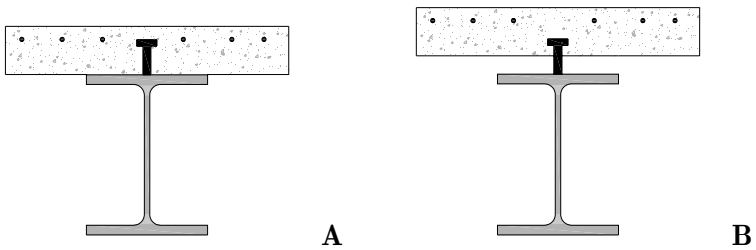

Figure II.78. Types of composite beam cross sections met within the investigated frames

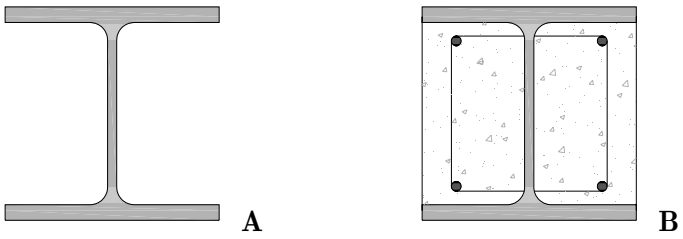

Figure II.79. Types of columns met within the investigated frames

The steel material and the joint behaviour are modelled through an elastic-perfectly plastic bilinear law (as illustrated in *Figure II.45*). For the concrete material, a parabolic behaviour law with account of tension stiffening as presented in *Figure II.46* is used. For the material properties, the characteristic values are used.

Through preliminary investigations performed before the parametrical study, an important phenomenon has been highlighted: even if the cross sections of a composite sway frame can be considered as Class 1 cross sections according to the recommendations given in Eurocode 4 *[6]*, it has been observed that the ductility of the concrete is sometimes not sufficient to allow the development of a full plastic mechanism within the frame. Indeed, the ultimate deformation allowed in the concrete in compression, i.e. $\varepsilon_{cu} = 0,35$ % (defined according to Eurocode 2 *[33]*) was reached before the formation of the plastic mechanism. This phenomenon leads to a limitation of the ultimate loads that the frame could sustain. As this problem can be considered as a problem of cross section classification, which is not under investigation within the present thesis, this phenomenon has been bypassed assuming a sufficient ductility of the concrete to allow the development of the plastic mechanism. In future investigations, new criteria for the composite cross section classification, taking into account of the maximum deformation capacity of the concrete, should be developed.

The finite elements used within the modellings are the same than the ones used for the modelling of the actual composite structures (see *§ II.5*) and are presented in *§ II.4.3* (*Figure II.44*). The behaviour of the joints is modelled through rotational springs.

As for the parametrical study performed on the steel frames, the properties of the frames have been defined so as to cover the three types of plastic mechanisms, i.e. beam, combined and panel plastic mechanisms (obtained through first-order rigid-plastic analyses) with each type of structures and to obtain different types of collapse modes (plastic mechanisms or instability) through the full non-linear analyses. The parameters which are modified within these frames are:

- the type of structural elements (as mentioned previously);
- the height of the columns;

- the properties of the joints;
- the beam and column cross sections and;
- the applied loads.

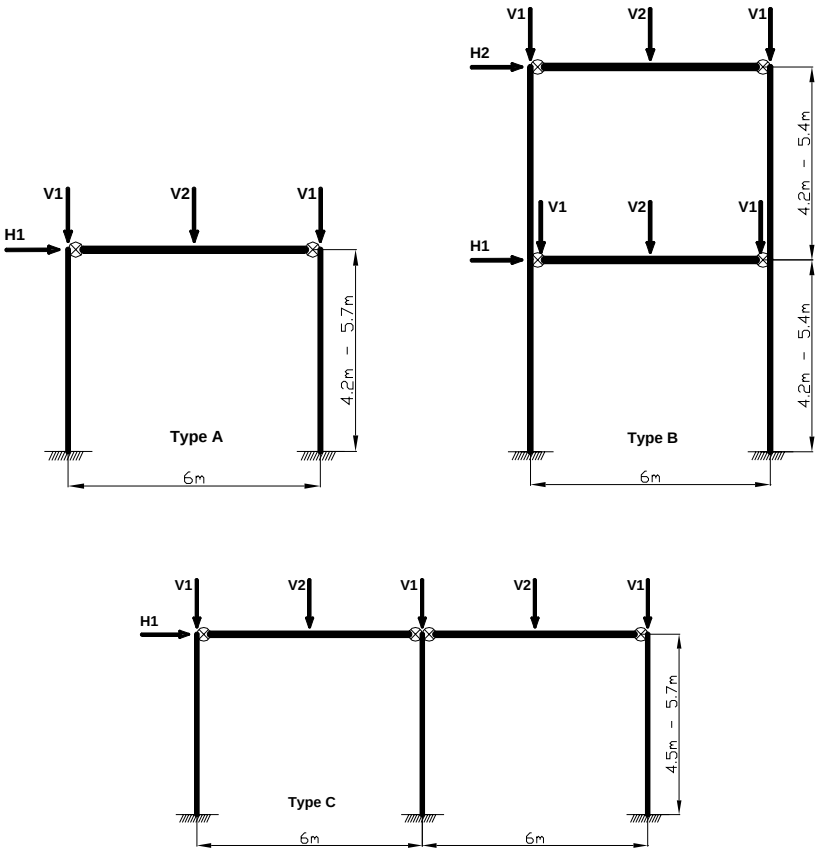

Figure II.80. Structure types A, B and C

For all these structures, the serviceability limit states have been checked and the displacements respect the limitations recommended in *Table II.3*.

The types of analyses which have been performed are:

- Critical elastic analyses (λ_{cr});
- First-order rigid-plastic analyses (computation of the three plastic load factors, i.e. $\lambda_{p,beam}$, $\lambda_{p,combined}$ and $\lambda_{p,panel}$);
- Full non-linear analyses (λ_u).

As mentioned in *§ II.5.2*, two types of λ_{cr} can be computed: cracked and uncracked ones. Within the present study, only the uncracked one is computed and used in the developed analytical method, as it is the easiest one to compute. The effects of the concrete cracking will be taken into account implicitly in the calibration of the coefficient μ (i.e. μ_{beam}, $\mu_{combined}$ and μ_{panel}).

For the computation of λ_{cr} and λ_u, the software FINELG is used; a pre-processor (based on Excel sheets and Visual Basic modules) has been developed for the generation of composite frame datafiles.

As recommended in Eurocode 4 *[6]*, an initial deformation is introduced in the computation. The formula to be used to estimate a value for the initial out-of-plumb ϕ is the same than the one proposed in Eurocode 3 *[12]* (see *Formula (2.25)*). Also, as for the steel frames, the shape of the initial deformation introduced in the computations is proportional to the first global instability mode obtained through the critical elastic analysis.

For the computation of the plastic load factors, a software based on an Excel sheet has been developed and validated through comparisons to numerical results. The *M-N* interaction in the columns for the computation of the plastic load factors is taken into account:

- through *Formula (2.29)* and *Formula (2.30)* for the steel columns;
- through the simplified method proposed in Eurocode 4 *[6]* for the composite columns which consists in evaluating the non-linear M-N interaction curve through a polygonal curve as illustrated in *Figure II.81.*

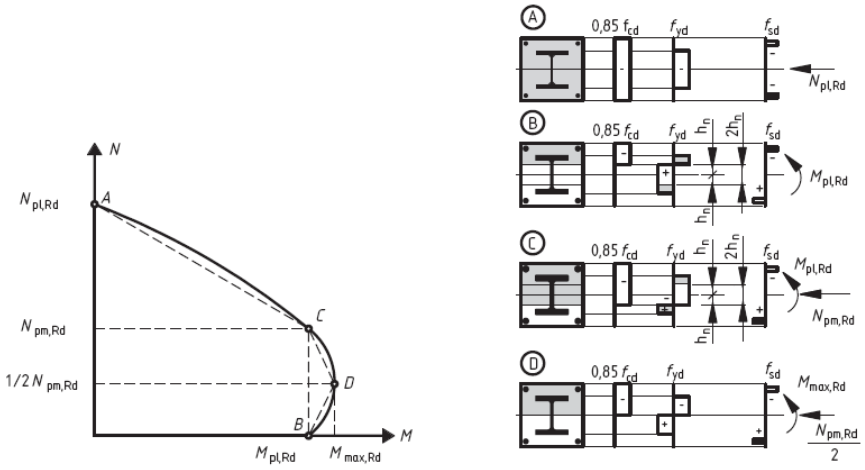

Figure II.81. Resistance M-N interaction curve of a composite column [6]

The main results of the parametrical study are presented in *§ II.6.2.2*; then, conclusions are drawn in *§ II.6.2.3*.

II.6.3.2. Parametrical study results

As mentioned above, the behaviour of 199 frames is investigated. As for the parametrical study performed on the steel frames, the results obtained with the new method and with the Merchant-Rankine approach are compared to the numerical results obtained through

the performed non-linear analyses considered as the "reference" ones. In the analytical methods, the values of λ_{cr} which are used are the numerical ones obtained through FINELG.

The investigated frames were defined so as to cover the different types of collapse modes (obtained through non-linear analyses) and to cover a wide range of λ_p/λ_{cr} values (from 0,05 to 0,31), λ_p being the minimum value of the three plastic load factors $\lambda_{p,beam}$, $\lambda_{p,combined}$ and $\lambda_{p,panel}$.

The three values of μ, i.e. μ_{beam}, $\mu_{combined}$ and μ_{panel}, calibrated so as to minimize the difference between the predicted values of λ_u through the new method and the ones numerically predicted are the following:

- $\mu_{beam} = 0{,}02$;
- $\mu_{combined} = 0{,}42$ and;
- $\mu_{panel} = 0{,}7$.

It can be observed that these coefficients are higher than the ones calibrated for the steel structures (except for the values corresponding to the beam plastic mechanism which are very close), which means that, for a composite structure and a steel structure with the same value of λ_{cr} and the same values of plastic load factors $\lambda_{p,beam}$, $\lambda_{p,combined}$ and $\lambda_{p,panel}$, the ultimate load factor λ_u obtained through the new method would be smaller for the composite structure than for the steel one.

This observation is in line with the remark reported in *§ II.5.1* which is reminded here after. Composite sway frames present a particularity compared to steel ones: the concrete cracking. This phenomenon leads to an amplification of the lateral deflections and, consequently, to an amplification of the second-order effects, which reduces the ultimate resistance of the frames. In other words, for a same number of hinges formed at a given load level in a steel frame and in a composite frame respectively, larger sway displacements are reported in the composite one. So, this particularity is reflected within the developed method through the "μ" values which are higher for composite sway frames than for the steel ones. The fact that the μ factors associated to the beam plastic mechanism are very closed can be explained by the small influence of this type of collapse mode to the second order effects.

The comparison between the predicted values of λ_u obtained through the analytical methods (the new one and the Merchant-Rankine approach) and the numerical simulations is given in *Figure II.82* and *Figure II.83* for all the frames.

From *Figure II.82*, it can be observed, as for the steel sway frames (see *§ II.6.2.2*), that the new method gives more accurate results than the Merchant-Rankine approach; indeed, the points obtained through the new method are closer to the line "AB" than the ones obtained with the Merchant-Rankine approach. Also, more points on the "unsafe side" of the graph are present with the Merchant-Rankine approach than with the new method; indeed, 81 cases (i.e. 40,7 % of the investigated frames) are unsafe through the Merchant-Rankine approach for only 15 (i.e. 7,5 % of the investigated frames) cases through the new method.

From *Figure II.83*, it can be observed that the number of frames for which the differences on the value of λ_u is between 0 % and 10 % is equal to 167 with the new method (i.e. 83,9 % of the frames) and to 51 with the Merchant-Rankine approach (i.e. 25,6 % of the frames) which confirms the better accuracy of the proposed method, as observed for the steel sway frames.

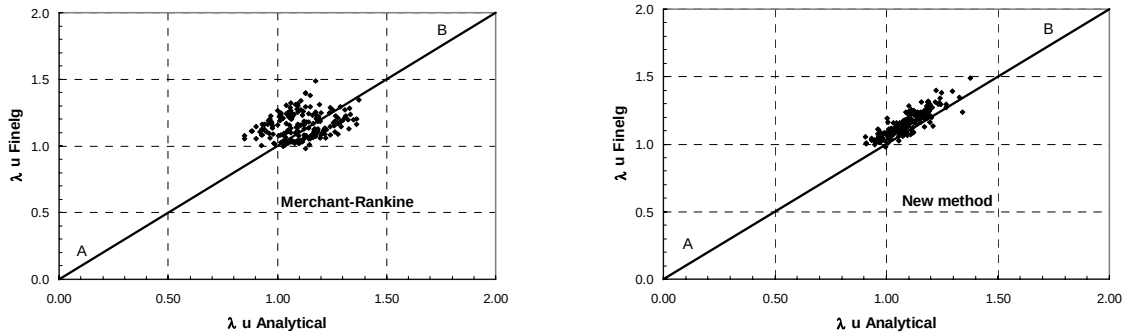

Figure II.82. Comparison between the analytical and the numerical results for the prediction of λ_u (all the investigated composite frames)

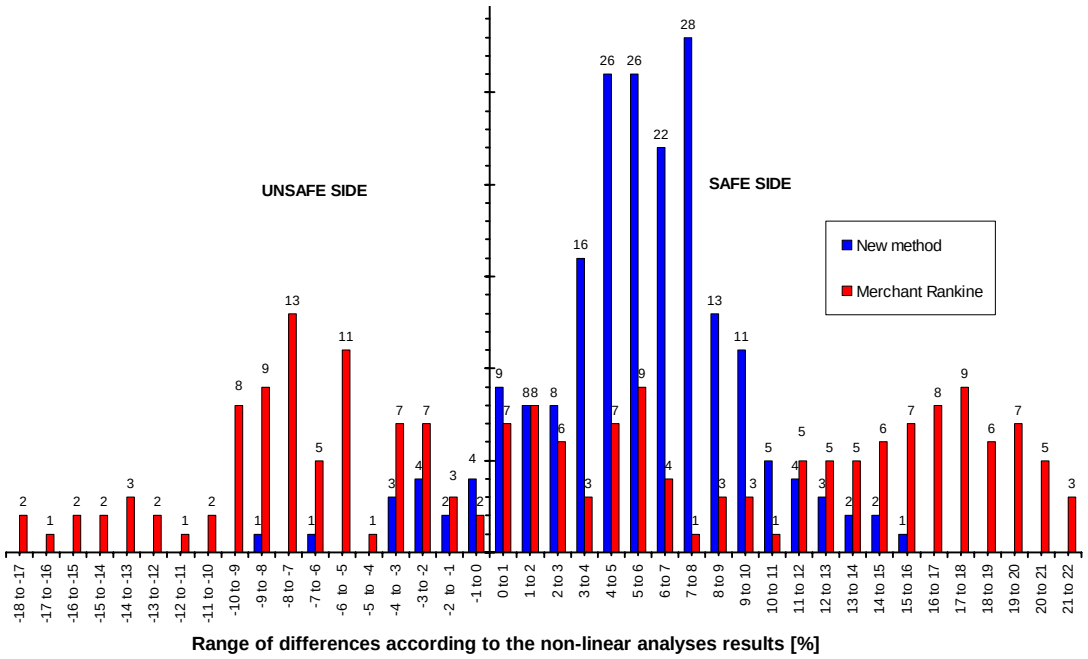

Figure II.83. Evaluation of the accuracy of the analytical methods (all the investigated composite frames)

Also, amongst the investigated composite frames, there are cases (38 in total, i.e. 19,1 % of the investigated composite frames) where the collapse mode associated to λ_u do not correspond to the one associated to λ_p. It is interesting to underline that, with the new method, the type of plastic mechanism associated to the minimum value of λ_u corresponds to the one appearing through the fully non-linear numerical analysis for 99,5 % of the investigated frames.

As previously mentioned, it is recommended to apply the Merchant-Rankine method to structures with a λ_p/λ_{cr} between 0,1 and 0,25. If only the frames respecting this condition are considered (which is the case for 150 of the investigated composite structures), the results presented in *Figure II.84* and in *Figure II.85* are obtained. From the latter, the previous observations are still valid; it can be observed that:

- Only 13 unsafe situations (i.e. 8,7 % of the considered frames) are obtained with the new method for 57 (i.e. 38 % of the considered frames) with the Merchant-Rankine approach.
- The number of frames for which the differences on the value of λ_u is between 0 % and 10 % is now equal to 131 with the new method (i.e. 87,3 % of the considered frames) and to 40 with the Merchant-Rankine approach (i.e. 26,7 % of the considered frames) which confirms the better accuracy of the proposed method.
- The type of plastic mechanism associated to the minimum value of λ_u obtained with the proposed new method corresponds to the one appearing through the fully non-linear numerical analysis for 100 % of the investigated frames.

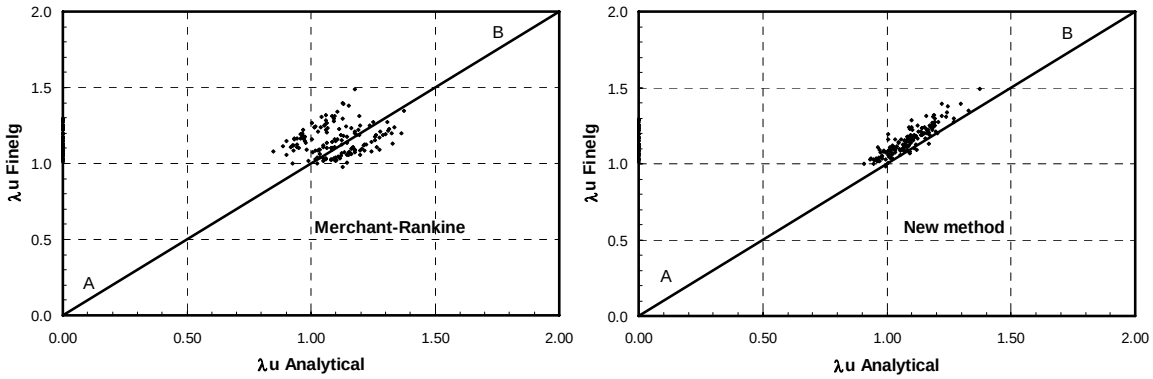

Figure II.84. Comparison between the analytical and the numerical results for the prediction of λ_u ($\lambda_p/\lambda_{cr} \in [0,1 ; 0,25]$)

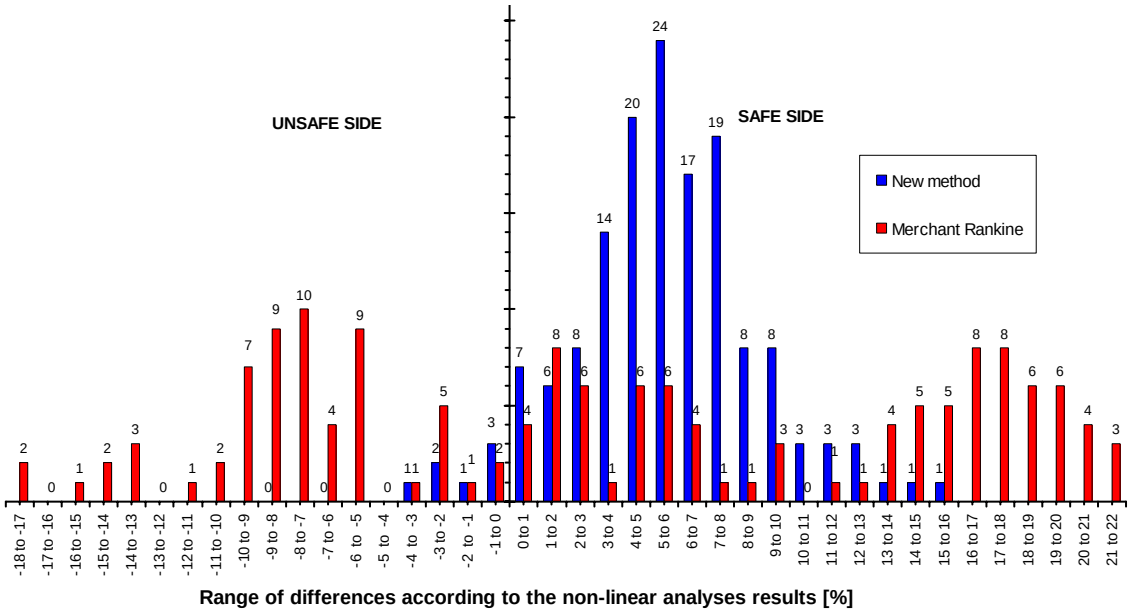

Figure II.85. Evaluation of the accuracy of the analytical methods ($\lambda_p/\lambda_{cr} \in [0,1 ; 0,25]$)

II.6.3.3. Conclusions

The calibration of the parameters μ needed to apply the new method to composite sway frames has been realised through a parametrical study on 199 composite frames. The main results of this parametrical study have been presented within this section. Also, it has been illustrated that the particularity of composite sway frames (according to steel ones) which is the concrete cracking is reflected in the parameters μ which have been calibrated.

Through this parametrical study, it has been demonstrated that the conclusions drawn for the steel sway frames in *§ II.6.2.3* are still valid for composite sway frames, i.e. safe results with a good accuracy obtained with the new method which is not the case with the Merchant-Rankine method. Also, the developed method is able to predict the collapse mode appearing at the ultimate limit state.

II.6.4. Application of the new method to the actual frames investigated in § II.5

Within this section, the developed method is applied to the actual frames investigated in *§ II.5* and characterised by a proportional loading (i.e. the "Ispra", the "Eisenach", the "UK" and the "Luxembourg" buildings – see *Appendix VI.4*).

The obtained results are given in *Table II.25* and compared to the ones obtained through the full non-linear analyses. It can be observed that good results are obtained through the new method except for the "Luxembourg" building for which an unsafe result is found (but the difference between the analytical result and the numerical one is small). Also, a

good agreement on the collapse modes associated to the ultimate load factors is obtained except for the "Luxembourg" building.

Table II.25. Results obtained through the new method for the actual buildings investigated in § II.5 and comparison to the non-linear analysis results

Structures	λ_u new method	λ_u MR	λ_u Non-linear analysis	Difference new method/non-linear analysis	Difference MR/non-linear analysis
"Ispra" building	1,69	1,43	1,79	5,6 %	20,1 %
"Eisenach" building	1,125	1,139	1,138	1,1 %	-0,1 %
"UK" building	1,87	1,88	2,01	7 %	6,5 %
"Luxembourg" building	1,25	1,210	1,209	-3,4 %	-0,2 %

II.6.5. Conclusions

Within the present paragraph, a new method based on the Ayrton-Perry formulation and aiming at predicting the ultimate load factor of steel and composite sway frames has been developed and validated through two parametrical studies.

In *Appendix VI.5.3*, it is shown that the developed method is easy to apply; it is possible, through limited analytical computations, to obtain an accurate estimation of the ultimate load factor which is practically always in the safe side. Also, the developed method is able to predict the collapse mode appearing at the ultimate limit state which is not the case with the simplified analytical methods as actually proposed in the codes.

The developed method has also been applied to the actual buildings investigated in *§ II.5*. It has been illustrated that the obtained results are very good except for one building for which an unsafe prediction of the ultimate load factor and a wrong collapse mode are predicted.

II.7. Part II conclusions

Moment resisting frames, without bracing systems, offer a flexible solution to the user of the buildings, especially for the internal arrangements and the exploitation of the buildings. When sufficient stiffness and strength with regard to lateral forces are achieved, such frames also offer a structural solution which can resist lateral loads. Obviously, the construction of tall buildings and large industrial halls without wind bracing systems is susceptible to make global instability a relevant failure mode. Although the Eurocode 3 dedicated to the design of steel structures covers this type of buildings, the latter is not

yet well covered by Eurocode 4 dedicated to the design of composite steel-concrete buildings.

The present part of the thesis was devoted to the study of the behaviour of composite sway frames. The main objective was to propose simplified analytical methods to design such frames.

The behaviour of composite sway frames is widely influenced by the response of the composite joints subjected to hogging and eventually to sagging bending moments. So, in a first paragraph, the behaviour of the latter was investigated through experimental and analytical studies. In a first part, experimental tests on double-sided and single-sided composite joints subjected to sagging and hogging bending moments were presented and analysed. Then, an analytical method recommended in the Eurocodes (called the "component method") was briefly described and the applicability of the latter to composite joints was investigated through comparisons of the so-obtained analytical predictions with the experimental results. In particular, a new collapse mode for single-sided composite joints subjected to hogging bending moment was identified and new formulas to predict the appearance of the latter were proposed and validated. Also, as the analytical method actually proposed in the Eurocodes does not cover the behaviour of composite joints subjected to sagging bending moments, an analytical procedure was developed and validated through comparisons with experimental results. From the presented investigations, it can be concluded that analytical tools to predict the behaviour of composite joints subjected to bending moments (sagging or hogging ones) are now available.

Then, in a second paragraph, the numerical tool used later on to investigate the behaviour of composite sway frames was validated through two main studies:

- The first one is a benchmark study performed amongst European institutes and coordinated by Liège University. The building used for this benchmark was tested at the Building Research Establishment in UK and the results numerically predicted by the institutes involved in the benchmark study were compared to the experimental results.
- The second one is a comparison to experimental results. The experimental test was performed on a composite sway frame at Bochum University. The design of the latter was performed in strong collaboration with Liège University.

From these studies, it can be concluded that the homemade finite element software FINELG is able to predict with a very good accuracy the response of composite sway frames.

In the following paragraph, these tools were used to investigate the behaviour of five actual composite sway buildings. The main obtained results were summarised within the thesis; the presented results come from a preliminary study presented in *[11]*. From this study, it was concluded that the behaviour of composite sway frames is close to the ones observed for steel sway frames. So, it was decided to investigate the applicability of simplified analytical methods, initially developed for steel sway frames, to composite sway frames. In a first step, the applicability of the elastic method named "Amplified Sway Moment Method" (ASMM) was investigated. It was shown that the applicability of this method can be extended to composite sway frames with good confidence; indeed, the predicted values of the elastic load factor through the ASMM were in good agreement with the numerically predicted ones obtained through fully non-linear analyses (considered as the "reference" results), even if the critical load factor used in this method is computed through the simplified method recommended in Eurocode 3 and 4. In a second step, the applicability of the plastic method named "Merchant-Rankine approach" (MR) was studied. It was demonstrated through this study that this approach shows the same level of accuracy than for steel sway frames:

- safe for beam plastic mechanisms;
- adequate for combined plastic mechanisms;
- unsafe for panel plastic mechanisms.

As the investigated plastic method (i.e. MR approach) did not give satisfactory results, it was decided to develop a new method. It was the scope of the last paragraph of the present part. The proposed method is founded on the Ayrton-Perry formulation which is the method recommended in the Eurocodes to deal with stability problems. The proposed method works as follows:

- in a first step, the critical load factor of the investigated frame has to be computed;
- then, the three main plastic load factors, i.e. the ones associated to a beam, a combined and a panel mechanisms, have to be determined;
- with these values, it is then possible to use the Ayrton-Perry formulation (presented in *Table II.24*) to compute three values of the ultimate load factor, one for each plastic load factors computed in the previous step;
- finally, the ultimate load factor of the investigated frame is taken as equal to the minimum value of the three ultimate load factors determined in the previous step.

To develop this new method, three coefficients influencing the values obtained through the Ayrton-Perry formulation had to be calibrated: one associated to the beam plastic

mechanism (μ_{beam}), one associated to the combined plastic mechanism ($\mu_{combined}$) and one associated to the panel plastic mechanism μ_{panel}). This calibration was performed through parametrical studies.

A first parametrical study was performed on steel sway frames; indeed, as the MR approach does not give fully satisfactory results for this type of structures, it was decided to also develop the new method for such frames. Through this study, the three calibrated values which were obtained are:

- $\mu_{beam} = 0{,}07$;
- $\mu_{combined} = 0{,}29$ and;
- $\mu_{panel} = 0{,}596$.

The latter were defined so as to minimize the difference between the analytical results predicted through the developed new method and the ones obtained through fully non-linear numerical results, considered as the reference.

Through this parametrical study, it was shown that the developed method gives accurate results practically always on the safe side and in good agreement with the numerical results, what was not the case with the MR approach. One other interesting conclusion is the fact that the new method could be extended to more situations than the ones covered by the MR approach; indeed, the MR approach is limited to structure with a ratio between the minimum plastic load factor and the critical load factor belonging to the interval 0,1 – 0,25 while the developed method continues to produce satisfactory results for structures with a ratio higher than 0,25.

A second parametrical study was then performed on composite sway frames. Through this study, the three calibrated values which were obtained are:

- $\mu_{beam} = 0{,}02$;
- $\mu_{combined} = 0{,}42$ and;
- $\mu_{panel} = 0{,}7$.

The conclusions drawn for the steel sway frames are still valid when the developed method is applied to composite ones with these calibrated values of "μ"; the fact that the values of "μ" for the composite sway frames are higher than the ones for the steel sway frames (except for the one associated to the beam plastic mechanism) is justified by the concrete cracking to which higher sway displacements are associated and, accordingly, higher second order effects.

To conclude, the so-developed simplified analytical method is easy to apply, as only "simple" frame analyses are requested, and permits to predict, with a very good accuracy, the ultimate load factor of steel and composite sway frames and the associated collapse mode.

Some perspectives to this work and the personal contributions to this part are given in *§ IV.2* and *§ IV.3* respectively.

III. Development of membrane effects in steel and composite beams further to an exceptional action

III.1. Introduction

Recent events such as natural catastrophes (tsunami, hurricane, ...) or terrorism attacks have highlighted the necessity to ensure the structural integrity of buildings under exceptional events with the objective to save the life of the occupants and of the safety services (fireman, ambulance man, ...) and also to avoid collateral damages to the adjoining buildings.

The partial collapse of the Ronan Point Tower in 1968 in UK is considered as the starting point of the interest in the structural integrity of buildings but more recent catastrophes in the last decade such as the terrorist attack of the World Trade Center towers in 2001 or the tsunami associated to the Sumatra earthquake in 2004 have increased the interest of the engineering community and also of the population in this topic.

According to Eurocodes and some different other national design codes, the structural integrity of civil engineering structures should be ensured through appropriate measures but, in most of the cases, no precise practical guidelines on how to achieve this goal are provided; this observation is the results of a literature survey which is summarised in *§ III.2*.

On this topic, an European RFCS project called "Robust structures by joint ductility" *[4]* has been set up in 2004, for three years, with the aim to provide requirements and practical guidelines allowing to ensure the structural integrity of steel and composite structures under exceptional events through an appropriate robustness (see *§ I.1*).

The investigations performed at Liège University, as part of this European project, are mainly dedicated to the exceptional event "Loss of a column in a steel or steel-concrete composite building frame"; the main objective is to develop a simplified analytical procedure to predict the frame response further to a column loss.

To achieve this goal, a general concept devoted to the prediction of the response of a building frame further to a column loss has been built at Liège University; this concept is described in *§ III.3*. In particular, it is highlighted that an analytical method is requested to predict the response of a frame when the membrane effects, associated to the development of significant second order effects, appear within the structure (see *Figure III.1*).

The investigations presented within the present part of the thesis are dedicated to the development of this analytical method. These developments are founded on the knowledge relative to the structural behaviour of steel and composite structures subjected to

significant second order effects gained from the previous investigations presented in *Part II*.

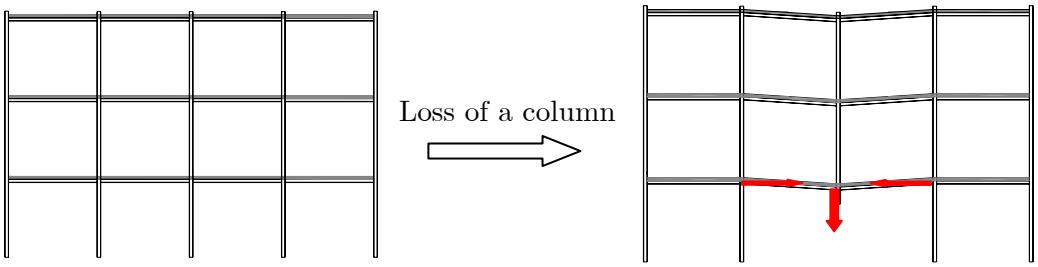

Figure III.1. Loss of a column in a frame

To develop this analytical method, a strategy is defined in *§ III.3.3*. This strategy involves experimental, numerical and analytical aspects. In particular, an experimental test performed at Liège University simulating the loss of a column in a composite frame is described in *§ III.4*. As in the previous part of the thesis, a particular attention is also paid to the behaviour of the beam-to-column joints which are here subjected to combined bending moments and tensile loads when the membrane forces develop within the structure (*§ III.5*). In addition, numerical investigations with a numerical tool validated in *§ III.6* are performed first to define a simplified substructure modelling able to reflect the global frame response and secondly to determine the parameters influencing its response (*§ III.7*).

The developed analytical method based on the simplified substructure modelling is finally described and validated through comparisons to experimental results in *§ III.8*. This method permits to predict the development of the membrane forces within the simplified substructure and their influence on the substructure response.

III.2. State-of-the-art knowledge on buildings subjected to exceptional events

III.2.1. Introduction

In the present paragraph, a summary of the state-of-the-art in the domain of buildings subjected to exceptional actions is presented. This summary is mainly dedicated to the exceptional situation "loss of a column in a steel or steel-concrete composite building", which is under investigation within the present part of the thesis.

The objective is to briefly describe information and design methods available in codes and standards and to highlight the requested investigations to develop and/or to improve design methods.

In *§ III.2.2*, some concepts (such as structural integrity, robustness, …) used in the following sections are first defined. Then, methods available in the main codes and standards dealing with the robustness of structures and the progressive collapse problem are briefly introduced in *§ III.2.3*. Finally, some results of recent international researches dealing with the robustness of structure further to the loss of a column are introduced in *§ III.2.4*.

III.2.2. Important definitions

A structure should be designed to behave properly under service loads (at SLS) and to resist design factored loads (at ULS). The type and the intensity of the loads to be considered in the design process may depend on different factors such as:

- the intended use of the structure : type of variable loads, …
- the location (region, altitude, …) : wind action, snow, level of seismic risk, …
- and even the risk of accidental loading : explosion, impact, flood, …

In practice, these individual loads are combined so as to finally derive the relevant load combination cases.

In this process, the risk of an *exceptional* (and therefore totally unexpected) *event* leading to other accidental loads than those already taken into consideration in the design process in itself is not at all covered. This is a quite critical situation where the *progressive collapse* of the structure, which is a catastrophic partial or total structural failure that results from an event that causes local structural damage and cannot be absorbed by the inherent continuity and ductility of the structural system, should be avoided. In other words, the *progressive collapse* is distinguished by a disproportionate damage according to the initiating event

To avoid it, the *structural integrity* should be ensured, i.e. the global structure should remain globally stable even if one part of it is destroyed by the *exceptional event* (explosion, impact, fire as a consequence of an earthquake, …). In conclusion, the *structural integrity* will be required when the structure is subjected to *exceptional loads* not explicitly considered in the definition of the design loads and load combination cases.

According to Eurocodes (*[46]* and *[47]*) and some different other national design codes (*[48], [49], [50]* and *[51]*), the *structural integrity* of civil engineering structures should be ensured through appropriate measures but, in most of the cases, no precise practical guidelines on how to achieve this goal are provided. Even basic requirements to fulfil are generally not clearly expressed.

Different strategies may therefore be contemplated (see *§ III.2.3*). One of them is to ensure certain *robustness* to the structure, i.e. an ability to resist locally the *exceptional loads* and ensure a *structural integrity* to the structure, at least for the time needed to safe lives and protect the direct environment. Obviously the objective could never be to resist to any *exceptional event*, whatever the intensity of the resultant actions and the importance of the structural part directly affected.

The *robustness* is required from the structural system not directly affected by the *exceptional event* (to avoid the local destruction of the structural element where the event occurs being often not possible). In this process, the ability to redistribute plastically extra forces resulting from the exceptional event is of high importance. This requires from all the structural elements and from the constitutive joints a high degree of plastic deformability under combined bending, shear, … or axial forces.

In the following section, a summary of the recommended methods available in different codes and standards to ensure the *structural integrity* (eventually through *robustness* requirements) of steel and/or steel-concrete composite structures subjected to the *exceptional event* "loss of a column in a building" are briefly described.

III.2.3. Codes and Standards

III.2.3.1. Introduction

Since the progressive collapse of the Ronan Point apartment tower in 1968 (UK – see *Figure III.2*), some codes and standards from Western Europe and North America have included some recommendations to avoid the progressive collapse of buildings.

Figure III.2. Ronan Point catastrophe in 1968 [52]

Recently, some interesting articles have been published, summarizing the information and the design procedures available in different codes and standards (*[52]*, *[53]*, *[54]*, *[55]* and *[56]*). The objective of the following sections is not to repeat all the information available in these articles but to give a brief description of recommendations provided in these codes and standards, with particular attention to the exceptional event "loss of a column in a building", in order to be able to highlight, at the end (i.e. in *§ III.2.5*), the limitations of these documents and the requested investigations in the field of robustness. The following sections are widely inspired from references indicated in the title of the latter.

III.2.3.2. British Standards ([52] and [48])

The British Standards were the first codes to propose recommendations to avoid the progressive collapse of buildings, strongly motivated by the catastrophic event of Ronan Point in 1968 (*Figure III.2*).

According to the British Standards, it is required that, in the event of an accident, the building will not suffer collapse to an extent disproportionate to the cause, i.e. to avoid the progressive collapse of the structure further to a limited collapse.

Three main methods are proposed to ensure that structures have a minimum level of strength to resist accidental loading. There are briefly described here below *[52]*:

- The "tying" method: this first design option consists in providing effective horizontal and vertical ties in accordance with the structural Codes of Practice. The provision of ties increases structural continuity creating a structure with a high degree of redundancy; providing the building with alternative load paths should part of the structure be removed by an accidental action. Generally, the ties are steel members or steel rebars; also, the beam-to-column joints have to be able to transfer the tying forces. The recommended minimum value for the tying force is equal to 75 kN.
- The "bridging" method: where "tying" is not feasible, it is recommended that the structure should be designed to bridge over a loss of an untied member and that the area of collapse be limited and localised. This is usually achieved by notionally removing each untied element (including load bearing vertical members and beams supporting one or more columns), one at a time, and checking that on its removal the affected zone does not extend further than the immediate adjacent stories and that the area of structure at risk of collapse is limited to the smaller of the following areas:
    - 15 % of the area of the considered storey or,

- 70 m²

The loads to be considered are one third of the characteristic imposed and wind loads and the full dead loads, except if the imposed load can be considered as a permanent one (mainly for storage buildings) where its full value has to be used in the computations.

- The "key element" method: if is not possible to bridge over the missing member, such a member should be designed as a protected (or key) element capable of sustaining additional loads related to a pressure of 34 kN/m². The value of 34 kN/m² was chosen with reference to a rounded estimated failure load of the load bearing flank wall at Ronan Point. This estimation was based on observational evidence. In practice, the 34 kN/m2 is used to determine a notional load that is applied sequentially to key elements and is not a specific overpressure that would result from a gas explosion. Such accidental design loading is assumed to act simultaneously with one third of all the normal characteristic loading.

The above requirements are considered to produce more robust structures which are more resistant to disproportionate failure due to various causes, such as impact as well as to gas explosions.

III.2.3.3. Eurocodes [46]

If reference is made to Eurocode 1 Part 1-7 *[46]* (new draft of the prestandard Eurocode 1 Part 2-7 *[47]*), it is mentioned in Principle 3.3.(1) that "*In the design, the potential damage to the structure arising from an unspecified cause shall be minimised, taking into account its use and exposure*". The possible strategies to be adopted in case of accidental design situations are presented in *Figure III.3*.

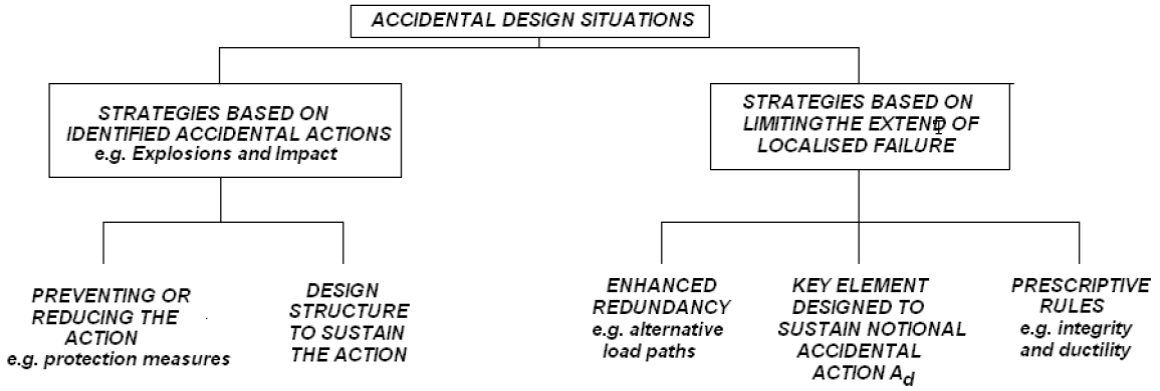

Figure III.3. Possible strategies for accidental design situations [46]

According to *[46]* and as illustrated in *Figure III.3*, measures to mitigate the risk of accidental actions should include, as appropriate, one or more of the following strategies:

- preventing the action from occurring or reducing the probability and/or magnitude of the action to an acceptable level through the structural design process (e.g. providing sacrificial venting components with a low mass and strength to reduce the effect of explosions);
- protecting the structure against the effects of an accidental action by reducing the actual loads on the structure;
- ensuring that the structure has sufficiently robustness by adopting one or more of the following approaches :
    - by designing certain key components of the structure on which its stability depends to be of enhanced strength so as to raise the probability of their survival following an accidental action. The notional accidental action recommended in *[46]* to design these key components is equal to 34 kN/m² as in the British Standards (see *§ III.2.3.2*)
    - by designing structural members to have sufficient ductility capable of absorbing significant strain energy without rupture.
    - by incorporating sufficient redundancy in the structure so as to facilitate the transfer of actions to alternative load paths following an accidental event.

The methods proposed in the Eurocode 1 *[46]* to ensure a sufficient robustness to the buildings are widely inspired from the British Standards method *[48]* (i.e. the tying, the bridging and the key element methods – see *§ III.2.3.2*). In particular, an informative annex (Annex A in *[46]*) titled "*Design for consequences of localised failure in a building structure from an unspecified cause*" provides rules and methods for designing buildings to sustain an extent of localised failure from an unspecified cause without disproportionate collapse. In the latter, a categorisation of building types/occupancies to consequence classes is given; in total, three consequence classes are identified (Class 1, Class 2 (lower risk and upper risk groups) and Class 3). The higher the class is, the more demanding the recommendations are.

III.2.3.4. United State General Services Administration guidelines [49]

The U.S. General Services Administration (GSA) developed a document titled "Progressive Collapse Analysis and Design Guidelines for New Federal Office Buildings and Major Modernization Projects" to ensure that the potential for progressive collapse is

addressed in the design, planning and construction of new buildings and major renovation projects.

The purpose of these guidelines is to:

- assist in the reduction of the potential for progressive collapse in new federal office buildings;
- assist in the assessment of the potential for progressive collapse in existing federal office buildings;
- assist in the development of potential upgrades to facilities if required.

The design method recommended in *[49]* is based on the alternate load path method and on a static linear elastic analysis with account of the dynamic aspect through an amplification factor (equal to 2) applied to the load combination to be considered: 2.(DL + 0,25.LL), where "DL" represents the dead loads and "LL" the live loads. As the method is based on a linear elastic analysis, the proposed procedure permits to have ratio between the so-obtained acting force in a member and the resistance of the latter higher than 1 to take into account, in an arbitrary way, of the plastic capacity of the members. Non linear analyses are permitted but they have to be performed by "experienced structural engineering analysts" and the obtained results have to be reviewed and approved by the project manager.

III.2.3.5. Unified Facilities Criteria (UFC) of the United State Department of Defence [50]

This document provides the design requirements necessary to reduce the potential of progressive collapse for new and existing Department of Defence (DoD) facilities that experience localized structural damage through normally unforeseeable events. This UFC incorporates a prudent, effective and uniform level of resistance to progressive collapse without expensive or radical changes to typical design practice.

The design requirements presented in this UFC were developed such that two structural response modes are available to provide different levels of resistance to progressive collapse. The first level of progressive collapse design employs the "tying" method, which are based on a "catenary" response of the structure. The second level employs the alternate path method, in which the structural mode is "flexural", as the building must bridge across a removed element (i.e. the "bridging" method according to the British Standards – see *§ III.2.3.2*). A significant portion of the design guidelines and criteria in this UFC are based on the British Standards approach.

The level of progressive collapse design is correlated to the level of protection; in total, four levels of protection are identified according to the type of building and its use:

- VLLOP : very low level of protection;
- LLOP : low level of protection;
- MLOP : medium level of protection and;
- HLOP : high level of protection.

For VLLOP and LLOP, only indirect design methods are used by specifying the level of tying forces; however, in the case that an adequate tie force cannot be developed in a vertical structural element, then the Alternate Path method is applied to verify that the structure can bridge over the deficient element. For MLOP and HLOP, the Alternate Path method is also applied to verify satisfactory flexural resistance in addition to the catenary resistance provided by the tie forces. Also, additional ductility requirements are specified for ground floor perimeter vertical load-bearing elements, to improve the resistance to progressive collapse.

III.2.3.6. United States Civilian Standards [57]

While general design guidances for reducing the potential of progressive collapse are discussed in various US design standards and building codes, none of them contains specific provisions for robustness design. In *[51]*, it is mentioned that the progressive collapse of a structure should be avoided if a structural member is locally damaged. As in the British standards, three methods are proposed including an indirect design approach, the alternative load path method and the specific local resistance design (i.e. design of key elements).

III.2.3.7. Canadian code

According to *[57]*, the Canadian code requires structures to be designed for adequate structural integrity in order to withstand all effects that may reasonably be expected to occur during their service life. Several general approaches, such as the provision of local resistance and redundancy as well as minimum tying force requirements, are also suggested; however, specific accidental load combinations are not proposed in this code.

III.2.3.8. Conclusions

In the present section, a brief description of recommendations provided in codes and standards from North America and Western Europe is given.

In a first step, the information available in the British Standards has been given. In particular, three recommended methods to avoid the progressive collapse in buildings have been described: the tying method, the bridging method and the key element method.

In addition, some values of accidental actions are proposed in the British Standards (for the pressure (34 kN/m^2) or for the tying force (75 kN), for instance); however, it is impossible to identify the scientific background from which these values are derived.

As mentioned in *[48]*, the recommended methods can be divided in two main families:

- the direct design methods which include explicit consideration of resistance to progressive collapse during the design process (i.e. the bridging method, the key element method and sometimes the tying method if the tie design is included in the design process) and;
- the indirect design methods in which the resistance to progressive collapse is considered implicitly through the provision of minimum levels of strength, continuity and ductility (i.e. mainly the tying method).

The other codes and standards are mainly inspired from the British Standards recommendations. In most of them, the same methods are proposed to ensure the robustness of structures; only some differences on the load combinations and on the ultimate values to be considered in case of an accidental event are observed.

III.2.4. Recent researches

Since some years, the topic "Robustness" has become a very fashion subject, in particular since the catastrophic event of the World Trade Center in 2001. It is confirmed by the different international projects and actions initiated in the last decade.

The objective of this section is not to reflect in details all the researches in the domain of robustness and progressive collapse. As for the codes and standards, recent publications deal with this subject (*[55]*, *[46]*, *[48]* and *[57]*) with the main objective to identify the domains for which additional investigations are requested. This point will be addressed in the conclusions presented in the following section.

The present paragraph only summarises recent researches realised at the Imperial College and presented in 2007 within the PhD thesis of Anastasios Vlassis (*[57]*, *[58]*, *[59]* and *[60]*) titled "Progressive collapse assessment of tall buildings". The reason is the fact that the thesis of Anastasios Vlassis and the present thesis, even if they have been developed in parallel without contacts, present some similarities, in particular on how to extract a simplified model from a structure to predict its global response and on the importance allocated to the influence of the joint behaviour on the structure response. However, the

performed developments are not overlapping but are complementary as explained here below.

The thesis of Anastasios Vlassis proposes a novel simplified framework for progressive collapse assessment of multi-storey buildings, considering sudden column loss as a design scenario. The proposed framework offers a practical means for assessing structural robustness at various levels of structural idealisation. Three main stages are utilised in the proposed assessment framework, including the determination of the nonlinear static response, dynamic assessment using a novel simplified approach and ductility assessment. The conceptual clarity of the proposed framework sheds considerable light on the adequacy of commonly advocated measures and indicators of structural robustness, culminating in the proposal of a single rational measure of robustness that is applicable to building structures subjected to sudden column loss.

In particular, a pseudo-static approach to predict the response of a structure further to the loss of a column with account of the dynamic aspects is developed. This method consists in predicting the non-linear static load-deflection response of the structure at the column loss level and to determine the corresponding maximum dynamic displacements; the latter are obtained by expressing the equivalence between external work and internal energy obtained when the two depicted hatched areas illustrated in *Figure III.4* are equal. The maximum dynamic displacements can be computed for different values of loads and reported in a load vs. dynamic displacement curve which represents the pseudo-static response (see *Figure III.4*).

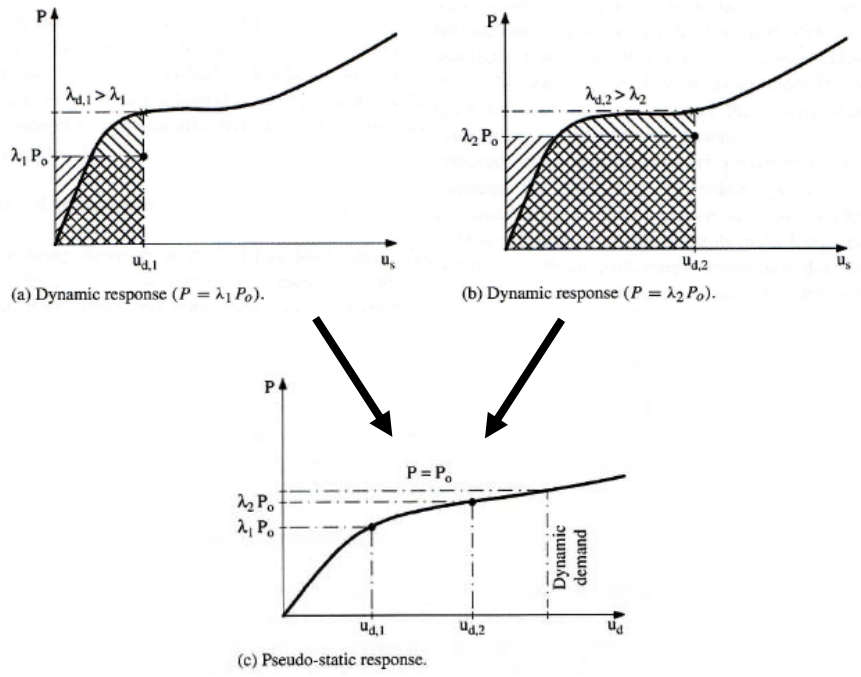

Figure III.4. Illustration of the pseudo-static method developed in the Vlassis thesis [58]

The developed method is very easy to apply; the accuracy of the method is linked to the accuracy of the load-deflection response curve which is used within the method. In the Vlassis thesis, the models which are presented to compute this curve are based on rough assumptions, in particular for the computation of the parameters to be used within the models.

At Liège University, a general concept (see *§ III.3*) aiming at predicting analytically the "static" structural response of a building further to the loss of a column has been defined and validated; the present part of the thesis contributes to these developments and validations. The developed analytical tools permit to estimate with a very good accuracy the load-deflection curve at the top of the loss column.

So, by merging the developments of the Vlassis thesis and the developments performed at Liège University, it will be possible to predict, with a very good accuracy the dynamic response of a structure further to the loss of a column through "static" analytical analyses.

In addition, a mechanical model based on the component method is presented in Vlassis thesis to predict the behaviour of steel and steel-concrete composite joints subjected to combined bending moments and tensile loads. Even if this model is inspired from the component method, some important phenomena (such as group effects – see *§ III.5.3.2.B*), which can significantly influence the response of the joints, are not taken into account; also, what can be criticized is the fact that the developed model has not been validated through comparisons to experimental tests. Within the present thesis, an analytical model based on *[61]* will be extended to steel-concrete composite joints and validated through comparisons to experimental tests.

Since July 2007, Liège University and Imperial College are in contact to create exchanges on these domains.

III.2.5. Conclusions

Since the Ronan Point catastrophic collapse, some codes and standards have been completed with recommendations to ensure the structural integrity of buildings. The first ones to introduce such recommendations were the British Standards and the Canadian code. The other codes and standards (Eurocodes, United State Civilian Standards, the Unified Safety Criteria for the US department of defence, the US General Services Administration guidelines, ...) are mainly inspired from the British Standards, with some differences concerning the accidental loads and the load combinations to be considered at the ultimate limit state.

However, it is impossible to find solid scientific backgrounds to these documents, in particular for the recommended values of actions proposed in the latter. It is also highlighted in *[62]* that most of these codes and standards have references to structural integrity but not a complete set of criteria for progressive collapse.

It is why, in the last years, researches have been initiated in this domain; the interest in the structural integrity and the robustness aspects has recently increased worldwide since the catastrophic events of the World Trade Center and the Pentagon Building in 2001.

In 2005, some research issues and challenges have been identified in *[54]*, which reflects the domains to be investigated in the future in order to provide, at the end, the technical support and the scientific background for design methods to ensure the structural integrity of structures; these issues and challenges are summarised here below:

1. identification of hazard/collapse initiation scenarios and prediction of the magnitudes of abnormal loads generated in these scenarios;
2. understanding attributes of buildings that have withstood threats successfully and validation of non-linear structural analysis platforms through comparison between the analysis predictions and the actual response of these buildings;
3. conditional limit states and behavioural models with account of sources of load-carrying capacity that normally would not be considered in design (catenary actions, substantial inelastic behaviour of members and connections, …);
4. modelling of connection behaviour which is essential to develop the alternate load path and to achieve continuity and ductility;
5. development of structural analysis platforms with account of specific aspects appearing when subjected to exceptional actions (large deformations, dynamic effects, …);
6. developing tools for the design engineers which require analytical sophistication and engineering effort that are commensurate with the risk exposure.

Through the present part of the thesis, it is intended to contribute to different parts of these issues and challenges as listed here below:

- Point 2: the validity of the homemade FE tool FINELG to predict the response of frames further to a column loss is investigated through comparisons with experimental test results and a benchmark study;
- Point 3 and 6: a simplified analytical behavioural model is developed to predict the development of the catenary actions and the displacements in a structure further to the loss of a column;

- Point 4: the behaviour of the joints subjected to combined bending moments and tensile loads is investigated and an analytical method is proposed to predict the behaviour of structural joints when the catenary actions develop within a structure.

The simplified analytical behavioural model is developed in the static domain, i.e. the dynamic effects which could be associated to the sudden loss of a column are not considered. However, as briefly described in this section, a PhD thesis presented at the Imperial College *[57]* proposes a pseudo-static method to predict the dynamic response of a structure further to the loss of a column from its static response. So, it will be possible, later on, to combine the simplified analytical model developed in the present thesis and the pseudo-static method proposed in *[57]* to predict the dynamic response of a structure.

The developments realised in this part are involved in a general concept developed at Liège University and presented in the following paragraph; at the end of this paragraph, the adopted strategy within the present part will be described.

III.3. Definition of the general concept adopted for the investigation of the exceptional event "loss of a column in a steel or composite frame"

III.3.1. Introduction

Through the state-of-the-art, it has been illustrated that some codes or standards recommend methods to ensure the robustness of structures and propose different methods (direct or indirect ones) to guarantee a sufficient robustness of these structures.

However, as mentioned in *§ III.2*, it is sometimes difficult to find a "scientific" background to the proposed methods. In addition, for most of the methods, only checks relative to the resistance are recommended although it is well known that, under exceptional actions, important deformations generally occur in the structures which requests to ensure a sufficient ductility of some structural elements to allow a redistribution of the internal forces.

So, as mentioned in the previous paragraph, it is needed to develop simplified methods which permit to predict the resistance of structures losing a column and to predict the requested ductility of some structural elements (beam-to-column joints, beams, …) to ensure a good redundancy.

The development of such simplified procedures is the scope of two complementary PhD theses developed at Liège University: the thesis of Luu Nguyen Nam Hai *[63]* and the present one. These theses are founded on a general concept which is first described in *§ III.3.2*; then, the followed strategy within the present part of the thesis is described in *§ III.3.3*.

III.3.2. Description of the adopted general concept

III.3.2.1. Definitions, main assumptions and objectives

The loss of a column can be associated to different types of exceptional actions: explosion, impact of a vehicle, … Under some of these exceptional actions, dynamic effects may play an important role; within the present work, it is assumed that the action associated to the column loss does not induce significant dynamic effects. So, the performed investigations are based on static approaches.

Accordingly, the column is assumed to be progressively removed from the frame and the normal load within this column varies progressively from the one appearing under the loads applied to the structure just before the occurrence of the exceptional action to 0 when the column is completely removed from the frame.

Also, the present study is limited to the investigation of the response of 2D steel or composite structures, i.e. the 3D effects which could influence the structural response (as the presence of secondary beams perpendicular to the considered plane or the distribution of the loads within the 3D slab) are not considered herein.

When a structure is losing a column, the latter can be divided in two parts (as illustrated in *Figure III.5* where a column at the ground floor is lost):

- the directly affected part which represents the part of the building which is directly affected by the loss of the column, i.e. the beams, the columns and the beam-to-column joints which are just above the loss column (in red in *Figure III.5*) and;

- the indirectly affected part which represents the rest of the building which is affected by the loads developing within the directly affected part and which influences the development of these loads (in blue in *Figure III.5*).

Within the present work, only the response of the directly affected part is under investigation; the behaviour of the indirectly affected part, i.e. its influence on the response of the directly affected part and its resistance when loaded by additional loads

coming from the directly affected part, is the topic of the thesis of Luu Nguyen Nam Hai *[63]*.

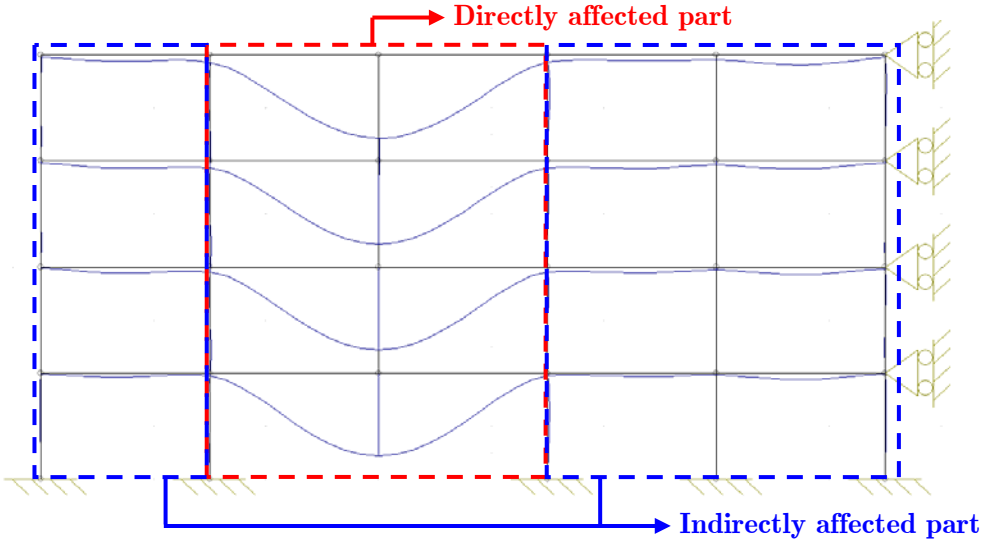

Figure III.5. Definition of directly and indirectly affected part

If a cut in the structure is realised at the top of the loss column, as illustrated in *Figure III.6*, different internal loads in the vertical direction can be identified:

- the shear loads V_1 and V_2 at the beam extremities closed to the loss column (left and right beams respectively);
- the axial load N_{up} in the column just above the loss column and;
- the axial load N_{lo} in the loss column.

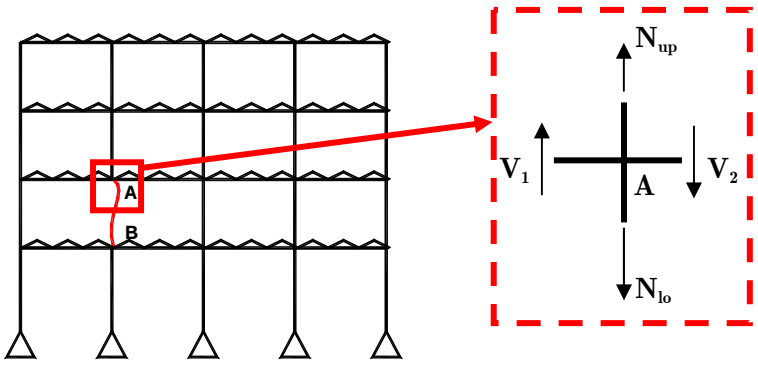

Figure III.6. Representation of a frame losing a column

The objective of the two PhD theses is to be able i) to predict the evolution of N_{lo} according to the vertical displacement of point "A" Δ_A, with due account to the eventual membrane forces developing in the directly affected part, in order to know the requested ductility within the different structural members and ii) to predict the loads developing in the directly affected part in order to check the resistance of the indirectly affected part supporting these additional loads.

III.3.2.2. Loss of a column in a structure

In *Figure III.7*, the curve representing the evolution of the normal load in column "AB" (N_{lo} – see *Figure III.6*) according to the vertical displacement at point "A" Δ_a is illustrated. Three phases are identified on this curve:

- At point (1), the frame is not loaded; so, N_{lo} and Δ_A are equal to 0.
- From point (1) to (2) (Phase 1), the design loads are progressively applied, i.e. the "conventional" loading is applied to the structure; so, N_{lo} progressively decreases (N_{lo} becomes negative as the column "AB" is subjected to compression) while Δ_A can be assumed to be equal to 0 during this phase (in reality, there is a small vertical displacement at point A associated to the compression of the columns below point "A"). It is assumed that no yielding appears in the investigated frame during this phase, i.e. the frame remains fully elastic.
- From point (2) to (5), the column is progressively disappearing. Indeed, from point (2), the compression in column "AB" N_{lo} is decreasing until reaching a value equal to 0 at point (5) which means that the column can be considered as fully destroyed. So, in this zone, the absolute value of N_{lo} is progressively decreasing while the value of Δ_A is increasing. This part of the graph is divided in two phases as represented in *Figure III.7*:
    - From point (2) to (4) (Phase 2): during this phase, the directly affected part passes from a fully elastic behaviour (from point (2) to (3)) to a plastic mechanism at point (4). At point (3), first plastic hinges are appearing in the directly affected part.
    - From point (4) to (5) (Phase 3): during this phase, high deformations of the directly affected part are observed and second order effects play an important role. In particular, significant catenary actions are developing in the bottom beams of the directly affected part.

It is only possible to pass from point (1) to (5) if:

- the loads which are reported from the directly affected part to the indirectly affected part do not induce the collapse of elements in the latter (for instance, buckling of the columns or formation of a plastic mechanism in the indirectly affected part);
- the compression loads appearing in the upper beams of the directly affected part associated to an "arch" effect (see *Figure III.8*), do not lead to the buckling of the latter;

- if the different structural elements possess a sufficient ductility to reach the vertical displacement corresponding to point (5).

It is possible that the complete removal of the column is reached (i.e. $N_{lo} = 0$) before reaching Phase 3. Also, if the loss column is an external one, it is not possible to develop Phase 3 as no catenary actions appear within directly affected part.

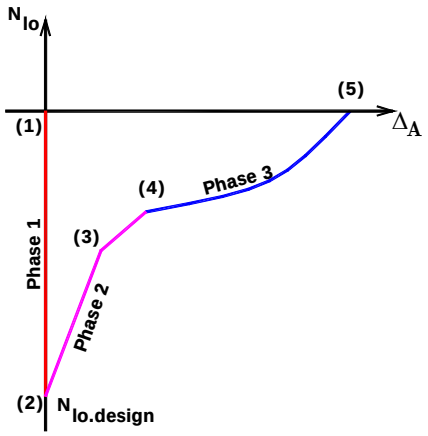

Figure III.7. Evolution of N_{lo} according to the vertical displacement at the top of the loss column

The investigation of the response of the frame during Phase 1 and 2 is the topic of the thesis of Luu Nguyen Nam Hai *[63]* while the response during Phase 3 is the subject of the present part of the thesis. The adopted strategy within this part is presented in the next section.

III.3.3. Adopted strategy within the thesis

As said in the previous section, the objective of the present part is to investigate the behaviour of the frame during Phase 3 (see *Figure III.7*).

At this phase, a plastic mechanism is formed in the directly affected part and the vertical displacement at point "A" rapidly increases. As a consequence, the second order effects developing in the directly affected part becomes significant. In particular, membrane forces develop in the bottom beams of the directly affected part while compression loads developed in the upper ones associated to an arch effect, as illustrated in *Figure III.8 [63]*.

Through parametrical studies performed on thousands of frames, it has been shown that the membrane forces developing in the beams of the storey just above the loss column are significantly more important than the ones developing in the other beams, as illustrated in *Figure III.8*.

Consequently, it is decided to investigate the behaviour of this storey only and to extract this storey from the frame to define a simplified substructure modelling able to simulate with a sufficient accuracy the behaviour of the directly affected part, as illustrated in

Figure III.9. One of the objectives of the present part of the thesis is to validate the simplified substructure modelling.

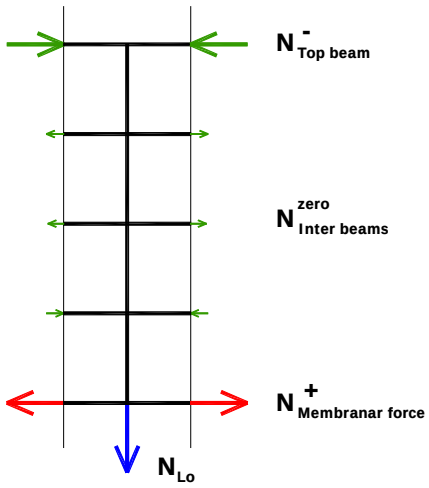

Figure III.8. Distribution of the membrane forces developing in the directly affected part

To be able to isolate the substructure, different parameters have to be defined:

- the lateral restraint K which represents the lateral stiffness of the indirectly affected part when the membrane forces develop in the directly affected part;
- the resistance F_{Rd} of the indirectly affected part, i.e. the maximum horizontal load coming from the directly affected part that the indirectly affected part can sustain;
- the loads p and Q that the system has to support.

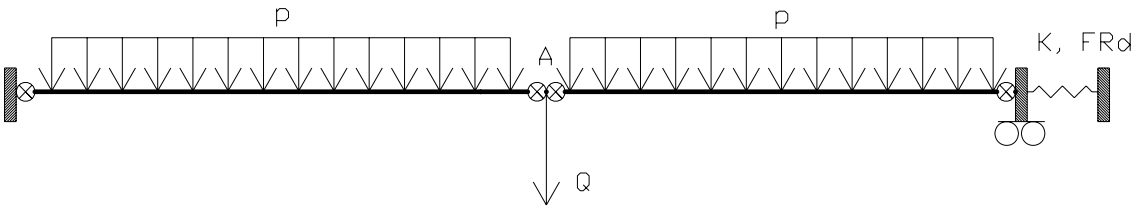

Figure III.9. Extracted subsystem

The beams and the joints of the substructure are the ones met in the bottom storey of the directly affected part. The uniformly distributed load p is the load applied on the bottom storey just before the column loss and is assumed to be constant.

The parameters K and F_{Rd} are properties of the indirectly affected part which influence the development of the membrane forces in the beams. Analytical methods aiming at predicting the values of these parameters have been developed and validated in the thesis of Luu Nguyen Nam Hai *[63]*, as one of the objective of the latter is to study the response of the indirectly affected part (see *§ III.7.3*).

The concentrated load Q represents the load to be supported by the substructure associated to the column loss (see *Formula (3.1)*) and varies during Phase 3. When the column is fully removed, the load "Q" to be supported comes from the upper storey.

$$Q = N_{lo} - N_{up} \tag{3.1}$$

At the end of Phase 2 (and at the beginning of Phase 3), i.e. at point (4) in *Figure III.8*, the values of N_{up} and N_{lo} are known through the theory developed in *[63]* and are equal to $N_{up,(4)}$ and $N_{lo,(4)}$ respectively; so, the value of Q when the plastic mechanism formed within the directly affected part is equal to $N_{lo,(4)}$ - $N_{up,(4)}$. At this moment, plastic hinges are formed within the simplified system as illustrated in *Figure III.10*; these plastic hinges can form in the beams or in the joints if the latter are partial-strength ones. This is the starting point of the development presented in this part.

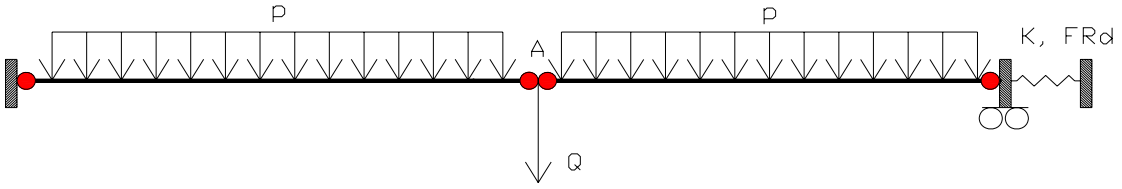

Figure III.10. Simplified subsystem at point (4) of Figure III.8 with plastic hinges represented in red

In addition, it is demonstrated through parametrical studies in *[63]* that, during Phase 3, the value of N_{up} can be assumed to be a constant equal to $N_{up,(4)}$ while the value of N_{lo} is varying. Accordingly, knowing the evolution of Q according to the vertical displacement of point "A" Δ_A when the plastic mechanism is formed, it is easy to derive the curve N_{lo} vs. Δ_A.

Within the simplified substructure, it is assumed that the system collapses when:

- the maximum deformation capacity is reached within a yielded section or joint;
- when F_{Rd} in the horizontal spring is reached;
- when the resistance to axial loads of the beams or the joints is reached.

In conclusion, the investigated structure is assumed to have a sufficient robustness if the point (5) of *Figure III.7* can be reached without exceeding the deformation capacity in the plastic hinges or the resistance to axial loads of the structural elements.

To validate the so-defined simplified substructure modelling and to investigate its behaviour when membrane forces develop, the strategy summarised in *Figure III.11* is followed.

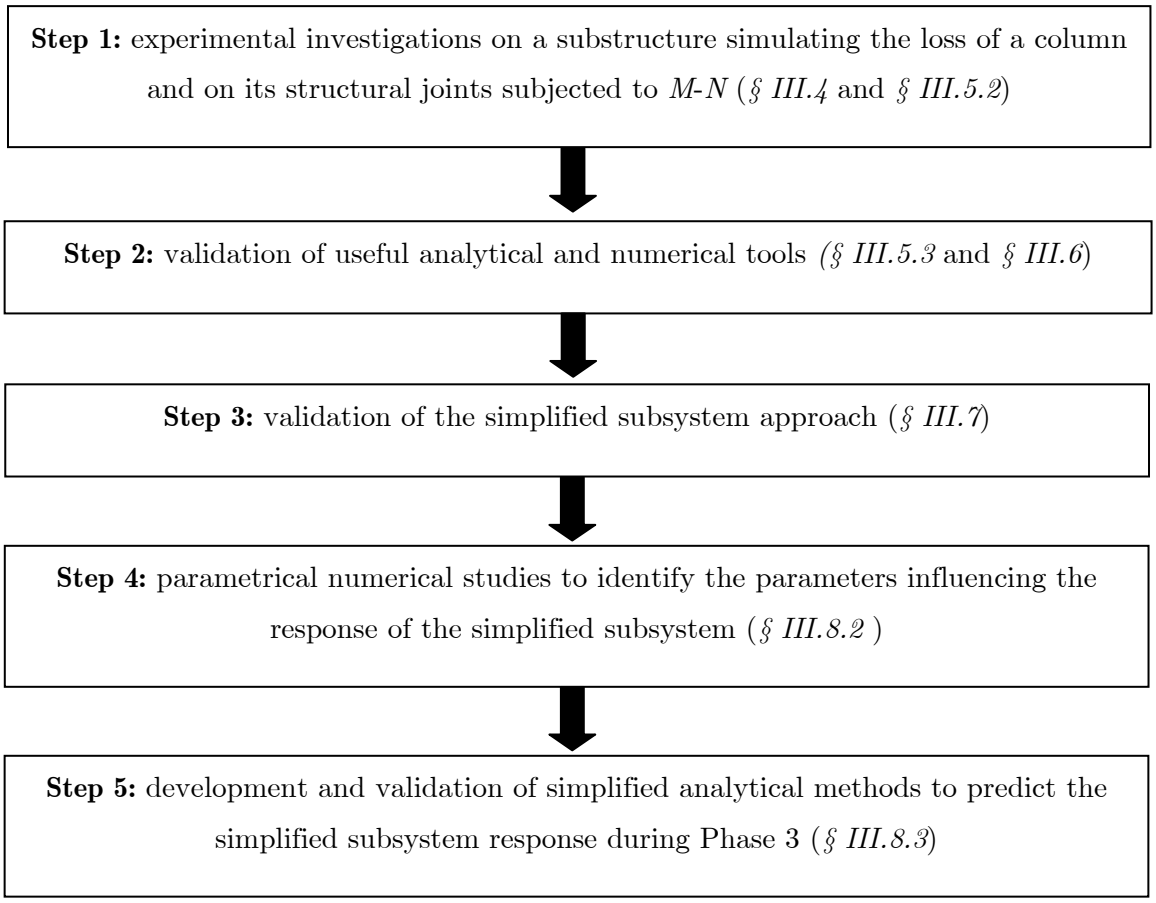

Figure III.11. Global strategy followed within the present part of the thesis

Within this strategy, analytical, numerical and experimental aspects are involved:

- In a first step, experimental investigations are conducted. In particular, a test on a substructure simulating the loss of a column in a composite structure has been conducted at Liège University; the latter is presented in *§ III.4*. In addition, tests in isolation on the substructure composite joints have been conducted at Stuttgart University to determine their behaviour under combined bending moments and axial tensile loads (*§ III.5.2*), situation which occurs when catenary actions develop within the frame.
- With the so-obtained experimental test results, analytical and numerical tools requested to investigate the behaviour of the simplified substructure are validated in Step 2. In *§ III.5.3*, an analytical method to predict the behaviour of composite joints subjected to combined bending moments and axial loads is developed and validated through comparisons with experimental test results. Then, the validity of the numerical tool FINELG to predict the behaviour of steel and composite frames further to the loss of a column is investigated in *§ III.6* through comparisons with the experimental results of the substructure test performed at Liège University (*§*

III.6.2) and through a benchmark study performed by different European institutions with different FE software (*§ III.6.3*).

- With the so-validated tools, the simplified substructure approach is then validated through Step 3 (*§ III.7*) and parametrical studies are conducted in Step 4 to identify the parameters influencing the response of the simplified substructure (*§ III.8.2*) and which have to be included in the developed simplified analytical approach presented in *§ III.8.3* (Step 5). This analytical approach is finally validated through comparisons with the substructure test results in *§ III.8.3.3*.

III.4. Experimental test simulating the loss of a column in a composite frame

III.4.1. Introduction

This paragraph presents the experimental test performed at Liège University as part of the "Robustness" project on a composite substructure simulating the loss of a column in a composite frame.

To define the tested substructure, an "actual" composite building is first designed according to the recommendations of Eurocode 4 *[6]*, so under "conventional" loading conditions (i.e. loads recommended in Eurocode 1 *[64]* for office buildings) with the aim to obtain realistic dimensions for the structure to be tested. The designed building is presented in *§ III.4.2*.

As it was not possible to test a full 2-D actual composite frame within the "Robustness" project, a substructure is then extracted from the actual building what is described in *§ III.4.2*; the extracted substructure is defined so as to respect the dimensions of the testing slab but also to exhibit a similar behaviour as the one which would be observed in the actual frame.

Finally, the accomplishment of the test as well as the test results are presented with details in *§ III.4.4*, putting into sight the main observations.

III.4.2. Design of an "actual" composite building according to Eurocode 4 recommendations

III.4.2.1. Introduction

As said in the previous section, an "actual" composite building is first designed in agreement with the recommendations of Eurocode 4 *[6]* under "conventional" loading. The

general layout of the building which is considered with one of its main frame is presented in *Figure III.12*.

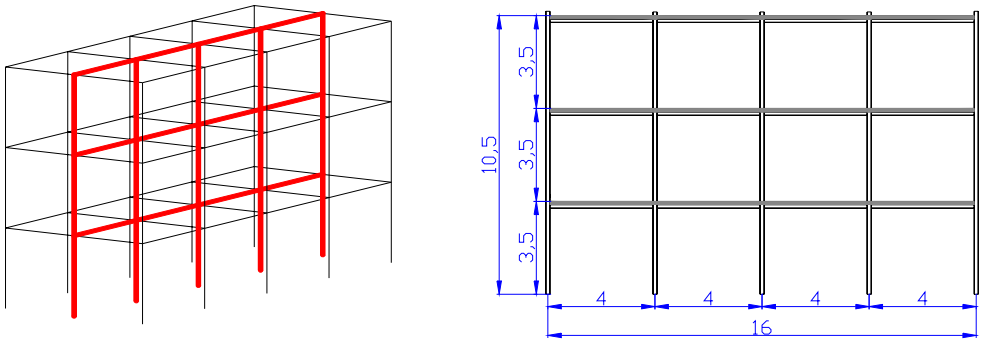

Figure III.12. 3D view of the designed building and representation of one of the main frames

The building is composed of three main frames with a space of 3 m between them. The main frames are four bays – three storeys ones with a total width of 16 m (bay span = 4 m) and a total height of 10,5 m (storey height = 3,5 m). The loads which have been considered for the design of the structural elements are the following:

- the self-weight;
- a permanent load of 2 kN/m²;
- an imposed load of 3 kN/m² (load recommended for office building in Eurocode 1 *[64]*).

The main frames are assumed to be braced and the column bases to be perfect hinges. In a first approach, the external joints are assumed to be fully pinned and the internal ones to be fully rigid; the validity of these assumptions will be checked later on in *§ III.4.2.3* presenting the joint design. The static scheme considered for the main frame design is presented in *Figure III.13*.

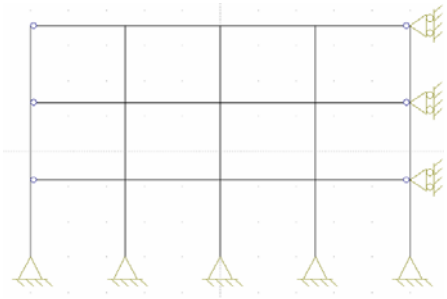

Figure III.13. Static scheme considered for the main frame design

III.4.2.2. Design of the structural members

The design of the main frame at the middle of the building is given with details in *[65]* and *[66]*; further to this design, the following structural members are defined:

- The slab is a reinforced concrete one with a thickness of 120 mm and made of a C25/30 concrete (f_{ck} = 25 N/mm²); it has been designed according to the rules given in Eurocode 2 *[67]*. The reinforcement is composed of two meshes: one place at the top with 10 mm rebars space of 200 mm and one place at the bottom with 10 mm rebars space of 150 mm. The steel grade for these rebars is S500C (high ductility rebars with f_{sk} = 450 N/mm²) and the cover is equal to 25 mm. The cross section of the slab is presented in *Figure III.14*.

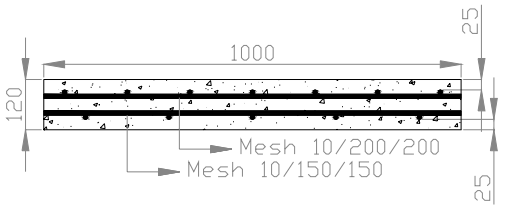

Figure III.14. Slab cross section

- The beams are composite ones (upper flange of the profile connected to the concrete slab); they have been designed according to the rules of Eurocode 4 *[6]*. The steel part of the beam is an IPE140 profile with a S355 steel grade (f_{yk} = 355 N/mm²); the composite beam cross section is presented in *Figure III.15*. A full connection between the profile and the concrete part has been designed; the number of studs (Nelson studs with a diameter equal to 16 mm and a height of 75 mm – f_u = 450 N/mm²) needed to ensure this full connection is presented in *Figure III.16*.

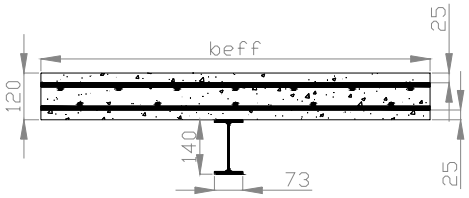

Figure III.15. Composite beam cross section

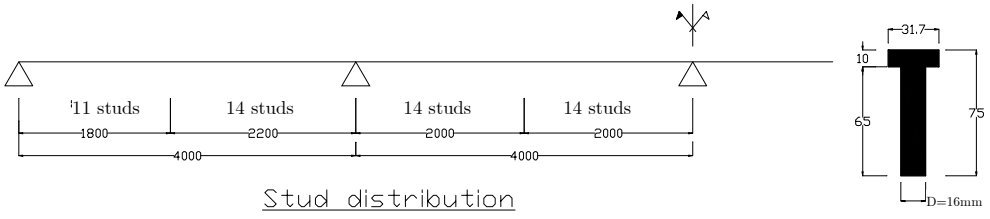

Figure III.16. Distribution of the studs along the composite beam length

- The columns are steel ones; they have been designed according to the rules given in Eurocode 3 *[12]*. The profile is an HEA160 one with a S355 steel grade.

III.4.2.3. Design of the structural joints subjected to hogging bending moments

A. Design of the external steel joints

For these joints, it is assumed that the concrete slab is stopped in front of the external columns (see *Figure III.17*); so, these joints are steel ones.

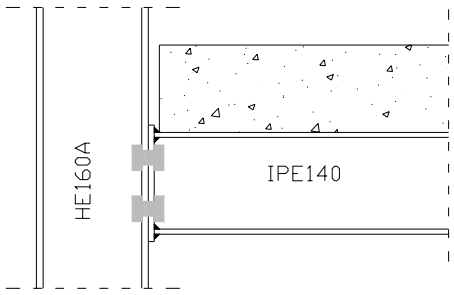

Figure III.17. External steel joint configuration

The joint properties have been chosen so as to ensure a ductile behaviour of the joint at failure and that, with account of the overstrength effects. To achieve this goal, only ductile components are activated at failure. The selected joint configuration is a flush-end plate bolted joint. *Figure III.18* presents the geometrical properties of the end-plate.

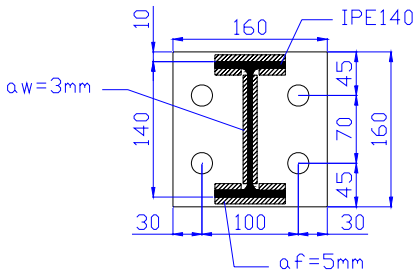

Figure III.18: geometrical properties of the end-plate

The bolts are M20 8.8 ones. The end-plate thickness is equal to 8 mm. The steel grade for all the steel components of the joint is S355 with a possible overstrength of 35 % (value proposed in Eurocode 8 for seismic design *[5]*), i.e. $f_{y,overstrength}$ equal to 480 N/mm².

Different states have been considered in the joint design so as to be sure that, even if overstrength occurs in some components, the joint still have a ductile mode of failure. The joint mechanical properties for these different states are summarised in *Table III.1*. The latter have been computed through the software CoP *[24]* which is in full agreement with the Eurocode 3 recommendations *[22]*.

Table III.1. Mechanical properties of the external steel joints with account of the overstrength effects

	Overstrength	M_{Rd} **[kNm]**	M_e **[kNm]**	**Failure mode**	V_{Rd} **[kN]**	$S_{j,ini}$ **[kNm/rad]**
Initial state	No overstrength	15,1	10,1	End-plate in bending	134,4	970
2° state	End-plate	16,6	11,1	Column flange in bending	134,4	970
3° state	End-plate + column	19,9	13,3	Beam flange in compression	134,4	970
4° state	End-plate + column + beam	20,5	13,7	End-plate in bending	134,4	970

The initial stiffness of the external joints is equal to 970 kNm/rad; the latter is higher than $0{,}5EI_b/L = 890$ kNm/rad (EI_b is the uncracked flexural stiffness of the composite cross section of the beam and L is the span of the beam), which is the upper limit under which a joint can be assumed as pinned. So, the assumption of pinned external joints in the actual composite building design is not validated. Accordingly, a computation of the internal frame modelled with the predicted properties of the joints has been performed and the internal forces have been compared to the resistance of the joint; the obtained results are presented later on in *§ III.4.2.4*.

B. Design of the internal composite joints

The steel components of these joints have the same configuration than the one used for the external steel joints presented in the previous section. A representation of one internal composite joint is given in *Figure III.19*.

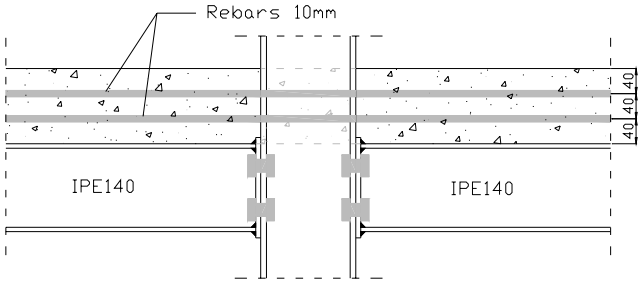

Figure III.19. Internal composite joint configuration

The mechanical properties of this joint configuration have been computed according to the procedure described in *[23]* which is in agreement with the Eurocode 4 recommendations *[6]*. The mechanical properties of the internal composite joints for different states of

overstrength are summarised in *Table III.2* (assuming that the internal joint is symmetrically loaded.

Table III.2. Mechanical properties of the internal composite joints with account of the overstrength effects

	Overstrength	M_{Rd} **[kNm]**	M_e **[kNm]**	**Failure mode**	V_{Rd} **[kN]**	$S_{j,ini}$ **[kNm/rad]**
Initial state	No overstrength	39,8	26,5	Beam flange in compression	134,4	7541
2° state	Beam	46,8	31,2	Column web in compression	134,4	7541
3° state	Beam + column	47	31,3	Reinforcement in tension + end-plate in bending	134,4	7541
4° state	Beam + column + end-plate	49,8	33,2	Beam flange in compression	134,4	7541

The initial stiffness of the internal joints is equal to 7541 kNm/rad; the latter is lower than $8EI_b/L$ = 14240 kNm/rad, which is the lower limit above which a joint can be assumed as rigid. So, the assumption of fully-rigid internal joints in the actual composite building design is not validated. As previously mentioned, a computation of the internal frame modelled with the predicted properties of the joints has been performed and the internal forces have been compared to the resistance of the joint (see *§ III.4.2.4*).

C. Conclusions

From the previous results, it can be concluded that all the structural joints are semi-rigid and partially resistant. The external steel joint failure is associated to components in tension while the internal composite joint failure to components in compression. It is due to the fact that, in the composite joint configuration, an additional component, which is the reinforcement in tension, is activated; so, the total resistance of the components in tension is increased.

All the failure modes for the two joint configurations are ductile ones, even if overstrength in some components occurs. Nevertheless, there is a difference in the post-limit behaviour of the two joints as the failure modes are not the same. This difference, illustrated in *Figure III.20*, is explained here below:

- For the internal joints with a failure associated to a component in compression: when M_{Rd} is reached, the joint can not sustain this bending moment (no plateau in

the behavioural curve) and the bending moment at the joint level decreases progressively.

- For the external joints with a failure associated to a component in tension: when M_{Rd} is reached, the joint can keep this bending moment (plateau in the behavioural curve).

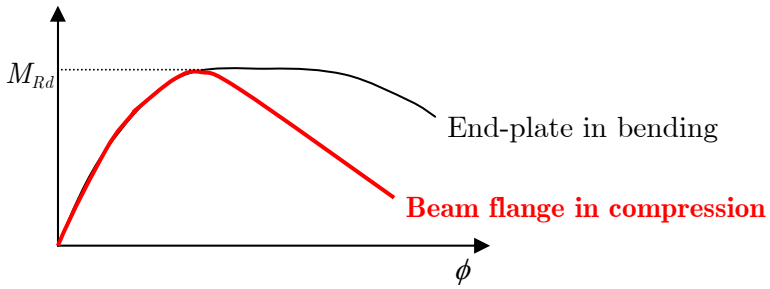

Figure III.20. Comparison of behavioural curves for different types of failure modes

In the present case, to ensure a good behaviour of the joint under exceptional loading, it is not necessary to keep the bending moment in the post-limit stage. Indeed, to have robustness, only ductility is requested. The rotation capacity of the joint must be sufficient so as to permit to pass from a behaviour of the joints in bending to a behaviour of the joints in tension (associated to the development of membrane forces within the beams).

In addition, when the joint will work in tension, the fact that the failure in bending is associated to a component in compression can have a positive effect. Indeed, if the failure in bending is associated to a component in tension, an important part of the resistance in tension is already "eaten" when the joint then works in tension; so, if the resistance is associated to a component in compression, the reserve of resistance in tension is bigger.

The behaviour of the so-designed composite joints has been experimentally investigated within the "Robustness" project, first under hogging and sagging bending moments (see *§ II.3.2.3*), and then, under combined tension forces and bending moments (see *§ III.5.2*). Through these investigations, the ductile behaviour of the joints was illustrated.

III.4.2.4. Verification of the internal main frame modelled with the predicted joint properties

As the stiffness properties of the joint computed in the previous section do not respect the initial assumptions, an elastic cracked analysis on the internal main frame (see *Figure III.12*) is once again performed through the software OSSA2D *[68]* (elastic linear software developed at Liège University – Argenco Department) with account of the predicted

properties of the joints. Different load cases are considered; some examples are presented in *Figure III.21*.

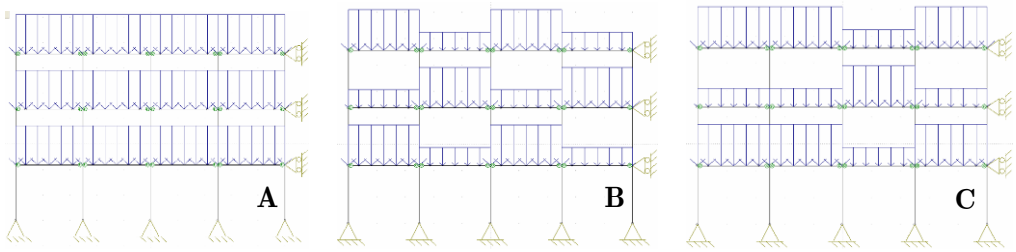

Figure III.21. Examples of considered load cases

The stiffness of the joints introduced in the modelling is equal to $S_{j,ini}/2$ as recommended in the Eurocodes for an elastic linear analysis. The extreme internal forces which are obtained through this analysis for the different load cases presented in *Figure III.21* are given in *Table III.3*; they are compared to the resistant forces of the structural elements.

Table III.3. Extreme internal forces in the internal main frame

	$M_{Ed,max}$ [kNm]	$V_{Ed,max}$ [kN]	M_{Rd} [kNm]	V_{Rd} [kN]
External joints	6	80	15,1	134,4
Internal joints	30	91	39,8	134,4
Mid-external span of the beam	73	-	92,6	-
Mid-internal span of the beam	67	-	89,3	-

In addition, a full non-linear analysis has also been performed through the homemade FEM software FINELG *[36]* validated (for "conventional" loading) in *§ II.4*. The joints and the steel materials have been modelled with elastic-perfectly plastic behavioural curves (see *Figure II.45*); the concrete has been modelled with a parabolic curve with tension stiffening (see *Figure II.46*). The mechanical properties which have been introduced are the characteristic ones; the loads are the design ones with the entire span fully loaded (load case A in *Figure III.21*).

Through this analysis, the collapse of the frame occurs with the formation of a beam plastic mechanism in the external composite right beam at the second storey for a load multiplier equal to 1,68. *Figure III.22* gives the deformation of the frame at collapse and the load multiplier of the design loads vs. deflection curve at mid-span of the external right beam at the second storey.

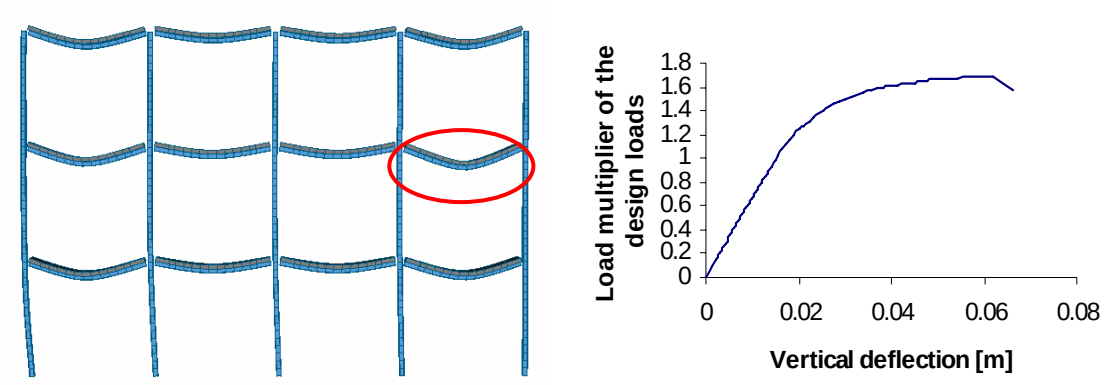

Figure III.22. Deformed shape at collapse and load multiplier-deflection curve obtained through the non-linear analysis

III.4.2.5. Conclusions

Through the presented design, a three storeys – four bays composite frame has been defined; all the structural members (i.e. the composite beams, the steel columns and the composite joints) have been designed in agreement with the Eurocodes. The joints have been designed so as to be partial-strength ones with ductile modes of collapse (taking into account of the possible material overstrength).

In the next section, the substructure tested in the Argenco laboratory (Liège University) is isolated from this "actual" building.

III.4.3. Extracted substructure tested at Liège University

III.4.3.1. Introduction

As mentioned in *§ III.4.1*, the scope of the substructure test is to investigate the behaviour of a composite structure further to the loss of a column.

According to the laboratory facilities, it was not possible to test the full actual composite frame previously described. So, a substructure has been extracted from the latter; this substructure has been designed so as to respect the laboratory facilities and to exhibit a behaviour as close as possible to the actual frame one.

In the present paragraph, the extracted substructure is described, putting into sight the main modifications according to the actual building.

III.4.3.2. Substructure geometric layout

To perform the test, the bottom storey is isolated from the internal frame of the actual building (see *Figure* III.23). According to the reaction slab dimensions in the laboratory, it is not possible to have a width of 16 m for the substructure (which is the width of the

actual frame). So, it is decided to reduce the width of the external spans as illustrated in *Figure* III.23.

Also, the width for the concrete slab of the substructure has to be fixed; the chosen width is equal to 500 mm (see *Figure III.24*). This width has been fixed so as to be sure that, during the loading, the distribution of the stresses within the concrete will be as close as possible to an uniform distribution; 500 mm corresponds to the value of the effective width of the concrete slab in the actual building for the hogging moment zone (according to the recommendations of Eurocode 4 *[6]*).

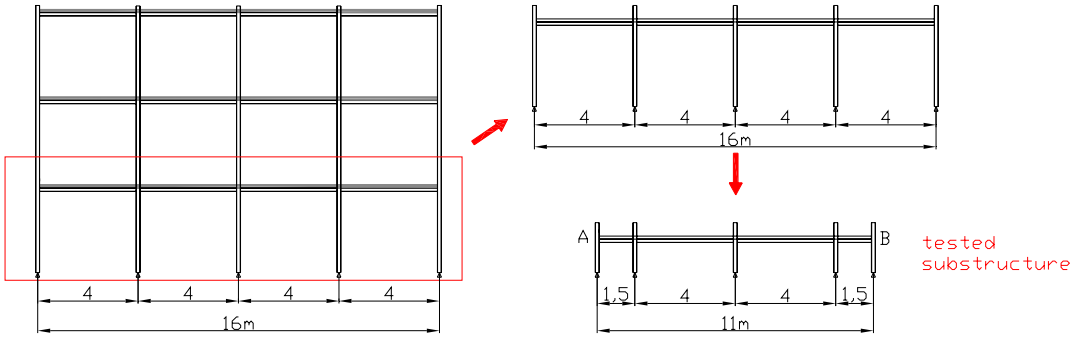

Figure III.23. From the actual frame to the tested substructure

III.4.3.3. Reinforcement and stud layouts of the substructure

The reinforcement and the stud layouts in the concrete slab have been fixed in strong collaboration with Stuttgart University.

First, it has been agreed to use six 8 mm rebars for the longitudinal reinforcement (151 mm²) instead of four 10 mm ones (157 mm²), which are the rebars included within the 500 mm width in the actual frame (see *§ III.4.2*). The scope of this modification is to increase the probability to have a distribution of small cracks along the slab during the loading instead of having big cracks which have to be avoided from the ductility point of view. For the transversal rebars, 10 mm rebars are used as illustrated in *Figure III.24.*

Secondly, the layout of the headed studs and the reinforcement has been chosen in a way that a tension band can develop in the concrete slab, with an especially high ductile behaviour. Therefore the distance between the first stud and the face of the column flange is increased compared to standard layout while the amount of reinforcement within this area is kept constant (see *Figure III.24*); this type of layout has already been investigated in a previous project conducted by Khulmann/Schäfer (*[69]* and *[70]*) and showed good results. Also, it has been decided to use studs with a diameter of 19 mm instead of studs

with a diameter of 16 mm which permits to limit the number of studs to ensure a full connection (23 studs in the internal composite beam instead of 28 – see *Figure III.16*).

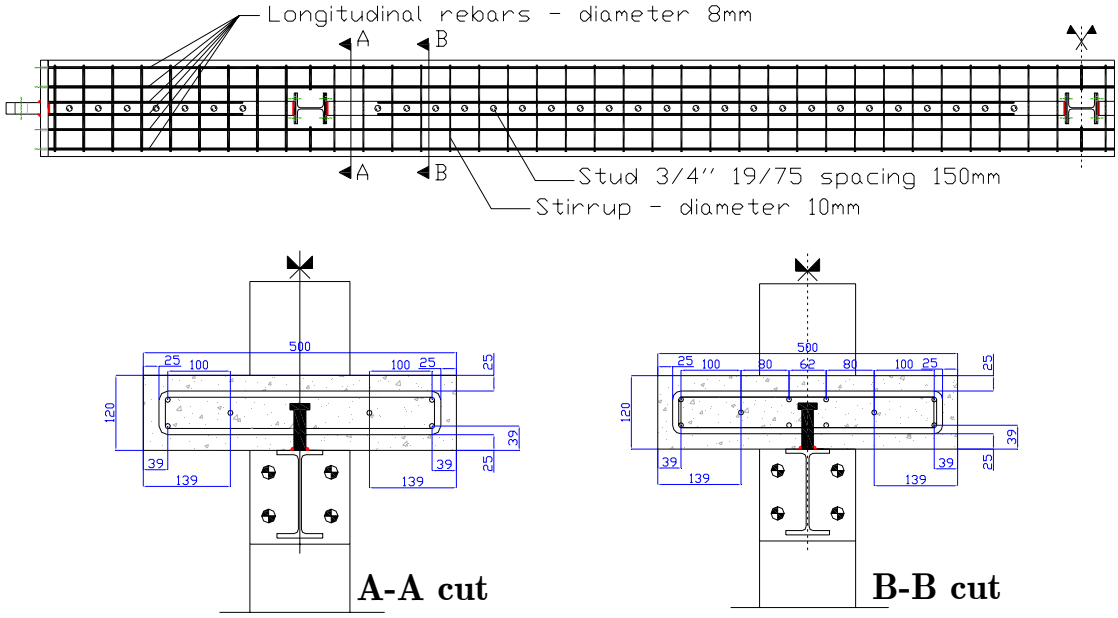

Figure III.24. Reinforcement and stud layouts

III.4.3.4. Joint and column base configurations within the substructure

At the column bases, actual hinges are placed with the column supports presented in *Figure III.25*; Teflon elements are put between the pin and the column support so as to limit the friction between these two elements during the loading.

The composite joint configuration in the substructure is the same than the one in the actual building (see *§ III.4.2.3.B*). However, for the joints between the external beams and the external columns (Beam A and Column A respectively in *Figure III.28*), it has been decided to place actual hinges (as shown in *Figure III.25*) instead of the actual external joints (see *Figure III.17*) so as to limit the number of parameters which could influence the response of the internal beams under investigation during the test (Beam B in *Figure III.28*).

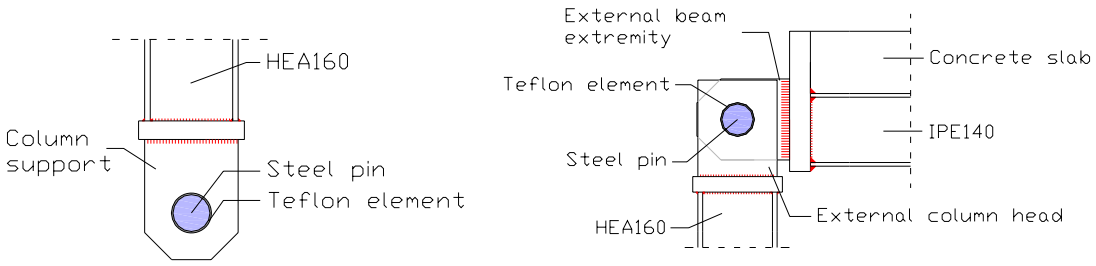

Figure III.25. Column support at the column bases and hinge between the external composite beam and the external steel column

III.4.3.5. Simulation of the lateral restraint during the test

As previously mentioned, the tested substructure is defined so as to exhibit a behaviour as close as possible to the actual frame one. By isolating the substructure from the actual frame, reducing the length of the external spans and placing actual hinges at the external joints, a key element is modified: the lateral restraint "*K*" coming from the directly affected part (see *Figure III.5*) and influencing the development of the catenary action which is under investigation (see *§ III.3.3*).

Different values of the lateral restraint "*K*" have been computed for the actual frame through an elastic linear analysis performed with the homemade software OSSA2D *[68]*, each "*K*" value corresponding to different positions of the column loss, as illustrated in *Figure III.26*. The computed values for "*K*" are presented in *Table III.4*.

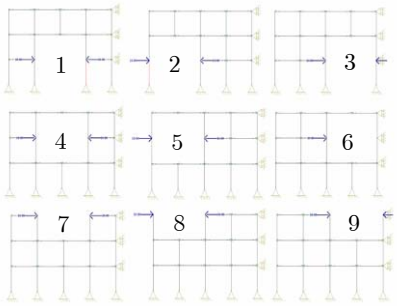

Figure III.26. Possible positions of column loss for the computation of "K"

Table III.4. Different computed values of "K"

K_1 *[kN/m]*	1639,3	K_4 *[kN/m]*	2040,8	K_7 *[kN/m]*	555,6
K_2 *[kN/m]*	793,7	K_5 *[kN/m]*	869,6	K_8 *[kN/m]*	138,3
K_3 *[kN/m]*	2564,1	K_6 *[kN/m]*	3333,3	K_9 *[kN/m]*	1010,1

For the test, "artificial" lateral restraints are placed each side of the substructure (see point A and B in *Figure* III.23) so as to replace the restraints released by the performed modifications; the scope of placing them each side of the substructure is to induce a "symmetric" response of the substructure during the test (see *Figure III.27*) which facilitates the application of the loads and the measurements.

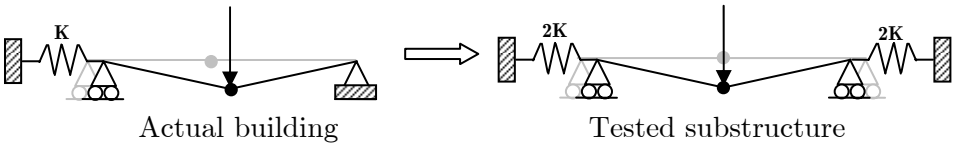

Figure III.27. Symmetric response of the tested substructure

In practice, these restraints is brought by two horizontal jacks (see *Figure III.28*) which are calibrated so as to exhibit a restraint close to the actual one corresponding to the loss of the column at the position 1 (see *Figure III.26*); as illustrated in *Figure III.29*, the restraint is assumed to be elastic from the beginning to the end of the test.

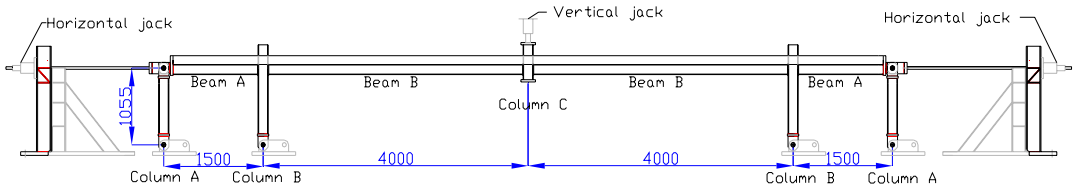

Figure III.28. Detailed drawing of the substructure test configuration

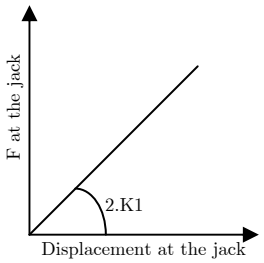

Figure III.29. Calibration of the horizontal external jacks

III.4.3.6. Conclusions

This section describes the substructure extracted from the actual building (designed in the previous section) to be tested at the laboratory of Liège University.

Some modifications have been realised to pass from the actual frame to the tested substructure so as to respect the laboratory facilities and to facilitate the interpretation of the results; all these modifications have been described and justified in the present section.

In the next section, the performance of the substructure test is described and the obtained results are presented.

III.4.4. Performed substructure test

III.4.4.1. Introduction

The test accomplishment and the obtained results are described in the present section. The latter is divided as follows:

- Annex tests aiming at characterising the properties of the constitutive materials are first presented in *§ III.4.4.2*;
- then, the measurements performed so as to have the actual geometrical properties of the tested specimen are explained in *§ III.4.4.3*;

- the latter is followed, in *§ III.4.4.4*, by the description of the loading sequence applied to the substructure during the test;
- the test equipment and the obtained measurements are then presented in *§ III.4.4.5*;
- finally, the test results are given in details in *§ III.4.4.6*.

III.4.4.2. Characterization of the constitutive materials

A. Member steel

As previously mentioned, different types of tests linked to the substructure test performed in Liège were performed within the "Robustness" project, in particular:

- tests in isolation on the composite joint configuration in Stuttgart and;
- component tests on the composite joint components in Trento.

In order to be able to compare the obtained results from the different laboratory, it was decided that all the steel members used for the different tests should come from the same production and rolling. So, the mechanical properties of the steel materials met within the substructure are the ones presented in *Appendix VI.1.2* for the joint specimens tested in Stuttgart.

B. Slab concrete (C25/30 concrete)

To characterise the resistance to compression of the concrete, twelve tests on cube and two on cylinder were performed. With the cubes, tests in compression at different days (3 cube tests at day 7, 14, 28 and the day of the test (day 72)) were performed to see the evolution of the concrete resistance as presented in *Figure III.30*; also, the equivalent resistances which would have been obtained on cylinder, which represents the characteristic value f_{ck} as defined in the codes, have been computed according to the Eurocode 2 rules *[67]*.

The results obtained through the compression tests performed on the two cylinders are also reported in *Figure III.30*; it can be observed that the cylinder resistances computed from the cube resistances are in good agreement with the cylinder test results.

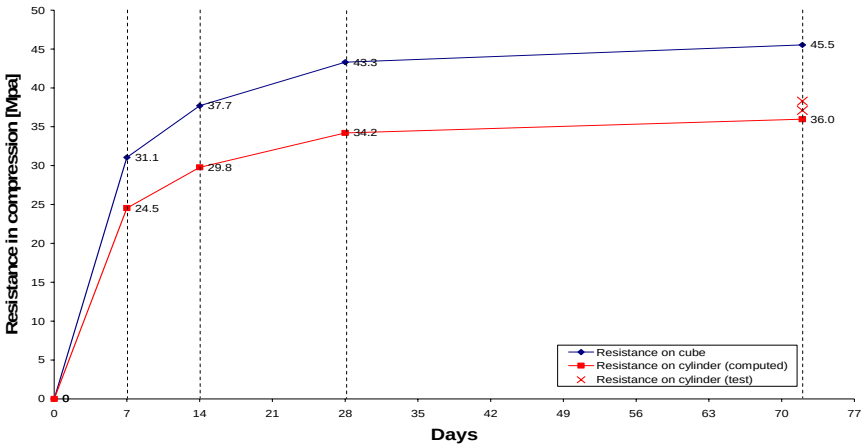

Figure III.30. Evolution of the concrete resistance to compression with time

III.4.4.3. Geometrical measurements

The scope of the geometrical measurements is to obtain the actual geometrical properties of the constitutive elements of the substructure. The main measurements which have been made deal with the actual dimensions of:

- the IPE140 and HEA160 profiles;
- the end-plate;
- the structural members;
- the substructure in global.

Also, the actual position of the rebars in the vicinity of the composite joints have been measured.

All these measurements are reported in *Appendix VI.6*.

III.4.4.4. Description of the loading sequence followed during the test

A. Introduction

All the actions applied on the substructure during the test have been applied "statically" (i.e. progressive removal of the column), which means that the dynamic aspects of the impact action and of the column loss itself have not been taken into account. It is justified here after:

- One objective of the performed test is to observe the "physic" phenomena linked to the loss of a column in a frame. So, that is why it was decided to remove progressively the column so as to be able to observe all these phenomena.

- Another reason is that the final aim of the test is to validate our numerical tools so as to perform parametrical numerical studies (see *§ III.6*). To reach this goal, it was needed to be able to measure all the displacements, rotations, loads and strains during the column loss, what was only possible with a progressive removal of the column.

B. Loading sequence

The loading sequence during the test was as follows:

- The substructure is first preloaded with an uniformly distributed load on the internal beams to simulate the reaction of the concrete slab on the main frame in the actual building (see *Figure III.12*); during this preloading, two locked jack are placed at the middle of the substructure to simulate the presence of the column, as illustrated in *Figure III.31*. In practice, the uniformly distributed load is applied with steel plates and concrete blocks, as shown in *Figure III.32*, which represents a total load of 6 kN/m; also, L shape profiles are placed so as to maintain the steel plates and the concrete blocks at their place when big deflection will occur (see *Figure III.32*). The 6 kN/m load is smaller than the one to be considered for the ULS verifications under the accidental combination of actions ($\cong$10 kN/m); however, it is the maximum load that can be "safely" applied in the laboratory during the test.

- In a second step, the support brought by the jacks is progressively removed by unlocking the jack; when the latter are removed, the free deflection of the system is observed. The further step is to impose a vertical displacement with two jacks on the column thus further deformation will occur (see *Figure III.33*). The applied displacement is increased until collapse of the substructure.

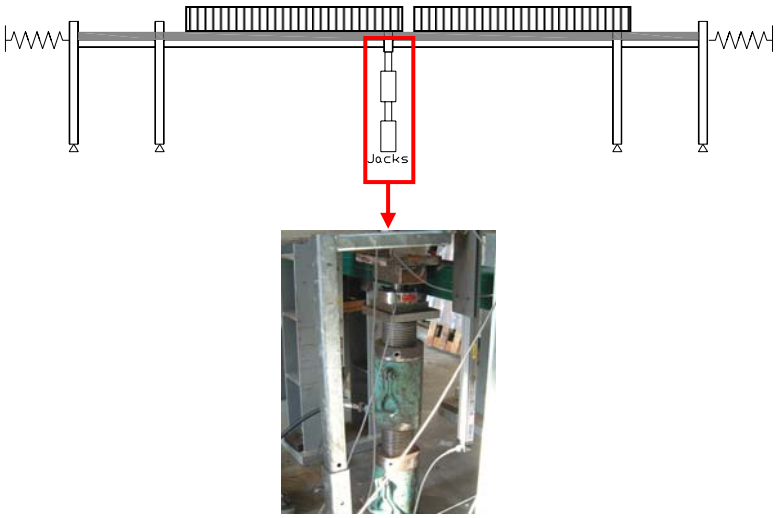

Figure III.31. Column at the middle simulated by two locked jacks

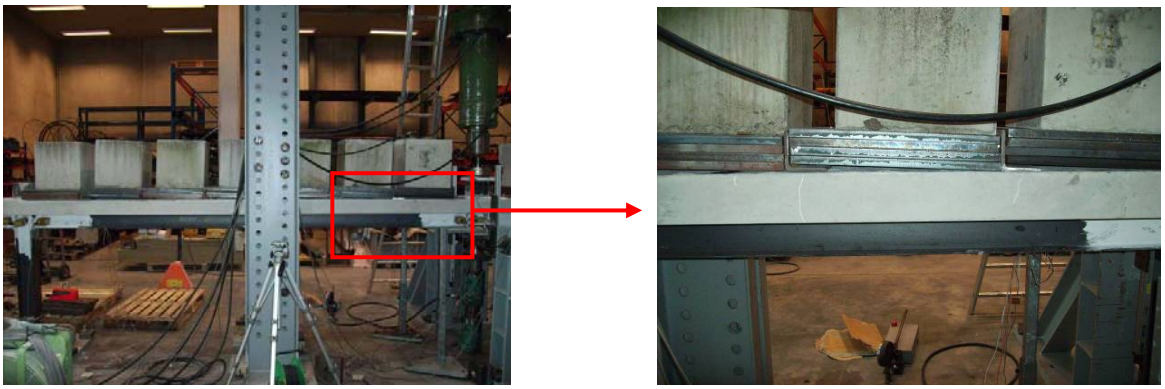

Figure III.32. Steel plates and concrete blocks simulating the uniformly distributed load

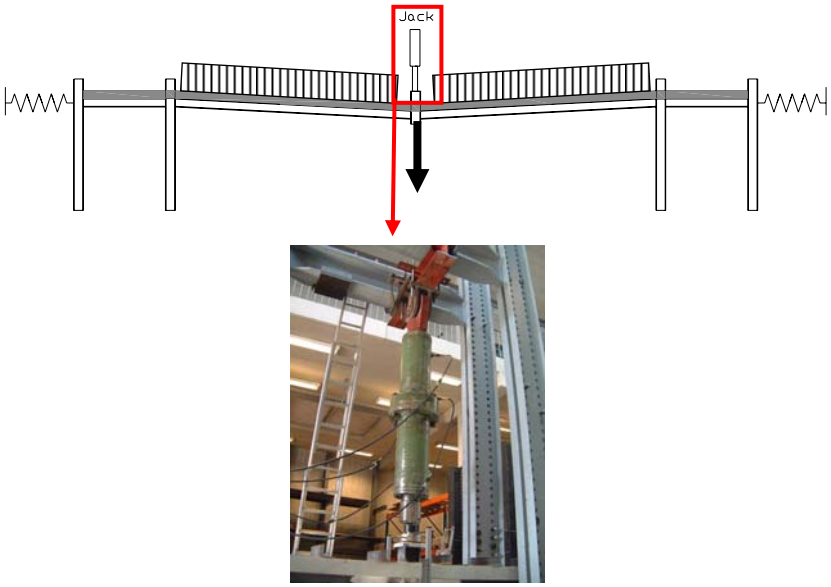

Figure III.33. Application of a vertical displacement with two vertical jacks

III.4.4.5. Test equipment

A. Hydraulic jacks (controlled displacement)

In total, six hydraulic jacks are used during the test:

- To simulate the presence of the column at the middle of the tested specimen, two screw jacks are placed (see *Figure III.31*).
- Then, for the increase of the vertical displacement at the middle until collapse, two hydraulic jacks are placed in tandem (see *Figure III.33*) so as to have a maximum displacement capacity of 800 mm.
- As previously mentioned, the lateral restraint is simulated each side of the substructure by hollow jacks (see *Figure III.34*) with a displacement capacity of 200 mm.

The applied loads at these jacks are measured through load cells.

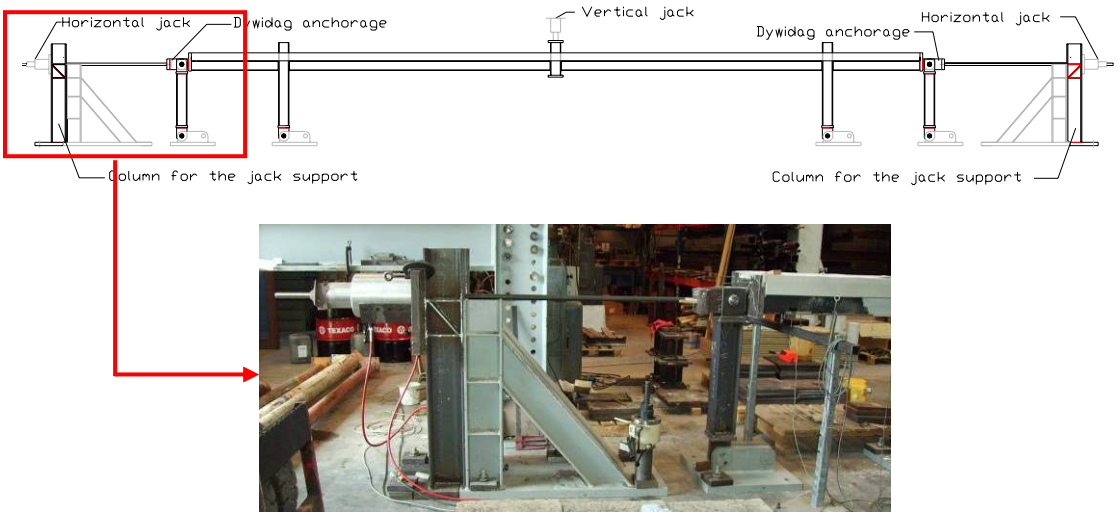

Figure III.34. Horizontal restraint simulated by horizontal hollow jacks

B. Displacement and rotational transducers

Five rotational transducers are placed in the vicinity of the joints as shown in *Figure III.35* and four displacement transducers are placed as follows (see *Figure III.36*):

- two at the middle of the substructure to measure the vertical displacement;
- one each side of the substructure to measure the horizontal displacement.

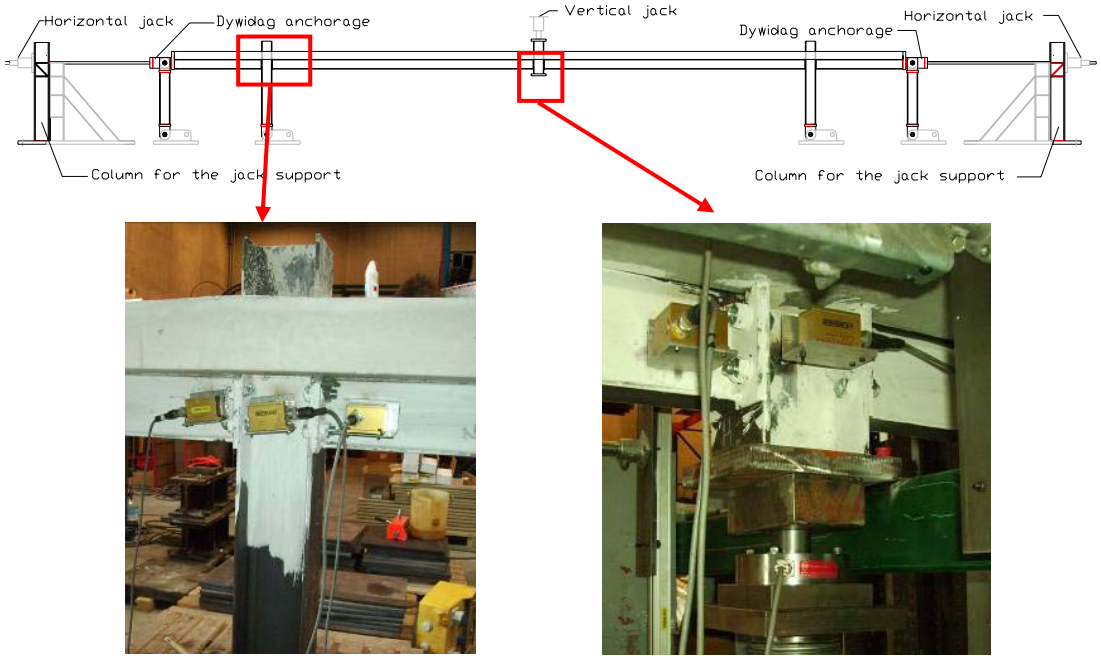

Figure III.35. Rotational transducers

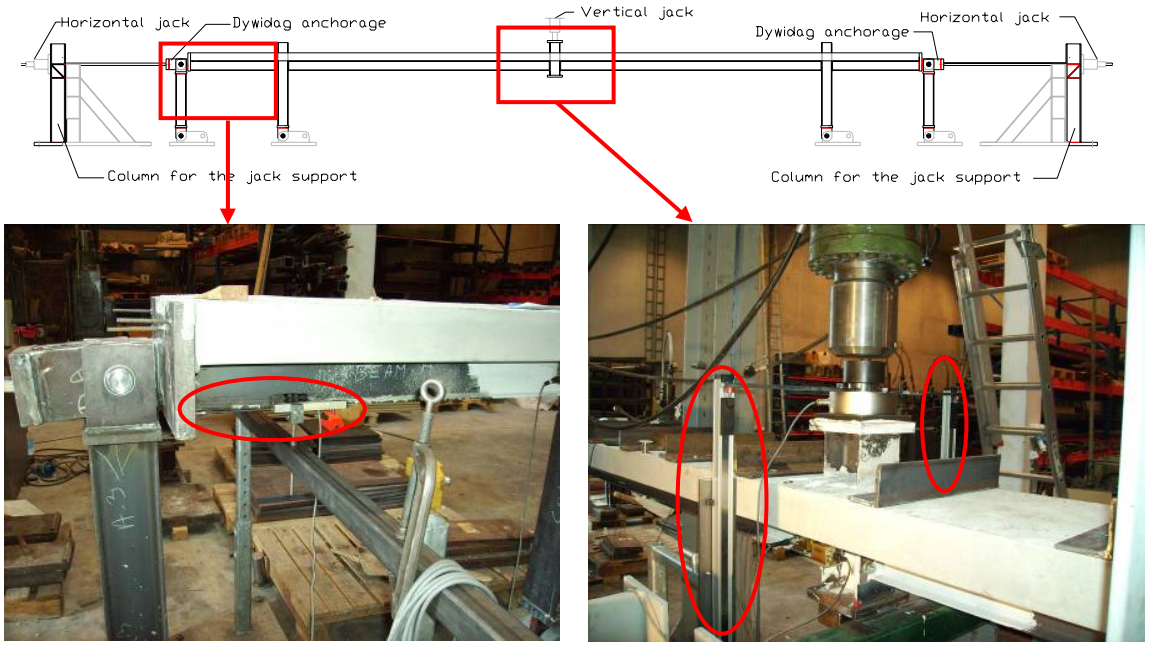

Figure III.36. Displacement transducers

C. Strain gauges

In total, twelve strain gauges are placed on the tested specimen: four strain gauges are glued on the bottom flange of the IPE140 profile at three different positions as illustrated in *Figure III.37* (position A and C at 500 mm from the adjacent column and position B at the middle).

The objective with these strain gauges is to have a rough estimation on how the strains (and the stresses) develop in the bottom flange during the test.

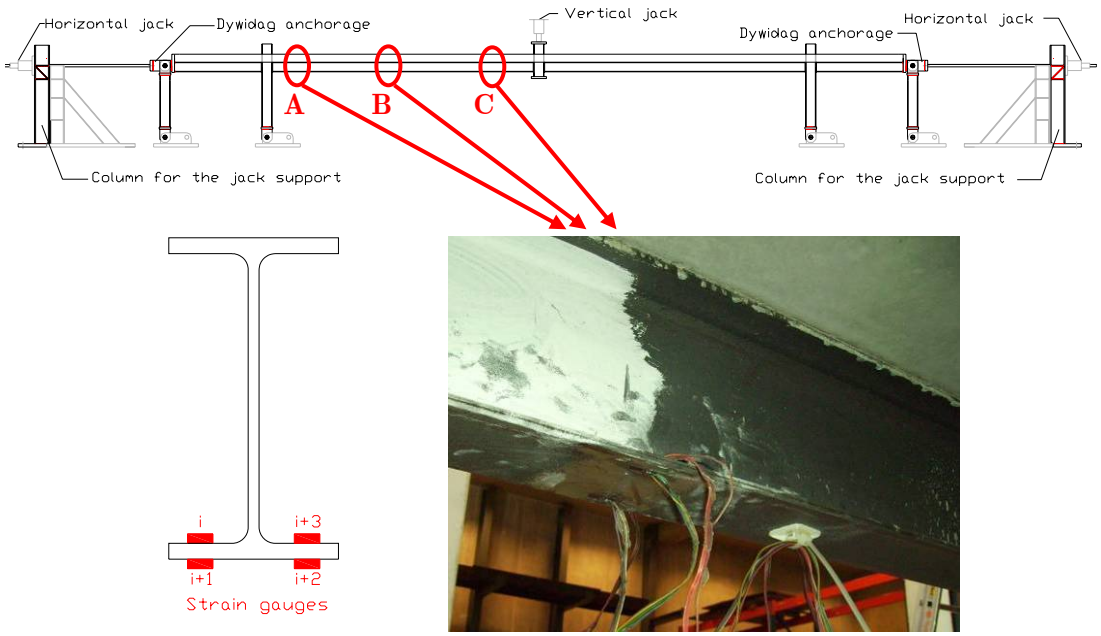

Figure III.37. Strain gauges at the IPE140 bottom flange

III.4.4.6. Substructure test results

As explained in *§ III.4.4.4*, a uniformly distributed load is first applied on the substructure with steel plates and concrete blocks. After the application of the latter, first small cracks are already observed in the concrete slab in the vicinity of the external composite joints, as shown in *Figure III.38*.

After the application of the uniform load, the jacks at the middle are unlocked and progressively removed. The system is completely released, i.e. the applied load at the jacks is equal to 0, when a deflection of 29 mm is reached. At this stage, the width of the cracks at the vicinity of the external joints is bigger and first steel yielding is observed in the column web panel of the internal composite joint.

This first step of the test is illustrated by the part "OA" of the curve presented in *Figure III.39* representing the evolution of the vertical load at the middle of the structure according to the vertical displacement. The vertical reaction which was associated to the uniformly distributed load and to the self-weight of the substructure is equal to 33,5 kN (value of the load at point "O"). From *Figure III.39*, it can be seen that the structure still be in the elastic range when "A" is reached.

Then, as previously mentioned, a vertical displacement is progressively imposed until collapse of the tested specimen. During this stage, two "unloading-reloading" are performed as illustrated in *Figure III.39*.

From point "A" to "B" in *Figure III.39*, the substructure enters in the yielding stage to finally form a beam plastic mechanism at point "B" with formation of the plastic hinges at the joint level. During this stage, the cracks in the vicinity of the external composite joints are more pronounced (see *Figure III.40*) and yielding of some steel components of the joints is observed (column web and beam flange in compression – see *Figure III.41* and *Figure III.42*). Also, for the internal composite joint, a detachment between the end-plate and the column flange is observed, as illustrated in *Figure III.42*.

From point "B" to "C" in *Figure III.39*, a plateau is observed which means that the vertical displacements increase with a constant vertical load (equal to 30 kN). During this stage, the concrete cracks in the vicinity of the external composite joints continue to develop and yielding spreads in the steel components. One important observation is that the concrete in the vicinity of the internal composite joint splits in compression as illustrated in *Figure III.43*.

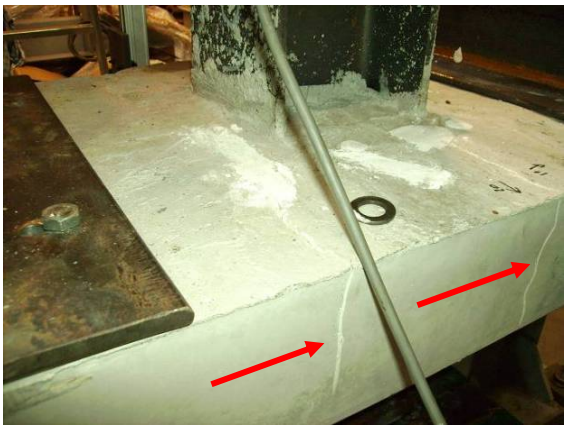

Figure III.38. First cracks in the vicinity of the external joints after the application of the uniformly distributed load

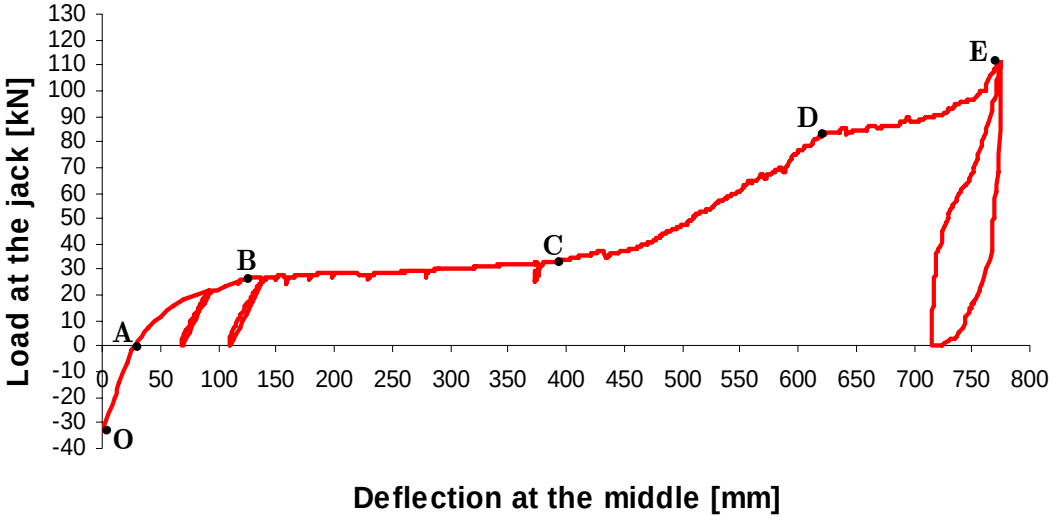

Figure III.39. Vertical load at the middle vs. vertical displacement curve

Figure III.40. Accentuated cracks in the vicinity of the external composite joints at the formation of the beam plastic mechanism

Figure III.41. Yielding of steel components at the external composite joints

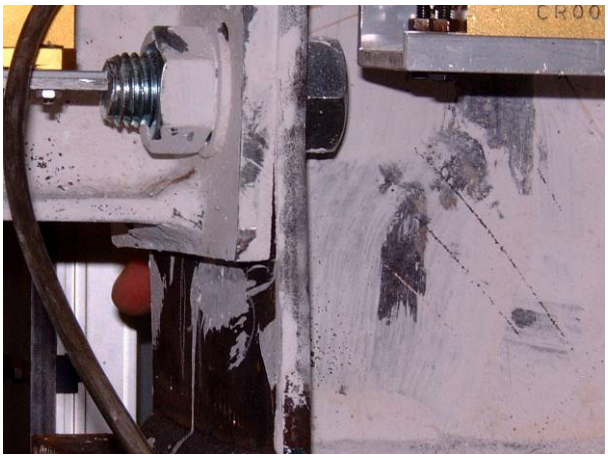

Figure III.42. Yielding of steel components at the internal composite joints

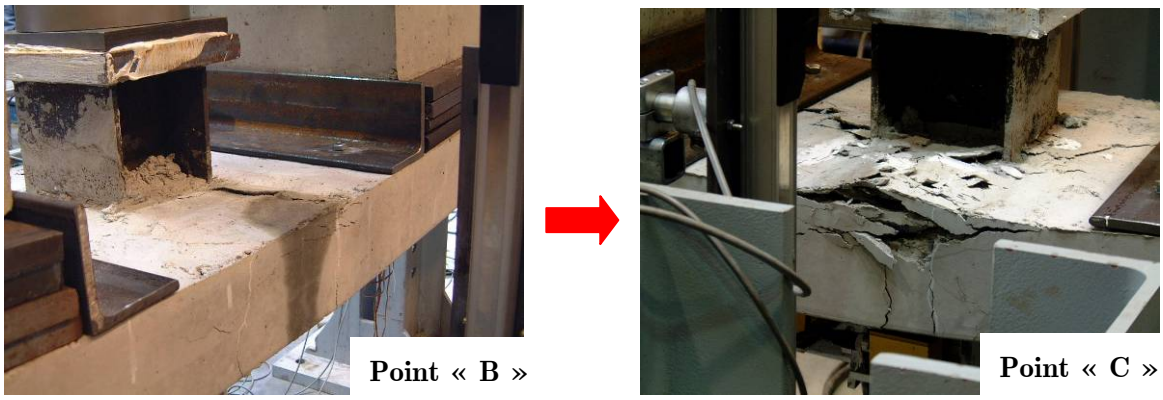

Figure III.43. Concrete splitting at the internal composite joint

Figure III.44 gives the horizontal displacements according the horizontal loads at the hollow jacks placed each side of the specimen (see *Figure III.34*). As previously mentioned (see *§ III.4.3.5*), these jacks have been calibrated so as to exhibit a linear elastic behaviour; it is confirmed by the curves presented in *Figure III.44* where the theoretical curve to which the jacks have been calibrated is reflected.

The horizontal jacks begin to be significantly activated at point "C" in *Figure III.39*; at this point, membrane forces start to develop as confirmed by the shape of the curve part

"CD" in *Figure III.39*. At point "D", the longitudinal rebars in the vicinity of the external composite joints completely collapse (see *Figure III.45*) and the external joints work as steel ones. The yielding also spreads in the different components of the internal and external composite joints as illustrated in *Figure III.46* and *Figure III.47*. At point "D", a loss of stiffness is observed in *Figure III.39* which is linked to the loss of the longitudinal rebars in the vicinity of the external joints; indeed, when these rebars are lost, the tensile stiffness of the external joints decreases, phenomenon which affects the development of the catenary actions.

However, it can be observed that the loss of the slab rebars do not affect the loading capacity of the substructure; indeed, after point "D", the vertical load at the vertical jacks still increases with the imposed displacement, as illustrated by part "DE" of the curve presented in *Figure III.39*.

This phenomenon is only possible if the steel connection is able to support, alone, the membrane forces developed in the system. In addition, associated to the loss of the rebars, the vertical displacements are increasing with a low variation of the vertical loads. These additional vertical displacements induce an increase of the membrane forces as confirmed by *Figure III.48* showing the evolution of the load in the horizontal jacks at the specimen extremities according to the vertical load at the vertical jacks. So, the steel connection working alone has also to be sufficiently resistant to support these additional membrane forces and sufficiently ductile to support the additional rotations associated to the vertical displacement. The capacity of steel, connection working alone, to support significant membrane forces has been confirmed by the tests performed in isolation at Stuttgart University on the substructure joint configuration; the latter are presented in *§ III.5*.

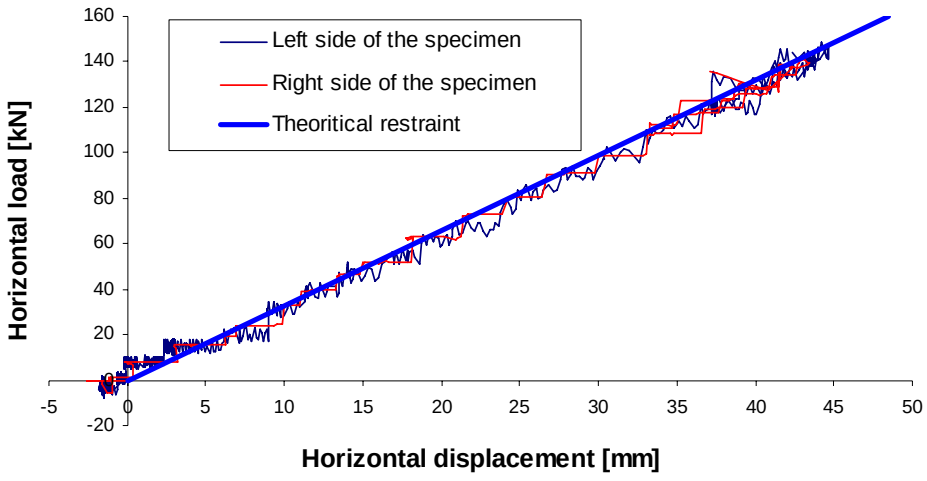

Figure III.44. Horizontal displacement vs. horizontal load at the hollow jacks curves

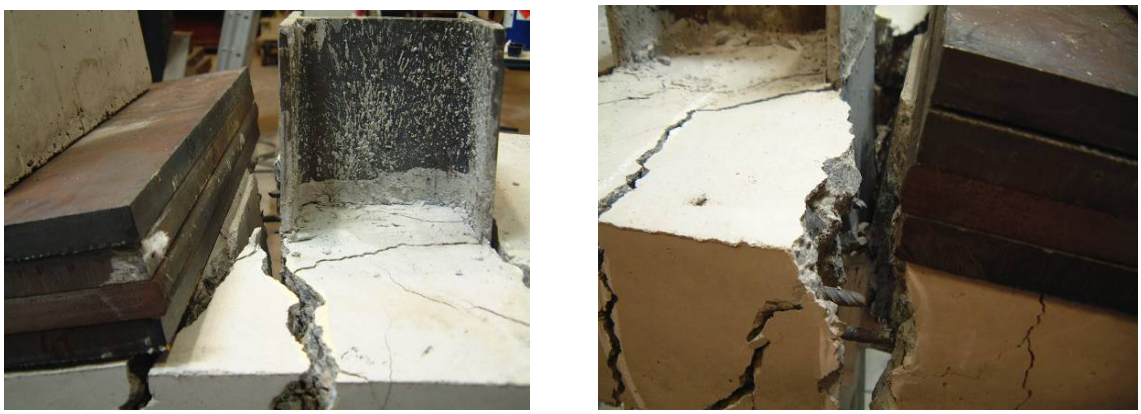

Figure III.45. Collapse of the longitudinal rebars in the vicinity of the external composite joints at point "D" of Figure III.39

Figure III.46. Yielding spread in the steel components of the external composite joints

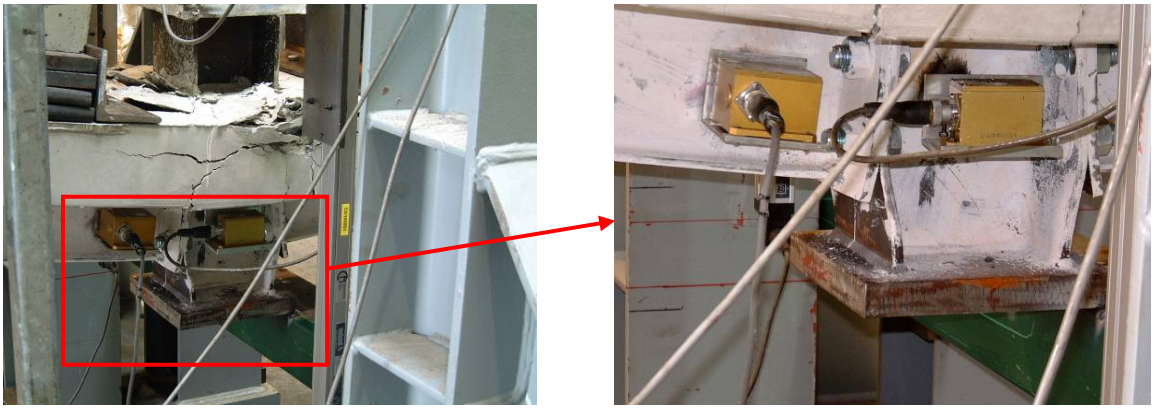

Figure III.47. State of the internal composite joint at point "D" of Figure III.39

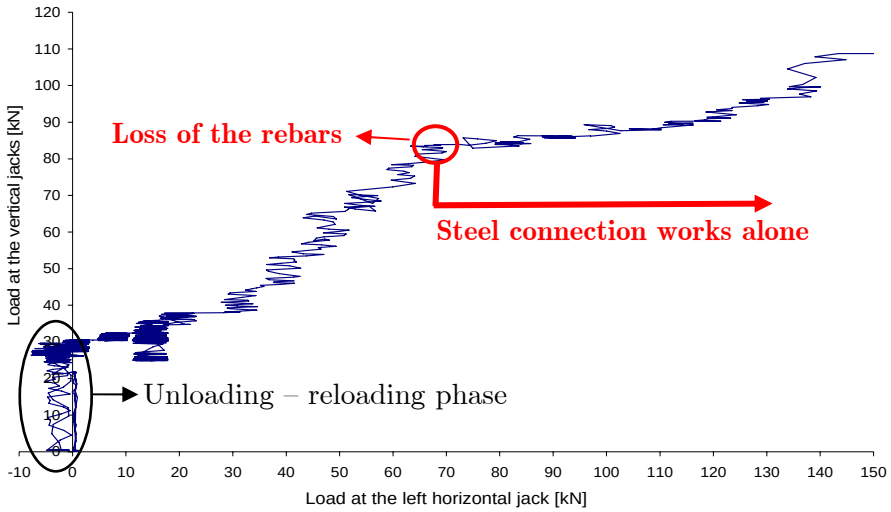

Figure III.48. Evolution of the load at the left horizontal jack according to the applied vertical load at the middle of the specimen

The test was stopped with the appearance of cracks at the bottom weld between the IPE140 profile and the end-plate at the internal composite joint (*Figure III.49*).

At the end of the test, a maximum vertical displacement of 775 mm is reached for a vertical load at the vertical jacks of 114 kN; the deformation of the specimen at this stage is presented in *Figure III.50*. The maximum horizontal displacement at each side of the structure is equal to 45 mm for a horizontal load of 147 kN; the observed horizontal displacement is illustrated in *Figure III.51*.

Also, at point E of *Figure III.39*, all the joint components of the internal and external composite joints suffer of big deformations and yielding as illustrated in *Figure III.52* and *Figure III.53* (where the damage concrete has been removed). In particular:

- For the external composite joints: yielding of the column web in compression, the beam flange and web in compression, the column flange in bending.
- For the internal composite joints: yielding of the column web in tension (Luders bands) associated to the membrane forces, column flange in bending, beam flange and web in tension.

The evolution of the joint rotations according to the load at the vertical jacks is given in *Figure III.54*. The maximum joint rotations reached at the end of the test are equal to 11° (192 mrad) and to 9,5° (166 mrad) for the internal and external composite joints respectively. It can be observed in *Figure III.54* that:

- The behaviours of the internal and external composite joints are very close.
- The joint rotations are mainly associated to the rotation of the yielded connections, what was already illustrated through the previous figures.

- The beam plastic mechanism develops with formation of plastic hinges in the joints.

From the maximum rotation values observed at the end of the test, it can be concluded that the joints exhibited a very ductile behaviour with a very high rotation capacity, as expected. Also, through these observations, it is confirmed that, even if the collapse mode under hogging bending moment is associated to the component "beam flange in compression" (as illustrated in *§ II.3.2.3.B*), the ductility of the joint is sufficient to develop the catenary action, as predicted in *§ III.4.2.3.C*.

Figure III.49. Cracks in the welds between the IPE140 profile and the end-plate

Figure III.50. Deformation of the specimen at point "E" of Figure III.39

Figure III.51. Horizontal displacement of the specimen at point "E" of Figure III.39

Figure III.52. External composite joints at the end of the test

Figure III.53. Internal composite joints at the end of the test

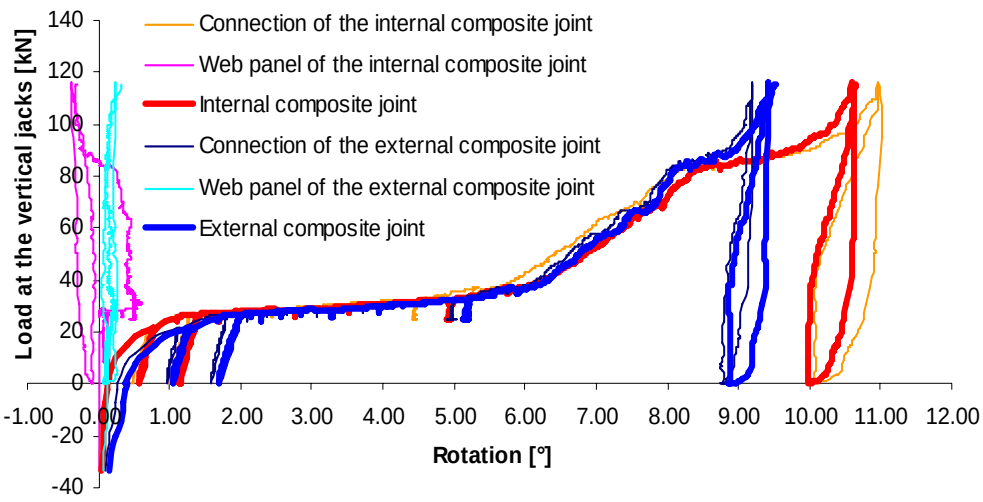

Figure III.54. Rotation of the internal and external composite joints

As mentioned in *§ III.4.4.5.C*, the evolution of the strains (through strain gauges) was registered. The obtained results are presented from Figure III.55 to Figure III.57 where the evolution of the stresses (computed with the young modulus equal to 210000 N/mm²) according to the load at the vertical jacks is reported; the position of the strain gauges in the specimen and in the cross sections are presented in *Figure III.37*. From these results, interesting observations can be made:

- The initial stresses which are observed are linked to the applied permanent loads. Indeed, the curves which are reported here represent the evolution of the stresses during the removal of the column at the middle; so, at the beginning of the curves, the permanent loads have already been applied.
- From the strain gauges at the left of the beam (position A in *Figure III.37*), it can be seen that the bottom flange is in compression but, when the plastic mechanism is formed (for a vertical load of about 30 kN), the compression stresses decrease with the development of the membrane forces. At the end of the test, the stresses are close to 0.
- The bottom flange at the middle of the beam (position B in *Figure III.37*) is in tension all along the loading and still in the elastic range. It seems that a problem occurred with the gauge 5 during the test; this gauge should not be taken into account for further investigations.
- At the right side of the beam (position C in *Figure III.37*), close to the internal composite joint, the bottom flange is in tension and, after the formation of the beam plastic mechanism, the latter yields with the development of the membrane forces (stresses close to 400 MPa which is the elastic limit of the IPE140 flange as presented in *Table VI.8*).
- In all the gauge measurements, it can be observed that the evolution of the strains (and the stresses) is affected by the collapse of the rebars at the external composite joints (for an applied vertical load of about 90 kN).

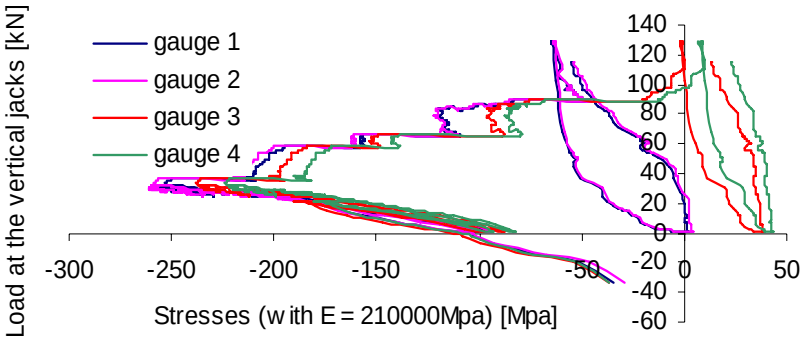

Figure III.55. Evolution of the stresses in the bottom flange at position A (see Figure III.37)

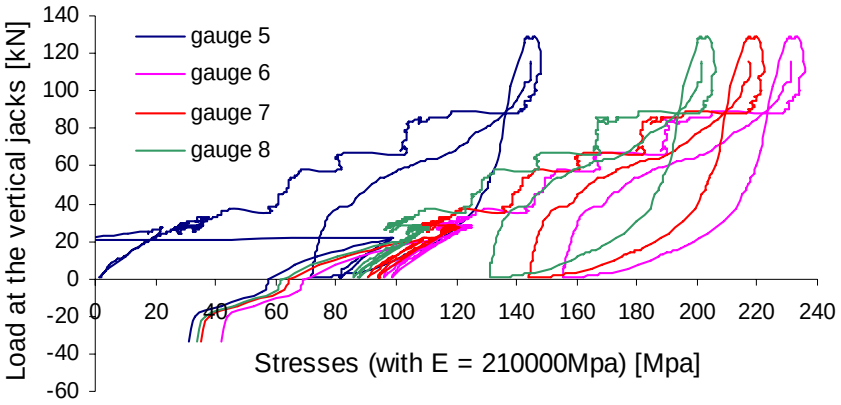

Figure III.56. Evolution of the stresses in the bottom flange at position B (see Figure III.37)

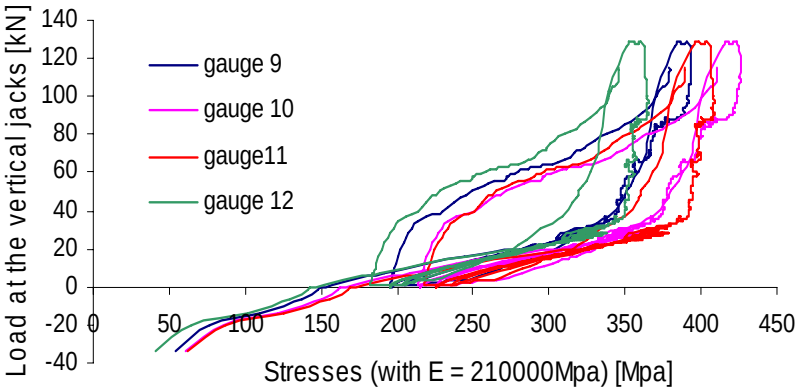

Figure III.57. Evolution of the stresses in the bottom flange at position C (see Figure III.37)

After the test, the steel plates and the concrete blocks were removed so as to see the disposition of the cracks along the concrete slab. As shown in Figure III.58, only two big cracks appeared during the test in the vicinity of the external composite joints what was not expected. Indeed, as mentioned in *§ III.4.3.3*, the studs layout (see *Figure III.24*) was fixed in agreement with the recommendation of a previous project *[69]* so as to have a good distribution of the cracks in the zone without studs; according to the presented results, the recommendation can not been validated. This observation can be explain by the fact that, in the tested substructure, the composite joint configuration are composed of flush end-plates with the upper part embedded in the concrete slab; so, when the end-plates deform, the embedded part deformation can easily initiate a crack in the reinforced concrete slab as illustrated in *Figure III.59*. However, the joints exhibited a very ductile behaviour during the test although to have one big crack is not the best situation from the ductility point of view.

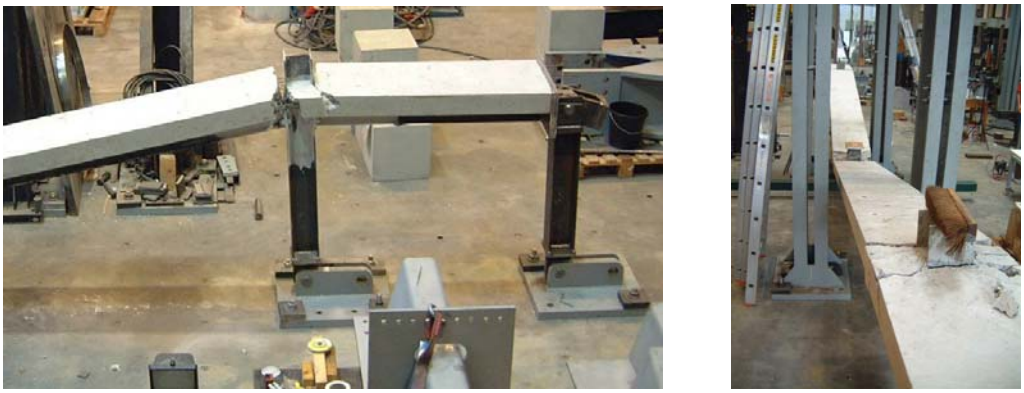

Figure III.58. Distribution of the cracks in the concrete slab

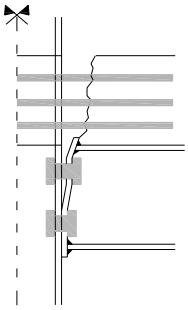

Figure III.59. Crack associated to the deformation of the end-plate embedded in the concrete slab

III.4.5. Conclusions

The objective of the performed test was to simulate the loss of a column in a composite frame to observe the development of the membrane forces in the structure after the loss of the column and the effects of these forces on the joint response.

The tested specimen was extracted from an actual frame designed in agreement with Eurocode 4 recommendations and that, for conventional loading, i.e. design loads recommended in Eurocode 1 without account of the exceptional loading "loss of a column". The tested specimen and the test configuration were defined so as to observe a behavioural response as close as possible to the one that the actual frame would have exhibited.

The main measurements which were registered are the vertical displacement at the column loss level, the rotations of the structural joints and the horizontal displacements and forces appearing at the specimen extremities.

The performed test, which constitutes a European first, was successful and all the phenomena under investigations were registered. Indeed, the development of the catenary action in the system was observed and the registered curves confirmed the development of membrane forces in the beams. Also, the composite joints loaded by combined tensile forces and bending moments exhibited a ductile behaviour as expected.

The results obtained through this test will be used later on to investigate the validity of the numerical tool (*§ III.6.2*) and of the developed analytical model (*§ III.8.3*).

III.5. Behaviour of composite joints subjected to combined bending moments and normal forces

III.5.1. Introduction

Through the substructure test presented in the previous paragraph, it was shown that the joints, when big deflection appears in a structure further to the loss of a column, are subjected to combined bending moments and tensile loads.

So, it is the reason why a particular attention is paid to the behaviour of joints subjected to such loading. Both experimental and analytical investigations are presented in the present paragraph; the latter is organised as follows:

- In *§ III.5.2*, the experimental tests performed at Stuttgart University (in strong collaboration with Liège University) are first described. The investigated composite joint configuration is exactly the same than the one met in the substructure. The objectives of these tests are:
    - to characterise the behaviour of the structural joint of the tested substructure subjected to combined bending moments and tensile loads in order to be able to introduce the actual properties of the joints within the analytical and numerical investigations performed on this structure and;
    - to validate an analytical procedure aiming at predicting the behaviour of composite joints subjected to combined normal forces and bending moments.
- In *§ III.5.3*, the developed analytical procedure is presented and validated. The latter is based on an analytical method developed for steel joints and is in full agreement with the component method recommended in the Eurocodes.
- Finally, conclusions are drawn in *§ III.5.4*.

III.5.2. Experimental tests

III.5.2.1. Introduction

Through the performed substructure test, it is not possible to derive accurate behavioural curves for the structural composite joints, the difficulty being the computation of accurate applied loads. So, it was decided within the "Robustness" project to perform tests in

isolation at Stuttgart University on the substructure composite joint configuration subjected to combined bending moments and normal forces ("*M-N*") (*[4]* and *[71]*). The objective of the tests was to derive the full *M-N* resistance interaction curve of the tested joints.

The test campaign realised at Stuttgart University is described in *§ II.3.2.3*. In total, five tests on the substructure composite joint configuration have been performed. They are distinguished by the loading sequences followed during the test as reminded here below:

- Three tests under hogging moments:
    - one test with the joint first loaded under hogging bending moments until reaching the ultimate resistance in bending and secondly, after having slightly reduced the applied bending moment, loaded under tension loads until the collapse of the joint (TEST 1) and;
    - two tests with the joint, first, loaded under hogging bending moments with the loading stopped just before reaching the ultimate resistance to bending and, secondly, loaded under tension loads until the collapse of the joint (TEST 2 & TEST 3).
- Two tests under sagging moments:
    - one test with the joint first loaded under sagging bending moments until reaching the ultimate resistance in bending and secondly, after having slightly reduced the applied bending moment, loaded under tension loads until the collapse of the joint (TEST 4) and;
    - one test with the joint, first, loaded under sagging bending moments with the loading stopped just before reaching the ultimate resisance to bending and, secondly, loaded under tension loads until the collapse of the joint (TEST 5).

Within the present section, *§ III.5.2.2* first describes how the loads were applied during the test and then, *§ III.5.2.3* presents the main obtained results.

III.5.2.2. Description of the test setup

The tested joint configuration is described in details in *§ II.3.2.3.A* and *§ III.4.2.3.B*. As mentioned in the previous section, the objective of the tests is to derive the full *M-N* resistance interaction curve of the tested joints, as illustrated in *Figure III.60*.

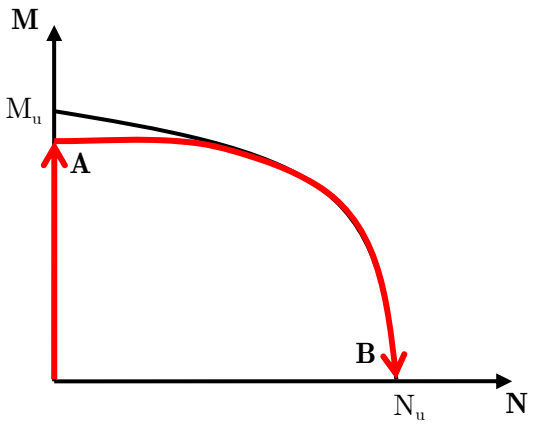

Figure III.60. M-N ultimate resistance curve of the joint to be characterised through the performed tests

To reach this goal, the loads were applied as follows:

- A bending moment is first applied to the joint through a vertical hydraulic jack, as illustrated in *Figure III.61*. In the latter, the joint subjected to a hogging bending moment is illustrated; when a sagging bending moment has to be applied to the joint, the tested specimen is inversed according to what is represented in *Figure III.61*. During this stage, the beam extremities are horizontally and vertically restrained. The applied load is stopped when the ultimate bending resistance is reached for TEST 1 and 4 and when the applied bending moment is close to the ultimate one for TEST 2, 3 and 5 (point A in *Figure III.60*). After reaching the ultimate bending resistance during TEST 1 and 4, the applied bending moments are slightly reduced to come back to point A (see *Figure III.60*).

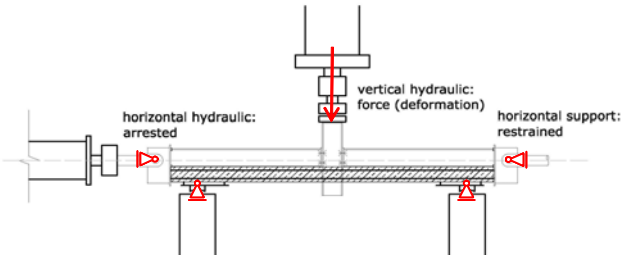

Figure III.61. Application of a bending moment to the tested specimen [71]

- Then, the beam left extremity is horizontally released and a tension horizontal load is applied through a horizontal jack (see *Figure III.62*). This load is increased until collapse of the tested specimen (point B in *Figure III.60*).

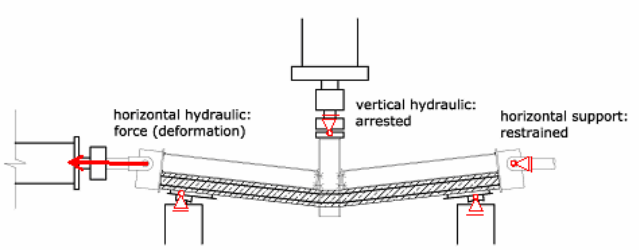

Figure III.62. Application of a tension load to the tested specimen [71]

The arrangement of the test equipment (mainly composed of extensional transducers) was chosen in order to derive the behaviour of the main components of the joints which contribute to the deformation capacity and to determine the single load deformation behaviour of the relevant components. The main obtained results are presented in the next section; more details are available in *[4]*.

III.5.2.3. Test results

A. Tested specimen subjected to combined hogging bending moments and normal forces – TEST 1, TEST 2 and TEST 3

By increasing the hogging bending moment during TEST 1, TEST 2 and TEST 3, first cracks in the concrete slab develop in front of the column, as observed through the substructure test (see *§ III.4.4.6*). Close to M_u, i.e. close to 60,6 kNm (see *§ II.3.2.3.B*), the concrete slab in front of the column is cracked over the total slab height.

Then, the horizontal tensile load is applied to the tested specimens. While applying this additional load, the cracks in the slab continue to develop and significant deformations of the steel components "end-plate in bending" and "column flange in bending" are observed (see *Figure III.63*).

Figure III.63. Tested specimen subjected to hogging bending moments and tension loads at the end of the test

The obtained *M-N* interaction curves are presented in *Figure III.64*. To compute the bending moments associated to the applied horizontal loads, a reference point within the

beam cross section had to be fixed; the latter is fixed at 94 mm of the bottom fibre of the bottom flange of the steel profile as illustrated in *Figure III.65*.

At point "A" of *Figure III.64* for TEST 1 and at point "A'" for TEST 2 and 3, a loss of resistance can be observed; the latter is associated to the collapse of the slab rebars in tension. The fact that this collapse does not occur for the same applied tensile load during TEST 1 and during TEST 2 and 3 is associated to the difference in the loading sequence. Indeed, during TEST 1, the ultimate bending resistance is first reached before applying the tensile load, what is not the case during TEST 2 and 3.

Also, the collapse of the rebars during the joint tests occurs for a tensile load equal to more or less 400 kN for TEST 1 and to more or less 550 kN for TEST 2 and 3, what is much higher than the tensile load at which the rebars collapsed during the substructure test (load in the horizontal jacks equal to 70 kN – see *Figure III.48*). This difference can be explained by the fact that, during the joint tests, the vertical displacements and, accordingly, the joint rotations are locked when the tensile loads are applied to the specimen, what was not the case during the substructure test. So, the requested ductility at the rebar level was higher during the substructure test than during the joint tests what explains the "premature" collapse of the rebars during the substructure test.

After the collapse of the rebars, the tested joints can be considered as steel ones. It can be observed that, after the resistance loss, the remaining steel components are able to sustain additional tension loads until a value equal to more or less 470 kN. This observation confirms what was observed during the substructure test at the slab rebars collapse, i.e. the capacity of the joint to sustain significant tensile loads after the rebars collapse. The maximum tension load reached during TEST 1 is equal to 470 kN, to 544 kN during TEST2 and to 581,7 kN during TEST 3.

Also, it can be seen in *Figure III.64* that the maximum tension load is reached for a bending moment which is not equal to 0; this is explained be the fact that the reference point (see *Figure III.65*) used to compute the applied bending moment do not correspond to the centre of tension of the joint. So, the bending moment when the maximum tension load is applied is equal to this tension load multiplied by the lever arm between the reference point and the centre of tension.

During the test, the axial deformation of the joint according to the applied horizontal load was measured; the so-obtained curves are reported in *Figure III.66*. These curves represent the axial deformation when a plastic hinge is formed at the joint level, i.e. when moving on the *M-N* resistant curve; it can be observed that the curve obtained through TEST 1 is slightly different of the ones obtained through TEST 2 and 3 and that a linear behaviour

links the horizontal load and the horizontal deformation until a value of 360 kN for TEST 1 and of 400 kN for TEST 2 and 3.

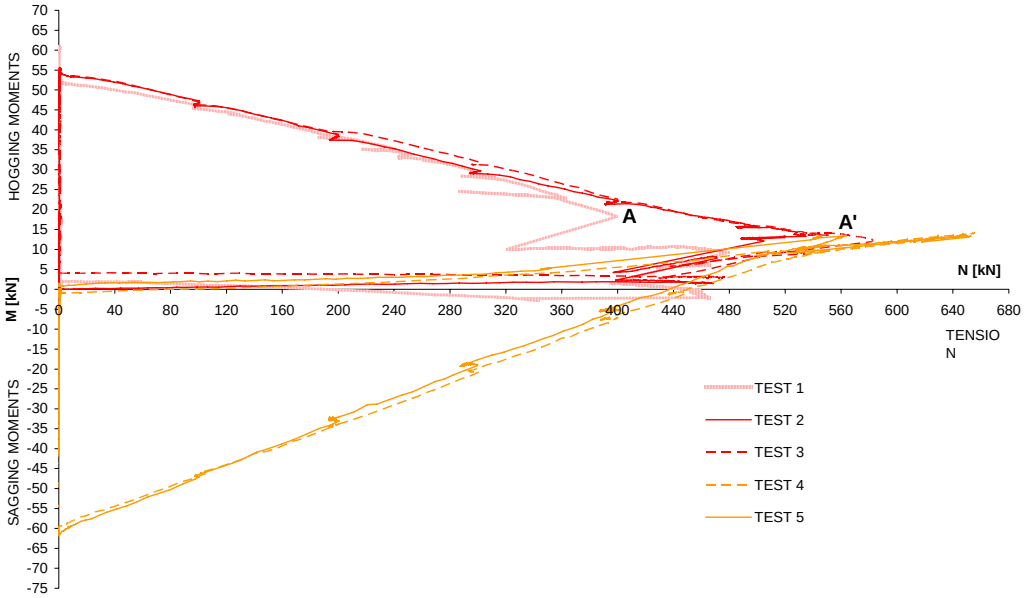

Figure III.64. M-N interaction curves experimentally obtained for TEST 1 to TEST 5

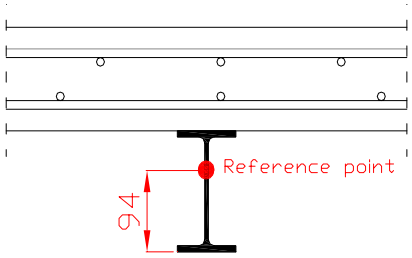

Figure III.65. Considered reference point to compute the applied bending moment at the joint

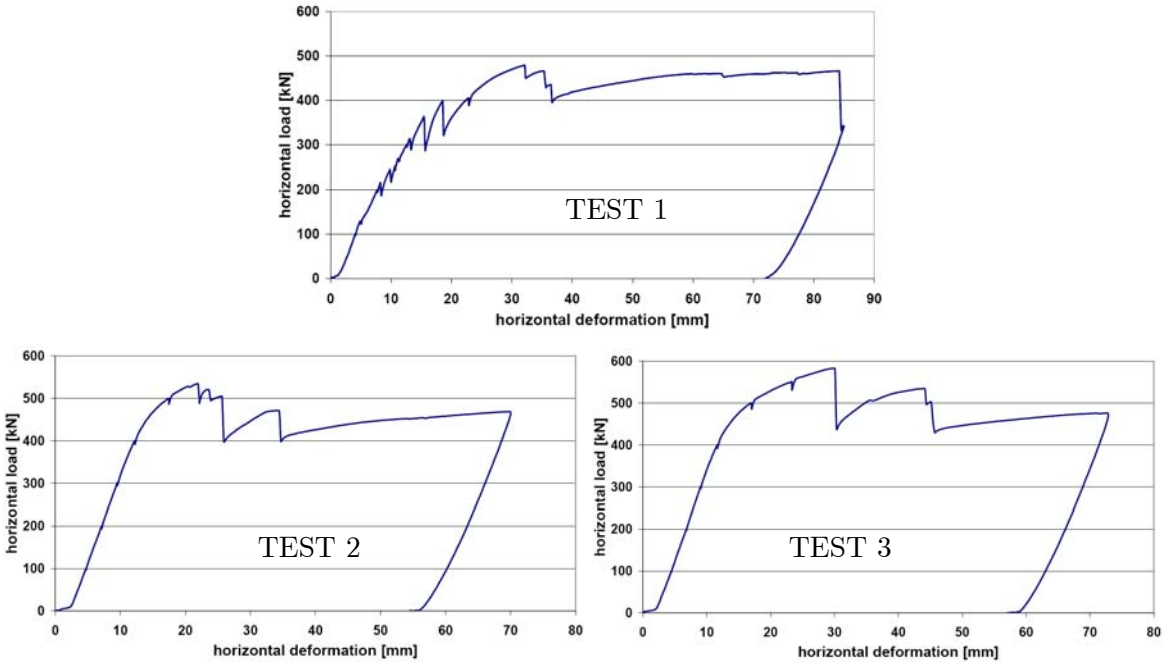

Figure III.66. Axial deformations of the joint measured during TEST 1, TEST 2 and 3

B. Tested specimen subjected to combined sagging bending moments and normal forces – TEST 4 and TEST 5

As previously mentioned, a sagging bending moment is first applied to the tested specimen. Close to M_u, i.e. close to 64,5 kNm (see *§ II.3.2.3.C*), a concrete crushing in the slab is observed in the vicinity of the column, as shown in *Figure III.67*; this crushing is associated to a lack of ductility of the concrete subjected to compression at the joint level.

Then, the horizontal tensile load is applied to the tested specimen. While applying this load, cracks in the concrete slab appear and some steel components exhibit big deformations, in particular the end-plate and the column flange in bending, as illustrated in *Figure III.68*.

The *M-N* resistance curves are also given in *Figure III.64*. At point "A'", the slab rebars collapse is observed as for the specimens subjected initially to hogging bending moments. Nevertheless, as illustrated through TEST 1, 2 and 3, the remaining steel components alone are able to sustain additional tension loads but which are much higher than the ones observed through TEST 1, 2 and 3. This difference can be explained by the membrane forces developing in the joint components in bending (see *Figure II.38*) as explained here below.

Under sagging moments, the collapse mode of the joint is associated to the component "column flange in bending". Accordingly, this component is activated since the beginning of the loading during TEST 4 and 5 while this component is significantly activated when tensile loads are applied to the tested specimen during TEST 1, 2 and 3 (the collapse mode when subjected to hogging bending moments is associated to the component "beam flange in compression"). As a consequence, the deformation of the component "column flange in bending" is more important during TEST 4 or 5 than during TEST 1, 2 or 3 for a same level of applied tension load. So, the membrane forces in this component are also more important during TEST 4 and 5, what can increase the resistance of this component and what justifies the higher tension loads supported during these tests.

The maximum tension load reached during the tests is equal to more or less 655 kN.

Figure III.67. Crushing of the concrete in the vicinity of the column

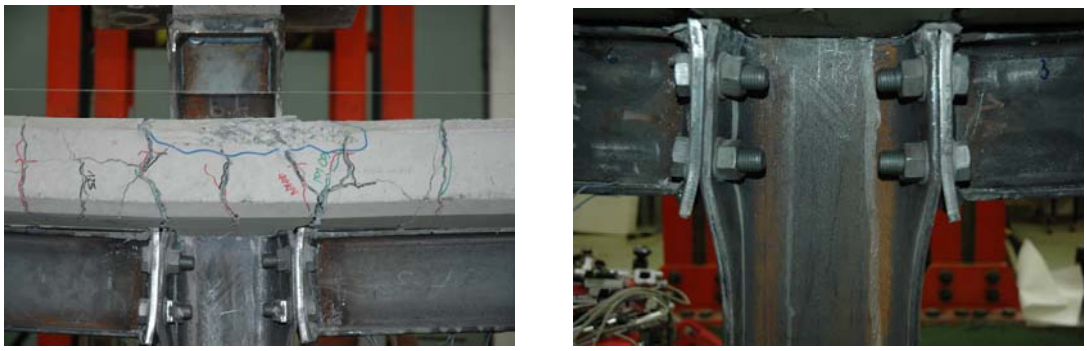

Figure III.68. Tested specimen at the end of the test under sagging bending moment and tension load

As for TEST 1, 2 and 3, the axial deformation of the joint according to the applied horizontal load was also measured; the obtained curves are reported in *Figure III.66*. It can be observed that a linear behaviour links the horizontal load and the horizontal deformation until a value of 500 kN for the horizontal load and that the obtained curves are similar.

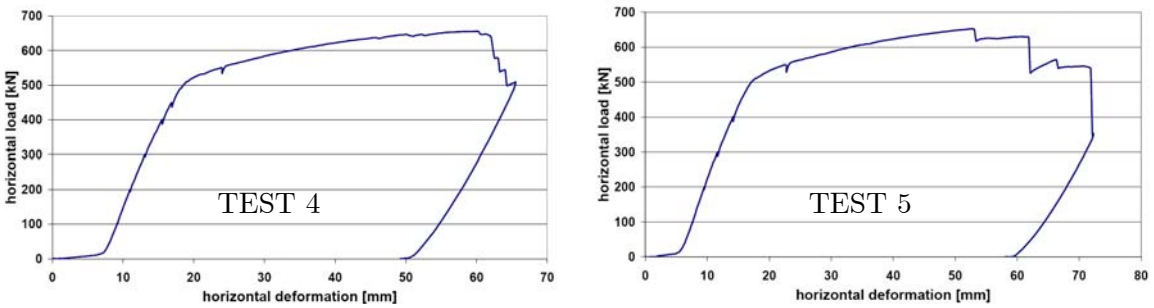

Figure III.69. Axial deformation of the joint measured during TEST 4 and TEST 5

C. Conclusions

This section presents the experimental tests performed at Stuttgart University on the composite joint configuration which is met in the tested substructure.

Through the performed tests, it was shown that only ductile components, i.e. rebars in tension, beam flange in compression, end-plate and column flange in bending, are activated to pass from a pure bending moment loading to the maximum tension load as expected from the design of the joint.

Also, through the *M-N* interaction curves obtained for the different tests and presented in *Figure III.64*, it can be seen that these curves (except for one test) converge to the same point at the end of the tests (i.e. point *A* in *Figure III.64*) what illustrates the good agreement between the obtained results.

In addition, the axial deformation of the tested joints according to the applied horizontal loads was measured during the test; this result will be useful when validating the simplified analytical procedure developed in *§ III.8*.

So, it can be concluded that the performed tests were successful and showed the ability of the joints to exhibit a ductile behaviour to pass from hogging or sagging bending moment to tensile load. The observations made during the composite joint tests in isolation are in line with what was observed during the substructure test presented in *§ III.4.4*.

The obtained results are used later on to validate an analytical procedure devoted to the prediction of the response of composite joints subjected to combined bending moments and axial loads (see *§ III.5.3*) and to introduce the actual properties of the substructure joints in the substructure numerical modelling for the validation of the numerical tool (see *§ III.6.2*).

III.5.3. Development and validation of an analytical procedure to predict the resistance of composite joints subjected to M-N

III.5.3.1. Introduction

The presence of axial loads in the beams has an influence on the rotational stiffness, the resistance moment and the rotation capacity of the joints. As the analytical method proposed in the Eurocodes, i.e. the component method (see *§ II.3.3.2*), is dedicated to the characterisation of the joint subjected to bending moment only, the proposed field of application is limited to joints in which the axial force N_{Ed} acting in the joint remains lower than 5 % of the axial design resistance of the connected beam cross section $N_{pl,Rd}$ *[22]*:

$$\left|\frac{N_{Ed}}{N_{pl,Rd}}\right| \leq 0,05 \tag{3.2}$$

Under this limit, it is assumed that the rotational response of the joints is not significantly affected by the axial loads. This limitation is a fully arbitrary one and is not at all scientifically justified. It has also to be underlined that this criterion only depends of the applied axial load N_{Ed} and of the plastic resistance of the beam $N_{pl,Rd}$ which is quite surprising as what is considered here is the influence of the applied axial load on the joint response.

If the criterion given in *Formula (3.2)* is not satisfied, the Eurocodes recommend to consider the resistant diagram defined by the polygon linking the four points

corresponding respectively to the hogging and sagging bending resistances in absence of axial force and to the tension and compression axial resistances in absence of bending.

In a previous study *[61]*, it was illustrated that the proposed method is quite questionable. So, in the PhD thesis of F. Cerfontaine *[61]* (and *[72]*), an improved design procedure, based on the component method concept, has been developed to predict the response of ductile and non-ductile steel joints subjected to combined axial loads and bending moments.

Within this section, the developed design procedure by F. Cerfontaine is first briefly described in *§ III.5.3.2*; as the studied joints within this section activate ductile components at collapse, only the procedure developed for ductile connections is presented in *§ III.5.3.2*. Then, the proposed procedure for steel joints is extended to composite joints and validated through comparisons to the experimental test results in *§ III.5.3.3*.

III.5.3.2. Brief description of the available analytical procedure for steel joints [72]

A. Introduction

Within this section, a brief description of the developed analytical procedure in the PhD thesis of F. Cerfontaine is given; this description is widely inspired from the article presented at the Eurosteel 2005 conference *[72]*.

The general concept of the developed method is first presented (*§ III.5.3.2.B*). Then, the convention used within the procedure is described (*§ III.5.3.2.C*). Finally, the principles on which the developed procedure is based are given (*§ III.5.3.2.D* to *§ III.5.3.2.F*).

B. General concept

In order to develop the improved design procedure according to the component method, which is still valid as the behaviour of the components is independent on the type of loading applied to the whole joint, a new assembly procedure was defined to cover the combined action of bending moments and axial loads. The main difficulty results from the modification of the list of active components within the joints according to the relative importance of the bending moment and axial load, and obviously according to the respective signs of the applied forces.

Two particular features of the component method had also to be carefully considered within the developed procedure:

- Group effects: these effects are likely to occur in plate components subjected to transverse bolt forces (i.e. mainly the components end-plate and column flange in

bending). Where a bolt force is applied, a yield plastic mechanism may develop in the plate component; if the bolt distances are high, separate yield lines will form in the plate component around the bolts (namely "individual bolt mechanism"), while a single yield plastic mechanism common to several bolts may develop when the distance between the latter decreases (namely "bolt group mechanism"). Group effects also affect the resistance of other components as the column web in tension and the beam web in tension.

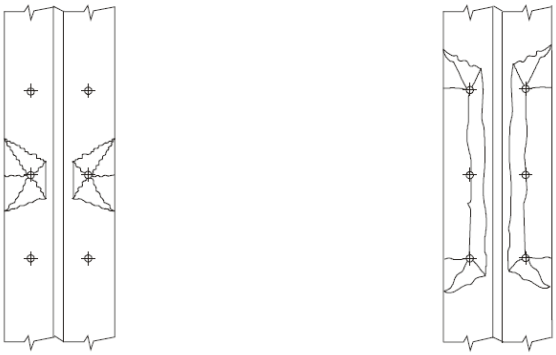

Individual bolt mechanism Bolt group mechanism

Figure III.70. Example of possible plastic mechanism in column flanges or end-plates [61]

- Component interaction: these ones may occur in components "extracted" from the column where three types of stresses interact: shear stresses in the web panel, longitudinal stresses due to axial and bending forces in the column and transversal stresses due to the load-introduction in the joint area (column web in tension, column web in compression and column web in shear).

One of the main difficulties was to introduce these effects in the developed procedure.

As mentioned in the previous section, only the procedure developed for joints activating ductile components at collapse is considered. So, the behaviour of each of the constitutive joint components is assumed to be infinitely ductile. As a result, a full plastic redistribution of the internal forces in the joint under bending moment and axial load may be contemplated as illustrated in *Figure III.71.*

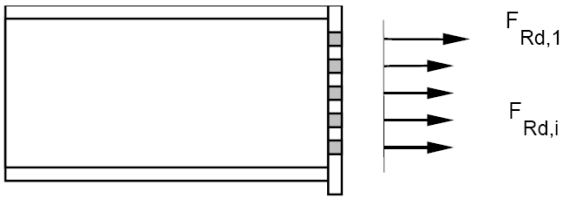

Figure III.71. Full plastic redistribution of the internal forces within a joint [23]

The so-derived ductile resistance interaction diagram corresponds to a plastic resistance surface; the actual applied bending moment and axial load (M_{Ed} and N_{Ed} respectively) in a

connection define a couple of values which should remain inside the interaction diagram so as to ensure the sufficient resistance of the studied connection.

C. Conventions

Within this section, developments are presented for the general case of a bolted end-plate steel connection with N_b bolt rows in which only tension loads may be transferred; in addition, two compression zones located at mid-thickness of the upper and lower beam flanges are identified (respectively noted "upper" or "up" and "lower" or "lo"). The compression zones are constituted of two components: the beam flange and web in compression and the column flange in compression.

So, this leads to a total of $N_b + 2 = n$ rows where internal forces may be transferred from the beam to the column. Conventionally, the tension forces are assumed to be positive (or equal to zero) while a compression force has a negative (or zero) value. All the rows are numbered from 1 to n by starting from the upper row. An example of row numbering is given in *Figure III.72*.

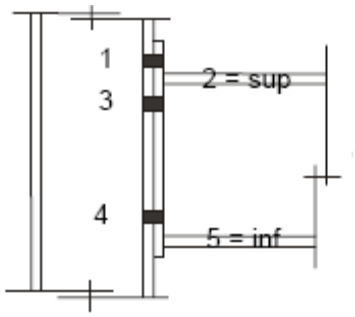

Figure III.72. Example of bolt row numbering with an extended end-plate connection

D. Equilibrium equations for the connection and load eccentricity

The evaluation of the resistance of the connection based on the static theorem requires at failure an equilibrium between the distribution of internal forces and the external applied loads. For connection subjected to a bending moment M_{Ed} and an axial load N_{Ed}, the equilibrium criteria are:

$$M_{Ed} = \sum_{i=1}^{n} h_i.F_i \text{ and } N_{Ed} = \sum_{i=1}^{n} F_i \tag{3.3}$$

where F_i is the load in row i and h_i is the corresponding lever arm; the latter is defined as the vertical distance between the reference beam point where M_{Ed} and N_{Ed} (see *Figure III.65* as an example) are computed and the row itself (h_i values are positive for rows located on the upper side of the reference point).

E. Resistance criteria

According to the static theorem, the resistance of each row, which is equal to the resistance of the weakest component in the row, should never be exceeded. At first sight, it looks easy as long as individual resistances of bolt-rows are considered but it is much more questionable when group effects (see *§ III.5.3.2.B*) develop in the connections.

Within the developed procedure, any group of rows noted [m, p], i.e. from row m to row p, in which group effects appear is considered as an equivalent fictitious row with an equivalent lever arm and a group resistance equal to that of the weakest group component. Therefore, the resistance criteria for each of the rows belonging to the [m, p] group may write, for any constitutive component α:

$$\sum_{i=m}^{p} F_i \leq F_{mp}^{Rd,\alpha} \text{ with } m = 1,...,p \text{ and } p = m, m+1,...,n \tag{3.4}$$

where $F_{mp}^{Rd,\alpha}$ is the resistance of the component α for the group of rows m to p. When m is equal to p, $F_{mp}^{Rd,\alpha}$ designates the individual resistance of the component a for row m. Such a resistance of the group of rows [m, p], noted F_{mp}^{Rd}, is defined as the smallest of the $F_{mp}^{Rd,\alpha}$ values.

This situation is illustrated in *Figure III.73* for a connection with three bolt rows (1, 2 and 3) but more generally covers the case of any connection with n rows in which group effects would develop in three bolt rows.

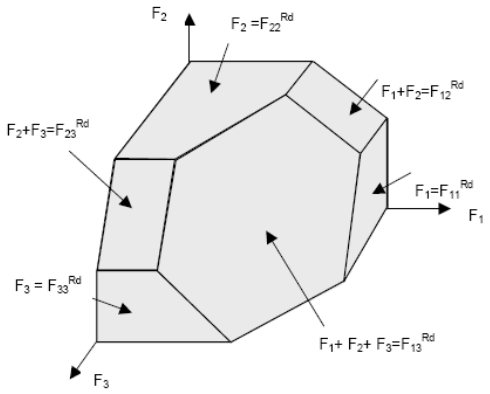

Figure III.73. Possible group effects between three bolt rows [61]

F. Definition of the failure criterion for the whole connection

Details about the application of the static theorem to a connection with n rows are given in *[61]*. This application leads to the following definition and writing of the *M-N* resistance interaction diagram: the interaction criterion between the bending moment and the axial force at failure is described by a set of $2n$ parallel straight line segments; the slope of each of the $2n$ parallel segments is equal to the value of the lever arm (h_k) and along these

segments, the force (F_k) in row k varies between 0 at one end and the maximum row resistance at the other end. An example of a M-N resistance interaction diagram is given in *Figure III.74* for a joint with four bolt rows (i.e. $2n$ = 2.(4+up+lo)=12 segments); for instance, to pass from point A to point B, the row 6 in compression is progressively activated (F_6 = 0 at point A where only the rows in tension are activated and $F_6 = F^{Rd,6}$ at point B).

It can be observed in *Figure III.74* that different values of bending moments correspond to the maximum tensile load; this phenomenon can be easily justified by the evolution of the loads within the rows involved in a group behaviour. This phenomenon will be illustrated latter on through the investigations performed in the next section.

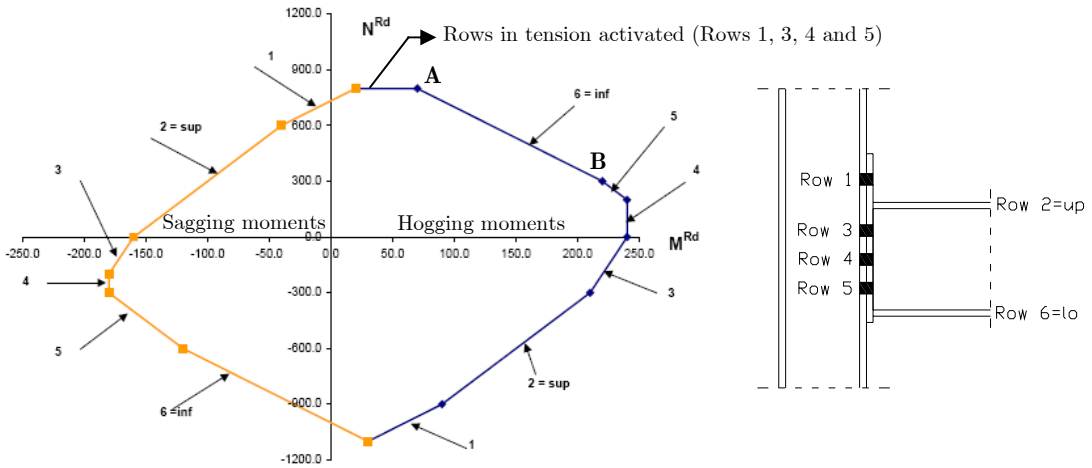

Figure III.74. Example of a M-N resistance interaction curve obtained for a four bolt row joint [61]

Each point of the curve is obtained by expressing the quite complex failure criteria given in *Formula (3.5)* for k from 1 to n; this criterion is defined so as to get maximum resistance bending moments by optimising the distributions of the loads amongst the bolt rows with account of the group effects.

Within this expression, it can be observed that two different resistances are attributed to the same row i (F_i^{Rd+} and F_i^{Rd-}). The evaluation procedure of the F_i^{Rd+} and F_i^{Rd-} values is illustrated in *Figure III.75* for a connection with three bolt rows where the black and white dots respectively show the successive steps for the evaluation of F_i^{Rd+} and F_i^{Rd-}; the objective of the evaluation procedure is to obtain the maximum resistant bending moment by maximising (or minimising if the sign of the bolt row resistance is negative) the loads in the bolt rows which are the most distant from the bolt row "k".

$$M = h_k.N + \sum_{i=1}^{n}(h_i - h_k).F_i^c$$

either $\left.\begin{array}{l} F_i^c = \max(F_i^{Rd+};0) \text{ if } i<k \\ F_i^c = \min(F_i^{Rd+};0) \text{ if } i>k \end{array}\right\}$ tension in the top rows 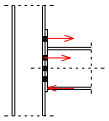

or $\left.\begin{array}{l} F_i^c = \min(F_i^{Rd-};0) \text{ if } i<k \\ F_i^c = \max(F_i^{Rd-};0) \text{ if } i>k \end{array}\right\}$ tension in the bottom rows 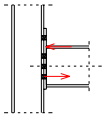 (3.5)

with $F_i^{Rd+} = \min(F_{mi}^{Rd} - \sum_{\substack{j=m \\ i\neq up,lo}}^{i-1} F_j^{Rd+}, m = 1,...,i)$ for $i<k$ and $F_i^{Rd+} = F_i^{Rd}$ for $i = up, lo > k$

$F_i^{Rd-} = \min(F_{im}^{Rd} - \sum_{\substack{j=i+1 \\ i\neq up,lo}}^{m} F_j^{Rd-}, m = i,...,n)$ for $i>k$ and $F_i^{Rd-} = F_i^{Rd}$ for $i = up, lo < k$

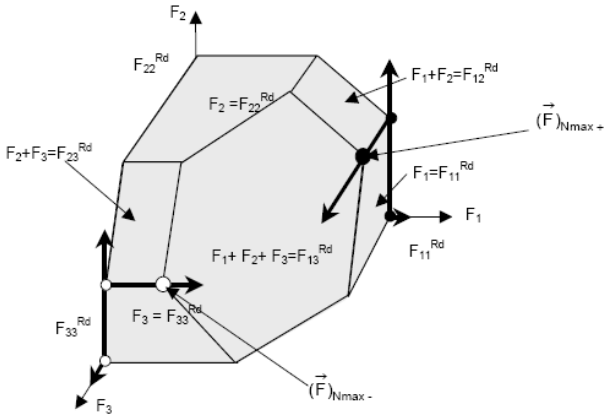

Figure III.75. Successive steps for the evaluation of F_i^{Rd+} and F_i^{Rd-} (black and white dots respectively) [61]

G. Conclusions

The quite complex criterion presented in *Formula (3.5)* has been introduced by F. Cerfontaine in a software named "ASCON" which allows the user to compute a resistance bending moment and a resistance axial load associated to a M_{Ed}-N_{Ed} couple. However, application rules are also proposed in *[61]* which allow a direct evaluation of the connection resistance for a given M_{Ed}-N_{Ed} couple through an analytical procedure.

The latter is extended to composite joints in the next section and applied to the tested joint configuration so as to predict its resistant *M-N* interaction curve and to compare the latter to the previously presented experimental test results.

III.5.3.3. Extension and validation of the analytical procedure to composite joints

A. Introduction

In the present section, the analytical procedure described in *§ III.5.3.2* is extended to predict the response of composite joints subjected to combined bending moments and normal loads in *§ III.5.3.3.B*.

Then, the proposed procedure is applied to the tested joint configuration in *§ III.5.3.3.C* so as to predict its resistance *M-N* interaction curve and to compare the obtained prediction to the experimental test results presented in *§ III.5.2*.

B. Extension of the analytical procedure to composite joints

The analytical procedure presented in *§ III.5.3.2* and developed by F. Cerfontaine is applicable to steel joints only.

In different references (as example in *[23]*) and in *§ II.3.3*, it is demonstrated that the component method can be easily applied to composite joint configurations to predict their behaviour under bending moments. The particularity of composite joint configurations is the fact that two main additional components are activated: the slab rebars in tension and the concrete slab in compression. As the analytical procedure presented in *§ III.5.3.2* is based on the component method concept, the latter is easily extended to composite joint configurations by including the behaviour of the two additional components into the procedure.

The component "slab rebars in tension" is already covered by Eurocode 4 *[6]* (in term of resistance and stiffness). What is assumed within the latter is the fact that this component can be considered as a bolt row and is activated in parallel with the other "tensile" components.

The same assumption is done herein. So, when computing the bending moment through *Formula (3.5)*, the resistance F_i^{Rd+} or F_i^{Rd-} associated to the rebars is computed according the same procedure as illustrated in *Figure III.75*.

For the component "concrete slab in compression", no rule is actually proposed within Eurocode 4 *[6]*. It is the reason why formulas were developed and validated in *§ II.3.3.4.B* to characterize this component (see *Formula (2.20)*, *Formula (2.21)* and *Formula (2.22)*). The latter are used within this section.

For each component i, its lever arm h_i has to be identified according to the convention presented in *§ III.5.3.2.C*. For the "steel" components (including the component "slab rebars in tension"), the computation of this lever arm is easy as the position of each component is clearly identified. So, when applying the failure criteria expressed through *Formula (3.5)*, each point of the interaction curves are obtained by assuming h_k equal to one of these lever arms.

For the component "concrete slab in compression", the lever arm depends of the height of concrete z which is assumed to work within the joint which evolutes according to the applied forces at the joint level; so, to use the failure criteria, it is not possible to identify "one" value of h_k characterising the component "concrete slab in compression". As a consequence, when the latter component is activated within a composite joint, the *M-N* resistance interaction curve is no more associated to a linear segment but to an incurve segment which is a function of the height of concrete z subjected to compression and its associated lever arm.

So, the M-N resistance interaction curve of a composite joint is not composed of $2.n$ parallel segments (as for steel joints – see *§ III.5.3.2.F*) but present a non-linear zone where the component "concrete slab in compression" is activated.

This observation is illustrated in the next section when this procedure is applied to the joint configuration tested at Stuttgart University.

C. Validation of the proposed analytical procedure

The validity of the proposed analytical procedure presented in the previous section is checked by computing the resistant *M-N* interaction curve of the composite joint configuration tested at Stuttgart University (see *§ III.5.2*) and comparing the obtained analytical curve with the experimental test results.

The computation details to obtain the analytical *M-N* resistance interaction curve are presented in *Appendix VI.7*. The comparison of the obtained analytical results to the experimental test results is presented in *Figure III.76*. On the latter, it can be observed that two analytical curves are reported:

- One named "plastic resistance curve" which is computed with the elastic strengths of the materials and;
- One named "ultimate resistance curve" which is computed with the ultimate strengths of the materials.

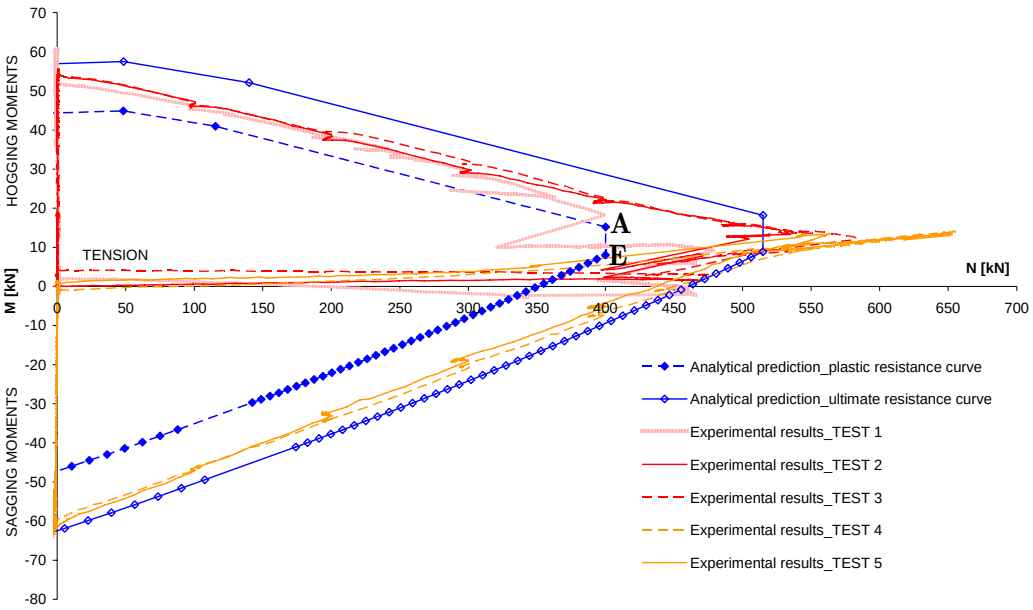

Figure III.76. Comparison of the resistance interaction curves

According to *Figure III.76*, the computed analytical curves are in very good agreement with the experimental results. Indeed, the experimental curves are between the plastic and ultimate analytical resistant curves which is in line with the loading sequence followed during the tests (see *§ III.5.2.2*).

In the hogging moment zone, it can be observed that for very small values of tensile loads, the experimental curves are close to the ultimate analytical one which is logical, as a bending moment close to the ultimate resistant bending moment of the joint is applied to the tested specimen before applying the tensile load. Then, when the tensile load is increasing, the experimental curves first deviate from the ultimate analytical one to finally come back close to the ultimate analytical curve (except for TEST 1). This phenomenon can be explained by the fact that, to pass from the ultimate hogging moment to the ultimate tensile resistant load, different components are activated; indeed, the component which is associated to the ultimate hogging moment is "beam flange in compression" while the one associated to the ultimate tensile load is the component "column flange in bending".

This phenomenon is not observed in the sagging moment zone; indeed, as shown in *Figure III.76*, the experimental curves are close to the ultimate analytical one from the pure bending to the ultimate tensile load. Again, it is in agreement with the component activated from the pure bending to the ultimate tensile load which is the same in the present case, i.e. the component "column flange in bending".

With the analytical procedure, it can be seen that different values of bending moments are associated to the maximum tensile load (vertical line "AE" in *Figure III.76*). This is

explained by the collapse mode associated to the maximum tensile load which includes two bolt rows involved in a group effect (see *AppendixVI.7*). Indeed, to pass from point "A" to point "E", there is a redistribution of loads between the bolt rows involved in the group effect, redistribution of loads which does not affect the value of the tensile load, as the sum of the bolt row loads is always equal to the group resistance, but affects the value of the bending moments, as the sum of the products "$h_i.F_i^{Rd}$" are not constant during the redistribution. This phenomenon is illustrated in *Figure III.77* where the distribution of the loads between the bolt rows at point A and point E of *Figure III.76* is given.

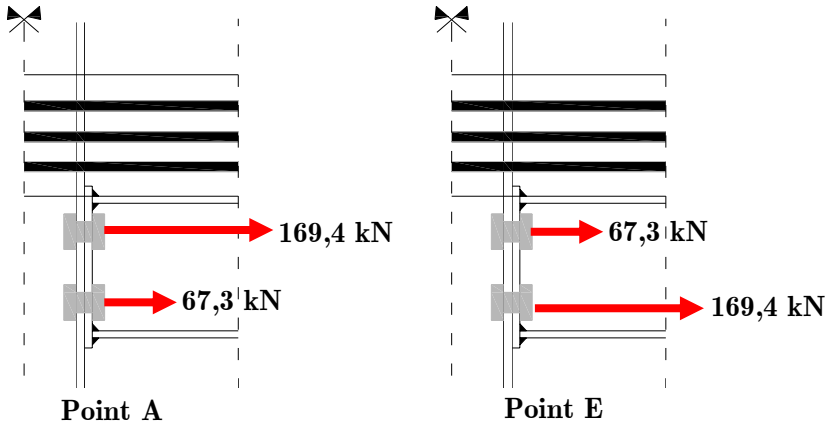

Figure III.77. Distribution of the loads within the bolt rows at point A and point E of Figure III.76

Also, in *Figure III.76*, it is shown that the maximum tensile load which can be supported by the joint is underestimated by the analytical procedure. This difference can be justified by the fact that the proposed analytical procedure does not take into account of the presence of membrane forces within the components "column flange in bending" and "end-plate in bending" associated to the big deformations of these components appearing when high tensile loads are applied to the joint. This phenomenon was already identified when investigating the behaviour of these joints subjected to bending moments (see *§ II.3.3.3.D* and *Figure II.38*).

D. Conclusions

In the present section, the analytical procedure to predict the *M-N* resistance interaction curve of joints, initially developed for steel joints, has been extended to composite joints.

The proposed procedure has been then applied to the tested composite joint configuration in order to compare the obtained analytical prediction with the experimental test results. It has been shown that the analytical prediction is in very good agreement with the experimental results which leads to the validation of the proposed procedure.

III.5.4. Conclusions

This paragraph is dedicated to the investigation of the behaviour of steel and composite joints subjected to combined axial loads and bending moments, loading situation appearing in structures when catenary actions develop further to the a column loss.

Experimental investigations have been first presented. The objective of the presented experimental tests (performed at Stuttgart University in strong collaboration with Liège University) was to derive the *M-N* resistance interaction curve (in the tensile zone) of the joint configuration met in the tested substructure. The obtained results have been presented in details, putting into sight the observed particularities. In particular, it was shown that only ductile components are activated to pass from the "pure" bending loading to the "pure" tensile loading, as expected from the joint design.

Then, an analytical procedure initially developed for steel joints and dedicated to the prediction of the behaviour of joints subjected to combined bending moments and axial loads has been extended to composite joints and validated through comparisons with experimental results.

Through the obtained results, it can be concluded that

- the actual behaviour of the substructure joints when catenary action developed is known and that;
- an analytical tool is now available to predict the resistance of composite joints subjected to combined bending moments and axial loads.

The performed analytical developments were only dedicated to the prediction of the *M-N* resistance curve of composite joints. However, an interaction between the bending stiffness and the axial stiffness also exists within the joint, what was not considered herein. In particular, it will be shown later on that a property which has to be known is the relation linking the axial deformation of the joint to the applied axial load (as illustrated in *Figure III.66* and *Figure III.69*) when moving on the *M-N* resistance curve. The prediction of this relation requests further researches and developments, what constitutes one of the perspectives of the present thesis (see *§ IV.8*).

III.6. Validation of the numerical tool

III.6.1. Introduction

In *§ II.4*, the use of FINELG to predict the response of composite non-sway and sway frames subjected to "conventional" loading was validated. In this paragraph, the use of

the latter to predict the response of steel and composites structures further to the loss of a column is investigated.

In a first step, the substructure tested at Liège University is modelled with FINELG and the so-obtained prediction is compared with the substructure experimental test results (*§ III.6.2*). Then, in a second step, a benchmark study performed on a steel frame losing a column at the first storey is presented in *§ III.6.3*.

III.6.2. Numerical simulation of the substructure test

III.6.2.1. Introduction

In this section, the FE software FINELG is used to simulate numerically the behaviour of the tested substructure. The defined model is first described in *§ III.6.2.2* and then, the comparison between the numerical and the experimental results is given in *§ III.6.2.3*.

III.6.2.2. Description of the numerical model

The substructure test is numerically computed through a 2D model with FINELG. The finite elements used to model this composite structure are the same than the ones already presented in *§ II.4.3*. The mechanical and the geometrical properties which have been introduced in the numerical modelling are the ones measured at the Argenco laboratory (see *§ III.4.4.2* and *Appendix VI.6* respectively). The steel materials are modelled with account of strain hardening effects (strain hardening stiffness equal to one fiftieth of the young modulus); the concrete material is modelled through a parabolic behaviour law with tension stiffening as presented in *Figure II.46*. Also, the behaviour of the substructure composite joints which have been implemented is the one observed through the isolated joint tests performed at Stuttgart University (see *§ III.5.2*). The load path defined in the numerical simulation is exactly the one followed during the test described in *§ III.4.4.4*.

The difficulty of the modelling is to introduce the actual behaviour of the joints within the simulation; indeed, the interaction within the joints between the axial loads and the bending moments (in term of resistance and stiffness) have to be reflected within the numerical simulation, as these interactions widely influence the development of the catenary action within the modelled structure. In the actual finite element codes, no finite element permits to model such combined interaction.

Within the present study, two different solutions have been investigated:

- The first one consists in modelling the joint behaviour with a rotational spring only. So, there is no joint interaction introduced in the modelling.

- The second one consists in modelling the joint behaviour through equivalent double-T beam elements exhibiting the same *M-N* resistance that the joint one. Also, the initial bending stiffnesses of the equivalent beams have been calibrated to exhibit the initial bending stiffnesses of the joints. In total, two equivalent double-T beams have been defined: one to model the behaviour of the joint subjected to hogging moments and one to model the behaviour of the joint subjected to sagging moments. The comparisons of the interaction resistance curves of the equivalent double-T elements with the joint ones (experimentally determined) are given in *Figure III.78*.

  With this solution, an important relation, which is the one linking the elongation of the joint with the applied axial load when moving on the resistant interaction curve, is not taken into account. Indeed, through a preliminary study, it has been illustrated that, if the elongation of the double-T beams when the plastic hinges are formed (numerically determined) is compared to the one experimentally determined for the joints (see *Figure III.66* and *Figure III.69*), the equivalent beam elongations are higher than the joint ones for the same applied axial load.

  To make up for this problem, the following trick is used: the lateral restraint at the substructure extremities (simulated by two horizontal jacks during the experimental test – see *Figure III.28*) is artificially increased to compensate this lack of axial stiffness within the joints. Indeed, the lateral restraint and the joints subjected to axial loads can be considered as springs in series as illustrated in *Figure III.79*. So, the "lack" of stiffness of the equivalent double-T beams can be compensated by an increase of the lateral restraint stiffness.

The comparison between the so-obtained results and the experimental one is presented in the following section.

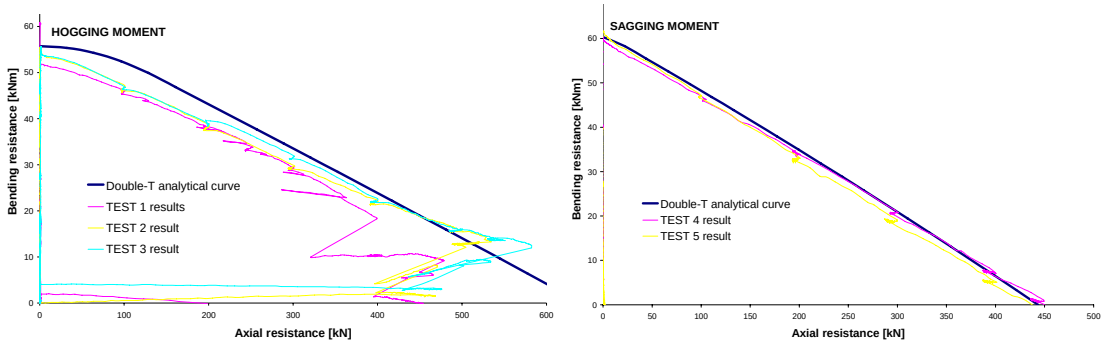

Figure III.78. Comparison between the M-N resistance interaction curves of the equivalent double-T elements and of the joints)

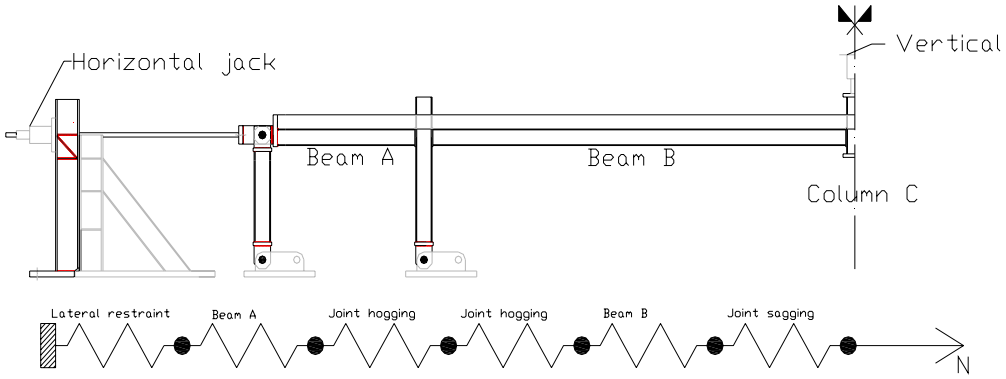

Figure III.79. Components influencing the axial stiffness of the substructure when the membrane forces develop within the tested substructure

Remark: the joints between beam B and column C (see *Figure III.79*) are first subjected to hogging moments and then to sagging moments. However, with the "double-T beam" solution, it is not possible to model, at the same time, the behaviour under hogging and sagging moments. The double-T beams which have been placed at these locations are the ones reflecting the behaviour under sagging moments as the main objective is to numerically predict the development of the membrane forces and their effect on the frame response, i.e. when a plastic hinge under sagging moment is formed at this location.

III.6.2.3. Comparison numerical predictions vs. experimental results

The comparisons between the numerical predictions and the experimental result are given in *Figure III.80*. It can be seen that, with the two solutions, the obtained results are not satisfactory, except for the modelling with the equivalent double-T beam elements until a deflection of 480 mm, when significant membrane forces begin to appear in the structure.

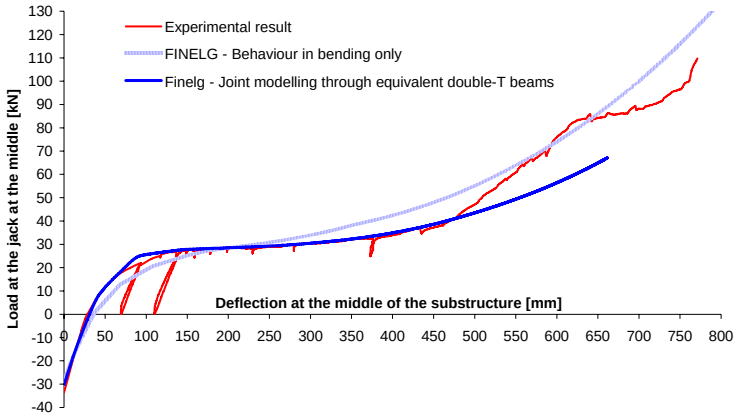

Figure III.80. Comparisons between the numerical predictions and the experimental results

None of the proposed solutions seems to be able to model the actual behaviour of the joints with a sufficient accuracy. Additional researches are requested to improve the numerical modelling of the behaviour of joints with account of the different interactions

appearing when catenary actions develop in a structure; this point is addressed in the perspective presented in *§ IV.2*.

III.6.3. Benchmark study

III.6.3.1. Introduction

Within the "Robustness" project, a benchmark study was performed to validate the software used within the project for the investigations of the exceptional situation "loss of a column in a steel frame".

The benchmark study was performed by three partners involved in the numerical investigations within the previously mentioned project:

- Liège University with FINELG;
- PSP (Professor Sedlaceck and Partner in Aachen) with ABAQUS and ;
- Stuttgart University with ANSYS.

The benchmark study is performed on a steel building designed by PSP, as coordinator of the study; the studied frame is first described in *§ III.6.3.2*. Then, the comparison between the obtained results is given in *§ III.6.3.3*.

III.6.3.2. Description of the investigated frame

The investigated frame is a 2D 7 bays – 6 storeys unbraced steel frame. The span of the beams is equal to 8,00 m for each bay and the height of each storey is equal to 3,50 m. The out-of-plane distance between the frames is equal to 5 m. The column bases are assumed to be fully fixed (all degrees of freedom fixed) and the joints are assumed as rigid and full strength ones. The frame has been designed by PSP *[73]* according to Eurocode 3 *[12]*; the applied loads considered for the frame design were the ones recommended in Eurocode 1 *[64]* for office buildings. The beams are IPE400v profile ones while the columns are HEA360 ones. The so-obtained structure is illustrated in *Figure III.81*.

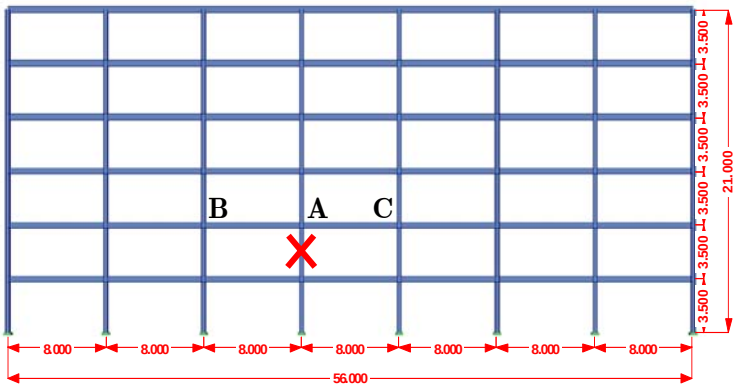

Figure III.81. Investigated steel frame within the benchmark study [56]

Full nonlinear analyses (i.e. with geometrical and material non-linearities) have been conducted through the different software. The steel material has been modelled through a tri-linear behaviour law as presented in *Figure III.82*. The loading sequence which has been followed for the benchmark study is the following:

- the design loads, as recommended in Eurocode 1 *[64]*, are first applied to the studied frame;
- then, the column marked by a cross in *Figure III.81* is progressively removed until reaching a value of the axial load equal to 0;
- finally, as the objective of the benchmark study is to compare the prediction obtained with the different software when significant second order effects developed within the structure, a concentrated load is applied at point "A".

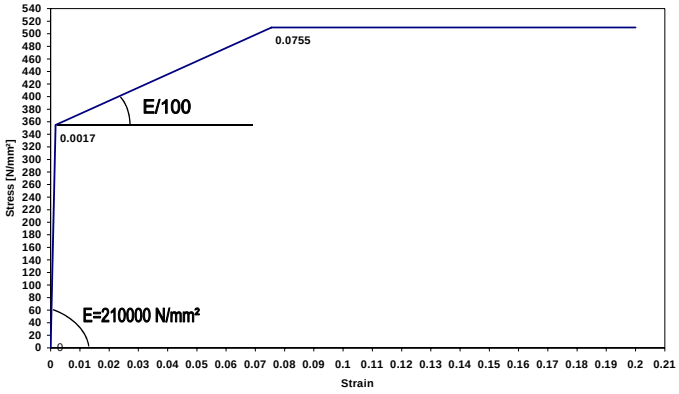

Figure III.82. Tri-linear behaviour law for the steel material used within the models [73]

The obtained results through the different software are compared in the next section.

III.6.3.3. Comparison of the numerical predictions obtained through different FE software

Some results obtained through the three different FE software are compared in *Figure III.83* and *Figure III.84*. It can be observed that a good agreement is obtained between the different predictions, in particular between FINELG and ABAQUS. With ANSYS, Stuttgart University met some problem of convergence leading to a premature stop of the simulation, i.e. before the formation of the panel plastic mechanism in the indirectly affected part as illustrated in *Figure III.83*.

Other results have been compared through the benchmark study; the latter are available in *[73]*. Through this study, it is shown that a very good agreement is obtained between the different software, what validates their further use to investigate the behaviour of steel frames (with fully rigid and full strength joints) further to the loss of a column.

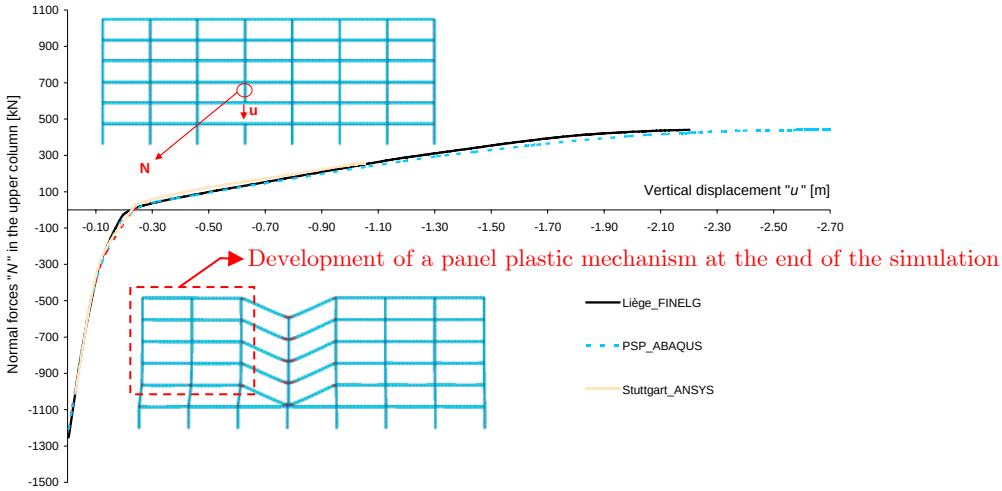

Figure III.83. Comparison of the vertical displacement at the top of the loss column vs. the axial load in the upper column curves

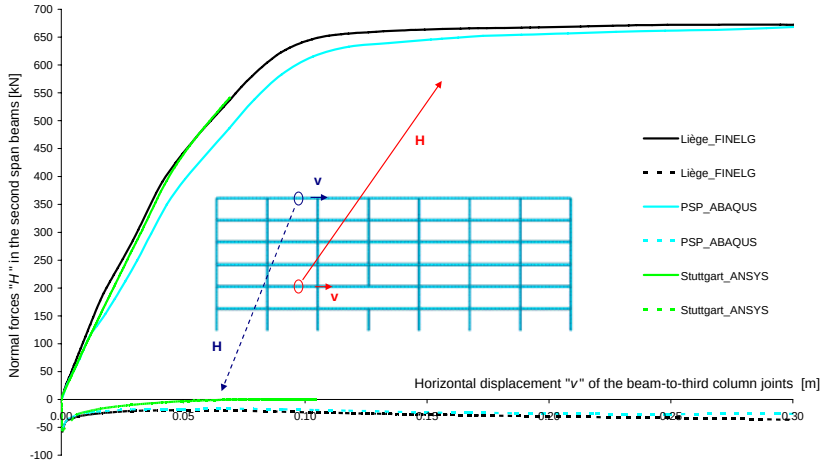

Figure III.84. Comparison of the horizontal displacement at the third columns vs. the axial loads within the second span beams

III.6.4. Conclusions

Within the present paragraph, the validity of the homemade finite element software FINELG to predict the structural response of a steel or composite frame further to a column loss is investigated.

In a first step, the substructure tested at the Argenco department of Liège University has been modelled with FINELG and the so-obtained numerical prediction has been compared to the experimental result. Through the performed comparisons, the difficulty to model the behaviour of the structural beam-to-column joints subjected to combined bending moments and tensile loads has been put into sight. In particular, a solution consisting in modelling the behaviour of the joints through equivalent double-T beams has been investigated; this solution gives good results if the membrane forces within the structure are not too important. When the influence of the membrane forces on the structure

response becomes significant, this solution does not produce accurate results. Additional developments are requested to model the behaviour of joints subjected to such loading; this point is addressed in the perspectives presented in *§ IV.2*.

In a second step, a benchmark study performed on a 2D steel frame with full-strength beam-to-column joints has been presented. The objective was to validate different software (FINELG, ANSYS and ABAQUS) used within the "Robustness" project to simulate the loss of a column in a steel building frame. The results obtained through the different software were in very good agreement what validates the used of the latter to predict the response of such frame. In particular, the so-validated software FINELG is used later on to perform numerical investigations on steel structures in *§ III.7.2* and *§ III.8.2*.

III.7. From the actual frame to a simplified substructure modelling

III.7.1. Introduction

As mentioned in the general concept presented in *§ III.3*, the adopted approach within the thesis to predict the behaviour of the frame when a plastic mechanism is formed in the directly affected part is to extract a simplified substructure from the frame under consideration. This simplified substructure is reminded in *Figure III.85*.

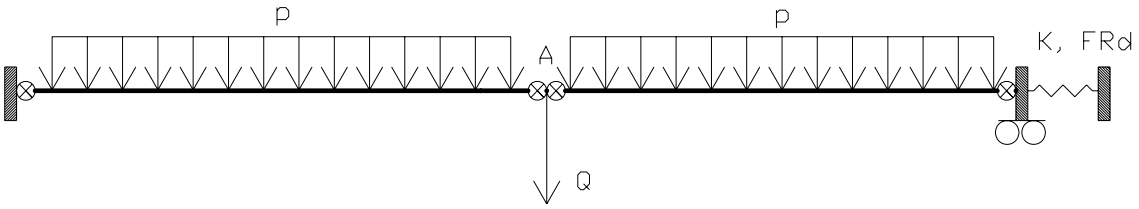

Figure III.85. Simplified substructure modelling

To be feasible, it has first to be confirmed that the simplified substructure modelling is able to predict the behaviour of the global frame with a sufficient accuracy. This validation has been performed in strong collaboration with PSP [74] through numerical investigations performed with validated FE software (see *§ III.6*). This validation is presented in *§ III.7.2*.

Then, the simplified substructure as presented in *Figure III.85* has to be defined. In particular, the value of K and F_{Rd} which are parameters coming from the indirectly affect part have to be estimated. The analytical methods to predict the latter have been developed in the thesis of Luu Nguyen Nam Hai [63]; *§ III.7.3* describes briefly the method used to estimate these values and the main properties influencing the latter.

III.7.2. Validation of the "simplified substructure approach"

The simplified substructure approach is validated through numerical investigations performed on the structure used for the benchmark study presented in *§ III.6.3*. An example of the performed comparisons is given in the present paragraph.

For the presented example, the loss of a column at the first storey of the structure as highlighted in *Figure III.81* is considered and the evolution of the vertical displacement of point "A" (see *Figure III.86*) according to Q ($=N_{lo}$ - N_{up} – see *Formula (3.1)*), obtained through a non-linear analysis performed with the global frame modelling, is compared to the one obtained through a non-linear analysis performed with the simplified subsystem modelling. The results presented herein have been obtained with the previously validate software FINELG (see *§ III.6.3*).

In order to compare the results, the parameters characterising the subsystem (see *Figure III.85*) have to be defined, i.e. the lateral stiffness of the indirectly affected part K and its resistance to horizontal loads F_{Rd}. As the objective here is to validate the simplified substructure approach, the values of K and F_{Rd} are extracted from the global frame non-linear numerical analysis to obtain values as accurate as possible.

As shown in *Figure III.85*, the horizontal restraint coming from the indirectly affected part is simulated by one horizontal spring. So, to define K and F_{Rd}, the evolution of the horizontal displacement of points "B" and "C" (see *Figure III.86*) according to the horizontal load H_B and H_C (associated to the catenary action) has to be first determined and then summed so as to simulate, through the horizontal spring, the global behaviour of the indirectly affected part. The obtained results are presented in *Figure III.87*.

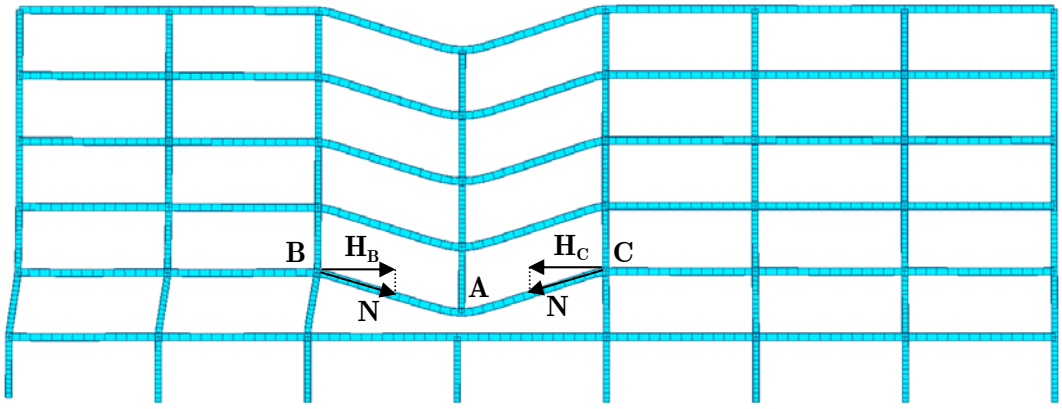

Figure III.86. Definition of the horizontal load to be considered for the prediction of K and F_{Rd}

In *Figure III.87*, it can be observed that no horizontal displacement appears before reaching a horizontal load equal to 92 kN; the passage from a horizontal load equal to 0 to 92 kN corresponds to the development of Phase 1 and 2 as illustrated in *Figure III.7*. When the plastic mechanism is formed in the directly affected part, i.e. at the beginning of Phase 3, the values of the horizontal displacements significantly increase, particularly for point "B"; the maximum horizontal load which is reached is equal to 1053 kN and corresponds to the development of a panel plastic mechanism on the left side of the structure in the indirectly affected part, as illustrated in *Figure III.83*.

As the objective with the simplified substructure is to predict the development of the catenary action within the directly affected part, i.e. to predict the behaviour of the structure during Phase 3, it is important to have a good estimation of the lateral restraint coming from the indirectly affected part for a value of the horizontal load higher than 92 kN. Also, it is decided to model the lateral restraint within the simplified substructure through a bilinear behaviour law as reported in *Figure III.87*. Accordingly, the so-obtained values for K and F_{Rd} are respectively equal to 8008 kN/m and 961 kN (= 1053 kN – 92 kN).

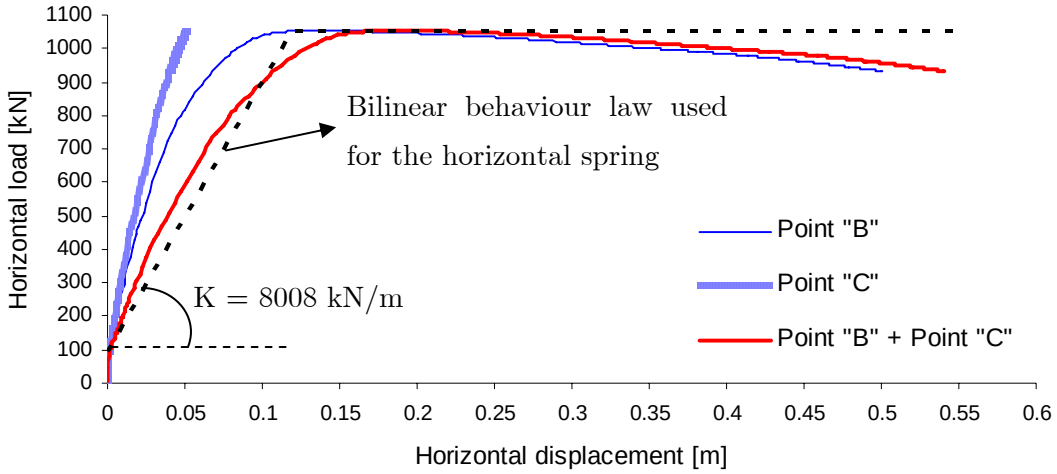

Figure III.87. Horizontal displacement vs. horizontal load at point "B" and "C" in the investigated structure (see Figure III.86)

The comparison of the results obtained through the global frame modelling and the simplified substructure modelling is given in *Figure III.88*. In the latter, a shaded zone is present; this zone limits the part of the graph which is linked to Phase 3. Indeed, from point (0) to (2), the curve is relative to Phase 1 (from (0) to (1)) and 2 (from (1) to (2)) while at point (3), the maximum value F_{Rd} is reached.

Within *Figure III.88*, two curves are reported for the simplified substructure modelling: one corresponds to the response of the system as presented in *Figure III.85* with the uniformly distributed load p equal to the uniform load applied to the modelled storey in

the global frame modelling and one corresponds to the same system assuming that p is equal to 0, i.e. only the concentrated load Q is applied to the system. It can be observed in *Figure III.88* that the two curves corresponding to the simplified subsystem modelling are exactly superposed during Phase 3 (from point (2) to point (3)). This observation can be explained by the fact that, when the plastic mechanism is formed within the structure, only the value of Q is varying and significantly affects the response of the structure.

In addition, it can be observed that, for Phase 3, a good agreement is obtained between the global frame modelling and the simplified substructure modelling.

Other comparisons have been performed by PSP with the validated software ABAQUS for different positions of column losses *[74]*; the conclusions drawn for the presented example have been confirmed, what validates the simplified substructure approach.

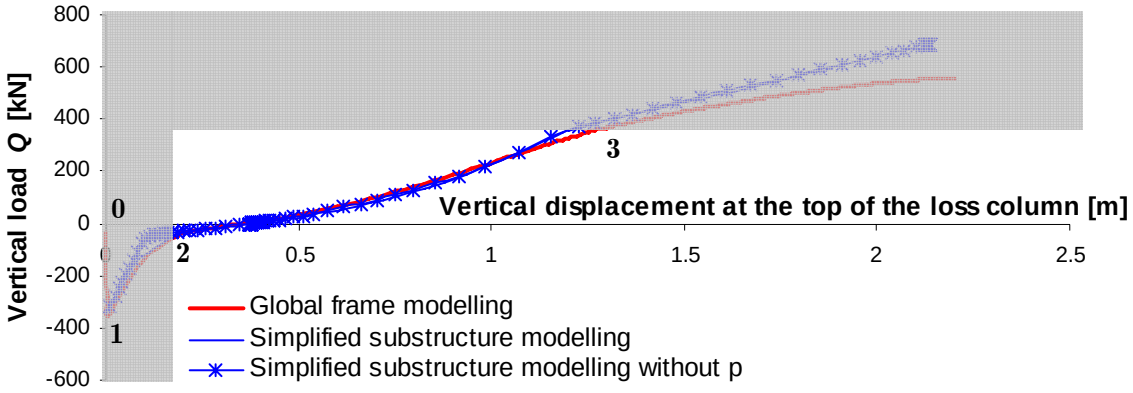

Figure III.88. Comparison between the results obtained through the global frame modelling and the simplified substructure modelling

Remark: it can be seen in *Figure III.88* that after point (3), the global frame modelling curve and the simplified substructure modelling curves diverge. It is explained by the behaviour law which is used for the horizontal spring; indeed, it can be observed in *Figure III.87* that, when the maximum horizontal load is reached, the value of the horizontal load is kept equal to F_{Rd} (= 961 kN) for the horizontal spring while, in the global frame modelling, it can be seen that this value is decreasing while the horizontal displacement is increasing. However, this difference is not significant as within the adopted concept, it is assumed that Phase 3 is stopped when F_{Rd} is reached within the subsystem (see *§ III.3.3*).

III.7.3. Definition of the simplified substructure properties

III.7.3.1. Introduction

As mentioned previously, two main parameters associated to the behaviour of the indirectly affected part, i.e. K and F_{Rd}, have to be estimated to define the simplified substructure. The developed analytical methods for the prediction of these parameters are presented in the thesis of Luu Nguyen Nam Hai *[63]*, as the latter are linked to indirectly affected part behaviour under investigation in this thesis (see *§ III.3*). The present section summarises briefly the developed methods to predict these parameters.

III.7.3.2. Estimation of K

The procedure developed to predict the value of K is based on spring models as represented in *Figure III.89*; the objective of the latter is to predict one value of K in order to define a bilinear behaviour law, as presented in *Figure III.87*, for the horizontal spring of the simplified substructure modelling. The method has been validated for braced and unbraced structures with or without semi-rigid joints.

This procedure takes into account of the column stiffnesses, including the restraints at their extremities (indicated in orange in *Figure III.89*), subjected to combined bending moments (associated to the horizontal loads applied to the indirectly affected part) and axial loads. Also, it has been shown in *[63]* that, for most of the cases, the elongation stiffness of the beams can be neglected within the evaluation of K.

With the proposed method detailed and validated through parametrical studies in *[63]*, accurate values of K (if compared to the one numerically predicted through full non-linear analyses) are obtained and can be introduced within the simplified substructure modelling

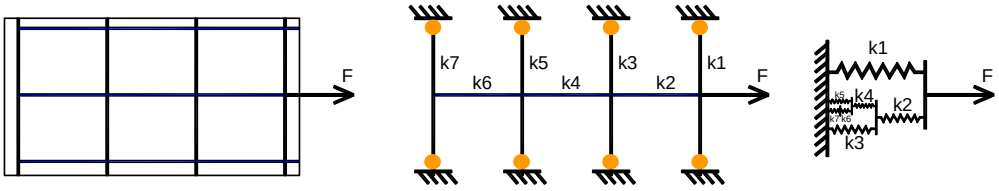

Figure III.89. Spring model used for the estimation of K

III.7.3.3. Estimation of F_{Rd}

Different collapse modes of the indirectly affected part can be associated to F_{Rd}:

- The development of a global plastic mechanism in the indirectly affected part. This situation is the one met within the benchmark study presented in *III.6.3* where a

panel plastic mechanism developed in the indirectly affected part on the left of the structure.

- The buckling of columns subjected to additional axial loads and bending moments associated to the development of the catenary actions within the directly affected part.

Methods to predict the horizontal loads associated to these possible collapse modes based on analytical models are presented in *[63]*. The particularities of these methods are linked to the performed assumptions, validated through parametrical studies, leading to simplified analytical methods.

The minimum value of F_{Rd} obtained for the different possible collapse modes is the one to be considered in the behaviour law of the simplified substructure horizontal spring.

III.7.4. Conclusions

Within the present paragraph, the simplified substructure approach has been first validated through comparisons between the results obtained through a non-linear analysis of the global frame modelling and the ones obtained through a non-linear analysis of the simplified substructure modelling. Through the presented example, it has been shown that a very good agreement between the results of the global frame modelling and of the simplified substructure modelling is obtained. This observation has been confirmed by PSP who performed the same type of comparisons for several positions of column loss within the frame [74].

In addition, it has been demonstrated that, to investigate the behaviour of the structure during Phase 3, it is not requested to take into account of the constant uniformly distributed load p applied on the beams as the only load which affects significantly the system response during Phase 3 is the concentrated load Q. This observation will be confirmed in the following paragraph through the development of the analytical method

Finally, a brief description of how to define the values of the parameters K and F_{Rd} associated to the indirectly affected part behaviour has been given, summarising the methods developed in the thesis of Luu Nguyen Nam Hai *[63]*. With these methods, it is possible to define a bilinear behaviour law for the horizontal spring of the simplified substructure.

III.8. Analytical method to predict the simplified substructure response with account of the development of the membrane forces

III.8.1. Introduction

In the previous paragraph, the validity of the simplified substructure approach has been demonstrated. Within the present paragraph, an analytical method able to predict the response of the simplified substructure is presented.

In a first step, numerical parametrical studies are carried out with the validated software FINELG in order to understand how the various parameters influence the response of the simplified substructure and to identify the parameters to be taken into account in the analytical procedure *[75]*; the latter is summarised in *§ III.8.2*.

Then, with the so-identified parameters, an analytical procedure is developed to determine the response of the simplified substructure, i.e. the evolution of the vertical displacement according to the applied concentrated load. The developed method is based on a rigid-perfectly plastic analysis and is described in *§ III.8.3*.

Finally, the developed analytical procedure is validated through comparison to the substructure experimental test results (see *§ III.4.4*).

III.8.2. Identification of the parameters to be considered

III.8.2.1. Introduction

In order to understand how the various parameters influence the response of the simplified substructure, an eleven-level parametric study has been first carried out. The main results are presented in the following section. In the latter, additional parametrical studies are also presented to investigate, with more details, the influence of some "key" parameters on the simplified substructure response and in particular, on the development of the catenary action:

- variation of the lateral restraint K;
- variation of the beam cross section A and;
- variation of the beam inertia I.

Remark: in all the investigated models, the resistance F_{Rd} of the horizontal spring is assumed to be equal to the axial resistance of the beam.

III.8.2.2. Parametrical studies

The different studied levels within the first parametrical study are illustrated in *Figure III.90* and their main properties are summarised in *Table III.5*.

The main parameters considered in this eleven-level study are the following ones:

- The beam response: the stiffness of the beams in bending (EI) and under axial force (EA) are varied, as well as the yield strength f_y of the constitutive material; a high value of EI allows to simulate "rigid" beams, while the adoption of high values of f_y enables to simulate a fully elastic response of the beam elements.
- The K restraint: the importance of the membrane effects in the beam increases with the K values, while the beam transverse displacements at failure decrease. For high values of K high tying forces are obtained at beam ends, while demand in terms of rotational capacity is requested at beam ends when large displacements occur in the beam, i.e. for low values of K.
- The resistance properties of the beam end sections: in this study, no connection is assumed to act at beam ends; so possible plastic hinges develop in the beam itself for an axial force equal to $N_{pl,Rd}$ (tension resistance of the beam cross section), for a bending moment equal to $M_{pl,Rd}$ (bending resistance of the beam cross section) or under a combination of bending moment and axial forces. In the parametric study, no interaction between axial forces and bending moments is first contemplated (Level 1 to 7); then a non-linear interaction resistance curve characterising the beam cross section is considered (Level 8 to 11).

As previously mentioned, additional parametrical studies are performed to vary "key parameters" identified through the "eleven-level" parametrical study. The starting points for these parametrical studies are Level 1 (i.e. "Rigid system") and/or Level 9 (i.e. "Bi-encased beam" with a high value of K). For these two levels, the parameters which are varied are:

- the stiffness of the horizontal spring K ($K \in]\infty; 3000kN/m]$);
- the beam cross section A_b ($A_b \in]\infty; 0,125.A_{IPE200}]$) and;
- the beam moment of inertia I_b ($I_b \in]\infty; 0,25.I_{IPE200}]$).

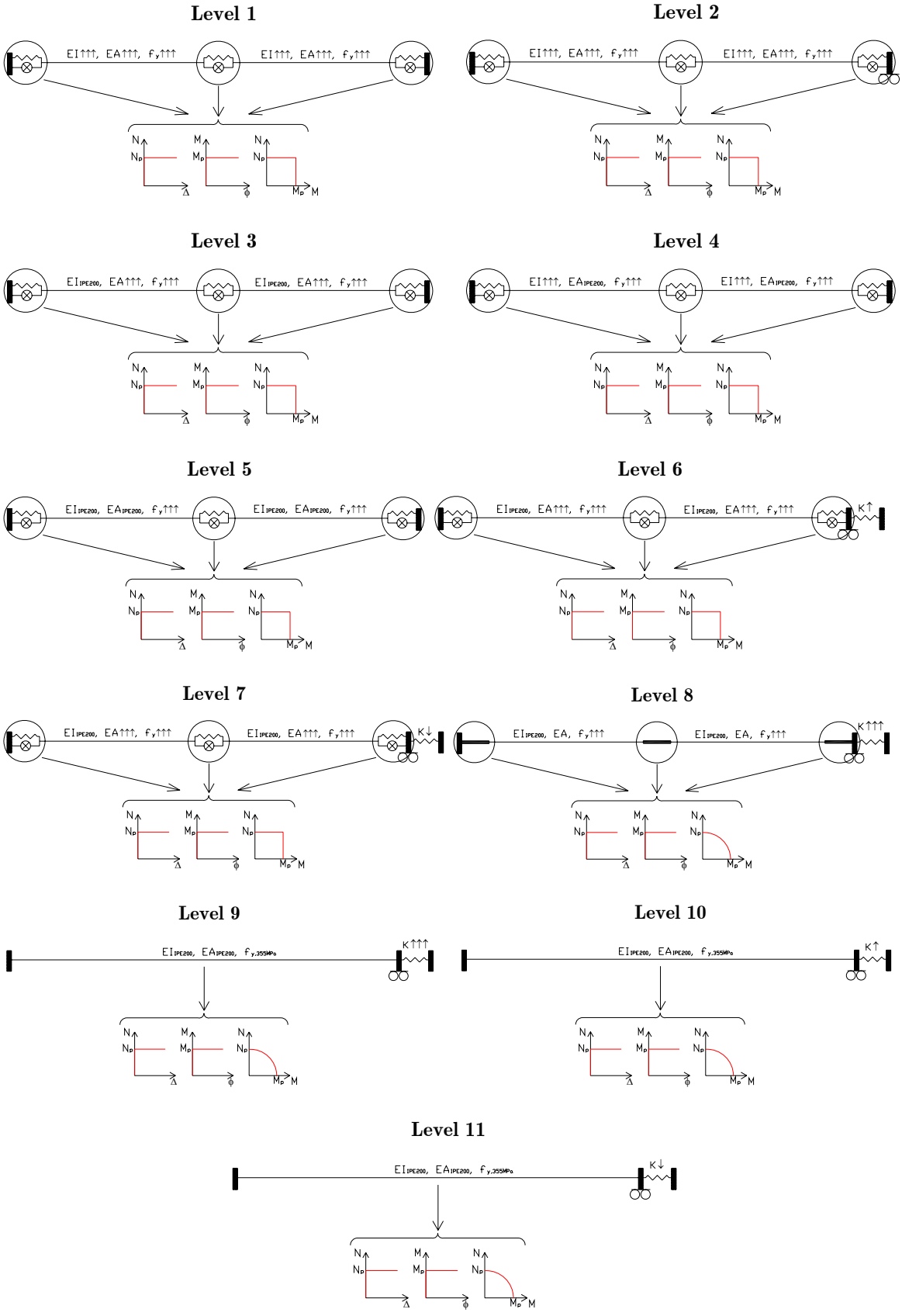

Figure III.90. The eleven levels of the first parametric study

Table III.5. Main properties of the studied levels

Level	L_{beams} [m]	EI	EA	$f_{y,beams}$ [MPa]	K [kN/m]	M-N interaction
Level 1	4	∞	∞	∞	∞	-
Level 2	4	∞	∞	∞	0	-
Level 3	4	IPE200	∞	∞	∞	-
Level 4	4	∞	IPE200	∞	∞	-
Level 5	4	IPE200	IPE200	∞	∞	-
Level 6	4	IPE200	∞	∞	900000	-
Level 7	4	IPE200	∞	∞	10	-
Level 8	4	IPE200	IPE200	∞	∞	IPE200_355Mpa
Level 9	4	IPE200	IPE200	355	∞	IPE200_355Mpa
Level 10	4	IPE200	IPE200	355	900000	IPE200_355Mpa
Level 11	4	IPE200	IPE200	355	10000	IPE200_355Mpa

Full non-linear 2-D numerical analyses are performed through the validated software FINELG (see *§ III.6.3*), with due account of geometrical and material non linearities. The beams are modelled by means of plane beam elements with three nodes as presented in *Figure II.44*. As a 2-D numerical analysis is performed, the out-of-plane buckling phenomena as lateral-torsional buckling are not taken into account in the computation.

In order to not restrict the development of the catenary action in the numerical modelling, the plastic strain limitations have been desactivated in the software. So, it is assumed that the different members of the simplified subsystem have an infinite ductility. In conclusion, the collapse of the subsystem is assumed to be achieved when the axial forces in the system reach the resistance F_{Rd} of the horizontal spring or the axial resistance of the beam $N_{pl,Rd}$. For level 9 to 11, the steel beams are assumed to have an elastic limit equal to 355 Mpa; in these cases, the steel material is modelled through an elastic-perfectly plastic law. In the other levels, the steel beams are assumed to be perfectly elastic ones.

A uniformly distributed load is applied and increased until collapse of the system (which corresponds to the achievement of the axial plastic resistance of the translational springs or of the beam ($N_{pl,Rd}$) in the present cases). Some of the obtained results for the additional parametrical studies are illustrated from *Figure III.91* to *Figure III.93*; more details are available in *[75]*.

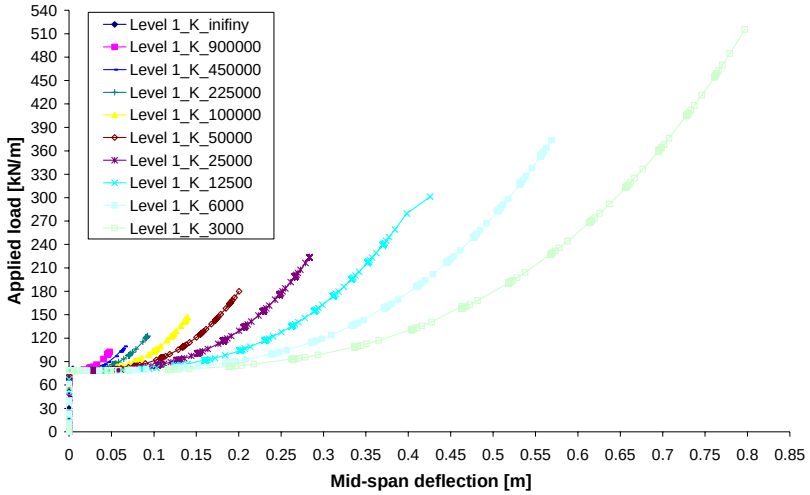

Figure III.91. Variation of K – Results for "Level 1" substructure – Mid-span deflection vs. applied load curve

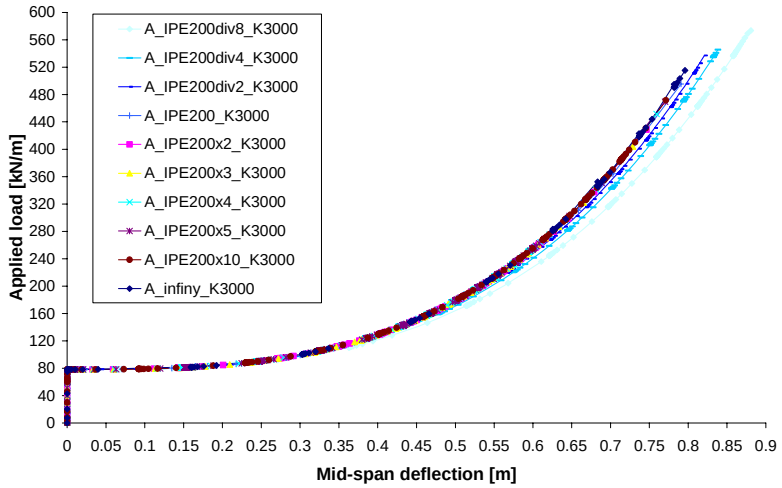

Figure III.92. Variation of A – Results for "Level 1" substructure with K = 3000kN/m – Mid-span deflection vs. applied load curve

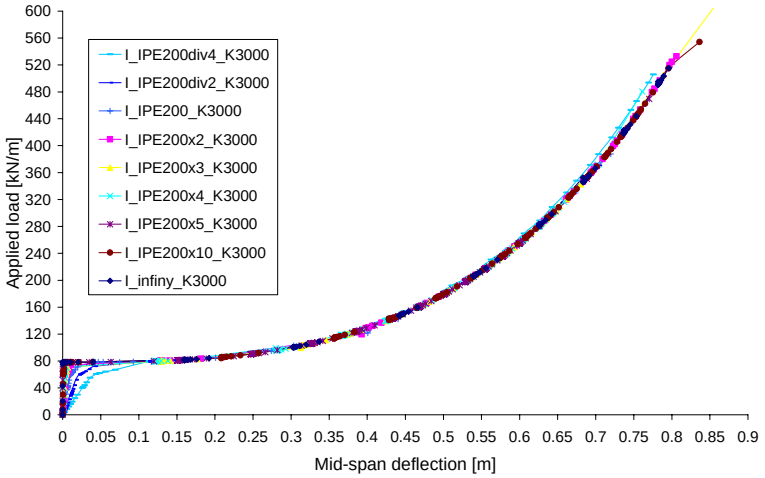

Figure III.93. Variation of I – Results for "Level 9" substructure with K = 3000kN/m – Mid-span deflection vs. applied load curve

The main conclusions drawn for the performed parametrical studies are summarised here below:

- The maximum applied load which can be reached depends of the value of K. It increases with decreasing values of K. The needs in term of ductility increase also when the K value is decreasing (see *Figure III.91*).
- The development of the catenary action depends on the relative values between the axial beam stiffness EA/L and the stiffness of the spring K. In practical situations, it has been shown in *[75]* that the influence of the axial beam stiffness may be neglected (see *Figure III.92*).
- The influence of the bending stiffness EI/L on the development of the catenary action may be neglected (see *Figure III.93*).
- The *M-N* interaction and the localised elongation at the plastic hinge level associated to the development of the catenary actions have a significant influence on the beam response and in particular, on the vertical displacement measured at mid-span of the simplified substructure.

III.8.2.3. Conclusion

Through the performed parametrical studies summarised in the present section, the parameters to be considered in the analytical model to predict the simplified substructure response have been identified. These parameters are:

- the lateral restraint K simulated by the horizontal spring with a stiffness "K";
- the *M-N* interaction at the plastic hinge level (developing in the beams or in the partial-strength joints);
- the elongation of the plastic hinges associated to the development of the catenary action.

On the other side, it has been demonstrated that it is not requested to take into account of the bending stiffness "EI/L" and the axial stiffness "EA/L" of the beams to predict with a good accuracy the development of the catenary actions (i.e. Phase 3 of the curve presented in *Figure III.7*) under investigation within the present part of the thesis.

In the next section, the analytical method (including the parameters identified within the present section) devoted to the prediction of the development of the catenary actions within the simplified substructure and their influence on the response of the latter is developed.

III.8.3. Development of an analytical method

III.8.3.1. Introduction

The objective of this section is to develop an analytical method to predict the development of the catenary action in the substructure model and to establish the link between the applied concentrated load Q and the vertical displacement at the application point of the load.

As the objective is to predict the behaviour in the post-plastic domain, i.e. after the formation of the beam plastic mechanism in the system, the analytical model is based on a rigid-plastic analysis. Also, as the deformations of the substructure are significant and influence its response, a second-order analysis is conducted.

The substructure to be investigated is reminded in *Figure III.94* with the definition of some parameters:

- p is the (constant) uniformly distributed load applied on the storey modelled by the simplified substructure;
- Q is the concentrated load associated to the column loss (see *Formula (3.1)* in *§ III.3.3*);
- L is the total initial length of the simplified substructure;
- Δ_A is the vertical displacement at the load application point;
- δ_K is the deformation of the horizontal spring simulating the lateral restraint coming from the indirectly affected part;
- δ_{N1} and δ_{N2} are the plastic elongations at each plastic hinges, i.e. the plastic elongation of a section or a joint when a plastic hinge is formed;
- θ is the rotation at the plastic hinges formed at the beam extremities.

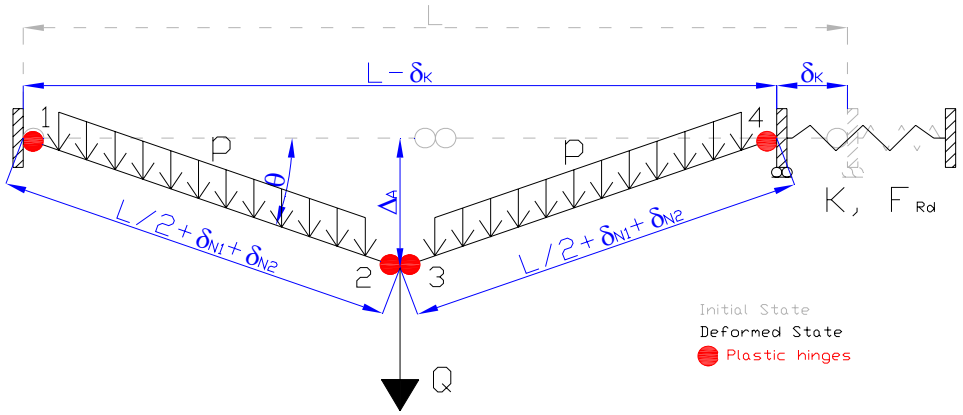

Figure III.94. Substructure to be investigated and definition of the main parameters

In *Figure III.94*, it can be observed that the concentrated load Q associated to the column loss is assumed to be applied at the middle of the simplified substructure, i.e. it is assumed that the beam spans each side of the loss column are equals. However, the theory developed in the following sections can be easily extended to situations where these spans are not equal.

In addition, it is assumed that the two plastic hinges 1 and 4 and the two plastic hinges 2 and 3 (see *Figure III.94*) have respectively the same resistance interaction curves (noted as couples of resistance (N_{Rd1}, M_{Rd1}) for the hinges 1 and 4 and (N_{Rd2}, M_{Rd2}) for the hinges 2 and 3). However, it is assumed that the shear forces do not affect the resistance of the plastic hinges, i.e. the shear forces, axial loads and bending moments interaction is not considered in the developed analytical method.

To find the link between the concentrated applied load Q and the vertical displacement Δ_A, different equations from the static and cinematic theories are used; they are detailed in *Appendix VI.8*. The so-obtained method is summarised in the next section.

III.8.3.2. Developed analytical method

In *Appendix VI.8*, two analytical models are presented:

- one with account of the uniformly distributed load p (*Appendix VI.8.2*) and;
- one without account of the uniformly distributed load p (*Appendix VI.8.3*).

The model which is presented herein is the second one, i.e. without account of the uniformly distributed load p; indeed, the formulas included in this model are more simple than the ones included in the first model and, in addition, it will be shown in *§ III.8.3.3* that the results obtained with the two models are exactly the same.

The substructure to be considered for the second analytical model is presented in *Figure VI.37* in *Appendix VI.8.3*. Through the development presented in the latter, two expressions are proposed i) for the evolution of the membrane forces ($N_{Rd} = N_{Rd1} = N_{Rd2}$ – see *Appendix VI.8.3*) developing in the substructure according to the variables Q and θ and ii) for the evolution of Q according to the variables N_{Rd}, M_{Rd1}, M_{Rd2} and θ (the other parameters are constant values):

$$N_{Rd} = \frac{K_N.(Sec(\theta).(2.K.L + Q.Tan(\theta)) - 2.K.L)}{8.K + 2.K_N.Sec^2(\theta)} \tag{3.6}$$

$$Q = Cos^2(\theta).[N_{Rd}.CoSec(\theta) - K.L.CoTan(\theta) + \frac{CoTan(\theta).\sqrt{Sec^4(\theta).(2.K^2.L^2 + N_{Rd}^2 - 4.K.L.N_{Rd}.Cos(\theta) + N_{Rd}^2.Cos(2\theta) + 8.K.M_{Rd1}.Sin(2\theta) + 8.K.M_{Rd2}.Sin(2\theta)}}{\sqrt{2}} - K.L.Tan(\theta) + 2.N_{Rd}.Sec(\theta).Tan(\theta)] \tag{3.7}$$

In *Formula (3.6)*, the parameter K_N is defined through *Formula (6.19)* in *Appendix VI.8.3* reminded here below (*Formula (3.8)*) and is an average value of the plastic elongation stiffnesses K_{N1} and K_{N2} linking the plastic elongations δ_{N1} and δ_{N2} at the plastic hinge level and the applied axial load N_{Rd} (as illustrated later on in *Figure III.96*).

$$K_N = \frac{2.K_{N1}.K_{N2}}{K_{N1} + K_{N2}} \tag{3.8}$$

Within *Formula (3.7)*, M_{Rd1} and M_{Rd2} can be expressed as functions of N_{Rd} as the bending resistances at the plastic hinge level and the membrane force N_{Rd} are linked through the *M-N* interaction resistance curves (of the beams or of the joints). So, Q can be expressed as a function of N_{Rd} and θ and, replacing N_{Rd} by its expression given in *Formula (3.6)* and by isolating Q from the so-obtained expression, as a function of θ only.

In addition, the link between Δ_A and θ can be expressed through the following formula (founded on *Formula (6.1)*, *Formula (6.17)* and *Formula (6.18)* of *Appendix VI.8*)

$$\Delta_A = (\frac{L}{2} + 2.\delta_N).Sin(\theta) = (\frac{L}{2} + 2.\frac{N_{Rd}}{K_N}).Sin(\theta) \tag{3.9}$$

In conclusion, a $Q - \Delta_A$ curve can be derived as illustrated in *Figure III.95*.

In the general concept presented in *§ III.3*, it was shown that the objective is to determine a link between the axial load in the loss column N_{lo} and the vertical displacement Δ_A (see *Figure III.95*). With the proposed analytical model, it is possible to derive this link during Phase 3 (i.e. when a plastic mechanism is formed in the directly affected part).

Indeed, through the theory developed in *[63]*, the vertical displacement Δ_A and the axial loads N_{lo} and N_{up} are known at the beginning of Phase 3 (i.e. Point (4) in *Figure III.95*); the latter are respectively called $\Delta_{A,(4)}$, $N_{lo,(4)}$ and $N_{up,(4)}$. So, the starting point of Phase 3 on the curve obtained through the theory developed herein is point "A" as illustrated in *Figure III.95*.

Also, as mentioned in *§ III.3.3*, it is demonstrated in *[63]* that N_{up} can be assumed as constant when the plastic mechanism is formed in the directly affected part and is equal to its value at point (4) of *Figure III.7*. Accordingly, from *Formula (3.1)*:

$$Q = N_{lo} - N_{up,(4)} \tag{3.10}$$

So, according to *Formula (3.10)*, the evolution of Q according to Δ_A from point "A" to point "B" of *Figure III.95* represents the evolution of N_{lo} according to Δ_A during Phase 3 (from $N_{lo,(4)}$ to 0) as illustrated in *Figure III.95*. In particular, it is possible to find the value of $\Delta_{A,(5)}$ corresponding to the complete column loss, i.e. when N_{lo} is equal to 0, as

illustrated by the arrows in *Figure III.95* and, accordingly, the requested deformation capacity at the plastic hinges level. Also, it is possible to check if the membrane forces within the beams are smaller than the beam or joint axial resistances and if the load applied to the indirectly affected part (see *Figure III.5*) which is equal to $N_{Rd}.Cos(\theta)$ is smaller than its resistance F_{Rd}.

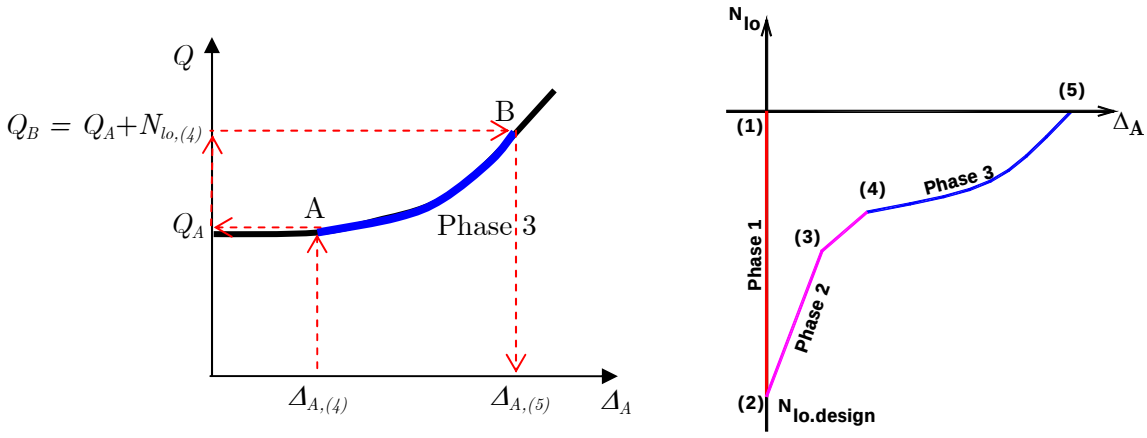

Developed analytical method — General concept

Figure III.95. From the developed theory to the general concept

These expressions are valid for steel or steel-concrete composite structures and are easy to apply. The constant parameters such as K, L and K_N are properties of the investigated structure. As mentioned previously, an analytical procedure to compute the lateral restraint K is available in *[63]* (see *§ III.7.3.2*). However, as mentioned in *§ III.5.4*, no analytical procedure is available to determine the link between the axial load N_{Rd} and its associated elongation δ_N (i.e. to compute K_{N1} or K_{N2}) for a joint subjected to combined bending moments and axial loads; also, if the plastic hinges form in the beams, an analytical procedure is not either available to predict this value. Additional investigations are requested on this topic not covered within the present thesis. This point will be addressed in the perspectives presented in *§ IV.2*.

The developed analytical method is validated in the next paragraph through comparisons to the experimental substructure test results.

III.8.3.3. Validation through comparisons to the substructure experimental test results

Within this section, the analytical models developed in *Appendix VI.8* are used to predict the response of the substructure tested at Liège University (see *§ III.4*).

The properties requested to define the simplified substructure model are the ones measured at the laboratory (see *§ III.4.4.2* and *§ III.4.4.3*).

As mentioned previously, the beam-to-column joints of the tested substructure are partial-strength ones which means that the plastic hinges formed at the joint level during the test. Accordingly, the *M-N* resistance interaction curves used to define the properties of the plastic hinges are the ones obtained through the experimental tests performed in isolation on the substructure joint configuration at Stuttgart University (see *§ III.5.2*).

In addition, the values of K_{N1} and K_{N2} are defined through the experimental test results as illustrated in *Figure III.96* here below representing the horizontal deformations of the joints according the applied axial load during TEST 1 (subjected to hogging moments) and TEST 4 (subjected to sagging moments). In fact, the results from TEST 1 and TEST 4 are chosen because the loading sequence followed during these tests is closer to how the joints were loaded during the substructure test than for the other tests performed in Stuttgart (i.e. TEST 2, 3 and 5); indeed, as mentioned in *§ III.5.2.1*, TEST 1 and 4 were performed to estimate the ultimate bending moments and after reaching these values of moments, a tensile load was applied while, for the other tests, the tensile load was applied before reaching the maximum bending moment. This difference of loading sequence does not influence the obtained *M-N* resistance curve (for a tensile load smaller than 400 kN – see *Figure III.64*) but influences the shape of horizontal deformation vs. horizontal load curves (see *Figure III.66* and *Figure III.69*).

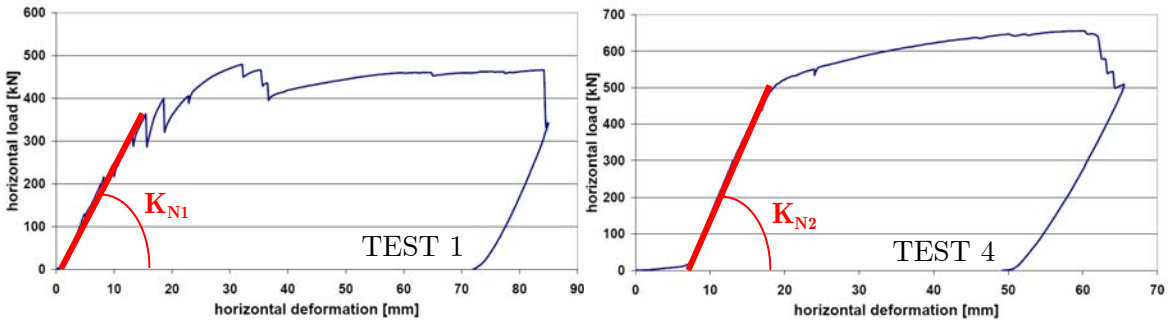

Figure III.96. Axial deformations of the joint measured during TEST 1 and 4

It can be observed that the values of K_{N1} and K_{N2} are only valid for tensile loads smaller than 375 kN and 500 kN respectively; however, the tensile loads which appeared during the substructure test were smaller than these values. The so-obtained values of K_{N1} and K_{N2} are respectively 25152 kN/m and 43478 kN/m.

Another parameter which is requested is the value of K characterising the lateral restrained of the indirectly affected part. Within the tested substructure, the indirectly affected part is identified in *Figure III.97* (one indirectly affected part each side of the substructure). The value of K has been determined numerically by modelling the indirectly affected part and applying a horizontal load as illustrated in *Figure III.97*. The so-obtained value of K is equal to 4280 kN/m.

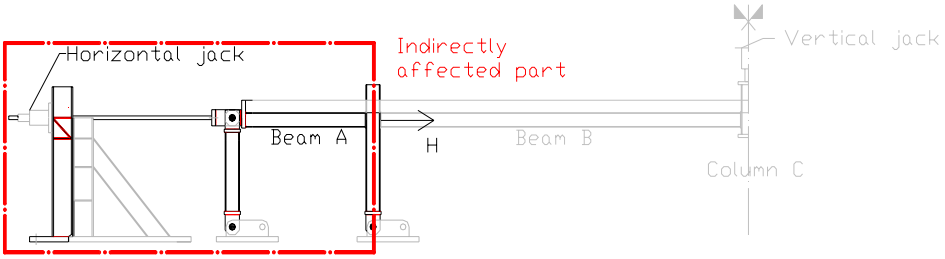

Figure III.97. Indirectly affected part of the substructure

The predictions obtained through the two analytical models (i.e. with and without the uniformly distributed load (including the self-weight of the beams and the weight of the concrete blocks and steel plates) – see *§ III.4.4.4*) are compared to the experimental test result in *Figure III.98*. In this figure, it can be seen that, as previously announced, the predictions obtained through the two analytical models are exactly the same and that these predictions are in very good agreement with the experimental result, what validates the developed analytical models.

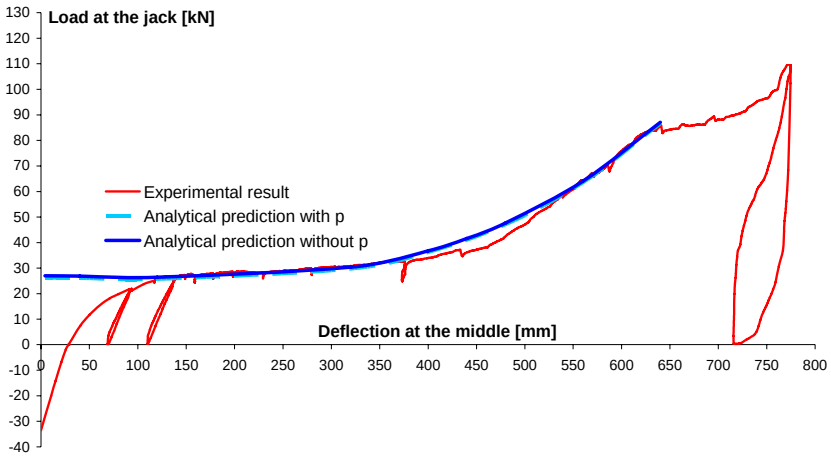

Figure III.98. Comparison between the analytical predictions and the experimental result

III.8.4. Conclusions

The present paragraph is dedicated to the presentation of the developed analytical method to predict the development of the membrane forces within a structure further to a column loss and their influence on the structure response.

Parametrical studies have been first conducted to identify the parameters influencing the response of the simplified substructure and which have to be considered within the developed analytical method. In particular, the influence of key parameters such as the lateral restraint K and the axial and bending stiffness of the beams has been investigated with more details.

Then, two analytical models, including the so-identified parameters, have been developed: one taking into account of the uniformly distributed load applied on the substructure and

one without account of this load, what leads to significant simplifications in the formulas to be considered.

The proposed analytical models have been finally validated through comparisons to the experimental result obtained for the substructure test; it has been illustrated that the predictions obtained through the two models are identical and that they are in good agreement with the experimental results.

With the so-validated analytical models, it is possible to predict the requested deformation capacity at the plastic hinge level at the end of the column loss and the loads to be supported by the indirectly affected part.

III.9. Part III conclusions

The investigations presented within the present part of the thesis were devoted to the study of the behaviour of steel and steel-concrete composite building frames further to a column loss and in particular, to the study of the response of these frames when significant membrane effects developed within the structure. These investigations were founded on the knowledge gained from the investigations presented in *Part II* on the structural behaviour of steel and composite buildings. Some of the investigations presented herein are part of a European project titled "Robust structures by joint ductility" in which Liège University was deeply involved.

In *§ III.2*, a general overview of the state-of-the-art knowledge on buildings subjected to exceptional actions has been first proposed with a particular attention paid to the exceptional event "loss of a column in a building"; the proposed overview have mainly focused on important definitions, information available in the actual codes and standards and recent researches. In particular, topics for which additional researches are requested have been presented and a clear link with the developments presented within the thesis has been highlighted.

To investigate the response of a frame further to a column loss, a general concept has been developed at Liège University; the latter has been presented in *§ III.3*. Within this general concept, the frame is divided in two parts: the directly affected part gathering the beams, the columns and the joints just above the loss column and the indirectly affected part gathering the rest of the frame. Also, the response of the frame is divided in three phases:

- Phase 1 corresponding to the response of the frame subjected to "conventional" loading just before the column loss;

- Phase 2 corresponding to the elasto-plastic response of the frame when the column is progressively removed from the frame and;
- Phase 3 corresponding to the "fully" plastic response of the frame when the column is progressively removed, i.e. when a plastic mechanism is formed within the directly affected part.

The developments presented herein were mainly dedicated to the study of the response of a frame during Phase 3 with the objectives to validate a simplified substructure modelling able to simulate the behaviour of a frame during Phase 3 and to propose a simplified analytical method able to predict the response of this simplified substructure (the two first phases are the topics of a complementary PhD thesis to be presented in summer 2008 at Liège University by H.N.N. Luu *[63]*). To achieve these objectives, a strategy has been developed and presented in *§ III.3.3*. Within this strategy, experimental, numerical and analytical aspects have been considered as summarised here below.

Within the previously mentioned European project, an experimental test on a substructure simulating the loss of a column in a composite building has been performed at Liège University with the objective to observe the development of the membrane forces within the substructure and their effects on the beam-to-column joint response. This test, which is a European first, has been described in details in *§ III.4*. Within this paragraph, the "actual" building from which this substructure was extracted has been first presented. Then, a description of how the substructure was extracted from this building has been given; the extraction of the substructure was performed so as to ensure that the response of the substructure observed during the test would reflect as close as possible the global response of the actual building. Finally, the obtained experimental results have been described and analysed in details; in particular, it has been shown that significant membrane forces developed within the substructure during the test.

Then, the behaviour of joints subjected to combined bending moments and axial loads has been investigated in *§ III.5*, loading condition which can appear at the joint level when membrane forces develop within a structure. Within this paragraph, experimental and analytical investigations have been conducted. The experimental tests have been performed at Stuttgart University, in strong collaboration with Liège University, to determine the response in isolation of the substructure composite joint configuration subjected to combined bending moments and tensile loads; the obtained results have been first analysed in details. Then, an analytical method, initially developed to predict the response of steel joints subjected to combined bending moments and axial loads, has been extended to composite joints. The proposed analytical method has been finally validated through comparisons with experimental results of the tests performed at Stuttgart

University. The proposed method permits to predict accurately the *M-N* resistance interaction curve of a composite joint, property which has to be known to be able to predict the response of a structure with partial-strength composite joints.

To validate the simplified substructure modelling and to develop the simplified analytical method, numerical investigations have been conducted with the homemade finite element software FINELG. The validity of the latter for the prediction of the response of a frame further to a column loss has been studied in *§ III.6*. In a first step, the numerical tool FINELG has been used to predict the response of the substructure tested at Liège University and the prediction has been compared to the experimental results. Through this study, the difficulty to model accurately the actual behaviour of beam-to-column joints subjected to combined bending moments and axial loads has been highlighted. In particular, the numerical predictions are not satisfactory when significant second order effects develop within the structure. Additional researches are requested on this topic; this point will be addressed in the perspective in *§ IV.2*. In a second step, a benchmark study has been conducted between the partners involved in the numerical investigations within the previously mentioned European project. This benchmark study has been performed on a steel structure with fully rigid and full strength joints and the loss of a column within this structure has been simulated. The responses obtained through different finite element software were in good agreement; in particular, the use of FINELG to predict the response of steel frames further to the loss of a column has been validated through this benchmark study.

With the so-validated numerical software FINELG, the simplified substructure modelling on which the developed analytical methods is founded has been validated through numerical investigations; through the validation, it has been illustrated that the proposed simplified substructure is able to simulate the global response of the directly affected part of the frame with a very good accuracy when the plastic mechanism is formed in the latter (i.e. during Phase 3). In addition, to define this simplified substructure, properties from the indirectly affected part are requested; so, the methods to predict the latter (developed in *[63]*) has been briefly described in this paragraph.

Finally, the developed analytical method to predict the development of the membrane forces within a structure further to a column loss and their influence on the structure response has been presented in *§ III.8*. Parametrical studies have been first conducted to identify the parameters influencing the response of the simplified substructure and which has to be considered within the analytical method. Then, two analytical models have been developed: one considering the uniformly distributed load applied on the substructure and one without account of this load. In *Appendix VI.8*, it has been illustrated that neglecting

the uniformly distributed load leads to significant simplifications in the formulas to be considered within the analytical model. The proposed analytical models have been finally validated through comparisons to the experimental result obtained for the substructure test; it has been illustrated that the predictions obtained through the two models are identical and that they are in very good agreement with the experimental results.

So, as a conclusion, the uniformly distributed load applied on the substructure model can be neglected; the so-obtained analytical model is very easy to apply and is able to predict the requested deformation capacity at the plastic hinge level at the end of the column loss and the loads to be supported by the indirectly affected part. However, within this method, a parameter linking the elongation of the plastic hinges and the applied tensile load has to be defined, what is not yet possible through analytical methods. This point will be addressed in the perspective presented in *§ IV.2*.

As mentioned previously, the presented developments are part of a general concept defined at Liège University. To obtain the complete response of the structure, the result obtained through the presented analytical model has to be linked to the responses obtained during Phase 1 and 2 investigated in *[63]*, investigations which are still in progress at the time of redaction the present thesis. An example of prediction of the complete response (i.e. from Phase 1 to Phase 3) of a steel frame will be given in *[63]* to be presented in summer 2008.

All the developments presented herein are founded on static approach, i.e. the dynamic effects which could be associated to a column loss have been neglected. As mentioned in *§ III.2*, a pseudo-static approach has been developed at the Imperial College of London to estimate the effect of the dynamic effect from the static response of a frame. Combining the theory developed herein and the one developed at the Imperial College, it would be possible to predict the response of a frame further to a column loss with account of the dynamic effects. This point is addressed later on in the perspective presented in *§ IV.2*.

IV. General conclusions, perspectives and personal contributions

IV.1. General conclusions

In the last decade, the Argenco department from Liège University had the opportunity to participate to European projects dedicated to the investigation of the behaviour of steel and steel-concrete composite building frames. As part of these projects, two main research topics were covered at Liège University:

- the behaviour of steel-concrete composite sway building frames subjected to significant second-order effects under "conventional" loading and;
- the behaviour of steel and steel-concrete building frames subjected to an exceptional event leading to the loss of a column.

The developments presented within the present thesis are directly linked to these topics. Two main objectives have been achieved through these developments:

- a simplified analytical method to predict the ultimate load factor of steel and steel-concrete composite sway frames was first developed and validated in *Part II* and;
- founded on the knowledge gained from *Part II* on the structural behaviour of steel and composite frames, a simplified analytical method to predict the development of the membrane effects within a structure further to a column loss and their effects on the structural response was proposed and validated in *Part III*.

To achieve these objectives, experimental, numerical and analytical investigations included in global strategies defined for each topic were conducted with a particular attention paid to the joint behaviour.

The conclusions relative to these two investigated topics were already detailed in *§ II.7* and *§ III.9*. Accordingly, the present paragraph only summarises the main accomplishments of the thesis within these topics. Some perspective and the personal contributions are described later on in *§ IV.2* and *§ IV.3* respectively.

IV.1.1. Main achievements related to the behaviour of composite sway frames subjected to "conventional" loading

Prediction of the response of composite joints subjected to bending moments:

The behaviour of composite sway frames is widely influenced by the response of the composite joints subjected to hogging and eventually to sagging bending moments. So, in a first section, the behaviour of these joints has been investigated through experimental

and analytical studies. In a first part, experimental tests (performed within the previously mentioned European projects) on double-sided and single-sided composite joints subjected to sagging and hogging bending moments have been presented and analysed. In particular, a new collapse mode for single-sided composite joints subjected to hogging bending moment was identified and new formulas to predict the appearance of the latter were proposed and validated. Also, as the analytical method actually proposed in the Eurocodes does not cover the behaviour of composite joints subjected to sagging bending moments, an analytical procedure was developed and validated through comparisons with experimental results. With the presented investigations, it can be concluded that analytical tools to predict the behaviour of composite joints subjected to bending moments (sagging or hogging ones) are now available and sufficiently accurate; in particular, these tools can be used to characterise the joints to be considered within the numerical and analytical computations of composite sway frames.

Validation of the homemade finite element software FINELG to predict the response of composite sway frames:

Within the thesis, numerical investigations were conducted to predict the response of composite sway frames. The numerical tool which was used is the homemade finite element software FINELG; the use of the latter was validated through two main studies:

- The first one was a benchmark study performed amongst European institutes and coordinated by Liège University. The building used for this benchmark was tested at the Building Research Establishment in UK and the results numerically predicted by the institutes involved in the benchmark study were compared to the experimental results.
- The second one was a comparison to experimental results. The experimental test was performed on a composite sway frame at Bochum University. The design of the tested frame was performed in strong collaboration with Liège University.

From these studies, it was concluded that the homemade finite element software FINELG can be used with good confidence to predict the response of composite sway frames.

Validation of the applicability of the Amplified Sway Moment method to composite sway frames:

Through preliminary numerical investigations performed on actual building frames and summarised within the thesis, it was illustrated that composite sway frames exhibit a similar behaviour to steel sway frames. So, it was decided to investigate the applicability of simplified analytical methods, initially developed for steel sway frames, to composite sway frames. In particular, the applicability of the elastic method named “Amplified Sway

Moment Method" (ASMM) and proposed in Eurocode 3 was investigated. It was shown that the applicability of this method can be extended to composite sway frames with good confidence; indeed, for all the studied actual composite frames, the predicted values of the elastic load factor through the ASMM were in good agreement with the numerically predicted ones obtained through fully non-linear analyses (obtained through the previously validated software FINELG and considered as the "reference" results), even if the critical load factor used in this method is computed through a simplified method recommended in Eurocode 3 and 4.

Development of a simplified analytical method to predict the ultimate load factor of steel and composite sway frames:

Within the thesis, the applicability of the plastic method named "Merchant-Rankine approach" (MR) was studied. It was demonstrated through this study that this approach exhibits the same level of accuracy than for steel sway frames, i.e. safe for beam plastic mechanisms, adequate for combined plastic mechanisms and unsafe for panel plastic mechanisms. As the investigated plastic method did not give satisfactory results, it was decided to develop a new method founded on Ayrton-Perry formulation able to predict the ultimate load factor of steel and composite sway frames.

To develop this new method, it was necessary to calibrate a coefficient (named μ in the thesis) influencing the values obtained through the Ayrton-Perry formulation. In the present case, three values of μ, one associated to the beam plastic mechanism, one associated to the combined one and one associated to the panel one, were calibrated. This calibration was performed through parametrical studies performed i) on steel frames and ii) on composite frames; the so-obtained values of μ are different if steel frames or composite frames are considered.

Through the parametrical studies, it was shown that the developed method, which is easy to apply, gives accurate predictions of the ultimate load factors, practically always on the safe side and in good agreement with the numerical results, what was not the case with the MR approach. It was also demonstrated that the developed method is able to predict the plastic mechanism associated to the ultimate load factor. Another interesting conclusion is the fact that the new method could be extended to more situations than the ones covered by the MR approach; indeed, the MR approach is limited to structure with a ratio between the minimum plastic load factor and the critical load factor belonging to the interval 0,1 – 0,25 while the developed method continues to produce satisfactory results for structures with a ratio higher than 0,25.

IV.1.2. Main achievements related to the development of membrane effects in structural steel or composite beams further to a column loss

Experimental test on a substructure simulating the loss of a column in a composite frame:

Within the European project "Robustness", an experimental test on a substructure simulating the loss of a column in a composite building was performed at Liège University with the objective to observe the development of the membrane forces within the substructure and their effects on the beam-to-column joint response.

The obtained experimental results were presented and analysed in details within the thesis. In particular, from the presented results, it was illustrated that the test objectives were achieved.

Development of an analytical method to predict the composite joint response subjected to combined bending moments and axial loads:

When the membrane forces develop within a structure, the beam-to-column joints initially loaded by pure bending moments are progressively subjected to combined bending moments and axial loads. The behaviour of joints subjected to such loading was investigated herein. Experimental and analytical investigations were conducted. The experimental joint tests in isolation were performed at Stuttgart University (within the European project "Robustness"), in strong collaboration with Liège University, to determine the response in isolation of the substructure composite joint configuration subjected to combined bending moments and tensile loads; the obtained results were analysed in details within the thesis. Then, an analytical method, initially developed to predict the response of steel joints subjected to combined bending moments and axial loads, was extended to composite joints. The proposed analytical method was finally validated through comparisons to the experimental results of the tests performed at Stuttgart University.

The developed method permits to predict with a good accuracy the *M-N* resistance interaction curve of a composite joint, property which has to be known to predict the response of a structure with partial-strength composite joints when significant membrane forces appear.

Validation of the homemade finite element software FINELG for the prediction of the response of a frame further to a column loss:

To develop the simplified analytical method, numerical investigations were conducted with the homemade finite element software FINELG. Accordingly, the validity of the latter for the prediction of the response of a frame further to a column loss was studied.

Firstly, the numerical tool FINELG was used to predict the response of the substructure tested at Liège University and the prediction was compared to the experimental results. Through this study, it was shown that the numerical prediction is not in good agreement with the experimental results. This unsatisfactory result is associated to the difficulty to model accurately the actual behaviour of beam-to-column joints subjected to combined bending moments and axial loads.

Secondly, a benchmark study was conducted between the partners involved in the numerical investigations within the previously mentioned European project. This benchmark study was performed on a steel structure with fully rigid and partial strength joints and the loss of a column within this structure was simulated. Through this study, the use of FINELG to predict the response of such frames further to a column loss was validated.

Development of a simplified analytical method to predict the development of the membrane forces within a structure and their effects on the frame response:

Within the thesis, a simplified substructure modelling able to simulate the global response of a frame when significant membrane forces developed in the structure was first defined and validated through numerical investigations.

The developed simplified analytical method is founded on this simplified substructure modelling. Parametrical studies were conducted to determine the parameters influencing the response of the substructure and to be considered within the analytical model. Then, the analytical method was developed and presented in details. Finally, the proposed method was validated through comparisons to the experimental result obtained through the substructure test; it was illustrated that the prediction obtained through the analytical method are in very good agreement with the experimental results.

The so-obtained analytical method is very easy to apply and is able to predict the requested deformation capacity at the plastic hinge level at the end of the column loss and the loads to be supported by the rest of the structure not directly affected by the column loss.

IV.2. Perspectives

Through the performed developments to meet the objectives of the thesis, some requests of additional researches on different topics have been identified leading to some perspectives of the present work; the latter are listed here below:

- Experimental and analytical investigations on the behaviour of beam-to-column joints have been presented within the thesis. These investigations were mainly dedicated to the characterisation of the joints in terms of resistance and stiffness. An important joint property which has also to be considered is its ductility and in particular, its deformation capacity. Indeed, when performing plastic analysis or when looking the behaviour of a structure further to the loss of a column, a post-limit ductility can be requested at the joint level if the latter is partially resistant.

  However, no methods are proposed in the codes to predict this rotation capacity. Since some years, a step-by-step method is under development through diploma works at Liège University (*[76]* and *[77]*) to predict the rotation capacity of joints subjected to bending moments. In future, the proposed method needs to be improved and further developments are requested; in particular, this method should be extended to predict the deformation capacity of joints subjected to combined bending moments and axial loads. Another diploma work is actually under way on this topic at Liège University.

- Through the experimental tests performed on the beam-to-column joints, it has been put into sight that a loss of resistance associated to a lack of ductility of the concrete is observed in some cases. This phenomenon is not yet taken into account in the analytical methods to predict the response of the joints; additional investigations should be initiated to characterise this phenomenon and to propose analytical formulas to predict this type of collapse.

- Through the preformed investigations on the joints, a phenomenon have been highlighted which is the development of membrane forces within joint components subjected to bending (mainly, the column flange and the end-plate); this phenomenon is illustrated in *Figure II.38*.

  A clear link between the behaviour of the simplified substructure investigated in *§ III.8.3* and the behaviour of the component in bending can be established. Indeed, the physic of their behaviour is the same if:

- the "concentrated" plastic hinges of the simplified substructure are replaced by plastic hinge lines developing in the plates and;
- the horizontal spring, defined in the simplified substructure to simulate the lateral restraint coming from the indirectly affected part, simulates the behaviour of the bolts in shear when considering the behaviour of the joint components in bending.

It is intended, in a near future, to adapt the formulas developed to predict the development of the membrane forces within the simplified substructure to the situation met with the joint components in bending; the objective is to be able to predict with a better accuracy the post-elastic behaviour of a joint, with account of the membrane forces.

- A last perspective related to the behaviour of the joints concerns the prediction of the axial stiffness of the joint when moving on the M-N interaction resistance curve. Indeed, a link between the axial loads applied at the plastic hinge level of the simplified substructure and the elongation of these plastic hinges has to be established to apply the analytical method to predict the development of the membrane forces. What is actually available in the literature (and in particular in *[61]*) is a method to predict the axial stiffness of joints in the elastic range; what is requested here is the value of this stiffness in the post-elastic range, and in particular when the joints have already reached their plastic bending resistance. The same link has also to be characterised when the plastic hinges form in steel or composite beams. For this situation, methods to predict this property are not either available in the literature. So, investigations should also be performed to determine the axial stiffness of plastic hinges formed in steel or composite beams.

- When performing the parametrical study on the composite sway frames to develop the simplified analytical method based on the Ayrton-Perry formulation (see *§ II.6.3*), it was mentioned that problems were met with the deformation capacity of the concrete. Indeed, even if the cross sections of a composite sway frame can be considered as Class 1 cross sections according to the recommendations given in Eurocode 4 *[6]*, it has been highlighted, through preliminary investigations that the ductility of the concrete, as defined in Eurocode 2 *[33]*, is sometimes not sufficient to allow the development of a full plastic mechanism within the frame.

  More investigations on this topic should be performed. An idea would be to introduce an additional criterion relative to the ductility of the concrete when considering the classification of composite cross sections.

- The validation of the analytical method developed to predict the response of steel and composite sway frame have been performed through comparisons with numerical results obtained for "academic" structures. It would be interesting to apply the developed method to actual buildings to see if the very good accuracy of the method is kept for such buildings.

  Also, the method has been applied with accurate estimations of the critical load factor (obtained through the FE element software FINELG) and of the plastic load factors (account of the non-linear M-N interaction in the steel columns). The validity of the method should be also checked if these values are computed through simplified methods.

  A diploma work is actually under progress on these topics at Liège University.

- When validating the homemade FE element software FINELG for the prediction of the response of a structure further to the loss of a column, it has been put into sight that it is very difficult to introduce the joint behaviour in the numerical modelling, with account of its "*M-N*" behaviour (in terms of resistance and stiffness).

  A new finite element should be developed and introduced in FINELG, for instance a spring element with a coupling of the bending and axial stiffness and of the bending and axial resistances to reflect the behaviour of the beam-to-column joints. Prof. Luis Da Silva has already developed a general concept for this type of elements with also account of the shear forces applied to the joints *[78]*.

  The difficulties to develop such a finite element are numerical, because obtaining a good convergence with elements coupling different effects is complicated, and analytical, because analytical methods are requested to define the properties of such an element.

- As mentioned previously, the analytical method proposed to predict the response of the simplified substructure (*§ III.8.3*) simulating the response of a frame further to the loss of a column with account of the membrane forces is founded on a static approach.

  In *[57]*, a pseudo-static method is proposed to estimate the dynamic response of a structure further to the loss of a column from its static response (which is not accurately predicted in *[57]*).

It would be interesting to combine the developments of the present thesis, of [63] and of *[57]* and to validate the so-obtained global approach through comparisons to numerical results and experimental tests (if one day available).

In addition, to develop this method, it has been assumed that the shear forces at the plastic hinges do not influence their resistance. Through additional studies, the validity of this assumption should be investigated and solutions should be proposed to take into account of the effects of the shear forces if requested.

IV.3. Personal contributions

As mentioned in *§ I.2*, the personal contributions have not been directly indicated within the text of the thesis in order not to make the lecture unwieldy. However, it is important within a PhD thesis to put into sight these personal contributions. Accordingly, the main personal contributions to the presented investigations are listed here below:

- Realisation of experimental tests on beam-to-column composite joints within the "sway frames" European project (design, drawings and interpretation of the experimental results) (*§ II.3.2.2*);
- Identification of a new collapse mode through the performed experimental tests on the single-sided composite joints when subjected to hogging moments and development and validation of an analytical formula to predict the resistance associated to this new collapse mode (*§ II.3.3.3*);
- Development and validation of formulas to predict the resistance and the stiffness of a new joint component ("concrete slab in compression") activated in composite joints subjected to sagging moments (*§ II.3.3.4*);
- Validation of the homemade FE software FINELG for the investigation of the behaviour of composite sway frames and coordination of a benchmark study within the "sway frames" European project (*§ II.4*);
- Contribution to the design of the composite sway frame and of its structural beam-to-column joints tested at Bochum University (Germany) within the "sway frames" European project (*§ II.4.5*);
- Numerical and analytical investigations of the behaviour of actual composite sway buildings (*§ II.5*);
- Development and validation of a new simplified analytical method, based on the Ayrton-Perry formulation, to predict the response of steel and composite sway frames (*§ II.6*);

- Development of a pre-processor to generate FINELG datafiles for composite frames (*§ II.6.3*);
- Carrying out of parametrical numerical studies on steel and composite sway frames (*§ II.6.2* and *§ II.6.3*);
- Contribution to the development of a general concept for the prediction of the response of a steel or composite frame further to the loss of a column (*§ III.3*);
- Realisation of an experimental test on a substructure simulating the loss of a column in a composite structure (design, drawings and interpretation of the results) within the "Robustness" European project (*§ III.4*);
- Contribution to the interpretation of the results of experimental tests performed in isolation at Stuttgart University on the substructure joint configuration subjected to combined bending moments and tensile loads (*§ III.5.2*);
- Extension and validation of an analytical procedure to predict the behaviour of composite joints subjected to combined bending moments and axial loads (*§ III.5.3*);
- Validation of the homemade FE software FINELG for the prediction of the response of steel frames with fully rigid and partial strength joints further to the loss of a column (*§ III.6*);
- Validation of the "simplified substructure approach" to predict the response of a frame further to the loss of a column *(§ III.7.2*);
- Carrying out of parametrical numerical studies to identify the parameters influencing the response of the simplified substructure model (*§ III.8.2*);
- Development and validation of a simplified analytical method able to predict the development of the catenary action within a structure further to a column loss and their influence on the structure response (*§ III.8.3* and *§ III.8.3.3*).

V. References

[1] D. Bitar, Y. Ryan, S. Caramelli, W. Salvatore, F. Taucer, J.P. Jaspart, J.F. Demonceau, M. Haller, J. Grijalvo, F.J. Heise, R. Kindmann, M. Kraus, B. Hoffmeister, M. Oppe and H. Stangenberg. Applicability of composite structures to sway frames. Final report, Report EUR 212913 EN, Science Research Development, European Commission, 2006.

[2] O.S. Bursi, S. Caramelli, G. Fabbrocino, J. Molina, W. Salvatore, F. Taucer & R. Zandonini. 3-D full-scale seismic testing of a steel-concrete composite building at ELSA. European commission, Directorate-General, Joint Research Center, EUR 21299 EN, 2004.

[3] Trento University. Prefabricated composite beam-to-concrete filled tube or partially reinforced-concrete reinforced-concrete-encased column connections for severe seismic and fire loadings. Final report of the RFCS project N° RFS-CR-03034, 2008 (to be published).

[4] Stuttgart University. Robust structures by joint ductility. Final report of the RFCS project N° RFS-CR-04046, 2008 (to be published).

[5] EN 1998-1. Eurocode 8: Design of structures for earthquake resistance – Part 1: General rules, seismic actions and rules for buildings. European committee for standardization, December 2004.

[6] EN 1994-1-1. Eurocode 4: Design of composite steel and concrete structures – Part 1-1: General rules and rules for buildings. European committee for standardization, December 2004.

[7] R.P. Johnson. Composite structures of steel and concrete – beams, slabs, columns and frames for buildings. Blackwell publishing, ISBN 1-4051-0035-4, 2004.

[8] D.J. Oehlers & M.A. Bradford. Composite steel and concrete structural members – Fundamental behaviour. Pergamon, ISBN 0 08 0419194, 1995.

[9] R.P. Johnson and D. Anderson. Designers' handbook to Eurocode 4 – Part 1.1: Design of composite steel and concrete structures. Eurocode design handbooks, ISBN 0 7277 1690 5, 1993.

[10] J.F. Demonceau & J.P. Jaspart. Presentation and analysis of tests on single-sided steel and composite joint configurations performed at Liège University. Internal report for the ECSC project 7210-PR-250 "Applicability of composite structures to sway frames", Liège University, August 2003.

[11] J.F. Demonceau. Applicability of composite structures to sway frames. Diploma work (2003 – 2004), Liège University, M&S Department.

[12] EN 1993-1-1. Eurocode 3: Design of steel structures – Part 1-1: General rules and rules for buildings. European committee for standardization, May 2005.

[13] Structural Steelwork Eurocodes – Development of a Trans-national Approach (SSDTA). Lecture 5: frame classification and joint representation. Eurocode 3.

[14] Structural Steelwork Eurocodes – Development of a Trans-national Approach (SSDTA). Lecture 6: choice of analysis and implications for design. Eurocode 3.

[15] R. Maquoi & J.P. Jaspart. A simple approach for the design of steel and composite frames accounting for effective overall stability. Festschrift Prof. Richard Greiner, Graz University, Austria, October 2001.

[16] E. Pecquet. Contribution to the development of computation rules for steel-concrete sway composite buildings. Diploma work (2001 – 2002), Liège University, M&S Department (in French).

[17] J. S. Hensman. Investigation of the wind-moment method for unbraced composite frames. PhD thesis, Nottingham University (U.K.), January 1998.

[18] J.S. Hensman & D.A. Nethercot. Numerical study of unbraced composite frames: generation of data to validate the use of the wind moment method of design. Journal of Constructional Steel Research 57, pp. 791-809, 2001.

[19] U. Kuhlmann & L. Rölle. Experimental tests on composite joints with biaxial loading. Internal report for the RFCS project RFS-CR-04046 "Robust structures by joint ductility", Stuttgart University, 2007.

[20] J.F. Demonceau & J.P. Jaspart. Predesign of the substructure to be tested at the University of Liège. Internal report for the RFCS project RFS-CR-04046 "Robust structures by joint ductility", Liège University, January 2006.

[21] Trento University. Partially reinforced-concrete-encased column joints for severe seismic loadings: tests and main results. Internal report for the RFCS project RFS-CR-03034 "Prefabricated composite beam-to-column filled tube or partially reinforced-concrete-encased column connections for severe seismic and fire loadings", March 2006.

[22] EN 1993-1-8. Eurocode 3: Design of steel structures – Part 1-8: Design of joints. European committee for standardization, May 2005.

[23] D. Anderson. Composite steel-concrete joints in frames for buildings: Design provisions. COST C1 – Semi-rigid behaviour of civil engineering structural connections, Luxembourg, 1999.

[24] www.connectionprogram.com

[25] J.P. Jaspart. Study of the semi-rigidity of beam-to-column joints and its influence on the resistance and stability of steel buildings. PhD thesis, Liège University, 1991 (in French).

[26] C. Doneux. Study of transfer mechanisms of bending moments at beam-to-column joints in composite structures loaded by a seismic action. PhD thesis, Liège University, 1991 (in French).

[27] A. Plumier & C. Doneux. Seismic behaviour and design of composite steel concrete structures. ECOCEST2 & ICON, 2001.

[28] F. Ferrario. Analysis and modelling of the seismic behaviour of high ductility steel-concrete composite structures. PhD thesis, Trento University, February 2004.

[29] A. Braconi, S. Caramelli, D. Licchesi & W. Salvatore. Applicability of composite structures to sway frames: steel-concrete composite 3-D frame: pilot tests on connections. Report for the ECSC project 7210-PR-250 "applicability of composite structures to sway frames", Pisa University, June 2003.

[30] I. Ryan & D. Bitar. Applicability of composite structures to sway frames: final test report – static and cyclic loading tests of full-scale 3D specimens (draft version). Report for the ECSC project 7210-PR-250 "applicability of composite structures to sway frames", CTICM, June 2003.

[31] J.Y. Richard Liew, T.H. Teo and N.E. Shanmugam. Composite joints subject to reversal of loading – Part 2: analytical assessments. Journal of Constructional Steel Research, pp. 247-268, 2004.

[32] K. Weynand. Column bases in steel building frames. COST C1 – Semi-rigid behaviour of civil engineering structural connections, Luxembourg, 1999.

[33] Eurocode 2 – Part 1. Design of concrete structures – General rules and rules for buildings. prEN 1991-1-1, draft for stage 49, July 2002.

[34] T. Q. Li, D. B. Moore, D. A. Nethercot & B. S. Choo. The experimental behaviour of a full-scale, semi-rigidly connected composite frame: overall considerations. Journal of Constructional Steel Research, Vol. 39, 1996.

[35] T. Q. Li, D. B. Moore, D. A. Nethercot & B. S. Choo. The experimental behaviour of a full-scale, semi-rigidly connected composite frame: detailed appraisal. Journal of Constructional Steel Research, Vol. 39, 1996.

[36] FINELG user's manual. Non-linear finite element analysis software. Version 8.2, July 1999.

[37] H. Somja. Contribution to the modelling of the behaviour of bridges during the construction phase with account of the geometrical and the material non-linearities (in French). PhD thesis, Liège University, 2004.

[38] J.F. Demonceau & J.P. Jaspart. Validation of the FEM technique for the numerical simulation of the response of composite building frames. Common report on a Benchmark study. Report for the ECSC project 7210-PR-250 "Applicability of composite structures to sway frames", Liège University, March 2003.

[39] M. Kraus. Applicability of composite structures to sway frames – Annual report 2002. Report for the ECSC project 7210-PR-250 "Applicability of composite structures to sway frames", Bochum University, 2002.

[40] J.F. Demonceau & J.P. Jaspart. Design of the joints of the 2-D frame to be tested in Bochum. Report for the ECSC project 7210-PR-250 "Applicability of composite structures to sway frames", Liège University, February 2003.

[41] J.F. Demonceau & J.P. Jaspart. Numerical studies of the 2-D frame to be tested in Bochum. Report for the ECSC project 7210-PR-250 "Applicability of composite structures to sway frames", Liège University, March 2003.

[42] S. Majkut. Extension of Eurocode 4 to the computation of composite sway buildings. Diploma work (2000 – 2001), Liège University, M&S Department (in French).

[43] T. V. Nguyen. Non-linear analysis of steel structures and extensions to composite structures. European Master in engineering Science of Mechanics of Construction, Polytechnic University of Ho Chi Minh City, 2004.

[44] M. Villette. Critical analysis of the treatment of members subjected to compression and bending and propositions of new formulations (in French). PhD thesis, Liège University, 2004.

[45] L. D. P. Ly, J.F. Demonceau and J.P. Jaspart. New simplified analytical method for the prediction of global stability of composite sway frames. Eurosteel 2008 proceedings, Graz, Austria, September 2008 (to be published).

[46] PrEN 1991-1-7. Eurocode 1 – Action on structures – Part 1-7: General actions – Accidental actions. European committee for standardization, final project team draft (stage 34), July 2004.

[47] ENV 1991-2-7. Eurocode 1: Basis of design and action on structures – Part 2-7 : Accidental actions due to impacts and explosions. European committee for standardization, final draft, June 1998.

[48] BS 5950-1:2000. Structural use of steelwork in building – Part 1: Code of practice for design – Rolled and welded sections. 2001.

[49] US General Services Administration (GSA). Progressive collapse analysis and design guidelines for new federal office buildings and major modernization projects. June 2003.

[50] UFC 4-023-03. Unified Facilities Criteria (UFC) - Design of buildings to resist progressive collapse. Department of Defence, USA, 25 January 2005.

[51] ASCE 7-02. Minimum design loads for buildings and other structures. American Society of Civil Engineering.

[52] D.B. Moore. The UK and European regulations for accidental actions. Workshop on prevention of progressive collapse, Multihazard Mitigation Council (MMC) of the National Institute of Building Sciences (NIBS), Illinois, July 2002.

[53] R. Shankar Nair. Progressive collapse basics. Proceedings of the Steel Conference and the Pacific structural Steel Conference (NASCC 2004), 2004.

[54] B. R. Ellingwood & D. O. Dusenberry. Building design for abnormal loads and progressive collapse. Computer-Aided Civil and Infrastructure Engineering 20, Blackwell Publishing, 2005.

[55] D. O. Dusenberry. Review of Existing Guidelines and Provisions Related to Progressive Collapse. Workshop on prevention of progressive collapse, Multihazard Mitigation Council (MMC) of the National Institute of Building Sciences (NIBS), Illinois, July 2002.

[56] Multihazard Mitigation Council. Prevention of progressive collapse: report on the July 2002 National Workshop and recommendations for future efforts. Prepared by the Multihazard Mitigation Council with funding from The National Institute of Standards and Technology in cooperation with the Defence Threat Reduction Agency, the General Services Administration, and the U.S. Army Engineering Research and Development Center, Washington, 2003.

[57] A. G. Vlassis. Progressive collapse assessment of tall buildings. Thesis submitted in fulfilment of the requirements for the degree of Doctor of Philosophy of the University of London and the Diploma of Imperial College London. April 2007.

[58] B.A. Izzuddin, A.G. Vlassis, A.Y. Elghazouli & D.A. Nethercot. Progressive collapse of multi-storey buildings due to sudden column loss – Part I: Simplified assessment framework. Engineering Structures, 2007 (doi:10.1016/j.engstruct.2007.07.011).

[59] B.A. Izzuddin, A.G. Vlassis, A.Y. Elghazouli & D.A. Nethercot. Progressive collapse of multi-storey buildings due to sudden column loss – Part II: Application. Engineering Structures, 2007 (doi:10.1016/j.engstruct.2007.08.011).

[60] B.A. Izzuddin, A.G. Vlassis, A.Y. Elghazouli & D.A. Nethercot. Assessment of progressive collapse in multi-storey buildings. Proceedings of the Institution of Civil Engineers – Structures & Buildings 160 – Issue SBI, 2007.

[61] F. Cerfontaine. Study of the interaction between bending moment and axial force in bolted joints (in French). PhD thesis presented at Liège University, 2003.

[62] J.R. Cagley. The design professional's concerns regarding progressive collapse design. Workshop on prevention of progressive collapse, Multihazard Mitigation Council (MMC) of the National Institute of Buidling Sciences (NIBS), Illinois, July 2002.

[63] H. N. N. Luu. Structural response of steel and composite building frames further to an impact leading to the loss of a column. PhD thesis presented at Liège University, 2008 (to be presented in summer 2008).

[64] EN 1991-1-1. Eurocode 1: Actions on structures – Part 1-1: General actions – Densities, self-weight, imposed loads for buildings. April 2002.

[65] J.F. Demonceau & J.P. Jaspart. Experimental test simulating the loss of a column in a composite building – Liège University. Internal report for the RFCS project RFS-CR-04046 "Robust structures by joint ductility", Liège University, September 2006.

[66] C. L. K. Nguyen. Evaluation of the so-called "K value". European Master in engineering Science of Mechanics of Construction, Polytechnic University of Ho Chi Minh City, 2005.

[67] EN 1992-1-1. Eurocode 2: Design of concrete structures – Part 1-1: General rules and rules for buildings. European committee for standardization, December 2004.

[68] Y. Duchêne & S. Guisse. WnOssa2D: computation software for 2D structures – User's manual (in French). 1995.

[69] U. Kuhlmann & M. Schäfer. Innovative verschieblichte Verbund-Rahmen mit teiltragfähigen Verbund-Knoten. Forschung für die Praxis P 505. Forschungsvereinigung Stahlanwendung e.V. im Stahl-Zentrum, 2004.

[70] M. Schäfer. Zum Rotationsnachweis teiltragfähiger Verbundknoten in verschieblichen Verbundrahmen. Universität Stuttgart, Mitteilungen des Instituts für Konstruktion und Entwurf, Nr. 2005-1, Dissertation, July 2005.

[71] U. Kuhlman, L. Rölle, J.P. Jaspart & J.F. Demonceau. Robustness – robust structures by joint ductility. COST C26 action titled "Urban habitat constructions under catastrophic events", proceedings of Workshop in Prague, March 2007.

[72] F. Cerfontaine & J.P. Jaspart. Resistance of joints submitted to combined axial force and bending – Analytical procedures and comparison with laboratory tests. Eurosteel 2005 proceedings, Maastricht, The Netherlands, June 2005.

[73] K. Weynand, C. Ziller, E. Busse & M. Lendering. System calculation – Benchmark model 3. Internal report for the RFCS project RFS-CR-04046 "Robust structures by joint ductility", PSP Technologien GmbH, March 2007.

[74] K. Weynand, C. Ziller, E. Busse & M. Lendering. Calibration of the simplified substructure. Internal report for the RFCS project RFS-CR-04046 "Robust structures by joint ductility", PSP Technologien GmbH, October 2007.

[75] J.F. Demonceau and J.P. Jaspart. Loss of a column in a office or residential building frame – First numerical investigations of the steel "two-beam" system. Internal report for the RFCS project RFS-CR-04046 "Robust structures by joint ductility", Liège University, May 2006.

[76] R. Leroy. Evaluation of the rotation capacity of steel and composite joints (in French). Diploma work presented at Liège University, 2006.

[77] D. Marechal. Evaluation of the rotation capacity of steel joints (in French). Diploma work presented at Liège University, 2004.

[78] L. Simoes da Silva. Towards a consistent design approach for steel joints under generalized loading. Journal of Constructional Steel Research, JCSR Special Issue "Imperial College Centenary - Utilisation of experimental data in steel Structures Research", submitted 2007.

[79] J.P. Jaspart & R. Maquoi. Investigation by testing of the structural response of semi-rigid joints. Testing of metals for structures; edited by F. M. Mazzolani, 1992.

[80] J.F. Demonceau & J.P. Jaspart. Design of the structure for the full scale test to be tested in Ispra – Pre-calculations at the University of Liège. Internal report for the ECSC project 7210-PR-250 "Applicability of composite structures to sway frames", Liège University, March 2002.

[81] A. Braconi, S. Caramelli & W. Salvatore. Applicability of composite structures to sway frames – Annual report 2001. Report for the ECSC project 7210-PR-250, Pisa University, 2001.

[82] G. Hanswille. Outstanding composite structures for buildings. Composite construction – conventional and innovative, conference report, September 16-18, 1997.

[83] E. Jöst, G. Hanswille, R. Heddrich, H. Muess & D.A. Williams. Die neue Opel-Lackiererei in Eisenach in feuerbeständiger Verbundbauweise. Ernst & Sohn Verlag für Architektur und technische Wissenschaften, Berlin, 1992.

VI. Appendixes

VI.1. Actual properties of the materials used for the experimental tests presented in the thesis

VI.1.1. Material properties – "Sway frames" project – Isolated single-sided composite joint test and Bochum frame test

The actual properties for the steel elements and the concrete are presented from *Table VI.1* to *Table VI.7*.

Table VI.1. Mechanical properties of the IPE300 steel

$f_{y,flange}$	327 Mpa	$f_{u,flange}$	465 Mpa
$f_{y,web}$	357 Mpa	$f_{u,web}$	480 Mpa

Table VI.2. Mechanical properties of the HEB260 steel

$f_{y,flange}$	285 Mpa	$f_{u,flange}$	414 Mpa
$f_{y,web}$	327 Mpa	$f_{u,web}$	429 Mpa

Table VI.3. Mechanical properties of the HEB280 steel

$f_{y,flange}$	299 Mpa	$f_{u,flange}$	429 Mpa
$f_{y,web}$	341 Mpa	$f_{u,web}$	450 Mpa

Table VI.4. Mechanical properties of the end-plate steel

$f_{y,15\ mm}$	383 Mpa	$f_{u,15\ mm}$	542 Mpa

Table VI.5. Mechanical properties of the rebar steel

f_y	520 Mpa	f_u	606 Mpa

Table VI.6. Concrete element properties – cube test values – Isolated single-sided composite joint test

$f_{ck,column}$	41,3 Mpa
$f_{ck,slab}$	44,7 Mpa

Table VI.7. Concrete element properties – cylinder test values – Bochum frame test

f_{ck}	44,9 Mpa

VI.1.2. Material properties – "Robustness" project – Isolated double-sided composite joint tests and substructure test

VI.1.2.1. Introduction

The steel materials used for these tests were tested in different European institutions. The obtained results in the different institutions are presented herein. For the analytical investigations, the average values for the different properties are used.

VI.1.2.2. Material properties

In the present paragraph, the comparison of the material test results performed in the different laboratories involved in the test campaign of the "Robustness" project is presented; the objective of this comparison is to confirm the fact that all the steel members come from the same rolling and to obtain average values which will be used later in the numerical and analytical investigations.

Remark: initially, it was planed that all the institutions involved in the experimental campaign of the project would perform coupon tests on all the members used for the tests. Unfortunately, some institutions were not able to perform coupon tests on the profiles as the additional pieces needed to perform these tests were not delivered. Only Stuttgart University and Profile Arbed Research (PARE) received such pieces for the IPE140 profiles and only Stuttgart University for the HEA160 profiles; so, in this paragraph, only the test results coming from these two institutions are reported for the profiles.

The obtained results for the different members and coming from the different institutions are presented from *Table VI.8* to *Table VI.11*.

Table VI.8. Mechanical properties of the IPE140 steel

IPE140	$f_{y,web}$ [Mpa]	$f_{y,flange}$ [Mpa]	$f_{y,average}$ [Mpa]	$f_{u,web}$ [Mpa]	$f_{u,flange}$ [Mpa]	$f_{u,average}$ [Mpa]	$\varepsilon_{u,average}$ [%]
PARE	467	420	444	561	548	555	31
Stuttgart	457	403	430	557	555	556	30
Average	462	412	437	559	552	556	31

Table VI.9. Mechanical properties of the HEA160 steel

HEA160	$f_{y,web}$ [Mpa]	$f_{y,flange}$ [Mpa]	$f_{y,average}$ [Mpa]	$f_{u,web}$ [Mpa]	$f_{u,flange}$ [Mpa]	$f_{u,average}$ [Mpa]	$\varepsilon_{u,average}$ [%]
Stuttgart	432	392	412	538	523	531	32

Table VI.10. Mechanical properties of the 8 mm rebar steel

8 mm rebars	$f_{y,average}$ [Mpa]	$f_{u,average}$ [Mpa]	$\varepsilon_{u,average}$ [%]
Pittini	523	646	8
Trento	521	652	16
Stuttgart	542	660	18
Liège	505	624	12
Average	523	646	14

Table VI.11. Mechanical properties of the 8 mm end-plate steel

8mm end-plate	$f_{y,long.}$ [Mpa]	$f_{y,trans.}$ [Mpa]	$f_{y,average}$ [Mpa]	$f_{u,long.}$ [Mpa]	$f_{u,trans.}$ [Mpa]	$f_{u,average}$ [Mpa]	$\varepsilon_{u,average}$ [%]
PARE	673	564	619	716	672	694	16
Stuttgart	-	569	569	-	663	663	19
Liège	665	561	613	701	653	677	15
Average	669	565	600	709	663	678	17

From this comparison, it can be concluded that the test results are in good agreement, what confirms that all the steel members come from the same rolling.

One important thing to be highlighted is the high elastic strength of the 8 mm end-plate; indeed, the average value of this elastic limit is equal to 600 Mpa while the steel grade which was order for these plates was S355. This phenomenon induces very high overstrength effect which was not expected and which is not reflected in the joint design.

VI.1.3. Material properties – "Precious" project – Isolated single-sided composite joint tests

Steel coupon tests and tests on concrete cubes and cylinder were performed at Trento University so as to characterise the properties of the material used within the tested specimens. These properties are presented from *Table VI.12* to *Table VI.16*.

Table VI.12. Mechanical properties of the IPE300 steel

$f_{y,flange}$	389 Mpa	$f_{u,flange}$	584 Mpa
$f_{y,web}$	469 Mpa	$f_{u,web}$	622 Mpa

Table VI.13. Mechanical properties of the HEB260 steel

$f_{y,flange}$	402 Mpa	$f_{u,flange}$	529 Mpa
$f_{y,web}$	438 Mpa	$f_{u,web}$	552 Mpa

Table VI.14. Mechanical properties of the en-plate steel

$f_{y,15\ mm}$	540 Mpa	$f_{u,15\ mm}$	637 Mpa

Table VI.15. Mechanical properties of the rebar steel

$f_{y,6\ mm}$	540 Mpa	$f_{u,6\ mm}$	639 Mpa
$f_{y,12\ mm}$	506 Mpa	$f_{u,12\ mm}$	599 Mpa

Table VI.16. Concrete element property – cube test value

f_{ck}	45,3 Mpa

VI.2. Exploitation of the apparatus measurements obtained for the experimental test performed at Liège University on isolated single-sided composite joints

VI.2.1. Introduction

In this paragraph, the general methods used to exploit the measurements obtained through the different apparatus during the experimental tests performed at Liège University on the isolated single-sided composite joints of the "Ispra" structure (see *§ II.3.2.2*) are presented. The methods presented here are in line with the procedures presented in *[79]* which can be considered as the reference document on how to extract the moment-rotation behaviour curves of joints.

VI.2.2. Computation of the bending moment applied at the joint

To compute the bending moment applied at the joint, the lever arm is taken as equal to the distance between the load application point and the middle of the column flange on the connection side.

VI.2.3. Rotational transducer measurements

The inclinometers are placed on the specimens in order to get the rotation of the web panel (γ), of the connection (φ) and to deduce the global rotation (ϕ) of the joint according to the applied load (or according to the applied moment). The formulas used to get these rotations are described here after in *Figure VI.1*. More details are given in *[79]*.

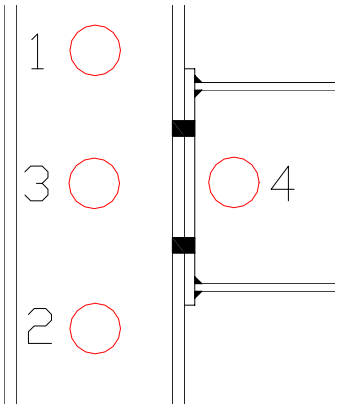

Web panel rotation:

$$\gamma = \text{Rot3} - \frac{\text{Rot1} + \text{Rot2}}{2}$$

Connection rotation:

$$\varphi = \text{Rot4} - \text{Rot3}$$

Global rotation of the joint:

$$\phi = \varphi + \gamma$$

Figure VI.1. Determination of the rotations of the joint components

VI.2.4. Translational transducer measurements

To obtain the joint behaviour through the translational transducer measurements, "parasite" displacements (given hereafter) have to be deduced from the vertical displacement measured at the beam end:

- Global rotation and vertical displacement of the system (*Figure VI.2*) ("rigid" body movement): the rotation of the system causes a vertical displacement at the beam end, which is given by the following formula:

$$D_1 = L_a \sin\theta + h\,(1 - \cos\theta) + D_{vb} \text{ with } \theta = \text{arctg}\left(\frac{D_{hh} + D_{hb}}{H}\right)$$

  where (cf. *Figure VI.2*):

  - L_a is the distance between the vertical translational transducer at the beam end and the middle axis of the column.

- h is the vertical distance between the load application point and the column support at the bottom.
- D_{vb} is the vertical displacement measured with a translational transducer at the bottom of the column.
- D_{hh} is the horizontal displacement measured with a translational transducer at the top of the column.
- D_{hb} is the horizontal displacement measured with a translational transducer at the bottom of the column.
- H is the distance between the two translational transducers measuring the horizontal displacement at the top and at the bottom of the column.

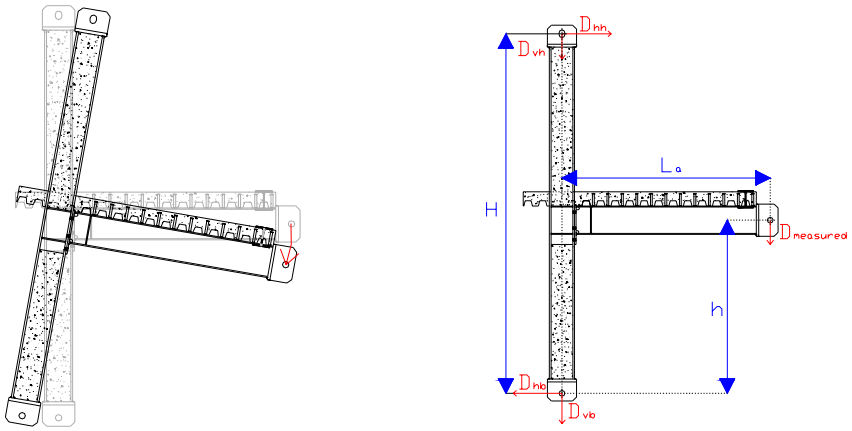

Figure VI.2. Rigid rotation of the system and parameters used for the determination of D_1

- Shortening of the column (*Figure VI.3*): the shortening of the column induces a vertical displacement at the beam end given by the following formula:

$$D_2 = D_{vh} - D_{vb}$$

where (cf. *Figure VI.2*):

- D_{vh} is the vertical displacement measured with a translational transducer at the top of the column.

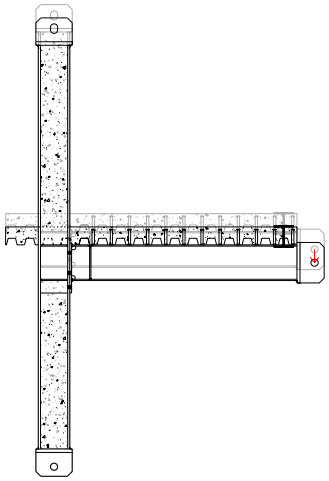

Figure VI.3. Shortening of the column

- Deformation of the beam and the column (*Figure VI.4*): this deformation induces a vertical displacement at the beam end (displacement D3) that can be estimated by means of the finite element software Finelg, which has been validated through benchmark studies in *§ II.4*. In the modelling, the joint is considered as rigid in order to get the displacement associated to the beam and column elements only.

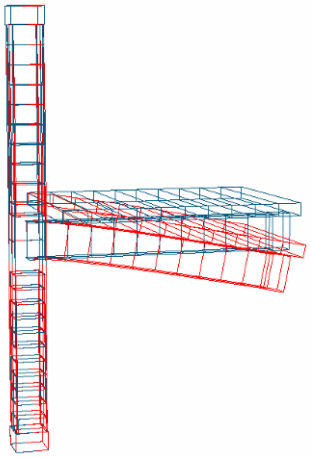

Figure VI.4. Estimation of the element deformations with Finelg

Considering these "parasite" displacements, the vertical beam end displacement due to the joint behaviour is given by the following formula: $D_{joint} = D_{measured} - D_1 - D_2 - D_3$. Obtaining this displacement, the M-ϕ behaviour curve of the joint can be drawn with $\phi = L_{beam}/D_{joint}$.

VI.3. Additional results for the benchmark study performed on the "UK" building (*§ II.4.4*)

VI.3.1. Frame A

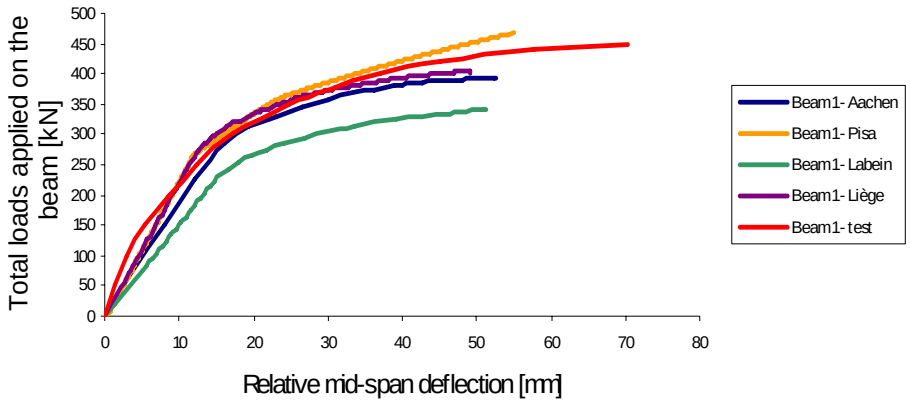

Figure VI.5. Relative mid-span deflection – beam 1 (see Figure II.49)

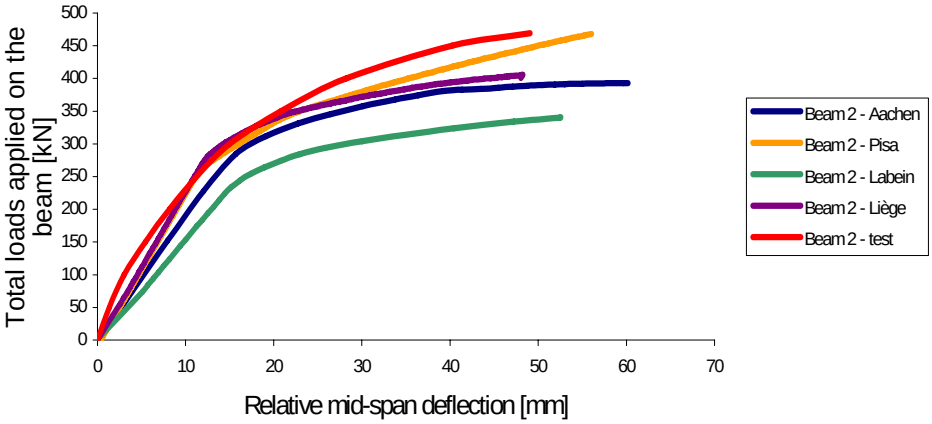

Figure VI.6. Relative mid-span deflection – beam 2 (see Figure II.49)

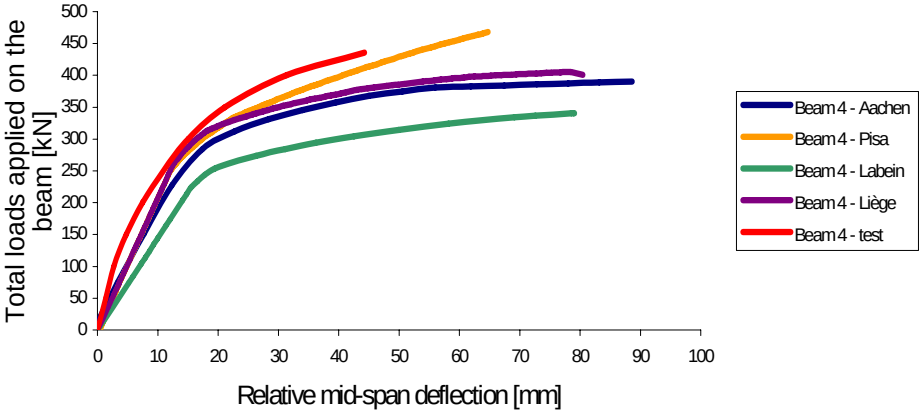

Figure VI.7. Relative mid-span deflection – beam 4 (see Figure II.49)

VI.3.2. Frame B

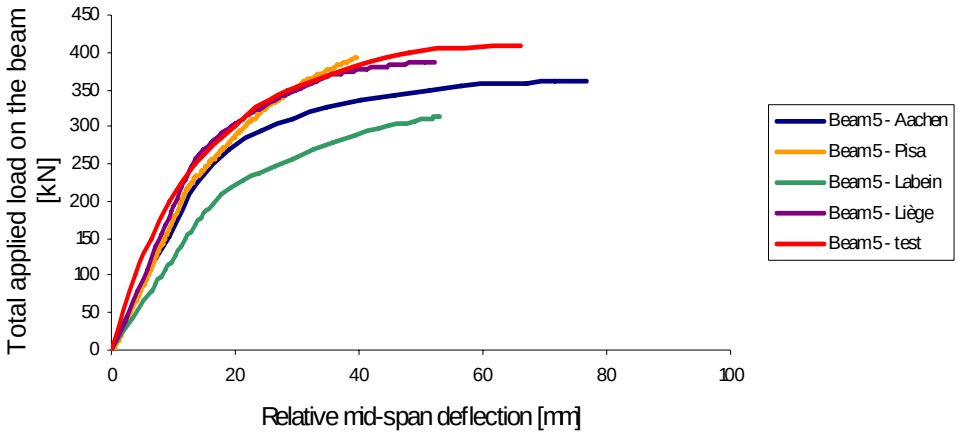

Figure VI.8. Relative mid-span deflection – beam 5 (see Figure II.49)

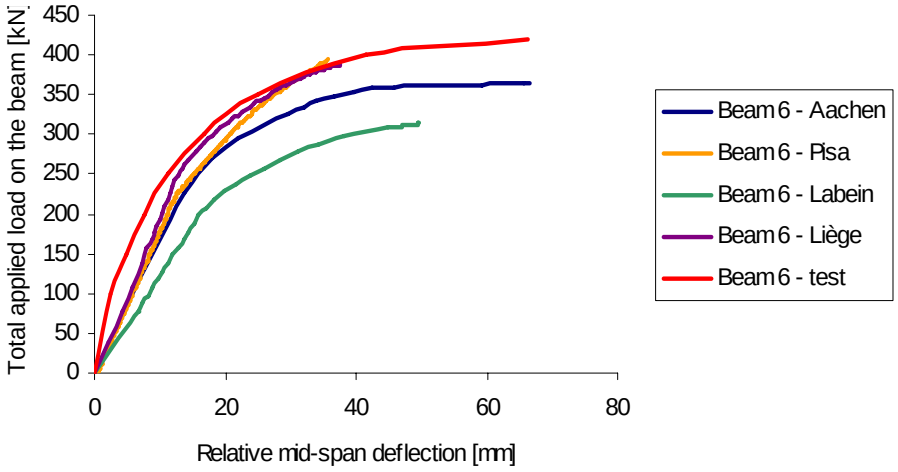

Figure VI.9. Relative mid-span deflection – beam 6 (see Figure II.49)

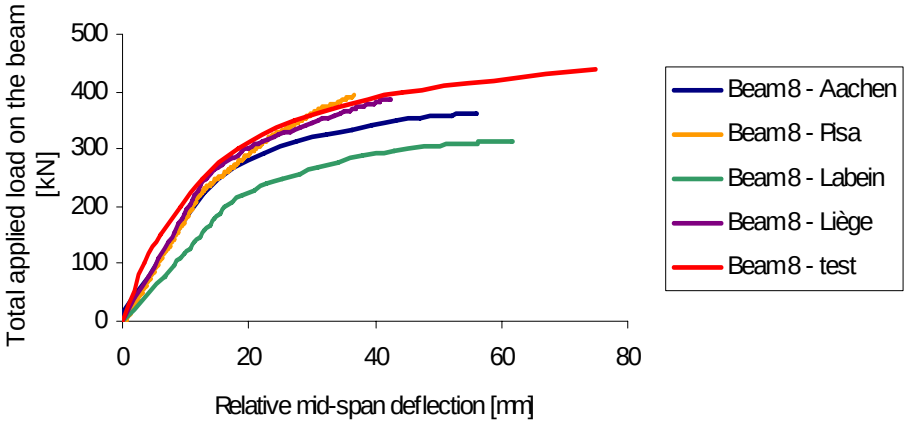

Figure VI.10. Relative mid-span deflection – beam 8 (see Figure II.49)

VI.3.3. Bending moment diagrams at collapse

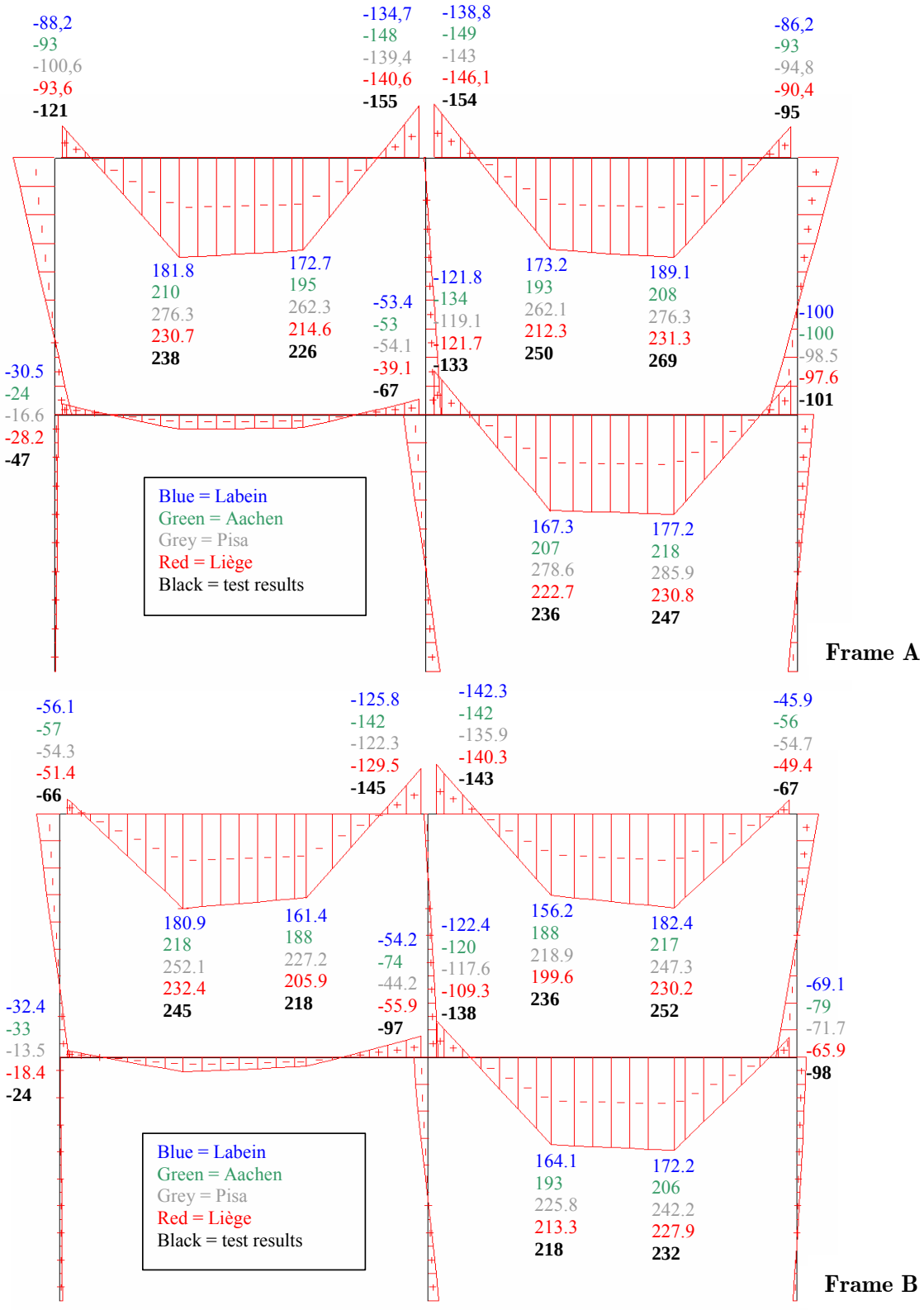

Figure VI.11. Diagram of bending moments at failure for Frame A and Frame B

VI.4. Investigated actual buildings

VI.4.1. Introduction

Five actual buildings in which sway effects are likely to occur under static loading have been selected:

- the "Ispra" building;
- the "Bochum" building;
- the "UK" building;
- the "Eisenach" building;
- the "Luxembourg" building.

The difficulty in this task was to collect, for each building, enough data such as those on geometry, material properties and joint detailing; these ones strongly influence the global structural response. These structures are briefly described here below.

VI.4.2. "Ispra" building

This 3-D full-scale building has been tested in Ispra (Italy) under seismic conditions in the field of the "sway frames" and "Ecoleader" projects (see *§ I.1 – [1]* and *[2]*). Tests on isolated joints have also been performed so as to get the actual properties of its constitutive structural joints.

Two different configurations of this structure have been considered within the "sway frames" project: they aimed at resisting respectively static loading and seismic loading (*[80]* and *[81]*). Only the investigations performed on the first configuration are developed in the present thesis, as a previous study *[16]* demonstrated that only this configuration can be qualified as sway under static loading with regards to Eurocode 3 criterion (see *§ II.2.2.3*). This is the latter which is described herein.

The "Ispra" building is 12 m long and is composed of two-storey two-bay frames that are 12 m large, 7 m high and 3 m spaced (*Figure VI.12*). These frames resist in-plane loading by frame action without exhibiting out-of-plane deformation because they are braced in the perpendicular direction.

The steel HEB200 columns are partially encased (*Figure VI.13.a*). The steel beams are made of IPE300 structural shapes; the upper flange of the profiles is connected to the composite slab by means of stud connectors. The slab reinforcement is constituted of a T6x6x150x150 mesh with two additional rebars with a diameter of 16 mm in the hogging

moment zones; the covering of the rebars is equal to 30 mm. The collaborating hollow rib is an EGB210 one with a thickness of 1mm, from BROLLO (Italy) and the ribs are perpendicular to the steel beam axis; the total height of the slab is equal to 120 mm.

All the moment resistant joints develop a composite action and are classified as semi-rigid and partial-strength. The end-plate thickness is equal to 12 mm and the bolts are M20 10.9 ones (*Figure VI.13.b*). The column bases are ideally pinned. One of the constitutive frames is represented in *Figure VI.14*.

The steel grades for the constitutive elements are:

- S235 for the profiles and for the joint components;
- S500 for the rebars;
- S320 for the hollow rib.

The concrete class for the composite slab and the composite columns is C25/30.

In addition to the self-weight of the structure, a permanent load of 1,5 kN/m^2 and an imposed service load of 5 kN/m^2 are uniformly applied on both floors. The wind loads are applied on the frame through concentrated loads at each floor level: 6.8 kN for the first level and 3.4 kN for the second one.

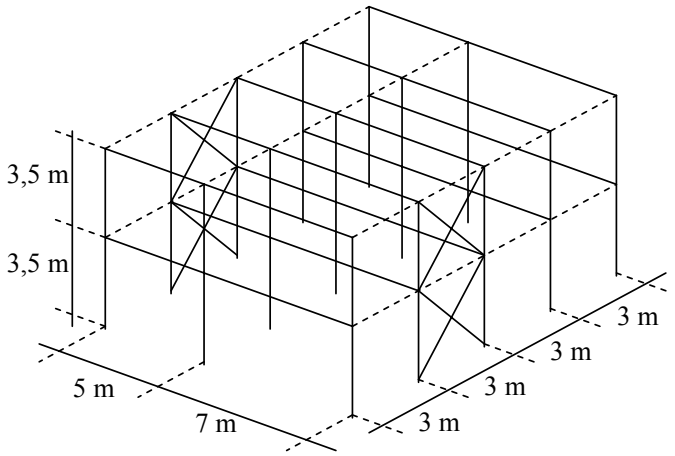

Figure VI.12. General layout of the 3-D "Ispra" building

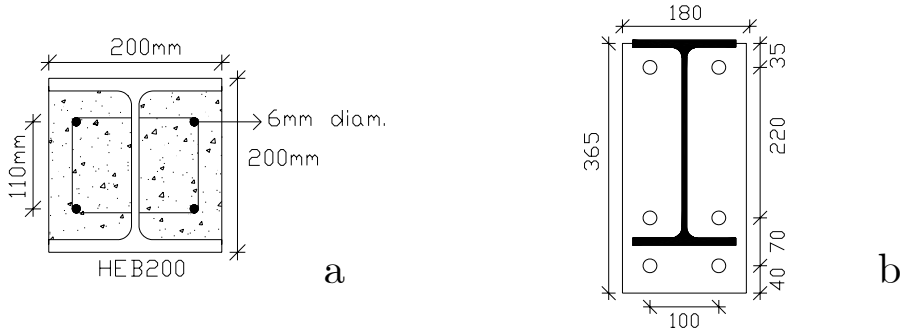

Figure VI.13. Composite column and joint details

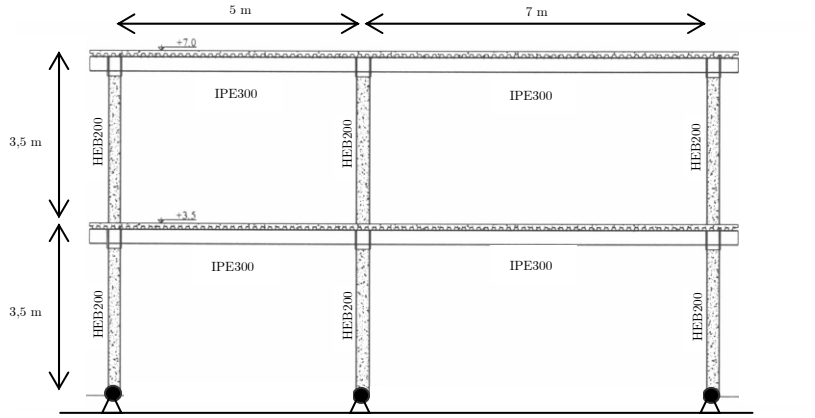

Figure VI.14. Isolated composite frame of the "Ispra" building

VI.4.3. "Bochum" building

It is a 2-D full-scale structure tested in Bochum (Germany) under static loading in the field of the "sway frames" project *[1]*. The latter is described in *§ II.4.5.2* and the applied loading in *§ II.4.5.3.B*.

VI.4.4. "UK" building

The "UK" building is a 3-D structure tested at BRE (Building Research Establishment), UK The test report is well documented (yield strengths, dimensions, type of loading); in particular, the behavioural curves of the structural joints are given (see *[34]* and *[35]*). In consequence, this building is the one used for the benchmark study presented in *§ II.4.4*. The description of the building is given in *§ II.4.4.1*.

For the numerical and analytical investigations presented in *§ II.5*, only Frame A is considered. Under the loading presented in *§ II.4.4.1*, this frame cannot be classified as a sway one if reference is made to the classification criterion given in the Eurocodes. In order to enter in the field of the present study (i.e. study of composite sway frames), modifications in the frame loading have been realised so as to obtain a $\lambda_{Ed}/\lambda_{cr}$ ratio which is higher than 0,1. The "Frame A" loading finally obtained is presented in *Figure VI.15*; the horizontal loads are supposed to represent wind actions and the vertical ones applied at the top of the columns to represent the gravity loads transmitted by upper storeys.

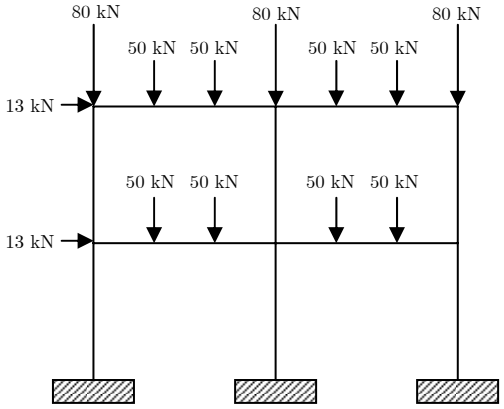

Figure VI.15. New frame loading for "Frame A" of the "UK" building

VI.4.5. "Eisenach" building

This structure is an unbraced factory building erected in Eisenach (Germany) and designed by Wuppertal University (*[82]* and *[83]*). The relevant data have been kindly provided by ARCELOR Group (formerly ProfilARBED Division). The building is 240 m long, 54 m width and 30,6 m height. The latter is composed of two or three-storey three-bay transversal frames which are spaced out 12 m apart (*Figure VI.16.a*); they resist in-plane loading by frame action without exhibiting out-of-plane deformations because they are braced in the perpendicular direction.

The slabs are composite ones (concrete slab with a collaborating sheet) and lean on secondary beams with an interval of 3 m. These secondary beams are supported by the principal beams represented in *Figure VI.16*. The columns are partially encased WPG profiles.

The available data only concern the two-storey two-bay frames. One of these frames has already been studied by M. Pecquet in his diploma work *[16]*. To respect the field of his work (i.e. study of sway composite structures), he realized some modification on the actual frame (represented in *Figure VI.16.b*); the main modifications made in the frame were to substitute the second level steel trusses by composite beams (so as to get a "full" composite frame) and to increase the thickness of the column flanges to resist to the additional dead loads brought by the new composite beams. The static scheme of the so-obtained substitute frame is given in *Figure VI.16.b* (g = permanent loads and q = variable loads); the latter is used for the numerical investigations presented in *§ II.5.2*. More details about this frame are available in *[16]*.

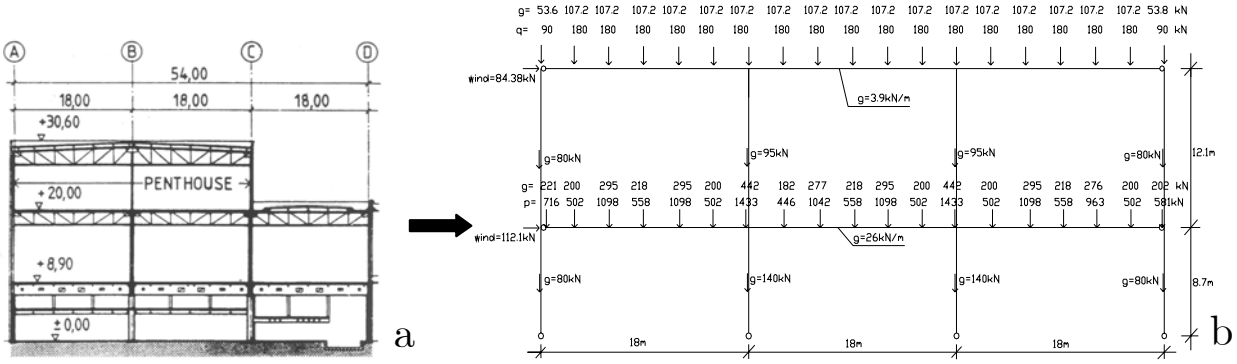

Figure VI.16. From the actual "Eisenach" structure to the substitute frame

The steel grade ordered for the structural elements is S355. The concrete grade for the slab and for the composite column is C30/37 with S500 rebars. The single-sided joints of the frame are assimilated to hinges and the double-sided joints to fully rigid ones.

VI.4.6. "Luxembourg" building

This is a bank office building located in Luxembourg (Grand-Duchy of Luxembourg). The relevant data have also been kindly provided by ARCELOR Group. This building is constituted of composite frames linked together by steel profiles. The height-storey three-bay frame is 38,8 m width and 26,2 m height (*Figure VI.17.a*). The actual "Luxembourg" structure is a braced one; indeed, concrete cores are present in the building and ensure its stability under transversal loading. Nevertheless, a frame of this structure has been isolated and assumed to be unbraced so as to satisfy the theme of the work.

As well as the slab, the beams or the columns are composite ones. This building was studied by Ms. Majkut in her diploma work *[42]*; she realized some modifications on the actual frame (*Figure VI.17.a*) so as to obtain a composite frame which presents a sway behaviour. The obtained frame is presented in *Figure VI.17.b*; this is the latter which is studied in *§ II.5*.

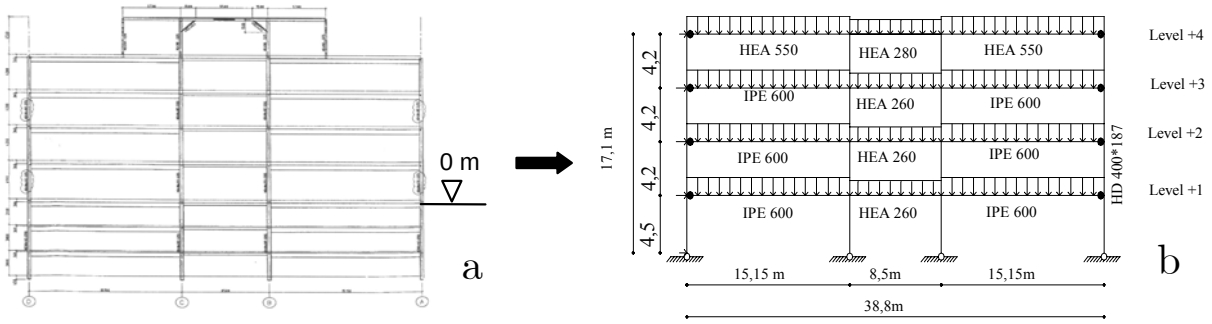

Figure VI.17. From the actual "Luxembourg" structure to the simplified substitute frame

The frame is loaded under permanent and variable uniform gravity loads and under concentrated horizontal loads at each storey level idealising the wind action; the values of these loads are presented in *Table VI.17*. The self-weight has to be added to the latter.

Table VI.17. Permanent and variable loads applied on the substitute frame of "Luxembourg" structure

Level	Permanent load (kN/m)	Variable load (kN/m)	Wind (kN)
1	31,5	22,5	14
2	31,5	22,5	20,4
3	31,5	22,5	20,9
4	36,5	21,4	7,6

Three different steel grades have been chosen for the beam and column profiles: S235, S355 and S460. The concrete class is C30/37 for all the concrete elements of the building, with S500 rebars for the reinforced concrete. More details about this structure are given in *[42]*.

VI.4.7. Conclusions

In this paragraph, five actual composite buildings in which sway effects are likely to occur under static loading are presented; two of them (the "Ispra" and the "Bochum" buildings) were designed at Liège University *[11]* in the field of the "sway frame" European project.

From these buildings, 2-D composite frames are isolated and are numerically and analytically investigated in *§ II.5*.

VI.5. Example of frame investigation in the framework of the parametrical study presented in § II.6.2

VI.5.1. Investigated frame

The investigated frame is a one bay – one storey steel structure (*Figure VI.18*). The beam is a IPE600 hot-rolled profile while the columns are HEB300 ones. The steel grade is S235 for all the elements. The joints are semi-rigid and partial-strength ones; their resistance to bending moments is equal to 159,6 kNm and their stiffness to 54765 kNm/rad. The applied loads are as follows:

- Two concentrated vertical loads at the top of the columns equal to 1700 kN;
- One concentrated vertical load at mid-span of the beam equal to 500 kN and;

- One concentrated horizontal load at the top of the left column equal to 100 kN.

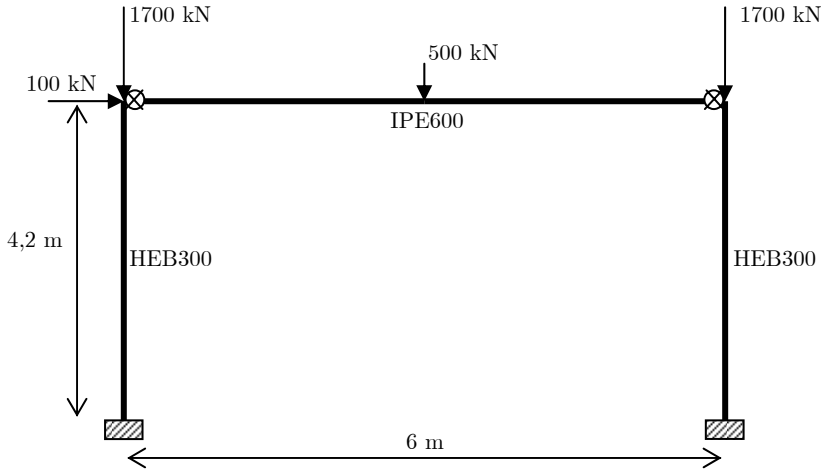

Figure VI.18. Investigated frame

VI.5.2. Numerical results

Through FINELG, a stability elastic analysis is first performed; the critical load factor (for the first global mode of instability - *Figure VI.19*) which is obtained through the latter is equal to 9,45 ($= \lambda_{cr}$) (all the applied load are increased by the same factor). So, if reference is made to the Eurocode 3 criteria (see *§ II.2.2.3.B*), the studied frame can be considered as "sway".

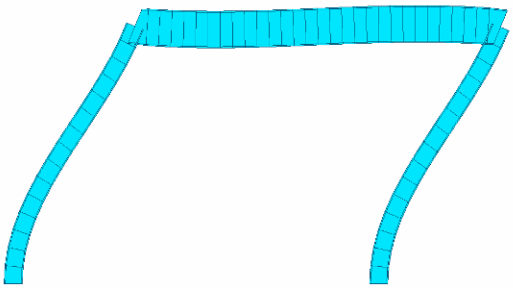

Figure VI.19. First global instability mode

Then, a full non-linear analysis (including the geometrical and the material non-linearities) is realised so as to compute the ultimate load factor (λ_u) of the frame. As mentioned in *§ II.6.2.1*, the shape of the initial deformation introduced in the computations is proportional to the first global instability mode obtained through the critical elastic analysis (*Figure VI.19*). The value of the initial deformation at the top of the frame is computed in agreement with *Formula (2.25)* as follows:

$$\delta_{ini} = \phi_{ini}.h_{struc} = \alpha_m.\alpha_h.\phi_0.h_{struc} = \sqrt{0,5.(1+\frac{1}{m})}.\frac{2}{\sqrt{h_{struc}}}.\frac{1}{200}.h_{struc}$$

with $h_{dtruc} = 4{,}2$ m and $m = 2$ ➔ $\delta_{ini} = \phi_{ini}.h_{struc} = 0{,}018$ m .

Through the non-linear analysis, a value of λ_u equal to 1,05 is obtained (see *Figure VI.20*). The collapse mode associated to the latter is the formation of a panel plastic mechanism, as illustrated in *Figure VI.21*, with development of plastic hinges at the joint level.

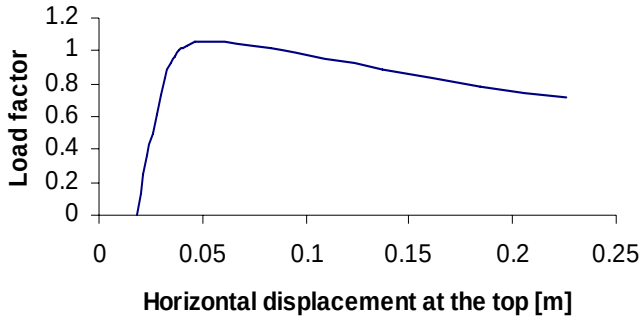

Figure VI.20. Horizontal displacement at the top vs. load factor curve

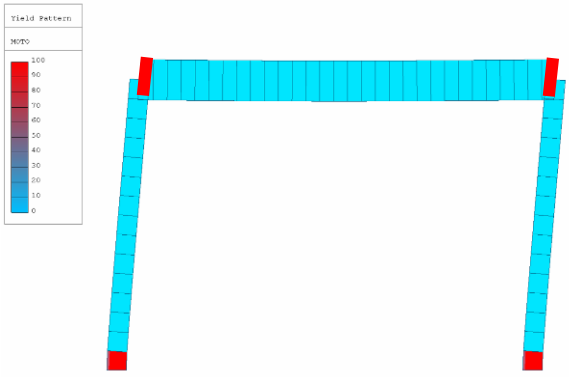

Figure VI.21. Frame deformation at the end of the non-linear simulation with the development of the yielding (in red)

VI.5.3. Analytical prediction of the ultimate load factor λ_u

The new method presented in *§ II.6.1* and the Merchant-Rankine approach (see *§ II.2.2.5.D*) are applied to the studied frame. To apply these two methods, a first-order rigid-plastic analysis is first realised so as to compute the three plastic load factors $\lambda_{p,beam}$, $\lambda_{p,combined}$ and $\lambda_{p,panel}$ respectively associated to a beam, combined and panel mechanism; as mentioned in *§ II.6.2.1*, the *M-N* interaction in the columns is taken into account through *Formula (2.29)* and *Formula (2.30)*. The obtained values are:

- $\lambda_{p,beam} = 1{,}29$
- $\boldsymbol{\lambda_{p,combined} = 1{,}20}$
- $\lambda_{p,panel} = 1{,}303$

It can be observed that the collapse mode associated to the first-order rigid-plastic analysis is a combined mechanism which is not in line with what is observed through the

full non-linear analysis (see previous section). This phenomenon can be explained by the fact that the development of a panel plastic mechanism is more affected by the second-order effects than a combined one. The latter is put into sight with more details in *[11]*.

Also, the ratio "λ_p/λ_{cr}" is equal to 0,12 which is between 0,1 and 0,25. So, the Merchant-Rankine approach can be used:

$$\frac{1}{\lambda_u} = \frac{1}{\lambda_p} + \frac{1}{\lambda_{cr}} = \frac{1}{1,2} + \frac{1}{9,45} \Rightarrow \lambda_u = 1,07$$

So, a difference of 2 % is obtained according to the fully non-linear analysis and the value obtained through the analytical method is bigger than the one obtained through FINELG. Also, it has to be notice that the value of λ_p which is used in the Merchant-Rankine approach is not the one corresponding to the plastic mechanism appearing at the ultimate state.

The new method is applied following the formulas proposed in *Table II.24*. The parameters μ_{beam}, $\mu_{combined}$ and μ_{panel} which are needed to apply the new method have been calibrated through the parametrical study presented in *§ II.6.2*. The proposed values in the latter are:

- $\mu_{beam} = 0{,}07$
- $\mu_{combined} = 0{,}29$
- $\mu_{panel} = 0{,}596$

$$\Rightarrow \begin{cases} \overline{\lambda}_{beam} = \sqrt{\dfrac{\lambda_{p,beam}}{\lambda_{cr}}} = 0,369 \\ \overline{\lambda}_{combined} = \sqrt{\dfrac{\lambda_{p,combined}}{\lambda_{cr}}} = 0,356 \\ \overline{\lambda}_{panel} = \sqrt{\dfrac{\lambda_{p,panel}}{\lambda_{cr}}} = 0,371 \end{cases} \Rightarrow \begin{cases} \phi_{beam} = 0,5.\left[1 + \mu_{beam}.(\overline{\lambda}_{beam}) + \overline{\lambda}_{beam}^{\,2}\right] = 0,581 \\ \phi_{combined} = 0,5.\left[1 + \mu_{combined}.(\overline{\lambda}_{combined}) + \overline{\lambda}_{combined}^{\,2}\right] = 0,615 \\ \phi_{panel} = 0,5.\left[1 + \mu_{panel}.(\overline{\lambda}_{panel}) + \overline{\lambda}_{panel}^{\,2}\right] = 0,679 \end{cases}$$

$$\Rightarrow \begin{cases} \chi_{beam} = \dfrac{1}{\phi_{beam} + \sqrt{\phi_{beam}^{\,2} - \overline{\lambda}_{beam}^{\,2}}} = 0,971 \\ \chi_{combined} = \dfrac{1}{\phi_{combined} + \sqrt{\phi_{combined}^{\,2} - \overline{\lambda}_{combined}^{\,2}}} = 0,896 \\ \chi_{panel} = \dfrac{1}{\phi_{panel} + \sqrt{\phi_{panel}^{\,2} - \overline{\lambda}_{panel}^{\,2}}} = 0,801 \end{cases} \Rightarrow \begin{cases} \lambda_{u,beam} = \chi_{beam}.\lambda_{p,beam} = 1,25 \\ \lambda_{u,combined} = \chi_{combined}.\lambda_{p,combined} = 1,08 \\ \lambda_{u,panel} = \chi_{panel}.\lambda_{p,panel} = 1,04 \end{cases}$$

$$\Rightarrow \lambda_u = \min\left(\lambda_{u,beam}; \lambda_{u,combined}; \lambda_{u,panel}\right) = 1,04$$

It can be observed that a very good accuracy is obtained with the new method (difference of 0,9 % on the safe side). It has also to be highlighted that the collapse mode associated to the minimum analytical ultimate load factor is a panel plastic mechanism which corresponds to the collapse mode appearing through the fully non-linear analysis.

VI.5.4. Conclusions

In the present paragraph, the study of a one bay – one storey steel frame has been detailed. Through the latter, it has been shown that the new method which is presented in *§ II.6* permits to obtain accurate results with a good agreement between the plastic mechanism associated to λ_u through the analytical method and the one appearing at collapse through a fully non-linear analysis.

This type of investigation has been performed on 181 steel frames and on 199 composite frames; the main results are summarised in *§ II.6.2.2*.

VI.6. Actual dimensions of the substructure (measured at the Argenco laboratory – Liège University)

The scope of the performed measurements is to get the actual properties of the constitutive members of the tested substructure (see *Figure* VI.22). The measured parameters are presented from *Figure VI.23* to *Figure* VI.29; the actual values of these parameters are given from *Table VI.18* to *Table VI.24*.

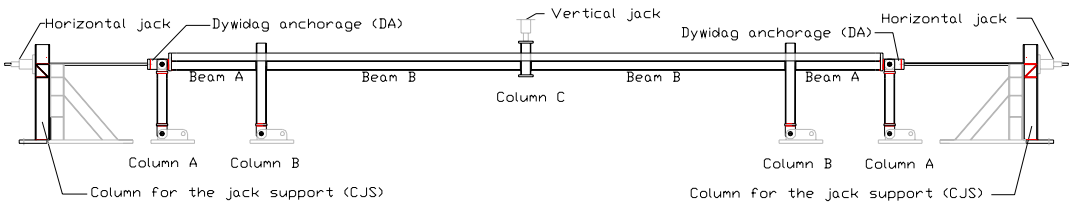

Figure VI.22. Tested substructure with the position of the constitutive members

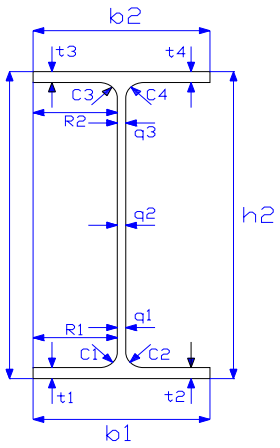

Figure VI.23. Measured parameters on the steel profiles

Table VI.18. Values of the measured parameters for the steel profiles

[mm]	*b1*	*b2*	*h1*	*h2*	*R1*	*R2*	*C1*	*C2*	*C3*	*C4*	*t1*	*t2*	*t3*	*t4*	*q1*	*q2*	*q3*
IPE140_Beam A	74,82	74,81	142	142	35	34	6,5	6,5	6,5	6,5	7,17	7,18	7,19	7,17	-	-	-
IPE140_Beam B	75,01	75,91	142	142	35	35	6,5	6,5	6,5	6,5	7,14	7,18	7,05	7,17	-	-	-
HEA160_Column B	161	161	154	154	76	77	15	15	15	15	8,64	8,03	8,44	8,52	6,21	6,23	6,24
HEA160_Column C	161	161	155	154	78	78	15	15	15	15	8,05	8,69	8,54	8,53	6,22	6,21	6,23

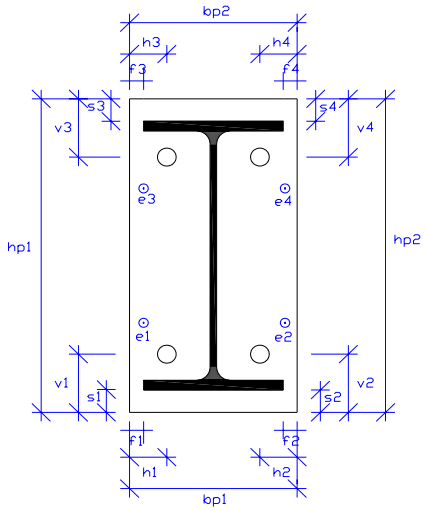

Figure VI.24. Measured parameters on the joint end-plates

Table VI.19. Values of the measured parameters for the end-plates in mm

Beam B - Column B LEFT	*hp1*	*hp2*	*bp1*	*bp2*	*v1*	*v2*	*v3*	*v4*	*s1*	*s2*	*s3*	*s4*
	161	161	159	159	45	46	45	44	9	9	10	11
	h1	*h2*	*h3*	*h4*	*f1*	*f2*	*f3*	*f4*	*e1*	*e2*	*e3*	*e4*
	30	29	30	30	42	43	43	42	9,17	9,14	9,16	9,15
Beam B - Column B RIGTH	*hp1*	*hp2*	*bp1*	*bp2*	*v1*	*v2*	*v3*	*v4*	*s1*	*s2*	*s3*	*s4*
	161	161	160	160	46	46	45	45	8	8	9	9
	h1	*h2*	*h3*	*h4*	*f1*	*f2*	*f3*	*f4*	*e1*	*e2*	*e3*	*e4*
	30	30	31	31	41	44	43	42	9,09	9,1	9,11	9,08
Beam B - Column C LEFT	*hp1*	*hp2*	*bp1*	*bp2*	*v1*	*v2*	*v3*	*v4*	*s1*	*s2*	*s3*	*s4*
	160	160	160	160	45	45	46	46	8	8	9	9
	h1	*h2*	*h3*	*h4*	*f1*	*f2*	*f3*	*f4*	*e1*	*e2*	*e3*	*e4*
	30	30	31	31	42	43	44	41	9,1	9,11	9,11	9,1
Beam B - Column C RIGTH	*hp1*	*hp2*	*bp1*	*bp2*	*v1*	*v2*	*v3*	*v4*	*s1*	*s2*	*s3*	*s4*
	160	161	161	161	46	46	45	45	9	9	9	9
	h1	*h2*	*h3*	*h4*	*f1*	*f2*	*f3*	*f4*	*e1*	*e2*	*e3*	*e4*
	30	31	30	30	42	42	43	42	9,08	9,09	9,11	9,1

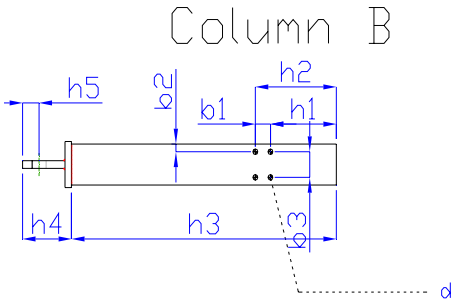

Figure VI.25. Measured parameters on the column B

Table VI.20. Values of the measured parameters for the column B

[mm]	*b1*	*b2*	*b3*	*h1*	*h2*	*h3*	*h4*	*h5*	*d*
Column B left	70	30	100	305	375	1225	228	78	22
Column B right	70	31	100	305	375	1225	225	75	22

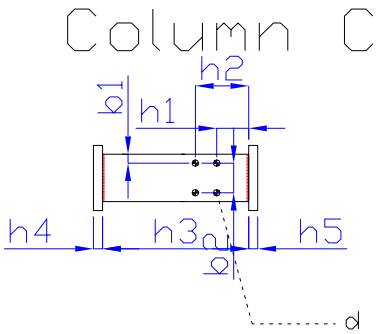

Figure VI.26. Measured parameters on the column C

Table VI.21. Values of the measured parameters for the column C

[mm]	*b1*	*b2*	*h1*	*h2*	*h3*	*h4*	*h5*	*d*
Column C left	31	100	105	173	480	29,91	29,72	22
Column C right	31	100	106	176	482	29,7	29,82	22

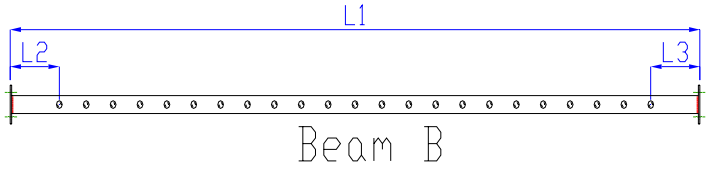

Figure VI.27. Measured parameters on the beam B

Table VI.22. Values of the measured parameters for the beam B

[mm]	*L1*	*L2*	*L3*
Beam B left	3850	275	277
Beam B right	380	275	277

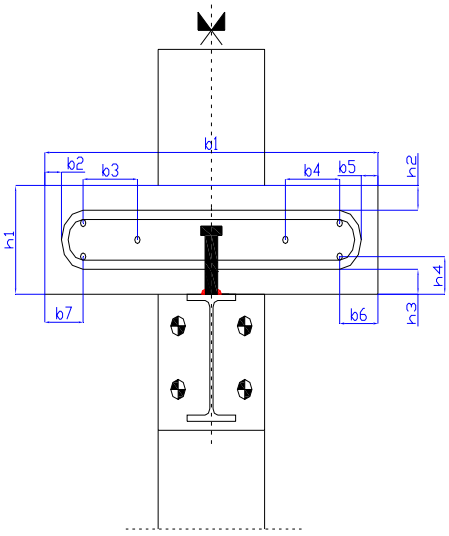

Figure VI.28. Measured parameters on the slab in the vicinity of the joints

Table VI.23. Values of the measured parameters for the slab

[mm]	*b1*	*b2*	*b3*	*b4*	*b5*	*b6*	*b7*	*h1*	*h2*	*h3*	*h4*
At Column B Left	497	27	100	107	24	53	50	121	43	25	42
At Column B right	492	24	95	100	22	49	48	121	35	24	46
At Column C	493	24	110	95	25	45	47	121	39	23	40

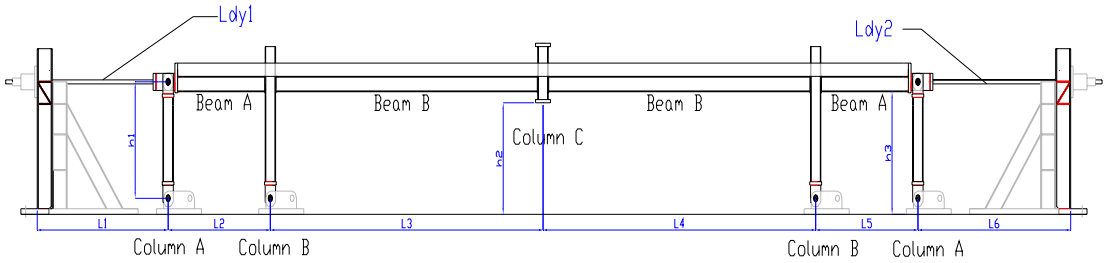

Figure VI.29. Measured parameters on the substructure

Table VI.24. Values of the measured parameters for the substructure

[mm]	L1	L2	L3	L4	L5	L6	h1	h2	h3	Ldy1	Ldy2
	1900	1500	4010	4005	1500	2245	1065	1033	1126	2410	2657

VI.7. Analytical prediction of the M-N resistance interaction curve of the substructure joint configuration

VI.7.1. Introduction

As mentioned in *§ III.5.3.3.C*, two *M-N* resistance interaction curves have been computed: one associated to the elastic strength of the materials and one associated to the ultimate strength. The computations presented herein are the ones used to obtain the interaction curve associated to the elastic strength.

As the objective is to compare the analytical prediction to experimental test results, the analytical computation of the *M-N* resistance interaction curve is performed using the actual properties of the materials, i.e. the ones presented in *Appendix VI.1.2*.

To be able to compute the resistance interaction curve, each joint component has to be characterised. This characterisation has been performed according to the rules recommended in the Eurocodes through the software CoP *[24]* and through a validated homemade software presented in *[11]*, except for the component "concrete slab in compression" which is not yet covered by the Eurocodes. The latter has been

characterised through hand-computations with the method proposed in *§ II.3.3.4.B* (see *Formula (2.22)*). The computation details are not presented herein.

The studied composite joint configuration is first reminded in *§ VI.7.2* with a summary of the results obtained for the component characterisation and then, the computation of the resistance interaction curve is presented in *§ VI.7.3*.

VI.7.2. Studied composite joint configuration

The studied composite joint configuration is reminded in *Figure VI.30*. The numbering of the rows (*Figure VI.31*) to be considered within the analytical procedure is realised according to the convention proposed for steel joint configurations presented in *§ III.5.3.2.C* with some adaptations to be applicable to composite joints configurations:

- The concrete slab (only activated when subjected to compression stresses) is divided in four "rows": one from the upper fibre of the concrete slab to the first layer of reinforcement (row 1), one from the first layer of reinforcement to the second layer of reinforcement (row 3), one from the second layer of reinforcement to the third layer of reinforcement (row 5) and one from the third layer of reinforcement to the lower fibre of the concrete slab (row 7).

- The slab rebars are numbered as bolt rows.

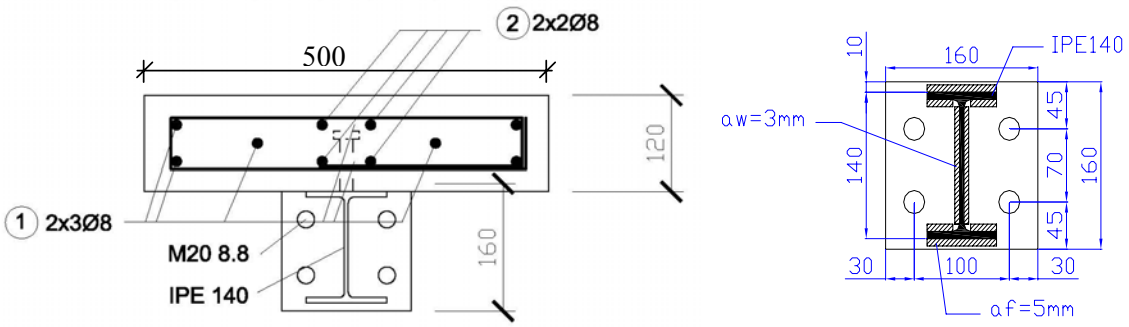

Figure VI.30. Studied double-sided composite joint configuration

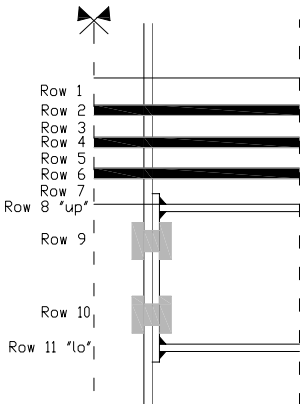

Figure VI.31. Row numbering

In order to be able to compare the analytical prediction to the experimental test results, the reference point where the axial load and the bending moments are assumed to be applied is the same than the one used to compute the applied bending moment and normal force during the test, i.e. the one presented in *Figure III.65*. So, having the position of this point, it is possible to compute the lever arm associated to each row; the associated resistance is also reported (with the nomenclature used in the failure criteria – see *Formula (3.5)*):

- $h_1 \in [127mm;166mm]$ $\left.\begin{array}{l} F_1^{Rd,+} = -266,4.z^+.24,8\text{=-}6,6.z^+kN \\ F_1^{Rd,-} = -6,6.z^-kN \end{array}\right\}$ with z^+ and z^- in mm $\left.\begin{array}{l} \\ z^+, z^- \in [0mm;39mm] \end{array}\right\}$
- $h_2 = 127mm$ $F_2^{Rd,+} = F_2^{Rd,-} = 54,4kN$
- $h_3 \in [106mm;127mm]$ $\left.\begin{array}{l} F_1^{Rd,+} = -6,6.z^+kN \\ F_1^{Rd,-} = -6,6.z^-kN \end{array}\right\}$ with z^+ and z^- in mm $\left.\begin{array}{l} \\ z^+, z^- \in [0mm;21mm] \end{array}\right\}$
- $h_4 = 106mm$ $F_4^{Rd,+} = F_4^{Rd,-} = 54,4kN$
- $h_5 \in [85mm;106mm]$ $\left.\begin{array}{l} F_1^{Rd,+} = -6,6.z^+kN \\ F_1^{Rd,-} = -6,6.z^-kN \end{array}\right\}$ with z^+ and z^- in mm $\left.\begin{array}{l} \\ z^+, z^- \in [0mm;21mm] \end{array}\right\}$
- $h_6 = 85mm$ $F_6^{Rd,+} = F_6^{Rd,-} = 54,4kN$
- $h_7 \in [46mm;85mm]$ $\left.\begin{array}{l} F_1^{Rd,+} = -6,6.z^+kN \\ F_1^{Rd,-} = -6,6.z^-kN \end{array}\right\}$ with z^+ and z^- in mm $\left.\begin{array}{l} \\ z^+, z^- \in [0mm;39mm] \end{array}\right\}$
- $h_8 = 42,6mm$ $F_8^{Rd,+} = F_8^{Rd,-} = -284,6kN$
- $h_9 = 11mm$ $F_9^{Rd,+} = 169,4kN$ and $F_9^{Rd,-} = 67,3kN$
- $h_{10} = -59mm$ $F_{10}^{Rd,+} = 67,3kN$ and $F_{10}^{Rd,-} = 169,4kN$
- $h_{11} = -90,6mm$ $F_{11}^{Rd,+} = F_{11}^{Rd,-} = -284,6kN$

where z^+ and z^- are defined in *Figure VI.32*. To compute the resistance of the component "concrete slab in compression", the value of $b_{eff,conn}$ is taken as equal to 266,4 mm, in agreement with *Formula (2.20)*.

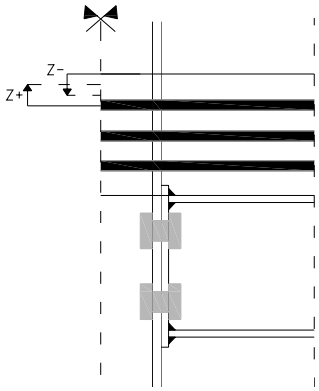

Figure VI.32. Definition of z^+ *and* z^-

As mentioned in *§ III.5.3.3.B*, it is not possible for the component "concrete slab in compression" to obtain one specific value of lever arm as the latter is linked to the height of concrete which is assumed to be in compression. It is the reason why a domain and not one value is given for the lever arms associated to this component. As an example, if the height of concrete subjected to compression in row 1 is equal to 39 mm (i.e. all the row is subjected to compression), the lever arm is equal to 146,5 mm (the resultant force is assumed to be applied at mid-height of the zone subjected to compression).

For the bolt rows (i.e. row 9 and 10), the resistance is associated to a group effect. Indeed, the individual resistance of a bolt row is equal to 169,4 kN while the resistance of the group is equal to 236,7 kN (which is smaller than 2.169,4 = 338,8 kN). So, it is the reason why, when computing the values of $F^{Rd,+}$ (see *Figure III.75*), the upper bolt row resistance is taken as equal to 169,4 kN ($=F_9^{Rd,+}$) and the lower bolt row resistance to 236,7 – 169,4 = 67,3 kN ($=F_{10}^{Rd,+}$); when computing the values of $F^{Rd,-}$, it is the opposite, i.e. the upper bolt row resistance is equal to 67,3 kN ($=F_9^{Rd,-}$) and the lower bolt row resistance to 169,4 kN ($=F_{10}^{Rd,-}$). The computation of these values is graphically illustrated in *Figure VI.33*.

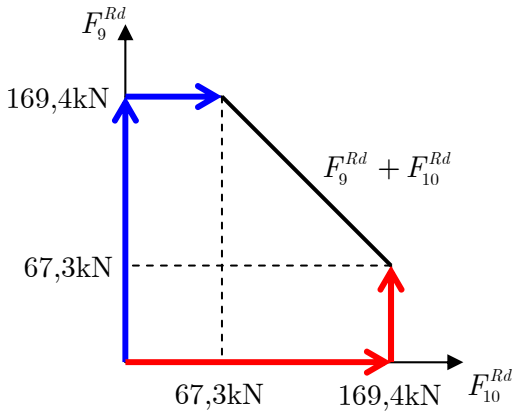

Figure VI.33. Computation of $F^{Rd,+}$ *(in blue) and* $F^{Rd,-}$ *(in red) for the bolt rows*

VI.7.3. Computation of the M-N resistance interaction curve

VI.7.3.1. Introduction

With the parameters characterised in the previous section, it is now possible to compute the *M-N* resistance interaction curve. As the scope of this Appendix is to predict analytically the interaction curve in order to compare it, later on, to the experimental test results, only the part of the curve in the tensile zone is computed as the experimental tests were performed on the joints subjected to combined tensile loads and bending moments.

To compute the resistance to axial loads and the resistance to bending moments, the formulas proposed in *§ III.5.3.2.D* (*Formula (3.3)*) are used. The different points of the *M-N* resistance interaction curve are computed first in *§ VI.7.3.2* and *§ VI.7.3.3*; then, the so-obtained *M-N* resistance interaction curve is drawn in *§ VI.7.3.4* (*Figure VI.34*).

VI.7.3.2. Upper rows in tension ($F_i^{Rd,+}$)

A. Point A: all the rows are in tension

$N = \sum_i F_i^{Rd,+} = F_2^{Rd,+} + F_4^{Rd,+} + F_6^{Rd,+} + F_9^{Rd,+} + F_{10}^{Rd,+} = 3.54{,}4 + 169{,}4 + 67{,}3 = 399{,}9$ kN

$M = \sum_i h_i.F_i^{Rd,+} = (127 + 106 + 85).54{,}4 + 11.169{,}4 - 59.67{,}3 = 15{,}2$ kNm

B. Point B: rows 1 to 10 in tension and row 11 in compression

$N = F_2^{Rd,+} + F_4^{Rd,+} + F_6^{Rd,+} + F_9^{Rd,+} + F_{10}^{Rd,+} + F_{11}^{Rd,+} = 3.54{,}4 + 169{,}4 + 67{,}3 - 284{,}6 = 115{,}3$ kN

$M = \sum_i h_i.F_i^{Rd,+} = (127 + 106 + 85).54{,}4 + 11.169{,}4 - 59.67{,}3 - 90{,}6.(-284{,}6) = 41$ kNm

C. Point C: rows 1 to 9 in tension and rows 10 and 11 in compression

$N = F_2^{Rd,+} + F_4^{Rd,+} + F_6^{Rd,+} + F_9^{Rd,+} + F_{11}^{Rd,+} = 3.54{,}4 + 169{,}4 - 284{,}6 = 48$ kN

$M = \sum_i h_i.F_i^{Rd,+} = (127 + 106 + 85).54{,}4 + 11.169{,}4 - 90{,}6.(-284{,}6) = 45$ kNm

D. Point D: rows 1 to 8 in tension and rows 9 to 11 in compression

$N = F_2^{Rd,+} + F_4^{Rd,+} + F_6^{Rd,+} + F_{11}^{Rd,+} = 3.54{,}4 - 284{,}6 = -121{,}4$ kN

$M = \sum_i h_i.F_i^{Rd,+} = (127 + 106 + 85).54{,}4 - 90{,}6.(-284{,}6) = 43{,}1$ kNm

It can be observed that this point enters in the compression "zone" of the interaction curve. So, the computation for the case "upper rows in tension" is stopped here.

VI.7.3.3. Lower rows in tension ($F_i^{Rd,-}$)

A. Point E: all the rows are in tension

$$N = \sum_i F_i^{Rd,+} = F_2^{Rd,-} + F_4^{Rd,-} + F_6^{Rd,-} + F_9^{Rd,-} + F_{10}^{Rd,-} = 3.54{,}4 + 67{,}3 + 169{,}4 = 399{,}9 \text{ kN}$$

$$M = \sum_i h_i.F_i^{Rd,+} = (127 + 106 + 85).54{,}4 + 11.67{,}3 - 59.169{,}4 = 8 \text{ kNm}$$

B. Zone F: rows 2 to 11 in tension and row 1 in compression

$$N = F_1^{Rd,-} + F_2^{Rd,-} + F_4^{Rd,-} + F_6^{Rd,-} + F_9^{Rd,-} + F_{10}^{Rd,-}$$

$$= -6{,}6.z^- + 3.54{,}4 + 67{,}3 + 169{,}4 = 399{,}9 - 6{,}6.z^- \text{kN with } z^- \text{ in mm}$$

$$M = \sum_i h_i.F_i^{Rd,+} = (166 - \frac{z^-}{2}).(-6{,}6.z^-) + (127 + 106 + 85).54{,}4 + 11.67{,}3 - 59.169{,}4$$

It can be observed that the M and N couples for this zone depends of the value of z^- (= height of concrete subjected to compression in row 1) which is between 0 mm and 39 mm. This zone in the *M-N* resistance interaction curve has been computed through an Excel sheet for different values of z^-. When z^- is equal to 0, the obtained point is point E; when z^- is equal to 39 mm, the obtained point is N = 142,5 kN and M = -29,66 kNm.

C. Zone G: rows 4 to 11 in tension and row 1 to 3 in compression

$$N = F_1^{Rd,-} + F_3^{Rd,-} + F_4^{Rd,-} + F_6^{Rd,-} + F_9^{Rd,-} + F_{10}^{Rd,-}$$

$$= -6{,}6.39 - 6{,}6.z^- + 2.54{,}4 + 67{,}3 + 169{,}4 = 142{,}5 - 6{,}6.z^- \text{kN with } z^- \text{ in mm}$$

$$M = \sum_i h_i.F_i^{Rd,+} = 146{,}5.(-257{,}4) + (166 - 39 - \frac{z^-}{2}).(-6{,}6.z^-) + (127 + 106 + 85).54{,}4 + 11.67{,}3 - 59.169{,}4$$

Again, as for the previous zone, it can be observed that the M and N couples for this zone depends of the value of z^- representing the height of concrete subjected to compression in row 3. This zone in the *M-N* resistance interaction curve has been computed through an Excel sheet for different values of z^-.

VI.7.3.4. Obtained M-N resistance interaction curves

As previously mentioned, the computations which are performed within this section are associated to the elastic strength of the materials. The same procedure has been followed

to compute the *M-N* interaction curve associated to the ultimate strength of the materials. The so-obtained curves are reported in *Figure VI.34*.

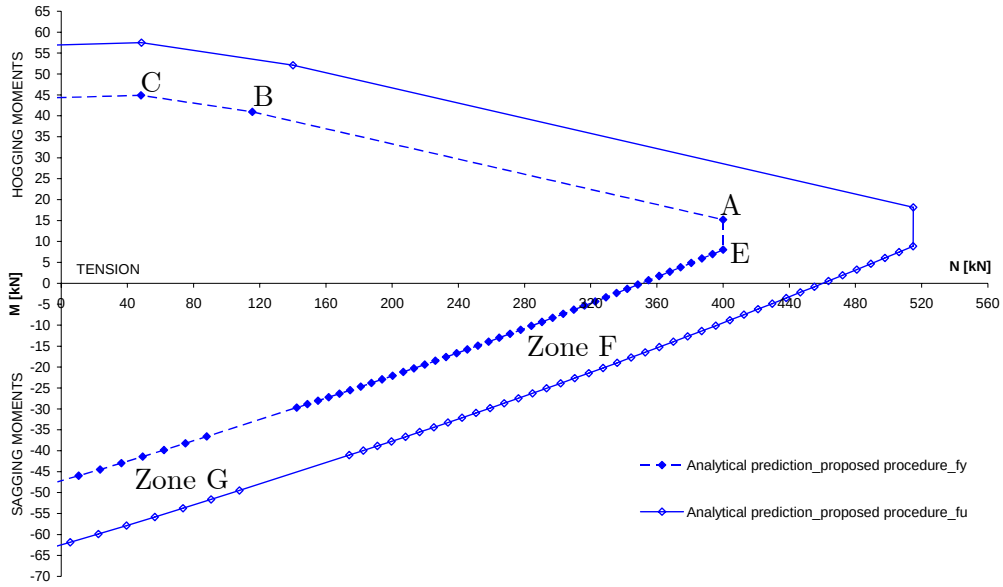

Figure VI.34. Resistance interaction curves predicted through the proposed procedure

Remark: the point D has not been reported in *Figure VI.34* has the latter is not in the tensile part of the graph.

VI.8. Details of computation relative to the developed analytical method to predict the development of the membrane forces in the simplified substructure and their effect in the substructure response

VI.8.1. Introduction

Within the present paragraph, the details of the developments leading to the definition of an analytical procedure to predict the response of the simplified substructure with account of the development of the membrane forces are presented. The simplified substructure to be investigated is reminded in *Figure VI.35*.

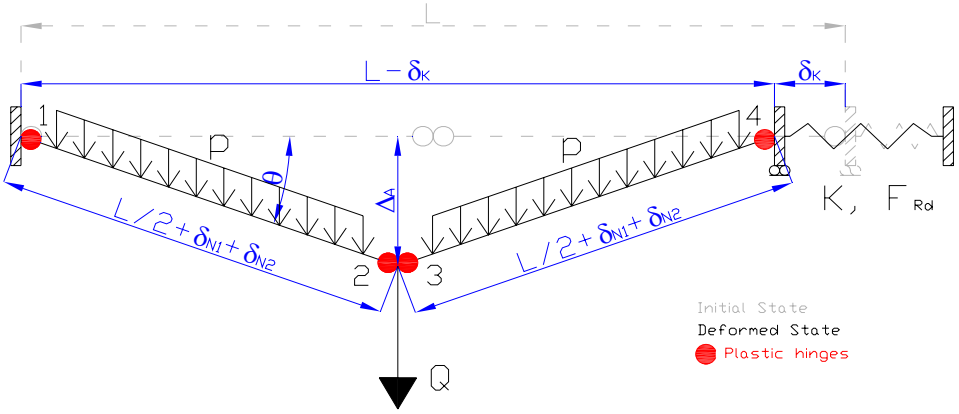

Figure VI.35. Substructure to be investigated and definition of the main parameters

The method which is developed is based on a second-order rigid-plastic analysis (see *§ II.2.2.4.F*). As mentioned in *§ III.8.3.1*, the concentrated load Q associated to the column loss (see *§ III.3.3*) is assumed to be applied at the middle of the simplified substructure, i.e. it is assumed that the beam spans each side of the loss column are equals. In addition, it is assumed that the two plastic hinges 1 and 4 and the two plastic hinges 2 and 3 (see *Figure VI.35*) have respectively the same resistance interaction curves. Accordingly, the parameters to be considered in the developed method are the followings:

- the uniformly distributed load p applied on the storey modelled by the simplified substructure (constant);
- the concentrated load Q associated to the column loss;
- the total initial length of the simplified substructure L (constant);
- the vertical displacement at the load application point Δ_A;
- the deformation of the horizontal spring simulating the lateral restraint coming from the indirectly affected part δ_K;
- the plastic elongation at each plastic hinges δ_{N1} (for hinges 1 and 4) and δ_{N2} (for hinges 2 and 3);
- the rotation at the plastic hinges at the beam extremities θ and;
- the axial and bending resistances at the plastic hinges N_{Rd1} and M_{Rd1} for the plastic hinges 1 and 4 and N_{Rd2} and M_{Rd2} for the plastic hinges 2 and 3.

Within the two following sections, two analytical procedures have been developed:

- one with account of the uniformly distributed load p (*§ VI.8.2*) and;
- one without account of the uniformly distributed load p (*§ VI.8.3*).

In *§ III.8.3.3*, it is shown that the results obtained with the two methods are identical; however neglecting p leads to significant simplifications of the formulas to be considered.

Remark: the main computations have been performed with the software MATHEMATICA.

VI.8.2. Analytical procedure with account of p

According to the compatibility of displacements:

- $\Delta_A = (\frac{L}{2} + \delta_{N1} + \delta_{N2}).Sin(\theta)$ (6.1)

- $(\frac{L}{2} + \delta_{N1} + \delta_{N2}) = \frac{(L - \delta_K)}{2.Cos(\theta)}$ (6.2)

➔ $\delta_K = L.(1 - Cos(\theta)) - 2.Cos(\theta).(\delta_{N1} + \delta_{N2})$ (6.3)

According to the equations of equilibrium (see *Figure VI.36*):

- $N_{Rd1} = (\frac{Q}{2} + \frac{pL}{2}).Sin(\theta) + K.\delta_K.Cos(\theta)$ (6.4)

- $N_{Rd2} = (N_{Rd1} - \frac{pL}{2}.Sin(\theta))$ (6.5)

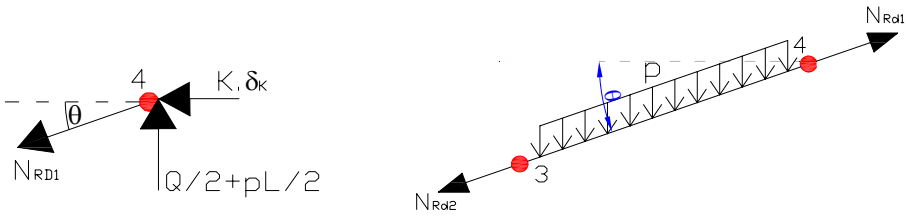

Figure VI.36. Cuts in the substructure to express equations of equilibrium

From *Formula (6.4)*, the following expression is obtained:

$$\delta_K = \frac{2.N_{Rd1} - (Q + p.L).Sin(\theta)}{2.K.Cos(\theta)} \quad (6.6)$$

So, from *Formula (6.3)* and *Formula (6.6)*, it is possible to find an expression of δ_{N1} as a function of the variables N_{Rd1}, θ and δ_{N2}:

$$\delta_{N1} = \frac{(Q + p.L).Sin(\theta) + 2.L.K.Cos(\theta).(1 - Cos(\theta)) - 2.N_{Rd1}}{4.K.Cos^2(\theta)} - \delta_{N2} \quad (6.7)$$

If the behaviour of the plastic hinges is considered, the link between the axial load N_{Rd} and the plastic elongation δ_N can be expressed as follows:

- $N_{Rd1} = K_{N1}.\delta_{N1}$ (6.8)

- $N_{Rd2} = K_{N2}.\delta_{N2}$ (6.9)

➔ With *Formula (6.5)*: $N_{Rd1} - \frac{pL}{2}.Sin(\theta) = K_{N2}.\delta_{N2}$ (6.10)

In these expressions, K_{N1} and K_{N2} represent the axial stiffnesses of the plastic hinges when subjected to the membrane forces.

So, from *Formula (6.8)* and *Formula (6.10)*, it is possible to find a relation linking δ_{N1} and δ_{N2}:

$$\delta_{N2} = \frac{K_{N1}.\delta_{N1} - \frac{pL}{2}.Sin(\theta)}{K_{N2}} \tag{6.11}$$

If δ_{N2} is replaced in *Formula (6.7)* by *Formula (6.11)*, an expression linking δ_{N1}, N_{Rd1} and θ is obtained:

$$\delta_{N1} = \frac{-2.K_{N2}.N_{Rd1}.Sec^2(\theta) - 2.K.L.(K_{N2} - p.Sin(\theta)) + K_{N2}.Sec(\theta).(2.K.L + (p.L + Q).Tan(\theta))}{4.K.(K_{N1} + K_{N2})} \tag{6.12}$$

At the end, it is possible to find an expression of N_{Rd1} as a function of the variables Q and θ if *Formula (6.12)* and *Formula (6.8)* are combined:

$$N_{Rd1} = \frac{K_{N1}.(-2.K.L.(K_{N2} - p.Sin(\theta)) + K_{N2}.Sec(\theta).(2.K.L + (p.L + Q).Tan(\theta)))}{4.K.(K_{N1} + K_{N2}) + 2.K_{N1}.K_{N2}.Sec^2(\theta)} \tag{6.13}$$

Looking now the equation of plasticity, the equality between the internal work and the external work can be expressed as follows:

$$(2.M_{Rd1} + 2.M_{Rd2}).\theta + 2.N_{Rd1}.\delta_{N1} + 2.N_{Rd2}.\delta_{N2} = Q.\Delta_A + p.L.\frac{L - \delta_K}{4}.Tan(\theta) - K.\delta_K.\delta_K \tag{6.14}$$

In the expression given in *Formula (6.14)*, the different displacements can be expressed as a function of θ through the formulas previously developed; accordingly, the displacements within this expression are derived according to θ as a second-order analysis is conducted. Then, the value of Q can be isolated. These operations have been performed through the software Mathematica. The so-obtained result is the following:

$$
\begin{aligned}
Q=\;&\frac{1}{2\,(KN1+KN2)}\Big(\cos[teta]^2\Big(2\,(KN1+KN2)\,NRd1\csc[teta]+\\
&\frac{1}{2}\sec[teta]^2\,(KN1\,L\,p\cos[2\,teta]+8\,(KN1+KN2)\,NRd1\sin[teta]-\\
&L\,((5\,KN1+2\,KN2)\,p+2\,K\,(KN1+KN2)\sin[2\,teta]))+\\
&\frac{1}{8}K\,(KN1+KN2)\cot[teta]\Big(-16\,L+\\
&\sqrt{2}\,\sqrt{\Big(\frac{1}{K^2\,(KN1+KN2)^2}\,(\sec[teta]^6\,(64\,K^2\,KN1^2\,L^2+128\,K^2\,KN1\,KN2\,L^2+64\,K^2\,KN2^2\,L^2+\\
&48\,KN1^2\,NRd1^2+96\,KN1\,KN2\,NRd1^2+48\,KN2^2\,NRd1^2+16\,K\,KN1\,L^2\,p^2+10\,KN1^2\,L^2\,p^2+\\
&16\,K\,KN2\,L^2\,p^2-24\,KN1\,KN2\,L^2\,p^2+16\,KN2^2\,L^2\,p^2-192\,K\,(KN1+KN2)^2\,L\,NRd1\cos[teta]+\\
&(64\,K^2\,(KN1+KN2)^2\,L^2+8\,K\,(KN1+KN2)\,L^2\,p^2+KN1^2\,(64\,NRd1^2-15\,L^2\,p^2)+\\
&16\,KN2^2\,(4\,NRd1^2-L^2\,p^2)+32\,KN1\,KN2\,(4\,NRd1^2+L^2\,p^2))\cos[2\,teta]-\\
&64\,K\,KN1^2\,L\,NRd1\cos[3\,teta]-128\,K\,KN1\,KN2\,L\,NRd1\cos[3\,teta]-64\,K\,KN2^2\,L\,NRd1\cos[3\,teta]+\\
&16\,KN1^2\,NRd1^2\cos[4\,teta]+32\,KN1\,KN2\,NRd1^2\cos[4\,teta]+16\,KN2^2\,NRd1^2\cos[4\,teta]-\\
&16\,K\,KN1\,L^2\,p^2\cos[4\,teta]+6\,KN1^2\,L^2\,p^2\cos[4\,teta]-16\,K\,KN2\,L^2\,p^2\cos[4\,teta]-\\
&8\,KN1\,KN2\,L^2\,p^2\cos[4\,teta]-8\,K\,KN1\,L^2\,p^2\cos[6\,teta]-KN1^2\,L^2\,p^2\cos[6\,teta]-\\
&8\,K\,KN2\,L^2\,p^2\cos[6\,teta]-16\,KN1^2\,L\,NRd1\,p\sin[teta]-16\,KN1\,KN2\,L\,NRd1\,p\sin[teta]+\\
&256\,K\,KN1^2\,MRd1\sin[2\,teta]+512\,K\,KN1\,KN2\,MRd1\sin[2\,teta]+256\,K\,KN2^2\,MRd1\sin[2\,teta]+\\
&256\,K\,KN1^2\,MRd2\sin[2\,teta]+512\,K\,KN1\,KN2\,MRd2\sin[2\,teta]+256\,K\,KN2^2\,MRd2\sin[2\,teta]+\\
&32\,K\,KN1^2\,L^2\,p\sin[2\,teta]+32\,K\,KN1\,KN2\,L^2\,p\sin[2\,teta]-24\,KN1^2\,L\,NRd1\,p\sin[3\,teta]-\\
&24\,KN1\,KN2\,L\,NRd1\,p\sin[3\,teta]+128\,K\,KN1^2\,MRd1\sin[4\,teta]+256\,K\,KN1\,KN2\,MRd1\sin[4\,teta]+\\
&128\,K\,KN2^2\,MRd1\sin[4\,teta]+128\,K\,KN1^2\,MRd2\sin[4\,teta]+256\,K\,KN1\,KN2\,MRd2\sin[4\,teta]+\\
&128\,K\,KN2^2\,MRd2\sin[4\,teta]+16\,K\,KN1^2\,L^2\,p\sin[4\,teta]+16\,K\,KN1\,KN2\,L^2\,p\sin[4\,teta]-\\
&8\,KN1^2\,L\,NRd1\,p\sin[5\,teta]-8\,KN1\,KN2\,L\,NRd1\,p\sin[5\,teta]))\Big)\Big)\Big)\Big)\Big)
\end{aligned}
\tag{6.15}
$$

It can be seen in *Formula (6.15)* that the variables included in this expression are θ, N_{Rd1}, M_{Rd1} and M_{Rd2}. Nevertheless, (N_{Rd1},M_{Rd1}) and (N_{Rd2},M_{Rd2}) are linked through the *M-N* interaction resistance curves (of the beams or of the joints); accordingly, M_{Rd1} and M_{Rd2} can be expressed as functions of N_{Rd1} and N_{Rd2} respectively. Also, N_{Rd2} can be expressed as a function of N_{Rd1} with *Formula (6.5)* and so, Q can be expressed as a function of N_{Rd1} and θ. Replacing N_{Rd1} by its expression given in *Formula (6.13)* and by isolating Q from the so-obtained expression, Q can be finally defined as a function of θ only.

The so-defined expression of Q is validated though comparison to the experimental results (see *§ III.8.3.3*). As it can be observed, the expression of Q is quite complex and not easy to apply. In the next section, the response of the substructure is predicted neglecting the uniformly distributed load p which will lead to significant simplifications of the expressions to be applied.

VI.8.3. Analytical procedure without account of p

The structure to be investigated is presented in *Figure VI.37*. If p is not included in the computations, the value of N in the beams is constant. So, the value of N_{Rd1} and N_{Rd2} applied at the plastic hinge level are the same:

$$\rightarrow \; N_{Rd1} = N_{Rd2} = N_{Rd} \tag{6.16}$$

In addition, as the axial load is the same, an average plastic deformation of the plastic hinges is defined:

$$\rightarrow \; \delta_N = \frac{\delta_{N1} + \delta_{N2}}{2} \tag{6.17}$$

$$\text{and } N_{Rd} = K_N.\delta_N \text{ with } K_N = \frac{2.K_{N1}.K_{N2}}{K_{N1} + K_{N2}} \tag{6.18) and (6.19}$$

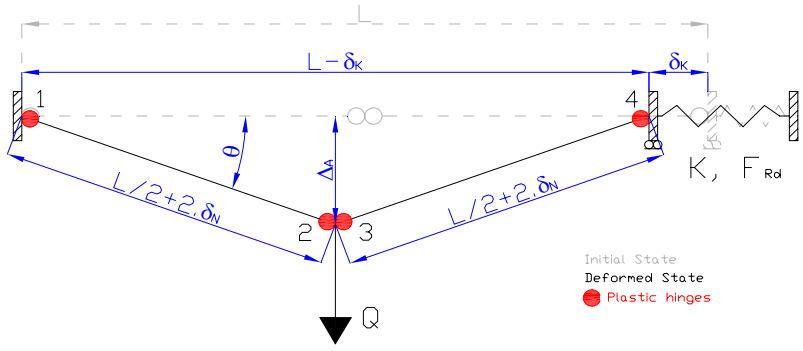

Figure VI.37. Substructure to be investigated and definition of the main parameters – p not included

If the same procedure than the one described in the previous section is followed, the expressions obtained for N_{Rd} and Q are:

$$N_{Rd} = \frac{K_N.(Sec(\theta).(2.K.L + Q.Tan(\theta)) - 2.K.L)}{8.K + 2.K_N.Sec^2(\theta)} \tag{6.20}$$

$$Q = Cos^2(\theta).[N_{Rd}.CoSec(\theta) - K.L.CoTan(\theta) + \frac{CoTan(\theta).\sqrt{Sec^4(\theta).(2.K^2.L^2 + N_{Rd}^2 - 4.K.L.N_{Rd}.Cos(\theta) + N_{Rd}^2.Cos(2\theta) + 8.K.M_{Rd1}.Sin(2\theta) + 8.K.M_{Rd2}.Sin(2\theta)}}{\sqrt{2}} - K.L.Tan(\theta) + 2.N_{Rd}.Sec(\theta).Tan(\theta)] \tag{6.21}$$

It can be seen that the variables included in the expression of N_{Rd} given in *Formula (6.20)* are only Q and θ while the variables included in the expression of Q given in *Formula (6.21)* are θ, N_{Rd}, M_{Rd1} and M_{Rd2}. Nevertheless, as in the previous section, (N_{Rd},M_{Rd1}) and (N_{Rd},M_{Rd2}) are linked through the *M-N* interaction resistance curves (of the beams or of the joints); accordingly, M_{Rd1} and M_{Rd2} can be expressed as functions of N_{Rd}. So, Q can be expressed as a function of N_{Rd} and θ and, replacing N_{Rd} by its expression given in *Formula (6.20)* and by isolating Q from the so-obtained expression, as a function of θ only.

It can also be observed that the expression given in *Formula (6.21)* is simpler. As mentioned previously, it is shown in *§ III.8.3.3* that the results obtained through *Formula (6.15)* and *Formula (6.21)* are exactly the same.

List of Figures

List of Tables